



uOttawa

L'Université canadienne
Canada's university

**FACULTÉ DES ÉTUDES SUPÉRIEURES
ET POSTDOCTORALES**



uOttawa

L'Université canadienne
Canada's university

**FACULTY OF GRADUATE AND
POSTDOCTORAL STUDIES**

Anthony Power

AUTEUR DE LA THÈSE / AUTHOR OF THESIS

Ph.D. (Biochemistry)

GRADE / DEGREE

Department of Biochemistry, Microbiology and Immunology

FACULTÉ, ÉCOLE, DÉPARTEMENT / FACULTY, SCHOOL, DEPARTMENT

A Cell Carriers for Systemic Delivery of Oncolytic Viruses

TITRE DE LA THÈSE / TITLE OF THESIS

John Bell

DIRECTEUR (DIRECTRICE) DE LA THÈSE / THESIS SUPERVISOR

CO-DIRECTEUR (CO-DIRECTRICE) DE LA THÈSE / THESIS CO-SUPERVISOR

Earl Brown

Robin Parks

Cahterine Tsifidis

**Kah-Whye Peng
Mayo Clinic Minnesota**

Gary W. Slater

Le Doyen de la Faculté des études supérieures et postdoctorales / Dean of the Faculty of Graduate and Postdoctoral Studies

CELL CARRIERS FOR SYSTEMIC DELIVERY OF ONCOLYTIC VIRUSES

By
Anthony Power

A thesis submitted in partial fulfillment of the requirements for the degree of
Doctor of Philosophy, specialization in Biochemistry.

University of Ottawa

Faculty of Medicine

January 12, 2010

Supervisor
Dr. John C. Bell, PhD

© Anthony Power, Ottawa, Ontario, Canada 2010



Library and Archives
Canada

Published Heritage
Branch

395 Wellington Street
Ottawa ON K1A 0N4
Canada

Bibliothèque et
Archives Canada

Direction du
Patrimoine de l'édition

395, rue Wellington
Ottawa ON K1A 0N4
Canada

Your file *Votre référence*
ISBN: 978-0-494-73907-5
Our file *Notre référence*
ISBN: 978-0-494-73907-5

NOTICE:

The author has granted a non-exclusive license allowing Library and Archives Canada to reproduce, publish, archive, preserve, conserve, communicate to the public by telecommunication or on the Internet, loan, distribute and sell theses worldwide, for commercial or non-commercial purposes, in microform, paper, electronic and/or any other formats.

The author retains copyright ownership and moral rights in this thesis. Neither the thesis nor substantial extracts from it may be printed or otherwise reproduced without the author's permission.

In compliance with the Canadian Privacy Act some supporting forms may have been removed from this thesis.

While these forms may be included in the document page count, their removal does not represent any loss of content from the thesis.

AVIS:

L'auteur a accordé une licence non exclusive permettant à la Bibliothèque et Archives Canada de reproduire, publier, archiver, sauvegarder, conserver, transmettre au public par télécommunication ou par l'Internet, prêter, distribuer et vendre des thèses partout dans le monde, à des fins commerciales ou autres, sur support microforme, papier, électronique et/ou autres formats.

L'auteur conserve la propriété du droit d'auteur et des droits moraux qui protègent cette thèse. Ni la thèse ni des extraits substantiels de celle-ci ne doivent être imprimés ou autrement reproduits sans son autorisation.

Conformément à la loi canadienne sur la protection de la vie privée, quelques formulaires secondaires ont été enlevés de cette thèse.

Bien que ces formulaires aient inclus dans la pagination, il n'y aura aucun contenu manquant.


Canada

CELL CARRIERS FOR SYSTEMIC DELIVERY OF ONCOLYTIC VIRUSES

By
Anthony Power

ABSTRACT

There is a clear need for novel therapeutics that can improve the treatment of metastatic cancers. Conditionally replicative oncolytic viruses represent one promising class of new agents that have garnered recent attention in laboratory and clinical studies. While much success has been achieved in targeting the replication and cytolytic effects of viruses to tumor cells, systemic delivery remains a major challenge. We have developed a murine tumor model in order to investigate potential obstacles to systemic delivery of oncolytic viruses in an immunocompetent host. We find that the *in vivo* delivery of naked virus particles to tumors is ablated by the humoral antiviral response elicited during repeated therapeutic administration. In contrast, live cell carriers avoid neutralization and deliver oncolytic virus to tumor beds in the presence of high-titer circulating antibodies. We investigated the properties of various mammalian cell lines as oncolytic virus carriers, and conclude with studies of a novel insect cell carrier system. The unique properties of this insect cell carrier platform make it an attractive technology for immediate clinical use as well as continued refinement in the lab.

ACKNOWLEDGMENTS

I would like to thank my supervisor John Bell for providing an inspiring and stimulating lab environment to work in over the years, for continual scientific and humanitarian support and always encouraging independence and initiative.

Dave Stojdl and Brian Lichty for showing me how to be a bench scientist, and continued support after moving on to start their own labs.

Ken Garson for many helpful suggestions, reagents, ideas, perpetual enthusiasm for science and swimming tips over the years.

Earl Brown for taking an interest in my project from the early days, and helping to infect me with virophilia.

Harry Atkins, for balanced perspective at many years of lab meetings and finding insect cells "cool."

All labmates past and present, for support through the ups and downs of research and memories of a truly unforgettable experience that I will always cherish.

Jenn Paterson, fellow honors and masters student, for her inspirational work ethic, scientific diligence, and many stimulating and rigorous discussions.

Long-term Baymate Rob Edge, for sharing great music, enthusiasm for all things science, and balanced humanity.

I thank my parents Rhonda and Tony, and sister Krista for encouraging me to follow my interests and their unconditional support and understanding.

To Allana, for fearlessly jumping into this adventure with me. Your unwavering commitment makes everything possible.

TABLE OF CONTENTS

ABSTRACT	II
ACKNOWLEDGMENTS	III
TABLE OF CONTENTS	IV
LIST OF ABBREVIATIONS	VI
LIST OF FIGURES.....	VIII
CHAPTER 1: INTRODUCTION	1
1.1 THE NEED FOR NOVEL APPROACHES TO SYSTEMIC CANCER THERAPY	1
1.2 EARLY STUDIES OF CANCER VIROTHERAPY: PROMISE AND PROBLEMS.....	1
1.3 ONCOLYTIC VIRUS RESEARCH AND THE MOLECULAR ERA: TARGETING TUMORS	2
1.4 THE PROBLEM OF HOST IMMUNITY: A 21ST CENTURY CHALLENGE FOR ONCOLYTIC VIROTHERAPY	8
1.5 MOLECULAR BIOLOGY OF VESICULAR STOMATITIS VIRUS	9
1.6 MOLECULAR BIOLOGY OF VACCINIA VIRUS	11
RATIONALE	11
AIMS AND APPROACH.....	12
CHAPTER 2: CELL-BASED DELIVERY OF AN ONCOLYTIC VIRUS CIRCUMVENTS ANTI-VIRAL IMMUNITY	13
CHAPTER 3: PROGRAMMABLE INSECT CELL CARRIERS FOR SYSTEMIC DELIVERY OF INTEGRATED CANCER BIOTHERAPY	42
CHAPTER 4: DISCUSSION.....	71
4.1 TARGETING VIROTHERAPEUTIC DELIVERY.....	71
4.2 EVASION OF ACQUIRED ANTIVIRAL IMMUNITY.....	74
4.3 BIOSAFETY.....	76
4.4 MANUFACTURING	77
4.5 A PROGRAMMABLE CELL PLATFORM FOR INTEGRATED CANCER BIOTHERAPY.....	78
4.6 CONCLUSIONS	79
REFERENCES	80
APPENDICES	A.1
APPENDIX I. TAMING THE TROJAN HORSE: OPTIMIZING DYNAMIC CARRIER CELL/ONCOLYTIC VIRUS SYSTEMS FOR CANCER BIOTHERAPY.....	A.1
APPENDIX II. IN VIVO VIROTHERAPY AND REPORTER GENE IMAGING OF MULTIPLE MYELOMA USING AN ATTENUATED VESICULAR STOMATITIS VIRUS ENCODING THE SODIUM IODIDE SYMPORTER GENE	A.2

APPENDIX III. CELL-BASED DELIVERY OF ONCOLYTIC VIRUSES: A NEW STRATEGIC ALLIANCE FOR A BIOLOGICAL STRIKE AGAINST CANCER	A.3
APPENDIX IV. EFFECTS OF INTRAVENOUSLY ADMINISTERED RECOMBINANT VESICULAR STOMATITIS VIRUS (VSV(DELTAM51)) ON MULTIFOCAL AND INVASIVE GLIOMAS.....	A.4
APPENDIX V.: VESICULAR STOMATITIS VIRUS: RE-INVENTING THE BULLET.	A.5
APPENDIX VI.: VSV STRAINS WITH DEFECTS IN THEIR ABILITY TO SHUTDOWN INNATE IMMUNITY ARE POTENT SYSTEMIC ANTI-CANCER AGENTS... ..	A.6
CURRICULUM VITAE.....	A.7

LIST OF ABBREVIATIONS

AV3	attenuated virus 3
BEV-1	bovine enterovirus 1
CFSE	carboxyfluorescein succinimidyl ester
CIK	cytokine-induced killer cells
D-MEM	dulbecco's modified eagle medium
dsDNA	double-stranded DNA
FCS	fetal calf serum
FLUC	firefly luciferase
GFP	green fluorescent protein
HSV-1	herpes simplex virus 1
IFN	interferon
IFNAR	interferon alpha receptor
IV	intravenous
IVIS	in vivo imaging system
IP	intraperitoneal
IRF-9	interferon regulatory factor-9
ISG	interferon stimulated gene
ISGF3	interferon-stimulated gene factor 3
Jak	Janus kinase
MACS	magnetic-activated cell sorting
mRFP	monomeric red fluorescent protein
mRNA	messenger ribonucleic acid
miRNA	micro ribonucleic acid
mirT	microRNA target site
NDV	Newcastle disease virus
NCI	National Cancer Institute
OV	oncolytic virus
PBS	phosphate-buffered saline
pfu	plaque-forming units
PKR	protein kinase R
RLUC	<i>renilla reniformis</i> luciferase
RNA	ribonucleic acid
RNP	ribonucleoprotein
STAT	signal transducer and activator of transcription

TK	thymidine kinase
VGf	viral growth factor
VSV	vesicular stomatitis virus
VV	vaccinia virus
VVdd	vaccinia virus double deleted (TK and VGf genes knocked out)
YFP	yellow fluorescent protein

LIST OF FIGURES

CHAPTER 1

Figure 1.1 <i>Antiviral Signaling Through the Type I Interferon Pathway</i>	4
Figure 1.2 <i>VSV Genome and Virion Structure</i>	10

CHAPTER 2

Figure 2.1 <i>Humoral Immune Response Impairs Systemic Tumor Therapy with Oncolytic VSV</i>	17
Figure 2.2 <i>Trojan Horse Delivery of Oncolytic VSV to Lung Tumors in Syngeneic Carrier Cells</i>	19
Figure 2.3 <i>Dual-enzyme in vivo luminescence imaging of VSV delivery by autologous and xenogeneic carcinoma cells</i>	21
Figure 2.4 <i>Dual-enzyme in vivo luminescence imaging of VSV delivery by murine leukemia cells</i>	23
Figure 2.5 <i>Cell-mediated systemic delivery and anti-tumor activity of VSV in the presence of circulating antibody</i>	25
Figure 2.6 <i>Enhancement of systemic therapy with VSV delivered in carrier cells</i>	27

CHAPTER 3

Figure 3.1 – <i>Establishment of Continuous Insect Cell Lines Propagating Oncolytic VSV-Δ51</i>	48
Figure 3.2 – <i>Persistently Infected Insect Cell Carriers Deliver Oncolytic Virus to Tumor Cells</i>	51
Figure 3.3 – <i>Arming Drosophilid Oncolytic Virus Carrier Cells with Additional Biotherapeutic Cargoes</i>	53

Figure 3.S1: *Insect cell carriers constitutively secreting vaccinia immunomodulators prime 786-0 human renal carcinoma cells for infection with oncolytic VSVΔ51*.....54

Figure 3.4 – *Insect Cell Carriers Deliver Multiple Integrated Biotherapeutics to Tumor Cells*.....56

Figure 3.S2: *Systemic biodistribution of mammalian carrier cells*.58

Figure 3.5 – *Systemic Delivery of Insect Cells Carrying Multiple Integrated Biotherapeutics*60

CHAPTER 1: INTRODUCTION

The work described in the following thesis examines the use of conditionally replicative “oncolytic” viruses as novel agents for systemic cancer therapy.

1.1 The Need for Novel Approaches to Systemic Cancer Therapy

Cancer is a group of diseases characterized by uncontrolled cell growth which frequently lead to death, and was responsible for killing an estimated 6.7 million people worldwide in 2002¹. Standard therapy currently consists of a combination of three primary modalities: surgery, radiation and chemotherapy². Surgery and radiation are effective against solid localized tumors, whereas systemically administered chemotherapeutics are necessary to treat disseminated hematological or metastatic disease². Although chemotherapeutics are commonly prescribed for cancer treatment, they are curative in only a small minority of cases³. Many patients do not respond to chemotherapy, and many others showing initial disease regression subsequently develop drug resistance and eventually relapse³. Furthermore, systemically administered chemotherapeutics reach every organ in the body but lack specificity for malignant cells. As a result they exhibit undesirable levels of toxicity to normal tissues at effective clinical doses³. The limitations of chemotherapeutics currently employed in the clinic thus provide strong impetus for the development of novel therapeutics that can be systemically delivered with less toxicity and greater efficacy.

1.2 Early Studies of Cancer Virotherapy: Promise and Problems

The concept of exploiting viral infection to treat malignancies emerged not long after the original identification of viruses as transmissible, subcellular agents capable of giving rise to

tissue damage in their hosts⁴. In pursuit of this goal, an extensive body of research was carried out during the early to mid 20th century investigating the effects of various naturally occurring virus strains on tumors⁵. Susceptibility of human and murine tumors to infection with many different viruses was noted, as were at least two overarching limitations to their clinical use. Firstly, viruses exhibiting the greatest antitumor effect were often those with the most devastating impact on normal tissues, many being neuropathogenic⁶. Thus it proved difficult to cure murine tumors without also seriously harming or killing the animal, delineating “the problem of host survival”. Secondly, it was noted that consecutive doses of viral agents would be susceptible to neutralization by adaptive immune responses mounted by the patient over the course of therapy⁷. Little progress could be made to overcome these problems without *in vitro* systems for culturing tumor cells and viruses, or any knowledge of their molecular genetics. A scattering of clinical trials continued, but without solutions to such problems, oncolytic viruses failed to gain acceptance as a proven mainstream medical therapy through the latter part of the 20th century, just as chemotherapies began to see increasingly widespread use.

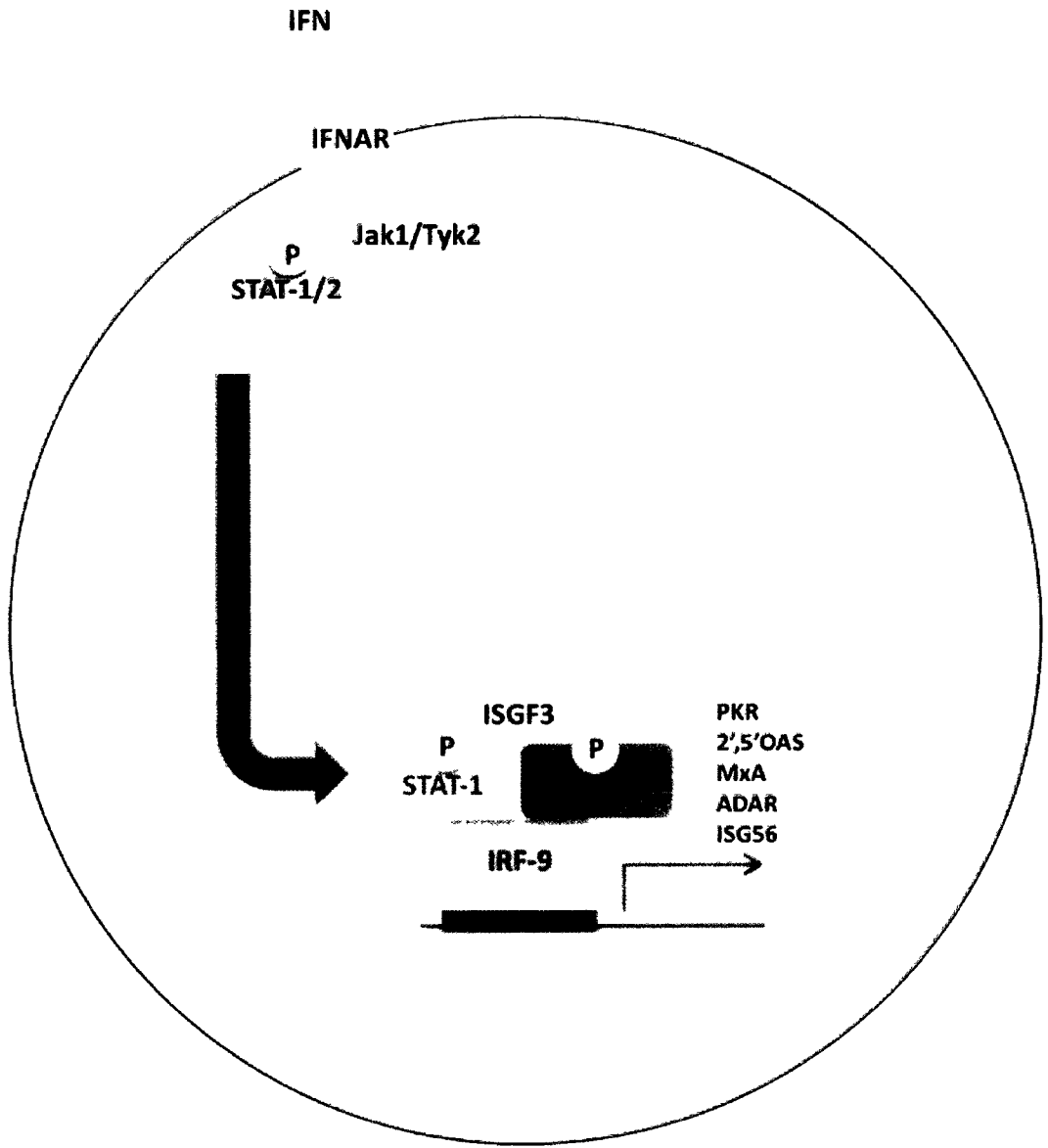
1.3 Oncolytic Virus Research and the Molecular Era: Targeting Tumors

Recent advances in cellular and molecular biology offer opportunities to overcome the problems that have limited the success of oncolytic virotherapy over the past century and there has been a resurgence of interest in the field. Chief among these advances has been the molecular characterization of selected or engineered viral mutants. Thus it has been possible to generate conditionally replicative viral mutants whose loss of function is complemented by genetic defects known to occur during tumorigenesis. For example, the

first oncolytic virus developed based on this strategy was a Herpes Simplex Virus 1 (HSV-1) mutant with a deletion of the thymidine kinase gene⁸. This gene is needed to promote the biosynthesis of nucleotides for virus replication to proceed in non-dividing cells, but its function is dispensable for growth in rapidly dividing transformed cells with high levels of available nucleotides. Thus the TK-deleted HSV-1 selectively replicated in tumor cells, and could safely induce tumor regression in mice⁸. A similar strategy has been used to develop E1B-deleted adenoviruses which conditionally replicate in p53-deficient tumor cells⁹. In addition, the viral growth factor (VGF) gene which encodes an activating ligand for cellular receptor tyrosine kinases has been deleted from vaccinia virus in order to target this virus to transformed cells with aberrantly activated growth signaling pathways¹⁰.

In addition to conditionally replicative viral mutants, studies in cultured human cell lines have revealed that some natural or wild-type strains possess an inherent tropism for tumor cells. These include bovine enterovirus 1 (BEV-1)¹¹, parvovirus¹², reovirus¹³, newcastle disease virus (NDV)¹⁴, vesicular stomatitis virus (VSV)¹⁵, and myxoma virus¹⁶. Investigation of the mechanism underlying this phenomenon has led to the understanding that defective anti-viral signaling, most notably in the type I interferon (IFN) pathway, is a common feature of many human cancers¹⁵.

The type I IFNs are a group of secreted cytokines that activate cellular Jak/STAT kinase signaling pathways by binding to a common type I interferon receptor (IFNAR) expressed on the surface of all nucleated mammalian cells¹⁷ (Figure 1.1). Janus tyrosine kinases (i.e. Jak1, Tyk2) are recruited to the activated IFNAR, leading to phosphorylation of intracellular



receptor chains. In turn, STAT1/2 monomers are recruited to the receptor and phosphorylated.

Activated STAT-1 and STAT-2 then dissociate from the IFNAR and join with the transcription factor IFN regulatory factor-9 (IRF-9) to form the IFN stimulated gene factor 3 (ISGF3), which translocates to the nucleus to activate the transcription of IFN stimulated genes (ISGs). These ISGs mediate the anti-viral, anti-proliferative and immunomodulatory functions of the IFN signaling pathway.

Type I IFNs play a crucial role in the innate defence against many viruses. For example VSV is highly sensitive to the effects of IFN, which potently blocks infection of cultured cells¹⁸. Likewise IFNAR-deficient mice are highly susceptible to infection with numerous viruses, particularly VSV¹⁹. In addition, productive viral infections in host organisms generally rely on the expression of one or more gene products that inactivate the IFN system¹⁷, further underscoring its central role in innate immunity.

In addition to antiviral functions, the IFN system exerts significant effects on cellular proliferation, playing a particularly important role in the regulation of normal hematopoiesis²⁰. For this reason preparations of recombinant interferon have undergone extensive clinical testing as cancer therapeutics. However these studies met with limited success as malignant cells frequently failed to respond to the regulatory effects of IFNs²¹.

The relevance of IFN unresponsiveness seen in many types of cancer cells led to the prediction that they could be preferentially infected and killed by IFN-sensitive viruses. This hypothesis was first tested with VSV, and it was shown that while normal cells were

resistant to infection, transformed cells were indeed well infected and susceptible to the virus' cytopathic effects in the presence of IFN¹⁵. Subsequent studies have shown loss of IFN responsiveness also leads to preferential infection of tumor cells by myxoma²² and parvoviruses²³. A survey of the NCI-60 cell panel revealed IFN-resistance and sensitivity to viral infection in the vast majority of human cancer cell lines, irrespective of their histological origins²⁴. Therefore it is likely that a variety of different molecular mechanisms underlie the susceptibility of tumors to infection depending on the disease type and the viral agent in question. As one of the first characterized examples, the susceptibility of cancer cells to reovirus was shown to be mediated by inactivation of the interferon-regulated, antiviral PKR gene product by oncogenic Ras signaling²⁵. Furthermore, the master tumor suppressor p53 plays a central role in ISG activation and its frequent inactivation, a nearly ubiquitous feature of tumor cells, increases susceptibility to viral infection. Thus innate antiviral immunity and cellular proliferation appear to be intimately linked through their common regulation by pleiotropic signaling pathways.

The discovery that tumor cells often exhibit defects in innate anti-viral signaling pathways has also suggested novel ways in which the specificity of oncolytic virus replication might be further improved. Many, if not all animal viruses encode gene products that counteract innate immune signaling and are required to productively infect normal cells. Viruses with loss-of-function mutations in such genes are therefore crippled in normal cells, but grow preferentially in transformed cells with defective antiviral defenses. Examples of conditionally replicative viral mutants that exploit this strategy are γ 34.5 gene-deleted HSV-1^{26, 27}, NS1-deleted influenza virus^{28, 29}, and M-mutated VSV²⁴. Each of these genes

functions to inactivate one or more components of the type I interferon signaling pathway in normal cells, however their functions are dispensable for growth in cancer cells with acquired innate immune defects.

As basic research into the mechanisms of gene regulation advances further, novel strategies for engineering tumor-specific viruses continue to emerge. For example, replacement of the poliovirus internal ribosome entry site with its counterpart from human rhinovirus ablates neuropathogenicity but does not hamper cytolytic replication in gliomas³⁰. The recent discovery and characterization of host cell regulatory microRNAs (miRNAs) has also been exploited for viral targeting. Since miRNAs generally appear to down-regulate expression of target genes and their expression is tissue-specific, it was hypothesized that insertion of certain miRNA target sequences (miRT) into the regulatory regions of viral genes could confer tumor tropism. For example, the let-7 miRNAs show tumor suppressor activity and their expression is frequently lost in cancers³¹. Target sites for this miRNA were therefore inserted into the 3' untranslated region of the matrix gene, in order to ablate the neurotropism exhibited by wt-VSV in laboratory mice³². In a similar approach, tissue-specific miRT were used to diminish the muscle tropism of an oncolytic picornavirus, preventing the development of lethal myositis in mice³³. Tissue-specific miRT have also been used to ablate the hepatotoxicity of wild-type adenovirus³⁴.

To summarize, a variety of different targeting strategies can be used to engineer tumor specific replication into virtually any genetically tractable viral platform. Future research is likely to present novel molecular targeting opportunities, while genomic sequencing and synthesis technologies should continue to offer a steady supply of replicating vector

platforms. Thus it appears that one of the major long-standing challenges to the success of oncolytic virotherapy, attenuating virulence without compromising tumor-specific replication and cytolysis, has largely been overcome.

1.4 The Problem of Host Immunity: A 21st Century Challenge for Oncolytic Virotherapy

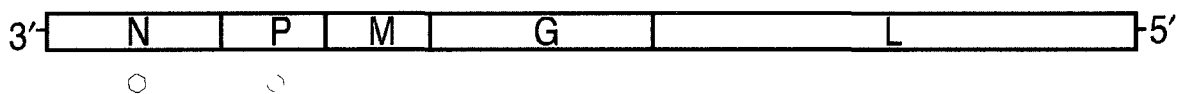
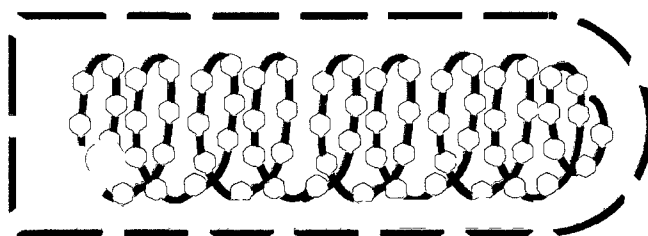
While major advances have been made in redirecting viral tropism to malignant tissues, the delivery of virotherapeutics to tumors in the face of a hostile host immune system remains a major challenge. Systemically administered viruses are susceptible to both innate and adaptive immune effectors. In naïve animals and humans circulating blood serum proteins such as complement and natural antibodies³⁵⁻³⁷ can bind to and inactivate viral vectors, either directly or by promoting their clearance by cells of the reticuloendothelial system. Viruses may also be sequestered by binding and/or uptake by blood cells^{38, 39}, or cleared from the circulation entirely by organs such as the liver^{40, 41} which specialize in this task. Despite these innate barriers, several studies have shown that it is possible, in naïve mice, to deliver oncolytic viruses to tumors by systemic administration^{15, 42-45}. However, hosts which have been pre-exposed to viral agents also develop lasting adaptive immunity, mediated by circulating immunoglobulins which can increase the neutralizing capacity of serum by several thousand-fold or more, as well as cellular components. The question of adaptive immunity is likely to be highly relevant to the outcome of virotherapy in the clinic, particularly for agents based on human pathogens, such as adenovirus, hsv-1, measles, vaccinia and reovirus, for which patients would be expected to possess some level of pre-existing immunity. For oncolytic vectors to which humans are not exposed naturally or through vaccination programs, there exists a window of opportunity to administer the

initial therapeutic dose to immunologically naïve patients. However, repeated dosing regimens would be subject to the adaptive response evolving during therapy.

1.5 Molecular Biology of Vesicular Stomatitis Virus

The work described in the following thesis exploits a mutant strain of VSV (described in Appendix VI) as a model oncolytic therapeutic. VSV belongs to the family of *Rhabdoviridae*, so named due to the bullet-shaped structure of the enveloped virion. The negative sense RNA genome is 11.1 kilobasepairs in length and encodes five genes (Figure 1.2). They are arrayed as individual, non-overlapping cistrons in a linear fashion in the order (3' to 5') N-P-M-G-L. The N gene encodes the nucleocapsid protein, which tightly associates with the RNA genome to form the mature viral RNP. Along with the phosphoprotein encoded by the P gene, it is a required co-factor for viral transcription and replication. These factors in turn associate with the viral RNA-dependent RNA polymerase encoded by the L gene to form the complete transcription/replication complex. The M gene of VSV encodes the matrix protein which functions in the inactivation of host gene expression and viral budding at the plasma membrane. The viral glycoprotein encoded by the G gene is a type I transmembrane protein arranged in homotrimeric spikes on the virion surface. It mediates host cell attachment and entry by orchestrating pH-dependent fusion between the viral envelope and endosomal membranes. As the sole viral polypeptide exposed on the outer virion surface, the G protein is also the exclusive target of virus neutralizing antibodies elicited during *in vivo* infection. The recombinant strains of VSV used in this thesis harbor deletions of Met-51 in the matrix protein as well as reporter transgenes between the G and L genes, and were generated by established techniques of reverse genetics (Appendix VI). The initial

Figure 1.2 VSV Genome and Virion Structure. Schematic depicting the linear arrangement of the 5 VSV genes on the negative strand RNA genome, and arrangement of the encoded proteins within the bullet-shaped, enveloped virion. The coiled nucleocapsid on the interior of the virion contains the RNA genome.



characterization of these oncolytic VSV mutants is described in Appendix VI. Further general background on VSV is reviewed in Appendix V.

1.6 Molecular Biology of Vaccinia Virus

Several experiments described in Chapter 3 of this thesis make use of a recombinant oncolytic strain of vaccinia virus generated by F. LeBoeuf of the Bell lab. Vaccinia virus is an enveloped virus with a linear dsDNA genome of approximately 190 kilobasepairs that is predicted to encode some 217 genes. The genome is flanked by 12 kbp inverted terminal repeats at each end. Incomplete base-pairing gives rise to terminal hairpin loops and the genome thus forms a continuous polynucleotide circle. The virion is brick-shaped, 300-400nm in diameter, and carries a full complement of enzymes required for the initial transcription of capped and polyadenylated mRNAs following entry into the cell.

Transcription and replication occur in cytoplasmic virus factories, largely independent of host cell factors (see Moss, B. (1990) Poxviridae and their Replication, in "Virology" (B.N. Fields et al., Eds.), 2nd ed. Raven Press, NY). Particularly relevant to the work described in this thesis is the fact that vaccinia virus encodes numerous secreted immunomodulatory proteins, such as B18r which binds and inactivates type I IFNs (Symons et al. (1995), *Cell*). The oncolytic strain used in these studies was a doubly-deleted vaccinia virus (VVdd) carrying deletions of the viral TK and VGF genes and harboring the mCherry fluorescent reporter transgene.

RATIONALE

Despite the well-established role of the adaptive immune response in preventing repeated viral infections and their associated pathogenesis, little experimental work had been done

to investigate its impact upon systemic oncolytic virotherapy prior to the undertaking of the studies described in this thesis. Consequently, the potential role of adaptive immunity has had little influence in the design of recent clinical trials of virotherapy. Although both pre-existing and induced neutralizing antibody titers have been detected repeatedly in human patients receiving systemic therapy⁴⁶⁻⁵¹, no effort has been made to avoid virus inactivation. This is likely a key reason why systemic anti-tumor efficacy has not yet been achieved in human oncolytic virus trials⁴⁶.

AIMS AND APPROACH

In the work described in the following thesis, we sought to investigate the impact of antiviral immunity on systemic oncolytic virus delivery, and to test strategies to overcome this obstacle. Recombinant strains of VSV were generated which carried an attenuating mutation in the matrix protein as well as a fluorescent reporter or bioluminescent transgene. These recombinant strains could be tracked *in vivo* to assess the delivery and spread of oncolytic viruses in an immunocompetent murine tumor model. This model system then allowed us to investigate the use of cell carriers as a novel strategy for immune evasion and systemic delivery of oncolytic virotherapy. The characteristics of a wide variety of putative carrier cell types from different lineages and species were compared *in vivo*, leading to the development of a novel insect cell platform for the propagation and systemic delivery of oncolytic viruses and other biotherapeutics.

CHAPTER 2: CELL-BASED DELIVERY OF AN ONCOLYTIC VIRUS CIRCUMVENTS ANTI-VIRAL IMMUNITY

Anthony T. Power¹, Jiahu Wang¹, Theresa Falls¹, Jennifer Paterson¹, Kelley Parato¹, Brian D. Lichty², David F. Stojdl³, Peter A.J. Forsyth⁴, Harry Atkins¹ and John C. Bell¹

¹ Department of Biochemistry Microbiology and Immunology, University of Ottawa, Ottawa Health Research Institute Centre for Cancer Therapeutics, Ottawa, Ontario Canada; ²Department of Pathology and Molecular Medicine, Centre for Gene Therapeutics, Michael DeGroote Centre for Learning & Discovery, McMaster University, Ottawa, Ontario, Canada; ³ Department of Biochemistry Microbiology and Immunology, University of Ottawa, Apoptosis Research Centre, Children's Hospital of Eastern Ontario, Ottawa, Ontario, Canada; ⁴Department of Medicine, Tom Baker Cancer Centre Calgary, Alberta, Canada.

To whom correspondence should be addressed:

John C. Bell, PhD.

Office: 613-737-7700 ext 70333, Cell: 613-286-2396; jbelle@ohri.ca

Keywords: Oncolytic virotherapy, oncolytic viruses, vesicular stomatitis virus, antibodies, immunity

Contribution of Authors: AT Power performed all experiments, created all figures and wrote the manuscript with review by JC Bell. AT Power and JC Bell designed all experiments. J. Wang generated recombinant lentiviruses expressing luciferase. T. Falls provided technical support for all animal experiments. J. Paterson helped generate recombinant VSVs expressing fluorescent transgenes and collaborated with AT Power in the initial development of the model for necroscopic imaging of VSV infection of murine tumors. B. Lichty and D. Stojdl contributed to the conceptualization of these experiments. AT Power performed IVIS imaging experiments with equipment provided by the lab of D. Stojdl. H. Atkins contributed leukemia cell lines and guidance concerning their experimental use.

Published: Molecular Therapy. 2007 Jan;15(1):123-30.

Abstract

Oncolytic viruses capable of tumor-selective replication and cytolysis have shown early promise as novel cancer therapeutics. However the host immune system remains a significant obstacle to effective systemic administration of virus in a clinical setting. Here, we demonstrate the severe negative impact of the adaptive immune response on the systemic delivery of oncolytic vesicular stomatitis virus (VSV) in an immune-competent murine tumor model, an effect mediated primarily by the neutralization of injected virions by circulating antibodies. We show that this obstacle can be overcome by administering virus within carrier cells that conceal viral antigen during delivery. Infected cells were delivered to tumor beds and released virus to infect malignant cells while sparing normal tissues. Repeated administration of VSV in carrier cells to animals bearing metastatic tumors greatly improved therapeutic efficacy when compared to naked virion injection. Whole-body molecular imaging revealed that carrier cells derived from solid tumors accumulate primarily in the lungs following intravenous injection, whereas leukemic carriers disseminate extensively throughout the body. Furthermore, xenogeneic cells were equally effective at delivering virus as syngeneic cells. These findings emphasize the importance of establishing cell-based delivery platforms in order to maximize the efficacy of oncolytic therapeutics as they move into the clinic.

INTRODUCTION

A variety of different replication-competent viruses have been selected or engineered to preferentially infect and kill cancer cells and are currently under clinical or preclinical study⁵². These novel therapeutics offer an unprecedented level of anti-tumor potency and, if administered systemically, could be particularly effective against disseminated disease. However, delivering an oncolytic virus to tumor cells through the circulatory system is a unique challenge in itself. Virus particles injected into the bloodstream are particularly vulnerable to inactivation by complement proteins^{53, 54}, uptake by the reticuloendothelial system^{55, 56} and neutralization by circulating antibodies^{53, 57-60}. Of these, host antibodies are likely to be the most restrictive barrier to therapy, as they mediate a long-lasting state of immunity to repeated infection.

Vesicular stomatitis virus (VSV) is an effective oncolytic therapeutic when administered intravenously in a variety of murine cancer models⁶¹⁻⁶⁴, however the impact of a pre-existing or evolving immune response has yet to be tested. Since robust adaptive immunity is elicited upon administration to mice⁶⁵ this system offers the valuable opportunity to study oncolytic virotherapy in the context of a fully functional host immune system.

Here we demonstrate the negative impact of humoral immunity on systemic delivery of VSV, underscoring the need for alternative approaches to oncolytic virus administration. Infected cells have shown promise as delivery vehicles for viral therapeutics⁶⁶⁻⁷³, and we now demonstrate that cellular carriers can shield oncolytic virus from neutralizing antibodies during delivery, providing a simple and effective means to enhance therapy in

the face of sterilizing anti-viral immunity. Furthermore we show that a wide variety of established, non-autologous cell lines, particularly those of hematological origin, could be the ideal platform for the construction of specialized biotherapeutic delivery vehicles to maximize the efficacy of oncolytic viruses when applied in the clinic.

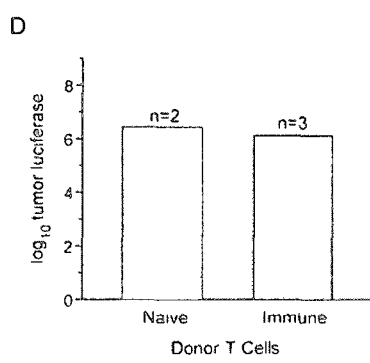
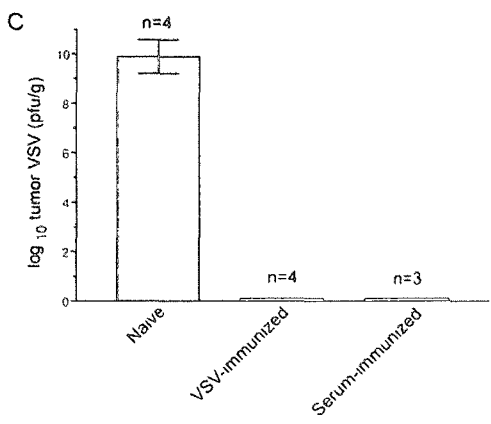
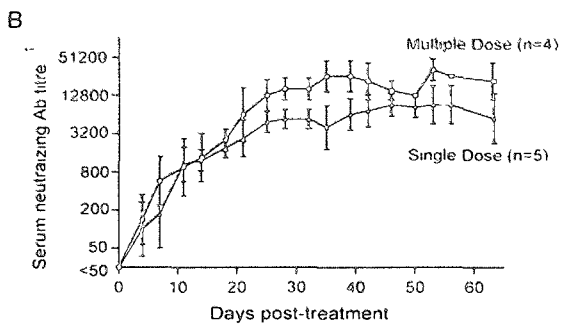
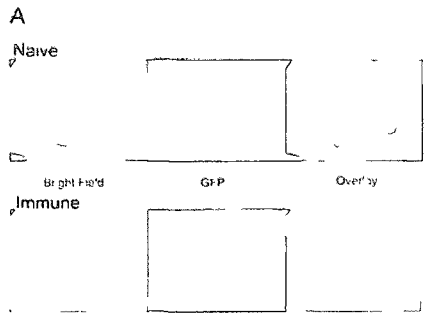
RESULTS

Circulating antibodies impair systemic therapy with VSV

To examine the impact of a pre-existing immune response upon therapy, we compared virus delivery in naïve animals to those immunized with an intravenous dose of 5×10^8 pfu VSV 6 weeks prior to treatment. As we have reported previously⁶¹, extensive tumor-specific replication, as evidenced by virus-associated fluorescence, is seen in CT26 tumors 24h following intravenous administration of VSV-GFP to naïve mice (Fig. 1A, upper panel). In contrast, no expression of virus-associated GFP was observed in tumors from pre-immunized mice (Fig. 1A, lower panel). Interestingly, the inhibition of delivery correlated with the onset of humoral immunity. Neutralizing titers were detectable in serum as early as 4 days into therapy and reached long-lasting plateau levels by 21-28 days (Fig. 1B), suggesting that circulating antibodies were responsible for impairing VSV delivery. To further investigate this possibility, we examined whether passive immunization with anti-VSV immune serum prior to treatment was sufficient to ablate infection of subcutaneous tumors. Quantitative analysis of tumor homogenates revealed nearly 10^{10} plaque-forming units (pfu)/g in tumors from naïve mice, whereas no virions were detected in tumors from

Figure 2.1 Humoral Immune Response Impairs Systemic Tumor Therapy with Oncolytic

VSV. (A) Composite bright-field/fluorescent microscopy images of subcutaneous tumors from either naïve (upper panels) or pre-immunized (lower panels) mice, 24h following intravenous administration of 5×10^8 VSV-GFP. **(B)** Kinetics of neutralizing antibody (NAb) response to either single (▲) or multiple dose (■) therapy with oncolytic VSV. Multiple dose group received 3 intravenous doses of 5×10^8 pfu per week over a total period of 7 weeks. Geometric mean NAb titers for each group +/- SD are shown **(C)** Quantitative analysis of VSV titers in subcutaneous tumors removed from either naïve, VSV-immunized, or passively-immunized mice 24h following intravenous therapy as described above. Bars represent mean \log_{10} titers +/- SD. **(D)** Quantitation of tumor luciferase activity in mice receiving a transfer of T lymphocytes from either naïve (dark bar) or VSV-immune (light bar) donors 24h prior to intravenous therapy with VSV-luciferase. Tumors were assayed 24h post-treatment. Bars represent mean relative luciferase units +/- SD.



mice pre-immunized with either live virus or anti-VSV immune serum (Fig. 1C). In contrast, adoptive transfer of purified immune T cells had no effect on tumor infection (Fig. 1D).

These results indicate that circulating antibodies rather than cellular responses elicited during oncolytic therapy are sufficient to ablate delivery of repeat virus doses, consistent with earlier observations that in the mouse, immunity to VSV is largely a humoral response

65 .

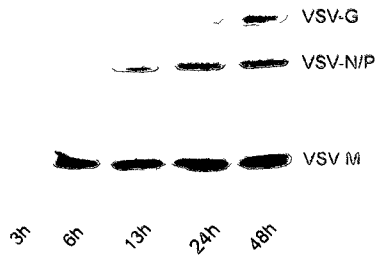
Systemic delivery of VSV using syngeneic carrier cells

We next tested whether an established syngeneic cell line could be used as a “*trojan horse*” vehicle to transiently sequester viral antigen during systemic delivery. As shown in figure 2A, CT26 murine colon carcinoma cells are readily infected with VSV and begin to accumulate viral protein within 6 hours. We therefore harvested cells after 3h of infection, prior to the onset of antigen expression, for administration to mice with established lung metastases. Microscopic examination of lungs 24h after intravenous injection of 10^6 VSV-infected cells revealed widespread expression of virally-encoded GFP within tumor nodules, but not in surrounding normal lung tissue (Fig. 2B). Nearly all visible tumor nodules were GFP-positive, indicative of highly efficient carrier cell delivery to the lungs. Similarly, dual-color fluorescence experiments revealed significant accumulation of CFSE-labeled carrier cells (Fig. 2C, green fluorescent dye) in the lungs within 30 min of injection, which released VSV-RFP to infect nearby metastases within 12h (Fig. 2C, red). Notably, CFSE-labeled cells were found distributed throughout normal lung tissue, whereas the replication of virus was confined exclusively to tumor nodules (Fig. 2C, white arrows).

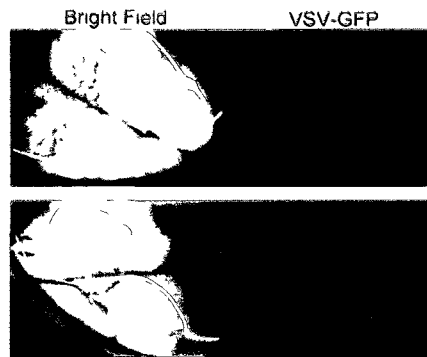
Figure 2.2 Trojan Horse Delivery of Oncolytic VSV to Lung Tumors in Syngeneic Carrier

Cells. (A) Western blot analysis showing timecourse of VSV protein synthesis in CT26 colon carcinoma carrier cells infected *in vitro*. **(B)** Balb/c mice with established CT26 lung tumors were treated IV with 10^6 trojan horse cells infected with VSV-GFP. Mice were euthanized and lungs were imaged under a dissecting microscope at 24h post-treatment. Bright field images (left) show distribution of tumor nodules, while green fluorescent images (right) show localization of viral replication. **(C)** Two-color fluorescent imaging of trojan horse delivery to lung metastases. The cellular fluorochrome CFSE was used to label CT26 trojan horse cells prior to infection with VSV-RFP and subsequent systemic infusion as above. At indicated timepoints mice were sacrificed and lungs were examined under a fluorescent dissecting microscope. Images shown are composites from CFSE (green, cellular label) and RFP (red, virus replication) channels. Lungs were examined under bright field to identify tumor nodules (arrows).

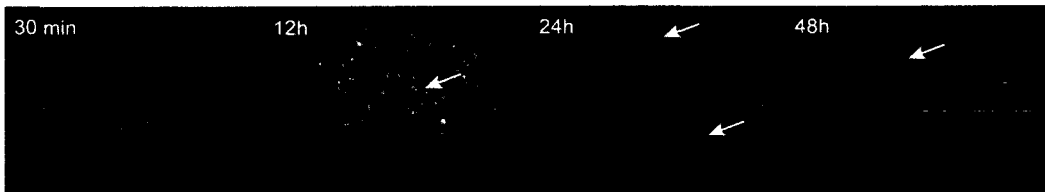
A



B



C



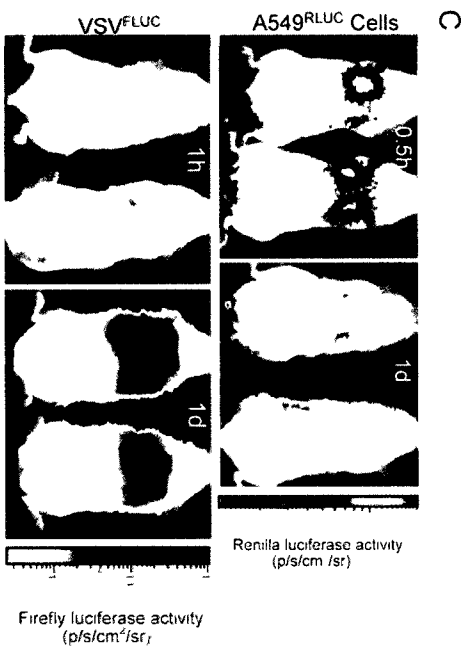
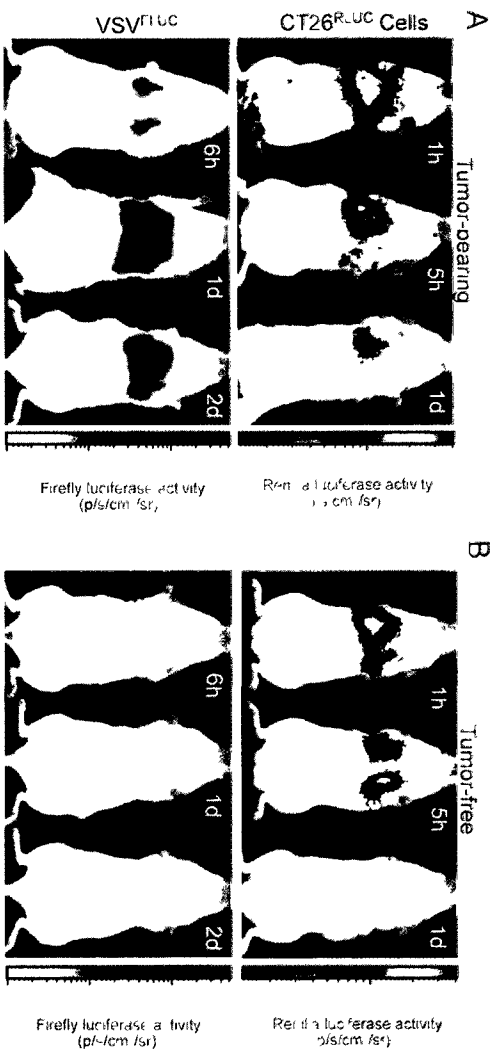
***In vivo* imaging of cell-based delivery**

In order to non-invasively visualize both the distribution of the cellular vehicle and the viral payload delivered *in vivo*, we created a cell line that expresses *Renilla reniformis* luciferase from an integrated cellular gene, CT26^{RLUC}, and a viral strain (VSV^{FLUC}) that expresses *firefly* luciferase from a viral promoter. This allowed us to independently follow the biodistribution of the carrier-cell and virus-associated luciferase enzymes by administering the appropriate substrate to treated mice and imaging bioluminescence with an *in vivo* imaging system (IVIS). Using the IVIS, we observed that syngeneic carrier cells accumulate rapidly in the lungs within the first hour following intravenous infusion, where they remain until releasing virus and undergoing lysis by 24h (Fig. 3A, upper panel). The lung-associated localization was not tumor-specific, as the same pattern was observed in the lungs of tumor-free mice (Fig. 3B upper panel). In contrast, virus-associated *FLUC* activity continued to increase and persisted well after the elimination of carrier cells in tumor-bearing, but not tumor-free lungs (Figs. 3A,B lower panels), confirming the release of virus and tumor-specific replication as detected by fluorescence imaging in the preceding experiments.

Xenogeneic carrier cells mediate systemic delivery of VSV in immune-competent animals

Past experience with cell-based therapies has led to the belief that autologous cells are the preferred source for viral carriers⁷⁴, since unlike histoincompatible allogeneic and xenogeneic cells they are not subject to immune rejection. To test this hypothesis experimentally, we used whole-body imaging to examine the capacity of labeled human A549^{RLUC} carcinoma cells to deliver VSV^{FLUC} to tumors in immune-competent mice. Human

Figure 2.3 Dual-enzyme in vivo luminescence imaging of VSV delivery by autologous and xenogeneic carcinoma cells. (A) Lung tumor-bearing mice were injected IV with 10^6 autologous CT26^{RLUC} carcinoma cells infected with VSV^{FLUC}. **(B)** Tumor-free mice were injected IV with 10^6 autologous CT26^{RLUC} carcinoma cells infected with VSV^{FLUC}. **(C)** Lung tumor-bearing mice were injected IV with 10^6 xenogeneic A549^{RLUC} human carcinoma cells infected with VSV^{FLUC}. At timepoints indicated mice were treated with the appropriate substrate to independently image cell-associated (*RLUC*, rainbow color scale) and virus-associated (*FLUC*, yellow-red color scale) enzyme expression.



carcinoma cells, like their mouse counterparts, accumulated in the lung within the first hour following IV administration and were eliminated by 24h (Fig. 3C, upper panels).

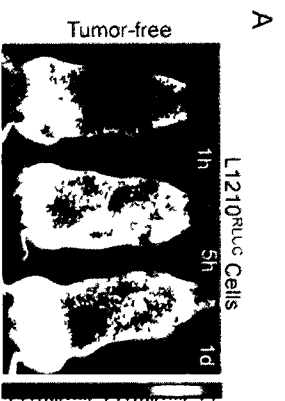
Surprisingly, the xenogeneic cells were equally capable of releasing VSV to infect lung tumors (Fig. 3C, lower panels). Thus cell-mediated delivery of VSV can be achieved using immunologically incompatible cells of allogeneic or xenogeneic background.

Leukemic carrier cells deliver VSV to disseminated tumor sites

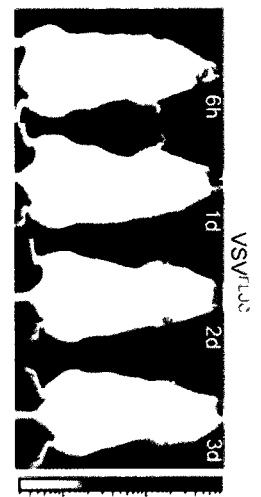
Although murine and human carcinoma cell lines efficiently delivered and released VSV to tumor cells *in vivo*, their apparent accumulation within lung microcapillaries prompted us to investigate whether a cell line derived from a hematological malignancy might more readily distribute throughout the circulatory system upon intravenous administration. In sharp contrast to carcinoma cells, a murine leukemia cell line (L1210^{RLUC}) showed a much more disseminated pattern of delivery following intravenous administration, with *RLUC*-tagged cells detectable not only in the lungs, but also throughout the abdominal cavity and lymphoid organs (Fig. 4A,B left panels). Infected L1210^{RLUC} cells retained the ability to deliver VSV^{FLUC} to lung tumors (Fig. 4B, right) and were also able to bypass the lung and deliver virus to subcutaneous tumors located on the hind flank of mice (Fig. 4C). As observed with carcinoma carriers, replication of VSV^{FLUC} was confined to carrier cells following injection into tumor-free mice, with no detectable replication persisting in normal tissues. Therefore leukemic carrier cells appear to be less restricted in their passage through the circulatory system and can disseminate virus to diverse anatomical locations.

Figure 2.4 Dual-enzyme *in vivo* luminescence imaging of VSV delivery by murine leukemia

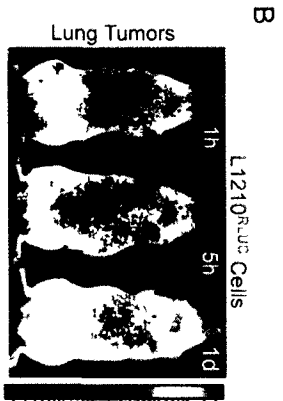
cells. (A) Tumor-free mice were injected IV with 10^6 murine L1210^{RLUC} cells infected with VSV^{FLUC}. (B) Lung tumor-bearing mice were injected IV with 10^6 murine L1210^{RLUC} cells infected with VSV^{FLUC}. (C) Subcutaneous tumor-bearing mice were injected IV with 10^6 murine L1210^{RLUC} cells infected with VSV^{FLUC}. At timepoints indicated mice were treated with the appropriate substrate to image cell-associated (*RLUC*, rainbow color scale) or virus-associated (*FLUC*, yellow-red color scale) enzyme expression.



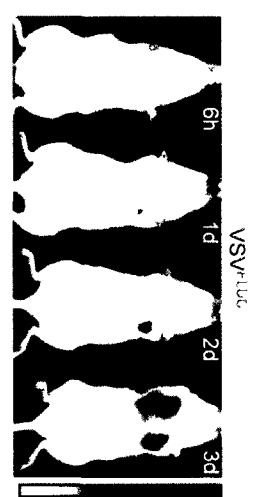
Renilla luciferase activity (p/s/cm /sr)



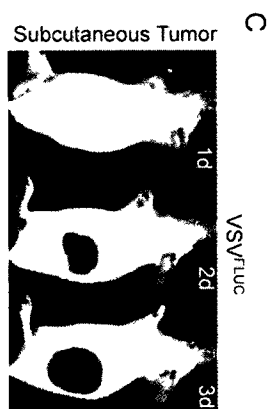
Firefly luciferase activity (p/s/cm /sr)



Renilla luciferase activity (p/s/cm /sr)



Firefly luciferase activity (p/s/cm /sr)



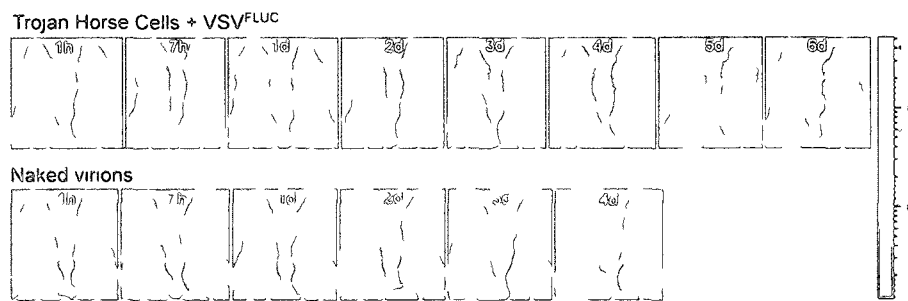
Firefly luciferase activity (p/s/cm /sr)

Immune evasion by cell-based delivery of VSV

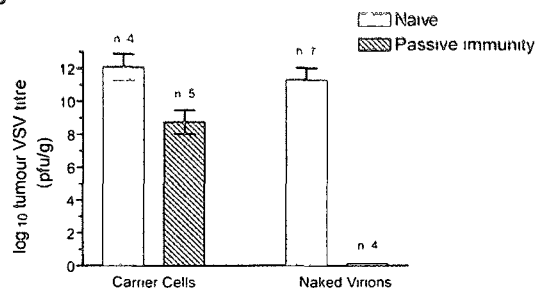
Given the effective systemic delivery achievable using cellular carriers, we asked whether this approach could protect a therapeutic dose of VSV from the detrimental effects of anti-viral antibodies. Administration of naked VSV^{FLUC} particles to mice did not lead to detectable infection of lung tumors when anti-VSV antibodies were present (Fig. 5A, lower panel). A transient, low-level of replication was detected only in the spleen at 7h. In contrast, carrier cells could bypass circulating antibody to reach the lungs and transfer virus to pre-existing tumor cells, with robust viral infection persisting for up to 6 days post-injection (Fig. 5A, upper panel). In a separate experiment, quantitative titers of virus were undetectable in lung tumors 24h following administration of naked virions to mice with pre-existing humoral immunity, whereas tumors treated with infected cells contained on the order of 10^9 virus particles, despite the presence of circulating antibodies (Figs. 5 B). Consistent with the ablation of viral delivery, mice with pre-existing immunity to VSV show no therapeutic response to multiple systemic doses of naked virions, succumbing to extensive tumor burden within the same time period (15d) as saline-treated controls (Fig. 5C). However administration of VSV-infected carrier cells could induce significant tumor regression (Fig. 5C, right). On autopsy we observed clearance of nearly all tumor nodules from the lungs and only one small residual nodule that had presumably escaped infection (white arrow). These data indicate that carrier cells can enable systemic VSV delivery and tumor oncolysis despite the presence of virus-neutralizing humoral immunity.

Figure 2.5 Cell-mediated systemic delivery and anti-tumor activity of VSV in the presence of circulating antibody (A) Mice were injected IP with immune serum containing antibodies against VSV and treated with VSV in carrier cells (upper panels) or as naked virions (lower panels). Mice were injected with luciferin and imaged at the indicated timepoints. **(B)** Quantitation of VSV in subcutaneous tumors 24h following IV administration of infected carrier cells or naked virions in the presence (shaded bars) or absence (hatched bars) of circulating anti-viral antibodies. Mean \log_{10} tumor titers \pm SD are plotted. **(C)** Post-mortem images of lung metastases following IV repeated administration of either saline (PBS), 5×10^8 naked VSV virions, or 10^6 VSV-infected carrier cells (3 doses/week over 4 weeks) in mice with pre-existing anti-viral immunity.

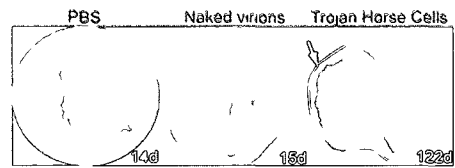
A



B



C

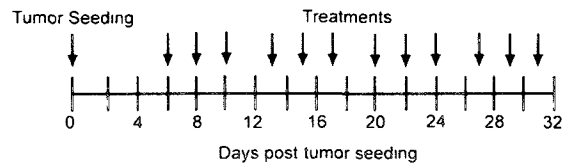


Enhanced efficacy of systemic therapy with repeated administration of VSV-infected cells

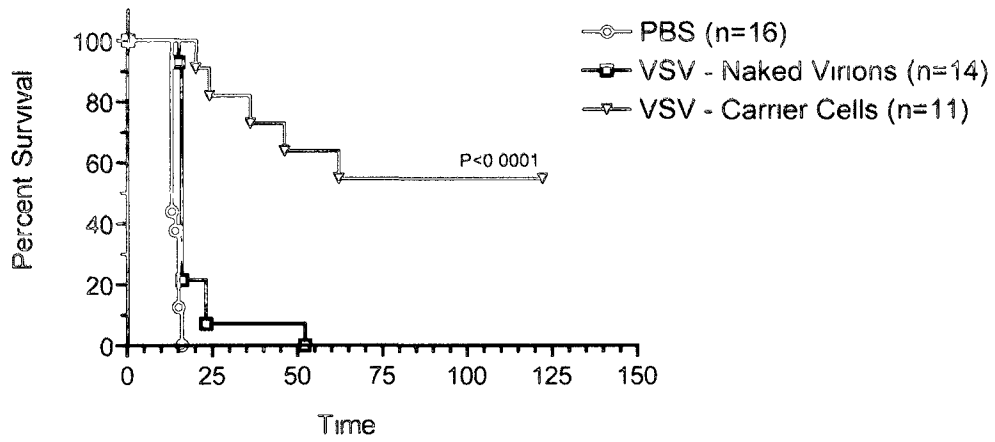
We next examined whether the cell-based delivery approach could enhance the therapeutic efficacy of a clinically-relevant dosing regimen in an animal tumor model. Since VSV is not a common pathogen in humans, patients are likely to be immunological naïve at the outset of therapy, but repeat virus doses will be exposed to an evolving adaptive response. We therefore chose to compare the anti-tumor efficacy of multiple VSV doses administered as naked virions or within infected carrier cells to initially naïve, but immune-competent mice with pre-established lung tumors. In this highly aggressive model of disease, saline-treated controls rapidly succumb to disease within 14 days due to the invasion of normal lung tissue by hundreds of metastatic tumor nodules (Fig 6B, -○-, 6c upper-left). We have previously shown that delivery of a single dose of VSV directly to the lungs via intranasal instillation induces lasting disease regression in this model⁶¹. However, repeated intravenous infusion of VSV particles has only a modest effect on tumor progression (Figs. 6B, , 6C upper-right), presumably since delivery to all tumor nodules is not achieved before continued dosing is rendered ineffective by the onset of humoral immunity (Fig. 1). In contrast, 12 administrations of VSV-infected carrier cells led to lasting cures in the majority of mice and significantly increased survival in all others (Fig. 6B ▽, 6C lower-left). These results suggest that hiding oncolytic virus within carrier cells during delivery can greatly increase the cumulative therapeutic benefit of systemic dosing regimens in the face of evolving anti-viral immunity.

Figure 2.6 Enhancement of systemic therapy with VSV delivered in carrier cells. Tumors were seeded in balc/c mice at day 0 by IV injection of 3×10^5 CT26 cells. Beginning at day 6, mice were treated IV with either saline (PBS), 5×10^8 pfu VSV as naked virions or 10^6 VSV-infected syngeneic carrier cells. Animals were dosed 3 days/week for 4 weeks as shown in **(A)** or until reaching tumor burden endpoints as plotted in **(B)**. **(C)** Representative photographs of lung tumor burdens at experimental endpoints for each treatment group.

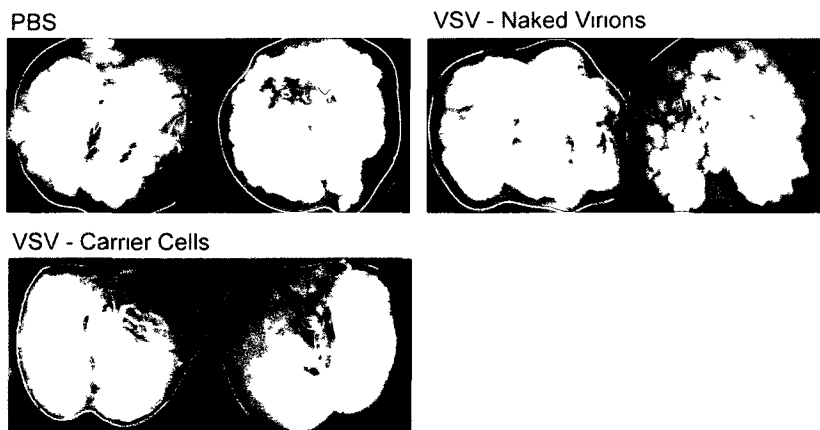
A



B



C



DISCUSSION

The adaptive immune system, evolved over millions of years to defend animals from invading pathogens, is a serious impediment to the prospect of using viruses as systemic therapeutics. We have shown that circulating antibodies elicited against an oncolytic strain of VSV in immune-competent animals are sufficient to ablate delivery of naked virions to tumors. However infected “trojan horse” cells conceal VSV from the host immune system to bypass this obstacle. Many oncolytic viruses are potent anti-tumor agents when directly injected into tumors⁷⁵⁻⁷⁸, but vulnerability to host defenses complicates their administration as systemic therapeutics. Serum factors such as complement proteins and antibodies can bind to and inactivate virus^{53, 54, 57-60}, whereas organ sinks such as the liver can remove it from the circulation altogether^{55, 56}. Excessive uptake of virus by the liver can also be responsible for toxic side-effects following systemic administration⁷⁹. The use of carrier cells to shield virions from systemic defenses thus offers a simple solution to the key problems associated with delivering VSV and other viral therapeutics to disseminated tumor sites.

We have shown that multiple doses of VSV administered systemically within carrier cells can induce complete disease regression in a lung model (Figure 6B,C) while a single dose cannot (data not shown). In contrast, even multiple doses of IV-injected naked VSV virions were largely ineffective in this model (Figure 6B,C). These findings indicate that stealth delivery contributes to the overall efficacy of multiple-dosing with VSV-laden carrier cells administered in the face of an evolving anti-viral immune response. It will be important in future studies to determine whether an immune response is mounted against the carrier

cell vehicle itself, and whether this has any effect on virus delivery. On the other hand, the immunogenicity of carrier cells may enhance therapy, since the activation of anti-tumor immunity during virotherapy appears to contribute some degree to eliminating tumors and may help to protect from disease recurrence. Indeed, HSV⁸⁰ and VSV (data not shown) appear to invoke cell-based anti-tumor responses in addition to killing malignant cells by direct infection and oncolysis. In similar fashion, tumor cells infected with Newcastle disease virus and injected into tumor-bearing animals have also been reported to activate anti-tumor immunity⁸¹. Thus the destruction of tumors by oncolytic viruses, whether administered as naked virions or within infected cells, is likely achieved through multiple mechanisms. Significant effort is now being made in our lab to understand how these mechanisms contribute to the overall potency of oncolytic virus therapy with these different delivery approaches.

The possibility of seeding *de novo* tumor growth is an important safety consideration if transformed cells are to be used as systemic therapeutics. To ensure that cells do not persist to form tumors, Coukos et al. have shown that HSV-infected carriers can be lethally irradiated prior to administration⁶⁷. Similarly, we have observed that the production of VSV is unimpaired by irradiation of infected cells (data not shown), and are currently investigating whether they retain the ability to deliver virus *in vivo*. Alternatively, allogeneic or xenogeneic carrier cells such as those described here would be eliminated by the patient's own immune system following virus delivery, avoiding the need for any special manipulation of carrier cells prior to administration. Inducible suicide programs could also be engineered into carrier cell lines to ensure they do not persist following injection into

the body. Combining these types of safeguards should ensure the safety of transformed cells lines for clinical administration, a tremendous advance over the use of autologous tumor^{66, 67} or normal cells^{68, 69, 71} since the former are renewable, rapidly propagated to large quantities and generally more permissive to oncolytic virus infection.

Previous studies have clearly demonstrated efficient delivery of therapeutic viruses to lung tumors^{66, 82}. and we have shown here that certain cell types, particularly those derived from solid tumors, accumulate rapidly and exclusively within the lungs, the site of the first microcapillary bed encountered following intravenous injection. While such a vehicle could be useful for delivering virus specifically to the tumor site in patients with primary or metastatic disease localized to the lung, it is clear that carrier cells must be capable of bypassing lung capillaries to reach metastases found at other anatomical locations. Blood cells normally traffic throughout the circulation and our studies suggest that they may be the ideal vehicle for delivering virus to disseminated sites. We found that a leukemia cell line was able to largely bypass the lungs and could deliver VSV to more distally-located tumors. Similarly, previous studies have established that leukocyte-derived CIK cells can deliver oncolytic vaccinia virus to hind flank tumors upon intravenous administration⁶⁹. The small size of leukocyte-derived carriers is likely a crucial parameter that facilitates their passage through blood vessels to achieve this widespread dissemination, although other factors such as structural rigidity⁸³, chemotactic responses⁸⁴ and adhesion molecule expression⁸⁵ are also known to influence blood cell circulation.

A live-cell carrier for therapeutic delivery is an attractive alternative to the various chemicals that can be used to encapsulate virions⁸⁶⁻⁹¹. Infected-cell carriers have the

unique ability to produce a burst of virus upon delivery to the tumor site, thereby amplifying the effective therapeutic dose by several orders of magnitude. In addition, the cell can be engineered to have limited or no innate anti-viral response thus increasing the output of therapeutic virus at the target site. Carrier cells could be made to express tumor antigens on their surface in the ideal context to stimulate immunity or perhaps surface molecules to facilitate retention in tumor beds. Our results suggest that an immortalized cell line of hematological origin could be an ideal foundation for constructing custom-built biotherapeutic vehicles with the potential to significantly enhance the delivery, selectivity and anti-tumor efficacy of systemic virotherapy.

MATERIALS AND METHODS

Viruses

The recombinant AV3 strain of VSV with an attenuating deletion of methionine 51 of the matrix protein and a transgene encoding eGFP⁶¹, RFP or eGFP-luciferase (see below) were propagated in Vero cells. Virions were purified from cell culture supernatants by passage through a 0.2um Steritop filter (Millipore) and centrifugation at 30,000 x g prior to resuspension in phosphate-buffered saline (Hyclone) for all animal studies.

Construction and Rescue of Recombinant VSV Strains

Two additional recombinant VSV genomes were generated by insertion of either the mRFP1⁹² or EGFPLuc (Clontech) reporter genes and rescued as described previously⁶¹.

Rescued viruses were propagated and purified as above.

Lentiviral transductions

A bicistronic lentivector was rescued by insertion of the *Renilla reniformis* luciferase gene (pGL3 R2.1, Promega) into the PmeI restriction site downstream from the EMCV IRES-driven GFP marker in pWPI and used to transduce target cell lines as described elsewhere⁹³. FACS sorting based on GFP expression yielded a population consisting of >90% transduced cells.

Cell Lines

Murine CT26 colon carcinoma, human A549 lung carcinoma, and L1210 murine leukemia cell lines (American Type Tissue Collection) were propagated in Dulbecco's Modified Eagle's Medium (Hyclone) supplemented with 10% fetal calf serum (Cansera).

Serum Neutralizing Antibody Assay

Two-fold serial dilutions of mouse serum were incubated with 300 pfu of VSV in a total volume of 60 ul for 90 min at 37°C and applied to Vero cell monolayers in a 96-well plate. Wells were examined for cytopathic effects (CPE) 48h post-inoculation. Neutralizing titer was taken as the highest dilution factor of serum that prevented the appearance of CPE.

Passive Immunizations

Serum was collected from donor mice 6 weeks following IV immunization with 5×10^8 pfu of VSV. Recipients were injected IP with 100ul immune serum 24h prior to therapeutic administration of VSV.

T Cell Purification and Adoptive Transfer

Single-cell suspensions of splenocytes from donor mice were purified on a MACS column using a Pan T Cell Isolation Kit (Miltenyi Biotec) to obtain an enriched population of untouched T cells. Each recipient was injected IV with a single spleen equivalent of purified T cells 24h prior to treatment with VSV.

Mice and Tumor Models

Female, 8-10 week old balb/c mice were obtained from Charles River Laboratories, and injected IV with 3×10^5 CT26 cells to establish lung tumors, or injected subcutaneously with 10^6 CT26 cells to establish hind flank tumors. Animals bearing lung tumors were euthanized upon signs of severe respiratory distress. All experiments were conducted with the approval of the University of Ottawa Animal Care and Veterinary Service.

***In vivo* imaging**

Mice were injected with either native coelenterazine (NanoLight Technology) (40ul IV at 1 mg/mL in 50% v/v methanol/PBS) to image *Renilla* luciferase activity, or d-luciferin (Molecular Imaging Products Company) (200ul IP at 10 mg/mL in PBS) for *Firefly* luciferase imaging. Mice were anesthetized under 3% isoflurane (Baxter Corp.) and imaged with the IVIS 200 Series Imaging System (Xenogen). Data acquisition and analysis was performed using Living Image v2.5 software. For each experiment, images were captured under identical exposure, aperture and pixel binning settings and bioluminescence is plotted on identical color scales.

Infection of carrier cells

Cells were infected at an MOI of 10 at 37°C for 2.5h, harvested (adherent lines were detached with 0.05% Trypsin-EDTA), washed to remove cell-free virions, and resuspended at a concentration of 10^7 cells/mL in PBS before intravenous tail-vein injection into mice at 3h post-infection (10^6 cells/mouse in 100ul). For fluorescent imaging experiments, cells

were stained with 5uM carboxyfluorescein succinimidyl ester (Molecular Probes) for 30min prior to infection following the manufacturer's protocol.

Fluorescent imaging

Mice were euthanized and tumors were examined using a Leica MZFLIII dissecting microscope with a standard GFP filter set. Images were captured with a Nikon Coolpix 100 camera. Overlays were generated using Adobe Photoshop CS v8.0 software.

Western blot detection of VSV proteins

Cell lysates were collected in 4% SDS sample buffer, run on a NuPAGE Bis-Tris 4-12% polyacrylamide gel, transferred to a nitrocellulose membrane and probed with polyclonal anti-VSV serum from hyperimmune rabbits.

Quantitation of VSV infection in tumors

Tumors were excised from euthanized mice and homogenized in PBS. The extent of VSV infection was measured either by plaque assay on Vero cells or luciferase assay (Promega) read on a luminometer (EG&G Berthold Lumat LB9507).

ACKNOWLEDGMENTS

This work was supported by a Terry Fox Program Project Grant and the National Cancer Institute of Canada. A.T.P. was supported by an Ontario Graduate Scholarship in Science and Technology and the Ottawa Health Research Institute. J.W. was supported by a Lymphoma Research Foundation of Canada Research Fellowship.

REFERENCES

1. Parato, K. A., Senger, D., Forsyth, P. A., and Bell, J. C. (2005). Recent progress in the battle between oncolytic viruses and tumours. *Nat.Rev.Cancer*. **5**: 965-976.
2. Ikeda, K., Ichikawa, T., Wakimoto, H., Silver, J. S., Deisboeck, T. S., Finkelstein, D., Harsh, G. R., Louis, D. N., Bartus, R. T., Hochberg, F. H., and Chiocca, E. A. (1999). Oncolytic virus therapy of multiple tumors in the brain requires suppression of innate and elicited antiviral responses. *Nat.Med*. **5**: 881-887.
3. Wakimoto, H., Ikeda, K., Abe, T., Ichikawa, T., Hochberg, F. H., Ezekowitz, R. A., Pasternack, M. S., and Chiocca, E. A. (2002). The complement response against an oncolytic virus is species-specific in its activation pathways. *Mol.Ther*. **5**: 275-282.
4. Worgall, S., Wolff, G., Falck-Pedersen, E., and Crystal, R. G. (1997). Innate immune mechanisms dominate elimination of adenoviral vectors following in vivo administration. *Hum.Gene Ther*. **8**: 37-44.
5. Ye, X., Jerebtsova, M., and Ray, P. E. (2000). Liver bypass significantly increases the transduction efficiency of recombinant adenoviral vectors in the lung, intestine, and kidney. *Hum.Gene Ther*. **11**: 621-627.
6. Hirasawa, K., Nishikawa, S. G., Norman, K. L., Coffey, M. C., Thompson, B. G., Yoon, C. S., Waisman, D. M., and Lee, P. W. (2003). Systemic reovirus therapy of metastatic cancer in immune-competent mice. *Cancer Res*. **63**: 348-353.
7. Lang, S. I., Giese, N. A., Rommelaere, J., Dinsart, C., and Cornelis, J. J. (2006). Humoral immune responses against minute virus of mice vectors. *J.Gene Med*.
8. Chen, Y., Yu, D. C., Charlton, D., and Henderson, D. R. (2000). Pre-existent adenovirus antibody inhibits systemic toxicity and antitumor activity of CN706 in the nude mouse LNCaP xenograft model: implications and proposals for human therapy. *Hum.Gene Ther*. **11**: 1553-1567.
9. Tsai, V., Johnson, D. E., Rahman, A., Wen, S. F., LaFace, D., Philopena, J., Nery, J., Zepeda, M., Maneval, D. C., Demers, G. W., and Ralston, R. (2004). Impact of

human neutralizing antibodies on antitumor efficacy of an oncolytic adenovirus in a murine model. *Clin.Cancer Res.* **10**: 7199-7206.

10. Stojdl, D. F., Lichty, B. D., tenOever, B. R., Paterson, J. M., Power, A. T., Knowles, S., Marius, R., Reynard, J., Poliquin, L., Atkins, H., Brown, E. G., Durbin, R. K., Durbin, J. E., Hiscott, J., and Bell, J. C. (2003). VSV strains with defects in their ability to shutdown innate immunity are potent systemic anti-cancer agents. *Cancer Cell.* **4**: 263-75.
11. Ebert, O., Harbaran, S., Shinozaki, K., and Woo, S. L. (2004). Systemic therapy of experimental breast cancer metastases by mutant vesicular stomatitis virus in immune-competent mice. *Cancer Gene Ther.*
12. Ahmed, M., Cramer, S. D., and Lyles, D. S. (2004). Sensitivity of prostate tumors to wild type and M protein mutant vesicular stomatitis viruses. *Virology.* **330**: 34-49.
13. Obuchi, M., Fernandez, M., and Barber, G. N. (2003). Development of recombinant vesicular stomatitis viruses that exploit defects in host defense to augment specific oncolytic activity. *J.Virol.* **77**: 8843-8856.
14. Gobet, R., Cerny, A., Ruedi, E., Hengartner, H., and Zinkernagel, R. M. (1988). The role of antibodies in natural and acquired resistance of mice to vesicular stomatitis virus. *Exp Cell Biol.* **56**: 175-80.
15. Garcia-Castro, J., Martinez-Palacio, J., Lillo, R., Garcia-Sanchez, F., Alemany, R., Madero, L., Bueren, J. A., and Ramirez, M. (2005). Tumor cells as cellular vehicles to deliver gene therapies to metastatic tumors. *Cancer Gene Ther.* **12**: 341-349.
16. Coukos, G., Makrigiannakis, A., Kang, E. H., Caparelli, D., Benjamin, I., Kaiser, L. R., Rubin, S. C., Albelda, S. M., and Molnar-Kimber, K. L. (1999). Use of carrier cells to deliver a replication-selective herpes simplex virus-1 mutant for the intraperitoneal therapy of epithelial ovarian cancer. *Clin.Cancer Res.* **5**: 1523-1537.
17. Komarova, S., Kawakami, Y., Stoff-Khalili, M. A., Curiel, D. T., and Pereboeva, L. (2006). Mesenchymal progenitor cells as cellular vehicles for delivery of oncolytic adenoviruses. *Mol.Cancer Ther.* **5**: 755-766.

18. Thorne, S. H., Negrin, R. S., and Contag, C. H. (2006). Synergistic antitumor effects of immune cell-viral biotherapy. *Science*. **311**: 1780-1784.
19. Raykov, Z., Balboni, G., Aprahamian, M., and Rommelaere, J. (2004). Carrier cell-mediated delivery of oncolytic parvoviruses for targeting metastases. *Int.J.Cancer*. **109**: 742-749.
20. Jevremovic, D., Gulati, R., Hennig, I., Diaz, R. M., Cole, C., Kleppe, L., Cosset, F. L., Simari, R. D., and Vile, R. G. (2004). Use of blood outgrowth endothelial cells as virus-producing vectors for gene delivery to tumors. *Am.J.Physiol Heart Circ.Physiol*. **287**: H494-H500.
21. Crittenden, M., Gough, M., Chester, J., Kottke, T., Thompson, J., Ruchatz, A., Clackson, T., Cosset, F. L., Chong, H., Diaz, R. M., Harrington, K., Alvarez, Vallina L., and Vile, R. (2003). Pharmacologically regulated production of targeted retrovirus from T cells for systemic antitumor gene therapy. *Cancer Res*. **63**: 3173-3180.
22. Raykov, Z., Balboni, G., Aprahamian, M., and Rommelaere, J. (2004). Carrier cell-mediated delivery of oncolytic parvoviruses for targeting metastases. *Int.J.Cancer*. **109**: 742-749.
23. Harrington, K., Alvarez-Vallina, L., Crittenden, M., Gough, M., Chong, H., Diaz, R. M., Vassaux, G., Lemoine, N., and Vile, R. (2002). Cells as vehicles for cancer gene therapy: the missing link between targeted vectors and systemic delivery? *Hum.Gene Ther*. **13**: 1263-1280.
24. Mineta, T., Rabkin, S. D., Yazaki, T., Hunter, W. D., and Martuza, R. L. (1995). Attenuated multi-mutated herpes simplex virus-1 for the treatment of malignant gliomas. *Nat.Med*. **1**: 938-943.
25. Bischoff, J. R., Kirn, D. H., Williams, A., Heise, C., Horn, S., Muna, M., Ng, L., Nye, J. A., Sampson-Johannes, A., Fattaey, A., and McCormick, F. (1996). An adenovirus mutant that replicates selectively in p53-deficient human tumor cells. *Science*. **274**: 373-376.
26. Coffey, M. C., Strong, J. E., Forsyth, P. A., and Lee, P. W. (1998). Reovirus therapy of tumors with activated Ras pathway. *Science*. **282**: 1332-1334.

27. Grote, D., Russell, S. J., Cornu, T. I., Cattaneo, R., Vile, R., Poland, G. A., and Fielding, A. K. (2001). Live attenuated measles virus induces regression of human lymphoma xenografts in immunodeficient mice. *Blood*. **97**: 3746-3754.
28. Wakimoto, H., Ikeda, K., Abe, T., Ichikawa, T., Hochberg, F. H., Ezekowitz, R. A., Pasternack, M. S., and Chiocca, E. A. (2002). The complement response against an oncolytic virus is species-specific in its activation pathways. *Mol. Ther.* **5**: 275-282.
29. Schiedner, G., Bloch, W., Hertel, S., Johnston, M., Molojavyi, A., Dries, V., Varga, G., Van Rooijen, N., and Kochanek, S. (2003). A hemodynamic response to intravenous adenovirus vector particles is caused by systemic Kupffer cell-mediated activation of endothelial cells. *Hum. Gene Ther.* **14**: 1631-1641.
30. Hummel, J. L., Safroneeva, E., and Mossman, K. L. (2005). The role of ICP0-Null HSV-1 and interferon signaling defects in the effective treatment of breast adenocarcinoma. *Mol. Ther.* **12**: 1101-1110.
31. Plaksin, D., Porgador, A., Vadai, E., Feldman, M., Schirmacher, V., and Eisenbach, L. (1994). Effective anti-metastatic melanoma vaccination with tumor cells transfected with MHC genes and/or infected with Newcastle disease virus (NDV). *Int. J. Cancer*. **59**: 796-801.
32. Cole, C., Qiao, J., Kottke, T., Diaz, R. M., Ahmed, A., Sanchez-Perez, L., Brunn, G., Thompson, J., Chester, J., and Vile, R. G. (2005). Tumor-targeted, systemic delivery of therapeutic viral vectors using hitchhiking on antigen-specific T cells. *Nat. Med.* **11**: 1073-1081.
33. Skalak, R. and Branemark, P. I. (1969). Deformation of red blood cells in capillaries. *Science*. **164**: 717-719.
34. Stein, J. V. and Nombela-Arrieta, C. (2005). Chemokine control of lymphocyte trafficking: a general overview. *Immunology*. **116**: 1-12.
35. Carlos, T. M. and Harlan, J. M. (1994). Leukocyte-endothelial adhesion molecules. *Blood*. **84**: 2068-2101.
36. Fisher, K. D., Stallwood, Y., Green, N. K., Ulbrich, K., Mautner, V., and Seymour, L. W. (2001). Polymer-coated adenovirus permits efficient retargeting and evades neutralising antibodies. *Gene Ther.* **8**: 341-348.

37. O'Riordan, C. R., Lachapelle, A., Delgado, C., Parkes, V., Wadsworth, S. C., Smith, A. E., and Francis, G. E. (1999). PEGylation of adenovirus with retention of infectivity and protection from neutralizing antibody in vitro and in vivo. *Hum. Gene Ther.* **10**: 1349-1358.
38. Chillon, M., Lee, J. H., Fasbender, A., and Welsh, M. J. (1998). Adenovirus complexed with polyethylene glycol and cationic lipid is shielded from neutralizing antibodies in vitro. *Gene Ther.* **5**: 995-1002.
39. Matthews, C., Jenkins, G., Hilfinger, J., and Davidson, B. (1999). Poly-L-lysine improves gene transfer with adenovirus formulated in PLGA microspheres. *Gene Ther.* **6**: 1558-1564.
40. Pearce, O. M., Fisher, K. D., Humphries, J., Seymour, L. W., Smith, A., and Davis, B. G. (2005). Glycoviruses: chemical glycosylation retargets adenoviral gene transfer. *Angew. Chem. Int. Ed Engl.* **44**: 1057-1061.
41. Green, N. K., Herbert, C. W., Hale, S. J., Hale, A. B., Mautner, V., Harkins, R., Hermiston, T., Ulbrich, K., Fisher, K. D., and Seymour, L. W. (2004). Extended plasma circulation time and decreased toxicity of polymer-coated adenovirus. *Gene Ther.* **11**: 1256-1263.
42. Campbell, R. E., Tour, O., Palmer, A. E., Steinbach, P. A., Baird, G. S., Zacharias, D. A., and Tsien, R. Y. (2002). A monomeric red fluorescent protein. *Proc. Natl. Acad. Sci. U.S.A.* **99**: 7877-7882.
43. Naldini, L., Blomer, U., Gallay, P., Ory, D., Mulligan, R., Gage, F. H., Verma, I. M., and Trono, D. (1996). In vivo gene delivery and stable transduction of nondividing cells by a lentiviral vector. *Science.* **272**: 263-267.

CHAPTER 3: PROGRAMMABLE INSECT CELL CARRIERS FOR SYSTEMIC DELIVERY OF INTEGRATED CANCER BIOTHERAPY

Power A.T.^{1,2}, LeBoeuf F.¹, Roy D.^{1,2}, Breton, S.^{1,2}, Falls T.¹, Ferreira L.¹, McCart J.A.,³
Kirn, D.H.⁴, Stojdl D.F.^{2,5}, Lichty, B.D.⁶, Atkins H.¹, Bell J.C.^{1,2}

¹Centre for Cancer Therapeutics, Ottawa Hospital Research Institute, Ottawa, Ontario, Canada; ²Department of Biochemistry, Microbiology and Immunology, University of Ottawa, Ottawa, Ontario, Canada; ³Division of Experimental Therapeutics, Toronto General Research Institute, Toronto, Canada; ⁴Jennerex Inc., San Francisco, California, USA; ⁵Apoptosis Research Center, Children's Hospital of Eastern Ontario, Ottawa, Ontario, Canada; ⁶Department of Pathology and Molecular Medicine, Centre for Gene Therapeutics, Michael DeGroote Centre for Learning and Discovery McMaster University, Ottawa, Ontario, Canada

To whom correspondence should be addressed:

John C. Bell, PhD.

Office: 613-737-7700 ext 70333, Cell: 613-286-2396; jbelle@ohri.ca

Keywords: oncolytic viruses, cancer therapeutics, biotherapeutics, biotherapy, gene delivery, cell delivery, cell carriers, virotherapy, systemic delivery, molecular engineering, insect cell expression

Contribution of Authors: AT Power performed all experiments with the exceptions noted, created all figures and wrote the manuscript with review by JC Bell. AT Power and JC Bell designed all experiments. Fabrice LeBoeuf provided VVdd-mCherry stocks, established the HT29 tumor model and helped design vaccinia immunomodulator and HT29 experiments. D. Roy performed the *in vitro* supernatant transfer experiments and doubly-armed insect cell carrier infections of tumor cell monolayers, with the guidance and protocols established by AT Power. F. LeBoeuf generated the recombinant VVdd-mCherry virus with help from S. Breton. T. Falls provided technical support for all animal experiments. L. Ferreira provided technical support with intravenous injections and performed the animal component of the circulatory half-life experiments. B. Lichty provided insect cell stocks. AT Power performed IVIS imaging experiments with equipment provided by the lab of D. Stojdl. H. Atkins contributed leukemia cell lines and helpful suggestions concerning their experimental use.

Submitted: Nature Biotechnology. Jan 15, 2010.

ABSTRACT

Due to cancer's genetic complexity, significant advances in the treatment of metastatic disease will require sophisticated, multi-pronged therapeutic approaches. Here we demonstrate the utility of a *Drosophila melanogaster* cell platform for the production and *in vivo* delivery of multi-gene biotherapeutic systems. We show that cultured *Drosophila* S2 cell carriers can stably propagate oncolytic viral therapeutics that are highly cytotoxic for mammalian cancer cells without adverse effects on insect cell viability or gene expression. These transporters can be modified to express banks of biotherapeutics with complementary activities that enhance anti-tumour activity. *Drosophila* cell carriers administered systemically to immunocompetent animals efficiently trafficked to tumors to deliver multiple biotherapeutics with little apparent off-target tissue homing or toxicity. Cells of this *Dipteran* invertebrate provide a genetically tractable platform supporting the integration of complex, multi-gene biotherapies while avoiding many of the barriers to systemic administration of mammalian cell carriers.

INTRODUCTION

The advent of high throughput sequencing and the molecular biology revolution has provided a rich library of biological parts with vast potential for technological application.

With this tool box of information it is now possible to create an integrated biological platform in which multiple genetically encoded therapeutics can be delivered as a single agent. Most efforts to date have relied on the simplicity of viruses or microbial cells to assemble multi-gene biosynthetic pathways^{1, 2}, sophisticated regulatory circuits^{3, 4} and minimal or synthetic genomes.^{5, 6} However, a standardized cell platform that can be programmed for the production and delivery of active biotherapeutics is currently lacking.

Genetically-encoded biotherapeutics with naturally evolved activities can be harnessed for the treatment of disease. In particular, proteins with the ability to regulate cell growth, modulate the host immune system or recognize tumor-specific antigens are of interest in the treatment of cancer. Although many tested agents demonstrate highly specific therapeutic effects when inoculated or expressed directly in tumors, they often lose potency when administered systemically due to poor stability in blood and/or rapid clearance from the circulation⁷. Incorporation of biotherapeutic genes into viral vectors can help to increase the efficiency of delivery to the tumor site. In particular, conditionally replicating oncolytic viruses (OVs) can be delivered systemically to tumors where they rapidly self-amplify to manufacture the therapeutic transgene specifically at the site of disease⁸. Host immunity remains a major challenge to the clinical realization of this goal⁹⁻¹¹.

We have recently demonstrated that cellular carriers can shield oncolytic virus from neutralization to achieve systemic delivery to tumors in the presence of circulating

antibodies¹⁰. Our group and others have investigated the ability of numerous mammalian cell types to function as oncolytic virus carriers for systemic therapy in pre-clinical models, including solid^{10, 12} and hematogenous^{10, 13} cell lines, cytokine-induced killer cells¹⁴, T cells^{15, 16}, primary monocytes¹⁷, and mesenchymal stem cells¹⁸⁻²⁰. However there remain significant obstacles to using any mammalian cell type for systemic oncolytic virus delivery in the clinical setting. Adherent solid tumor cells and mesenchymal stem cells are unable to traverse capillary beds and generally arrest within the vessels of the first organ they encounter^{10, 20}, while leukocyte-based carriers are able to re-circulate but still exhibit receptor-mediated homing to lymphoid organs and bone marrow^{10, 21, 22}. Thus interactions between mammalian carrier cells and off-target host tissues interfere with systemic tumor targeting. Secondly, primary cell types are often cumbersome to isolate and culture, while systemic administration of permanent cell lines carries the risk of tumorigenicity. Finally, OV infection is by design cytotoxic to mammalian host cells. This precludes the opportunity to genetically modify virus-laden carriers and complicates clinical delivery.

In order to move beyond the limitations of mammalian cells, we have investigated the potential of Dipteran insect cells as novel vehicles for systemic biotherapeutic delivery. Notably, established *Drosophila melanogaster* cell lines supported continuous propagation of multi-gene oncolytic virotherapeutics normally cytotoxic to mammalian cells, enabling the simultaneous production of secondary biotherapeutic gene products. Systemically-administered insect cell carriers were well tolerated, circulated extensively with little off-target tissue homing, and effectively delivered oncolytic virus to tumors in immunocompetent animals. Established *D. melanogaster* cell lines therefore offer a

genetically-tractable platform suitable for systemic delivery of multiple integrated biotherapies.

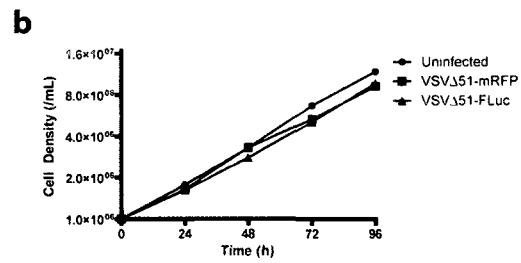
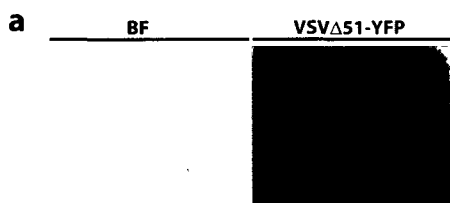
RESULTS

Establishment of Continuous *Dipteran* Cell Lines Propagating Oncolytic VSV Δ 51

Oncolytic virus preparations destined for use in research or clinical development are manufactured in mammalian or avian cell cultures. The OV's are propagated in these cell lines via a cytotoxic replicative cycle, in a batch production format followed by extensive purification and safety testing before a clinical grade product can be obtained. In contrast, insect cells can carry similar viruses as persistent infections while suffering little adverse effect²³. For example vesicular stomatitis virus (VSV), a highly effective oncolytic agent when administered to mammalian tumor cells^{24,25}, has been reported to infect and persist in cultured *Hemipteran*²⁶ or *Dipteran*²⁷ cells without detectable cytopathic effects. We tested whether cultured *Dipteran* cells could serve as carriers for the continuous growth of VSV- Δ 51, an engineered OV previously developed in our laboratory²⁴. Suspensions of the *D. melanogaster* S2 cell line were cultured in a minimal, serum-free medium formulation and infected with recombinant VSV- Δ 51 harboring a yellow fluorescent protein (YFP) reporter transgene to monitor viral persistence. We observed efficient infection of S2 cells with virtually all cells expressing virus-encoded YFP (Fig. 3.1a). During continued passaging over a period of months, VSV-infected S2 cell cultures showed similar log-phase growth kinetics to uninfected controls (Fig. 3.1b), with only a modest increase in doubling time from approximately 27h to 29h (Fig 3.1c). No change in the percentage of viable cells or average cell diameter was detected when infected S2 cultures were compared to uninfected controls (Fig. 3.1c). We have continued to monitor virus gene expression at the single cell level during continued passage of infected cell lines, and have found that they maintain a

Figure 3.1 – Establishment of Continuous Insect Cell Lines Propagating Oncolytic VSV-Δ51

a) Brightfield and corresponding fluorescent image of *Drosophila* S2 cells 7 days after infection with VSV-Δ51-YFP at a multiplicity of 10 pfu/cell. b) Log-phase growth curves comparing uninfected *Drosophila* S2 cells to two S2 lines persistently infected with VSV-Δ51 (VSV-Δ51-mRFP or VSV-Δ51-FLuc). c) Summary comparing doubling time (t_d), percentage of viable cells, and average cell diameter (d_{av}) of *Drosophila* S2 cultures either left uninfected or persistently infected with VSV-Δ51-mRFP or VSV-Δ51-FLuc.



c

S2 ^{mock}	27.0	98.5	13.1
S2 ^{VSVΔ51mRFP}	29.9	98.3	12.9
S2 ^{VSVΔ51FLuc}	29.3	98.5	12.0

homogeneously high level of infection throughout hundreds of doubling generations (Fig. 3.1a). To date, after more than one year of continuous culture and repeated freeze-thaws, we have not observed loss of viral persistence or even a detectable decrease in the percentage of infected *Dipteran* cells. Furthermore, a recombinant VSV-GFP lacking the naturally encoded glycoprotein gene also persisted long-term in S2 cells (data not shown), indicating that spread between cultured *Dipteran* cells is dispensable for the persistence of viral infection. Thus VSV appears to be maintained as an innocuous passenger in cultured *Dipteran* cells with continuous propagation of the viral genome in an intracellular form and vertical transmission to daughter cells.

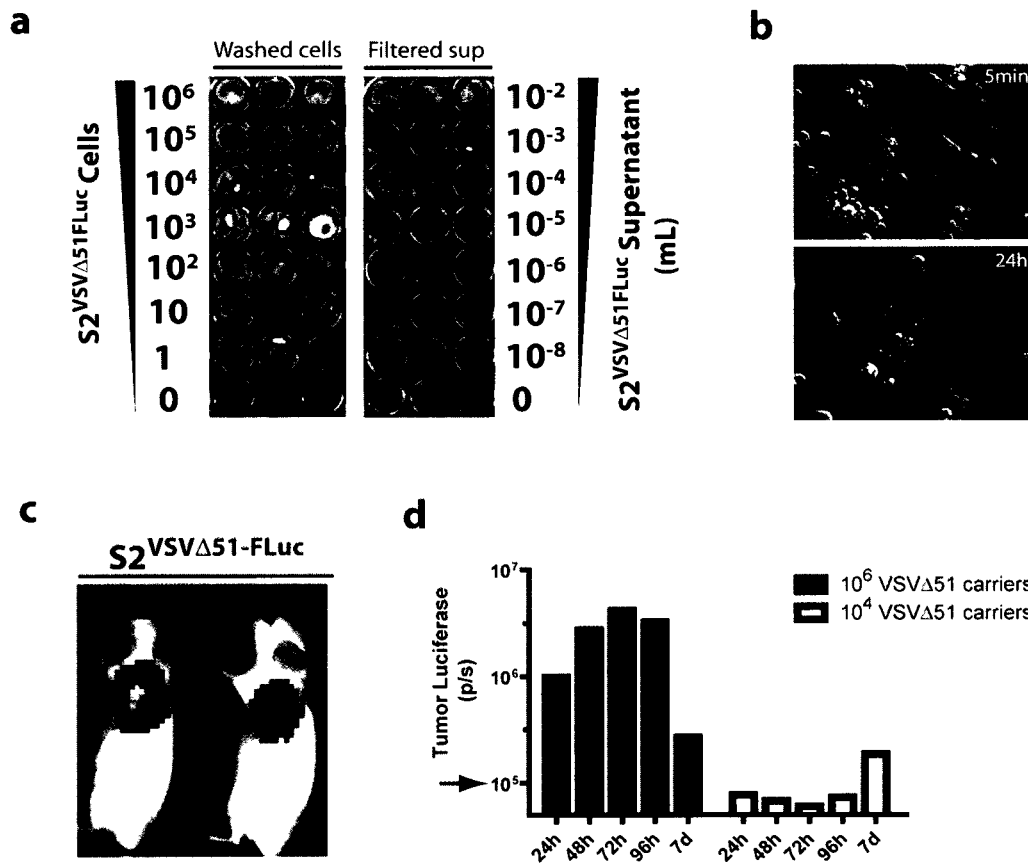
Persistently Infected Insect Cell Carriers Deliver Oncolytic VSV Δ 51 to Tumors

We examined whether persistently-infected *Dipteran* cell carriers could deliver oncolytic virus leading to infection of mammalian tumor cells *in vitro*. Carrier cell cultures harboring VSV Δ 51-Luciferase (S2^{VSV,51FLuc}) were harvested and divided into 0.2 μ m-filtered cell-free supernatant and washed cell pellet fractions. Serial dilutions of either cells or supernatant were then added to adherent monolayers of mammalian tumor cell lines. After 48h, the tumor cells were assayed for viral luciferase expression by bioluminescent imaging. As shown in figure 3.2a, few infectious particles were released into the culture supernatants of insect cell carriers. Limiting dilution analysis revealed approximately 10^4 infectious particles/mL in supernatants harvested from cultures containing 10^6 infected cells/mL. Therefore the quantity of infectious particles released from *Dipteran* cells was on the order of 0.01/cell, consistent with earlier reports²⁷. In contrast, the infected carriers themselves retained the ability to efficiently deliver VSV directly to tumor cells, with as little as a single

insect cell able to initiate a productive infection (Fig. 3.2a). Time-lapse microscopy of this insect cell-mediated delivery process revealed docking of fluorescently-labeled *Dipteran* carriers ($S2^{VSV_{\Delta 51}mRFP}$) to the surface of tumor cells within minutes of inoculation (Fig. 3.2b). Docking was followed by insect cell death and loss of visible viral transgene (mRFP) expression (Video S1), likely due to heat shock effects experienced under mammalian culture conditions. After a short eclipse period, the tumor cells began to show infection-associated rounding within several hours, followed by visible accumulation of the virus-encoded mRFP transgene, and ultimately lysis by approximately 24h. (Fig 3.2b, Video S1). We next examined whether insect cell carriers could deliver oncolytic virus to tumors growing in immunocompetent animals. *Drosophila* S2 cells carrying VSV- $\Delta 51$ -Luciferase were washed to remove cell-free particles and directly injected into solid subcutaneous tumors grown in syngeneic balb/c mice. Tumor luciferase expression was followed via longitudinal imaging. As shown (Fig 3.2c), robust VSV- $\Delta 51$ -Luciferase infection was observed specifically within tumors following administration of 10^6 insect cell carriers. Substantial signal (10-fold over background) was detectable by 24h post-injection and continually increased until peaking at 3d (Fig. 3.2d), identical to the previously reported replication kinetics of VSV- $\Delta 51$ administered as naked virions in this tumor model²⁸. Further characterization of the intratumoral dose-response revealed the minimal threshold number of insect cells carriers required to initiate a durable oncolytic virus infection. Injection of 10^4 cell carriers led to a minimally detectable and slow-evolving infection detectable at levels just over background by 7d (Fig. 3.2d). Thus similar to results of previous studies with naked

Figure 3.2 – Persistently Infected Insect Cell Carriers Deliver Oncolytic Virus to Tumor Cells

a) Limiting dilution assay of insect cell carriers. Serial dilutions of S2 cells persistently infected with VSV- Δ 51-FLuc or their filtered culture supernatants were overlaid onto monolayers of CT26 murine carcinoma cells. Viral luciferase activity was assayed by IVIS at 48h post-infection. b) Time-lapse images of insect cells delivering VSV- Δ 51-mRFP to CT26 murine carcinoma cells, at 5min and 24h post-inoculation. Composite images show bright field overlaid with red fluorescence. c) IVIS image shows luciferase activity at 3 days post-treatment, in duplicate mice bearing subcutaneous CT26 tumors treated by IT injection of 10^6 *Drosophila* S2 cells persistently infected with VSV- Δ 51-FLuc. The total luciferase signal for each tumor was digitally quantified at 24h, 48h, 72, 96h and 7d post-treatment and plotted in d).



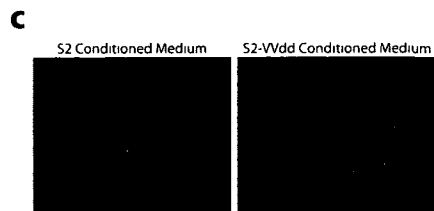
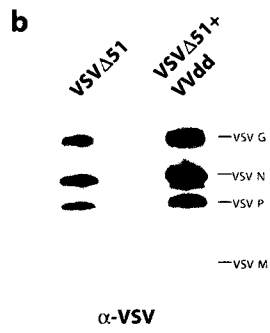
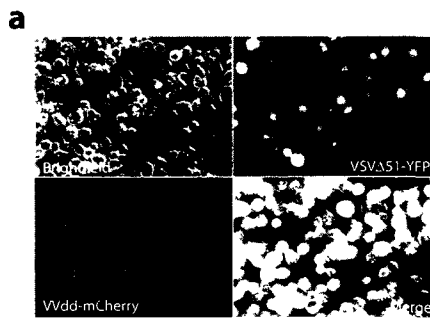
virions²⁵, a significant threshold dose was required to overcome the innate restrictions to oncolytic virus growth within the *in vivo* tumor microenvironment.

Insect Cells Carrying Oncolytic VSV Can Be Armed with Auxiliary Biotherapeutic Gene Cargoes

We examined whether insect cells carrying oncolytic VSVΔ51 could be armed with additional biotherapeutic gene products to overcome innate limitations to intratumoral oncolytic virus growth. Replication competent vaccinia vectors provide a robust platform for biotherapeutic transgene production²⁹, and their growth and cytopathic effects can be targeted specifically to tumors⁸. Furthermore they encode an array of secreted immunomodulators³⁰ with the ability to complement growth deficiencies of heterologous viruses^{31, 32}. We reasoned that insect cell carriers modified to constitutively secrete such immunomodulators should prime the tumor microenvironment to help promote oncolytic virus growth. Conditioned media from insect cells infected only with VVdd or from uninfected control S2 cells, were collected and passed through a 0.2um filter to remove free vaccinia particles. Tumor cell monolayers were subsequently infected with VSVΔ51-YFP viral particles in the presence of conditioned medium. The spread of the VSV-encoded YFP transgene and the production of virus were followed. At the limiting dose employed in this experiment VSVΔ51-YFP poorly infected tumor cells primed with control medium from uninfected insect cells, with minimal viral gene expression detected (Fig. 3.3c, S1). In contrast, tumor cells primed with conditioned medium from VVdd-infected S2 cells showed a robust VSV infection throughout the monolayer and production of nearly 100-fold greater titers of infectious virus (Fig. 3.3c, S1).

Figure 3.3 – Arming *Drosophilid* Oncolytic Virus Carrier Cells with Additional

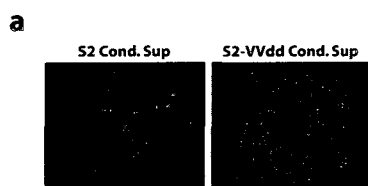
Biotherapeutic Cargoes a) Persistently infected VSV-Δ51-YFP cell carriers were superinfected with VVdd-mCherry at a multiplicity of 10 pfu/cell and imaged after 24h. b) Expression of VSV proteins in persistently infected S2 carriers in the presence or absence of vaccinia virus. S2^{VSV-Δ51-YFP} cell carriers were left uninfected or superinfected with VVdd for 24h, then harvested and subjected to immunoblotting with a polyclonal antibody recognizing the VSV proteins. c) Fluorescent images of monolayers of U2OS osteosarcoma cells infected with VSV-Δ51-YFP at a multiplicity of 10⁻⁵ pfu/cell for 48h in the presence of conditioned medium from mock- or VVdd infected *Drosophila* S2 cells. Supernatants from these tumor cells were collected at the same timepoint and titered for VSV production (d).



d

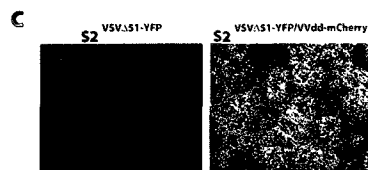
	VSV Production (pfu/mL)
S2 Conditioned Medium	7.6×10^7
S2-VVdd Conditioned Medium	5.0×10^9

Figure 3.S1: Insect cell carriers constitutively secreting vaccinia immunomodulators prime 786-0 human renal carcinoma cells for infection with oncolytic VSVΔ51. a) Monolayers of 786-0 cells were infected with VSVΔ51-YFP at a multiplicity of 10^{-5} pfu/cell, in the presence of conditioned medium from uninfected or vaccinia virus (VVdd) infected S2 insect cells. Fluorescent images were acquired at 36h post-infection. b) Shows the titers of VSVΔ51-YFP produced by 786-0 tumor cells after 36h during the same experiment. c) Monolayers of 786-0 cells were inoculated with singly-armed $S2^{VSV_{\Delta}51-YFP}$ or doubly-armed $S2^{VSV_{\Delta}51-YFP/VVdd-mCherry}$ insect cell carriers at a multiplicity of 0.01. Fluorescent images were acquired at 40h post-treatment. d) Shows titers of VSVΔ51-YFP produced by 786-0 tumor cells after 40h during the same experiment.



b

	VSV Production (pfu/mL)
S2 Conditioned Medium	5.2×10^5
S2-VVdd Conditioned Medium	5.0×10^7



d

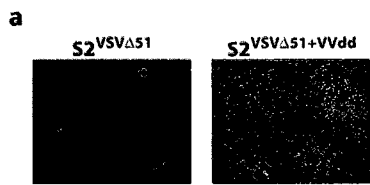
	VSV Production (pfu/mL)
S2 VSV Δ 51-YFP	8.1×10^3
S2 VSV Δ 51-YFP+VVdd-mCherry	3.3×10^8

Insect Cell Carriers Deliver Multiple Integrated Biotherapeutics to Tumor Cells

We next examined whether oncolytic VSV and complementing vaccinia virus immunomodulators could be integrated into insect cell transporters and delivered to tumor cells as a single therapeutic agent. To test this idea, we determined whether insect cells carrying VSV Δ 51 ($S2^{VSV_{\Delta}51YFP}$) could support super-infection with an oncolytic vaccinia strain (VVdd³³) tagged with the mCherry fluorescent reporter gene. Indeed, infection of $S2^{VSV_{\Delta}51YFP}$ carrier cells with VVdd-mCherry led to readily detectable vaccinia gene expression within 24h (Fig. 3.3a). Insect cells not only maintained VSV gene expression when superinfected with vaccinia virus, but it appeared that specific protein levels were significantly increased, as assessed by both viral reporter gene imaging and anti-VSV western blot (Fig 3.3a,b). Thus we were able to obtain a homogeneous population of carriers with virtually all cells infected with both VSV Δ 51-YFP and VVdd-mCherry (Fig. 3.3a). These doubly-armed cell carriers ($S2^{VSV_{\Delta}51YFP/VVddmCherry}$) were added to monolayers of mammalian tumor cells and infection was followed by fluorescent imaging and plaque assay. Insect cell carriers were administered at a minimal dose which resulted in little infection of tumor cells when VSV Δ 51 was delivered as a single agent (Fig 3.4a, 3.S1). However doubly-armed $S2^{VSV_{\Delta}51YFP/VVddmCherry}$ carriers constitutively secreting vaccinia immunomodulators could prime the tumor cell monolayers for infection and consequently a much more robust VSV Δ 51 infection was observed. Significantly greater viral spread was evident with extensive YFP expression throughout the monolayer (Fig. 3.4a, 3.S1), leading to dramatic increases in the titer of infectious VSV produced by the tumor cells (Fig 3.4b, 3.S1). We conducted similar experiments to determine whether insect cells could deliver this

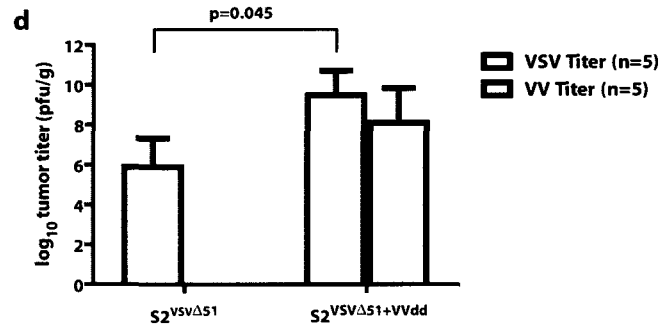
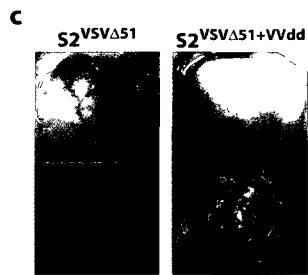
Figure 3.4 – Insect Cell Carriers Deliver Multiple Integrated Biotherapeutics to Tumor Cells

a) *Drosophila* S2^{VSV Δ 51YFP} or S2^{VSV Δ 51YFP/VVddmCherry} cell carriers were inoculated onto monolayers of U2OS osteosarcoma cells at a multiplicity of 0.001 for 48h. Composite YFP/mCherry fluorescent images are shown. b) Tumor cell supernatants from the same timepoint were titered for VSV production. c) *Drosophila* S2 cells infected with either VSV- Δ 51-YFP alone or with both VSV- Δ 51-YFP and VVdd-mCherry were injected IT into human HT29 tumors grown as xenografts in nude mice. At 3d post-infection tumors were removed and imaged. Brightfield and composite YFP/mCherry fluorescent images are shown. d) The same tumors were homogenized and titers of infectious VSV and VV were determined by plaque assay. Bars show mean log₁₀ titers +/- standard deviation. Bracketed bars show statistical significance at the indicated p value according to the two-tailed paired t-test.



b

VSV Production (pfu/mL)	
S2 ^{VSVΔ51} -YFP	3.4×10^7
S2 ^{VSVΔ51} -YFP+VVdd-mCherry	4.2×10^8

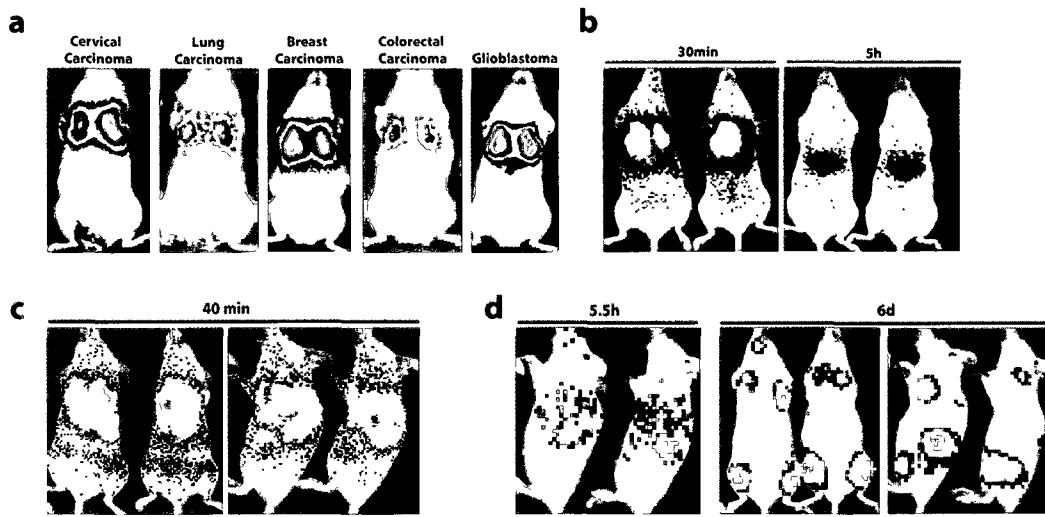


integrated biotherapeutic system to tumors *in vivo*. In order to rigorously test its activity within a restrictive microenvironment, the HT29 human colon carcinoma model was used, which has previously shown to be only partially sensitive to VSV Δ 51 *in vitro*³⁴. When HT29 tumors were grown as xenografts in nude mice and directly injected with insect cells carrying VSV Δ 51 as a single agent, little infection was detected by fluorescent imaging or plaque assay (Fig. 3.4c,d). However insect cells doubly infected with vaccinia and VSV led to a profound oncolytic virus infection within the tumor. Extensive spread of VSV was clear upon fluorescent imaging and we observed a 1000-fold increase in infectious virus recovered from the tumors (Fig. 3.4c,d). Additionally, VVdd-mCherry was delivered by the doubly infected carriers and also went on to infect the tumors (Fig. 3.4c,d). Thus insect cells carriers can deliver an integrated biotherapeutic system to tumors in order to promote oncolytic virus growth within a restrictive microenvironment.

Systemic Delivery of Insect Cells Carrying Multiple Integrated Biotherapeutics

The treatment of advanced disseminated cancers requires therapies that can be delivered systemically. We have previously demonstrated that mammalian carriers derived from leukocytic cell lineages show much improved circulatory distribution in comparison to their counterparts from solid tissues (ref. 10 and Fig. 3.S2). However, these mammalian carriers still express surface recognition molecules that facilitate their trafficking to, and accumulation in, lymphoid organs (ref. 10 and Fig. 3.S2) limiting their capacity for tumor-targeted biotherapeutic delivery. In contrast, insect cells which lack these homing receptors and are therefore incapable of interacting with mammalian host tissues could have a longer half-life in the circulation and thus be more available for tumour delivery. To test this idea,

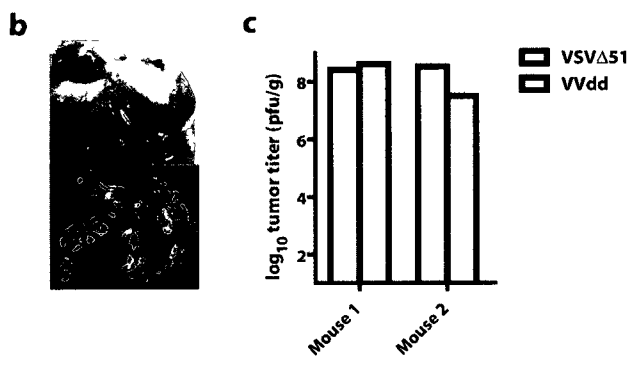
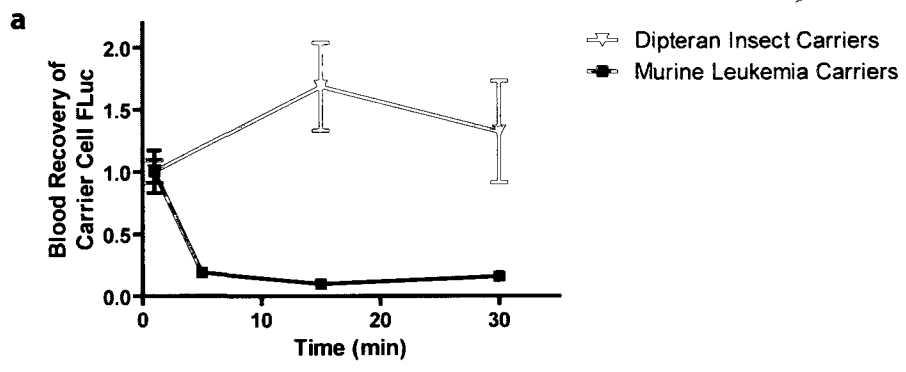
Figure 3.S2: Systemic biodistribution of mammalian carrier cells. Balb/c mice were injected intravenously with 10^6 of each firefly luciferase-tagged cell line and imaged by IVIS at timepoints as indicated. a) Solid tumor cell lines at 30min post-injection, HeLa cervical carcinoma (human), A549 lung carcinoma (human), MCF-7 breast carcinoma (human), CT26 colorectal carcinoma (murine), SF268 glioblastoma (human). b) Murine A20 lymphoma imaged at 30min and 5h post-injection. c) Murine L1210 leukemia cells imaged at 40min post-injection. Ventral and left-side (revealing spleen) views are shown. d) Murine L1210 leukemia cells imaged at 5.5h and 6d post-injection. Ventral and left-side (revealing spleen) views are shown.



we directly compared the circulatory half-life of insect cells harboring VSV Δ 51-Luciferase ($S2^{VSV_{\Delta}51FLuc}$) to murine leukemia carriers tagged with luciferase ($L1210^{FLuc}$). Carrier cells were injected intravenously into immunocompetent mice, and the cellular component of recovered blood was assayed for luciferase activity at various timepoints. Consistent with our imaging studies (ref 10 and Fig. 3.S2), mammalian leukemia cell carriers rapidly extravasated from the circulation, with a 90% decrease in their recovery from blood between 1min and 5min post-administration (Fig. 3.5a). In contrast, insect cell carriers failed to extravasate into non-tumor tissues and circulated at stable levels in the blood throughout the 30min of monitoring in this experiment. Importantly systemically administered insect cell carriers could deliver integrated biotherapeutics to distally located tumor beds. By 3d following intravenous administration of doubly-loaded carriers, extensive spread of both VSV Δ 51-YFP and VVdd-mCherry was visible in tumors (Fig. 3.5b), and high titers of each virus could be recovered (Fig. 3.5c).

Figure 3.5 – Systemic Delivery of Insect Cells Carrying Multiple Integrated Biotherapeutics

a) Circulatory kinetics of *Drosophila* S2 cell carriers administered systemically to immunocompetent balb/c mice. Mice were injected intravenously with either 10^7 L1210-FLuc murine leukemia cells or 10^7 S2 VSV- Δ 51-FLuc carriers. Blood samples were collected at 1, 5, 15 and 30min post injection, and the cellular fractions were assayed for luciferase activity in triplicate. Each point represents the mean of 3 triplicate measurements \pm standard deviation. b) Duplicate immunocompetent balb/c mice bearing CT26 tumors were treated intravenously with 10^7 *Drosophila* S2 cells carrying VSV- Δ 51-YFP and VVdd-mCherry. Tumors were excised after 72h and imaged. Brightfield and composite mCherry/YFP fluorescent images are shown. c) Each tumor was homogenized and titers of VSV- Δ 51 and VVdd were determined by plaque assay. Bars show individual viral titers for tumors of each of two mice.



DISCUSSION

The current standard of care for cancer, employing conventional chemotherapy and/or radiation therapy is unable to effect cures in the majority of patients with systemic disease. There is little doubt that sophisticated new therapeutic approaches need to be developed if significant success is to be attained in the treatment of metastatic cancers. A great deal of effort has been put toward the development of biotherapeutics including oncolytic viruses (OVs) with encouraging recent clinical results^{35,36}. To complement and augment OV therapeutics there has been an emerging interest in the use of cell carriers to enhance the systemic delivery of OVs³⁷. Mammalian carrier cells proposed to date are limited by one or more of the following features: cumbersome isolation and/or manufacturing protocols, limited viral productivity (in the case of non-tumor cells), off-target tissue homing tropisms, and safety concerns (in the case of tumorigenic cell lines).

To improve the clinical feasibility of the carrier cell approach, we have investigated whether insect cells persistently infected with an oncolytic virus could be exploited for systemic therapy. We observed that cultured *Drosophila melanogaster* cell populations continued to proliferate normally while maintaining a homogeneous infection with VSV Δ 51. Consistent with previous findings²⁷, these persistently infected *Dipteran* cell lines released on the order of only 0.01 infectious particles per cell into culture supernatants, much less than the hundreds to thousands typically produced by mammalian cell lines³⁸, and too little to be of therapeutic use. However insect cells directly harvested from these cultures remained highly infectious and effectively delivered oncolytic VSV to tumor cells through direct contact. Thus individual VSV Δ 51-infected *Dipteran* cells represent potent therapeutic

agents in their own right, and importantly, could deliver this oncolytic virus to tumors *in vivo* following either intratumoral or intravenous administration.

Unlike the mammalian cell lines typically used to propagate VSV, insect cell carriers remained viable and actively proliferated while infected with their oncolytic virus cargo, allowing further modification to express additional biotherapeutic gene products.

Illustrating this point, we have shown that *Dipteran* VSV carriers could be armed to constitutively secrete vaccinia virus-encoded immunomodulators that successfully primed the tumor microenvironment to promote oncolytic virus infection. Interestingly, the oncolytic vaccinia virus vector consisting of some 200 genes also productively infected the insect cell carriers and was delivered to tumors *in vivo*. These findings indicate that the insect cell platform has the capacity to simultaneously carry many integrated biotherapeutic genes and viruses to tumors upon systemic administration.

Insect cell lines capable of continuously propagating oncolytic viruses and other biotherapeutics therefore represent an attractive delivery platform with both immediate clinical utility and long-term potential for continued development. Insect cells stably propagating oncolytic virotherapeutics would be ideally suited to large-scale manufacturing³⁹, and could be systemically administered to patients without the drawbacks of off-target tissue homing and tumorigenicity that limits the safety of mammalian cell lines. Therefore a continuous insect cell line could be established as a standardized clinical vehicle, giving rise to a novel class of programmable cell biotherapies for cancer.

MATERIALS AND METHODS

Cells

Human (HT29, U2OS, 786-0, HeLa, SF268, A549, MCF-7) and murine (CT26-lacZ, L1210, A20) cell lines were cultured in Dulbecco's modified eagle medium (D-MEM, Hyclone, Logan, UT, USA) supplemented with 10% fetal calf serum (Cansera, Etobicoke, Canada). All mammalian cells were cultured at 37°C under 5% CO₂. *Drosophila melanogaster* Schneider line 2 (S2) cells were cultured in SF900II serum-free medium (Invitrogen) at 22°C under atmospheric pressures. Establishment of murine L1210 leukemia cells expressing an integrated firefly luciferase transgene (L1210-FLuc) has been described previously¹⁰. All cell lines were obtained from the American Type Culture Collection (ATCC, Manassas, VA, USA).

Viruses

Construction of recombinant strains of VSVΔ51 expressing eGFP-firefly luciferase or monomeric red fluorescent protein reporter transgenes (referred to herein as VSVΔ51-FLuc and VSVΔ51-mRFP, respectively) have been described previously^{10, 25}. An additional recombinant harboring a yellow fluorescent protein (YFP) reporter was generated by subcloning the YFP coding region between the XhoI and NheI sites of the pXN vector⁴⁰ and rescuing recombinant virus as described previously²⁵. All VSV stocks were propagated on Vero cells. For animal studies, VSV stocks were further purified from cell culture supernatants by filtration through a 0.2µm Steritop filter (Millipore, Billerica, MA, USA) and centrifugation at 30,000 x g before resuspension in phosphate-buffered saline (PBS) (Hyclone, Logan, UT, USA). Vaccinia VVdd-mCherry was made by insertion of mCherry-DNA

into the vaccinia thymidine kinase (TK) gene locus of VVdd³³ by homologous recombination. Successful recombinants were selected by mCherry expression and plaque-purified.. Vaccinia stocks were propagated on U2OS cells and cell-associated virus was collected by repeat (3) freeze-thaw cycles. Further purification of viral stocks were done by centrifugation at 20,700 x g through a 36% sucrose cushion (in 1mM Tris) before resuspension in 1mM Tris, pH 9.

Western blot detection of VSV proteins

Cell lysates were collected in 4% sodium dodecyl sulfate sample buffer, run on a NuPAGE Bis-Tris 4-12% polyacrylamide gel, transferred to a nitrocellulose membrane, and probed with polyclonal anti-VSV serum from hyperimmune rabbits.

Analysis of Cultured Insect Cells

Cell suspensions were counted on an automated cell viability analyzer (Beckman Coulter, Brea, California, USA), which determined the total cell concentration, viability by trypan blue exclusion, and average cell diameter.

Preparation of Insect Cell Conditioned Medium

Drosophila S2 cells were either mock infected or infected with VVdd-mCherry at a multiplicity of 10 pfu/cell for 24h, harvested and then pelleted by centrifugation. Supernatants were collected and passed through a 0.2um filter twice to eliminate cell-free vaccinia virions. To test for factors enhancing VSV infectivity, tumor cell monolayers were pre-treated for 5h with conditioned insect cell supernatant diluted into 50% 2X tumor cell

growth medium. Tumor cells were then infected with VSV in the presence of conditioned medium.

Mice and tumor models

CT26 tumors were established by subcutaneous injection of 1×10^6 cells into the hind or front flank of female 8- to 10-week old balb/c mice (Charles River Laboratories, Wilmington, MA). Palpable tumors were treated after approximately 10-14 days. HT29 (3×10^6) tumors were established subcutaneously in CD1 female nude mice (Charles River). Palpable tumors were treated approximately 14-21 days after injection. Intratumoral injections were performed under 3% isoflurane anesthesia. Intravenous injections were in the tail vein. All experiments were performed in accordance with institutional guidelines review board for animal care (University of Ottawa).

Bioluminescent and In vivo imaging

Mice were injected with *d*-luciferin (Molecular Imaging Products, Ann Arbor, MI, USA) (200ul intraperitoneally at 10mg/mL in PBS) for *Firefly* luciferase imaging. Mice were anesthetized under 3% isoflurane (Baxter Corp., Deerfield, IL, USA) and imaged with the *in vivo* imaging system (IVIS) 200 Series (Xenogen Corp., Hopkinton, MA, USA). Data acquisition and analysis was performed using Living Image v2.5 software. For *in vitro* imaging, cells were assayed in black multiwall plates (Sigma-Aldrich, Oakville, Canada). *d*-Luciferin substrate was diluted directly into the tissue culture medium, cells were incubated at room temperature for 5 min and then imaged using the IVIS 200. Bioluminescence signal from each well was quantified digitally with the Living Image 2.5 software.

Quantitation of Tumor Infection

Tumors were excised from euthanized mice and homogenized in PBS. Homogenates were serially diluted and plated onto Vero cells for 24h for VSV plaque assays, or U2OS cells for 72h for vaccinia virus plaque assays.

Fluorescent Imaging of Cell Infection *In Vitro*

Fluorescent images of infected cell cultures were acquired using the Axiovert S-100 (Carl Zeiss, Inc., Oberkochen, Germany) microscope equipped with a AxioCam camera (Carl Zeiss, Inc.). Axiovision 3.1 software (Carl Zeiss, Inc.) was used for digital image acquisition and Photoshop CS software (Adobe, San Jose, CA, USA) was used for post-acquisition image manipulation and creating 2-color overlays.

Fluorescent Imaging of *In Vivo* Tumor Infection

Mice were euthanized and dissected to expose tumors. Brightfield and fluorescent images were acquired using the M205-FA dissecting microscope/imaging system (Leica Microsystems Inc., Richmond Hill, ON, CANADA). The associated LAS FA6000 software was used for all image acquisition and post-imaging manipulations.

Live Cell Imaging

Time-lapse live-cell imaging was performed on an Axiovert 200M microscope. Cells were maintained at 37°C and 5% CO₂ throughout.

Infection and Preparation of Insect Cell Carriers

Drosophila S2 cells were initially infected with VSV Δ 51 at a multiplicity of 10pfu/cell.

Cultures were passaged continually at a density between 10^6 - 10^7 cells/mL to maintain log-phase growth. Doubly-infected carriers were generated by superinfecting S2-VSV Δ 51 carriers with VVdd-mCherry for 24h. For delivery to tumor cells, insect cells were washed three times in 10mL SF900II medium, and resuspended in a final volume of SF900II before inoculation onto cell monolayers or injection into animals.

Analysis of Circulatory Half-Life of Carrier Cells

Mice were injected intravenously with 10^7 carrier cells, and blood samples were collected by cardiac puncture from live mice under ketamine anesthesia. Pelleted total blood cells were directly resuspended in the lysis buffer supplied with the Luciferase Assay Kit (Stratagene, Cedar Creek, TX, USA) and firefly luciferase activity was assayed as per the manufacturer's protocol. Samples were imaged in a black 96-well plate (Sigma-Aldrich, Oakville, Canada) using the IVIS 200 (Xenongen, Alameda, CA, USA) and the total signal from each well was digitally quantified using the Living Image 2.5 software.

REFERENCES

1. Martin,V.J., Pitera,D.J., Withers,S.T., Newman,J.D., & Keasling,J.D. Engineering a mevalonate pathway in *Escherichia coli* for production of terpenoids. *Nat. Biotechnol.* **21**, 796-802 (2003).
2. Farmer,W.R. & Liao,J.C. Improving lycopene production in *Escherichia coli* by engineering metabolic control. *Nat. Biotechnol.* **18**, 533-537 (2000).
3. Elowitz,M.B. & Leibler,S. A synthetic oscillatory network of transcriptional regulators. *Nature* **403**, 335-338 (2000).
4. Gardner,T.S., Cantor,C.R., & Collins,J.J. Construction of a genetic toggle switch in *Escherichia coli*. *Nature* **403**, 339-342 (2000).
5. Posfai,G. *et al.* Emergent properties of reduced-genome *Escherichia coli*. *Science* **312**, 1044-1046 (2006).
6. Lartigue,C. *et al.* Creating bacterial strains from genomes that have been cloned and engineered in yeast. *Science* **325**, 1693-1696 (2009).
7. Antosova,Z., Mackova,M., Kral,V., & Macek,T. Therapeutic application of peptides and proteins: parenteral forever? *Trends Biotechnol.* **27**, 628-635 (2009).
8. Kim,J.H. *et al.* Systemic armed oncolytic and immunologic therapy for cancer with JX-594, a targeted poxvirus expressing GM-CSF. *Mol. Ther.* **14**, 361-370 (2006).
9. Chen,Y., Yu,D.C., Charlton,D., & Henderson,D.R. Pre-existent adenovirus antibody inhibits systemic toxicity and antitumor activity of CN706 in the nude mouse LNCaP xenograft model: implications and proposals for human therapy. *Hum. Gene Ther.* **11**, 1553-1567 (2000).
10. Power,A.T. *et al.* Carrier cell-based delivery of an oncolytic virus circumvents antiviral immunity. *Mol. Ther.* **15**, 123-130 (2007).
11. Lang,S.I., Giese,N.A., Rommelaere,J., Dinsart,C., & Cornelis,J.J. Humoral immune responses against minute virus of mice vectors. *J. Gene Med.* **8**, 1141-1150 (2006).
12. Raykov,Z., Balboni,G., Aprahamian,M., & Rommelaere,J. Carrier cell-mediated delivery of oncolytic parvoviruses for targeting metastases. *Int. J. Cancer* **109**, 742-749 (2004).
13. Iankov,I.D. *et al.* Infected cell carriers: a new strategy for systemic delivery of oncolytic measles viruses in cancer virotherapy. *Mol. Ther.* **15**, 114-122 (2007).
14. Thorne,S.H., Negrin,R.S., & Contag,C.H. Synergistic antitumor effects of immune cell-viral biotherapy. *Science* **311**, 1780-1784 (2006).

15. Ong, H.T., Hasegawa, K., Dietz, A.B., Russell, S.J., & Peng, K.W. Evaluation of T cells as carriers for systemic measles virotherapy in the presence of antiviral antibodies. *Gene Ther.* **14**, 324-333 (2007).
16. Cole, C. *et al.* Tumor-targeted, systemic delivery of therapeutic viral vectors using hitchhiking on antigen-specific T cells. *Nat. Med.* **11**, 1073-1081 (2005).
17. Peng, K.W. *et al.* Tumor-associated macrophages infiltrate plasmacytomas and can serve as cell carriers for oncolytic measles virotherapy of disseminated myeloma. *Am. J. Hematol.* **84**, 401-407 (2009).
18. Komarova, S., Kawakami, Y., Stoff-Khalili, M.A., Curiel, D.T., & Pereboeva, L. Mesenchymal progenitor cells as cellular vehicles for delivery of oncolytic adenoviruses. *Mol. Cancer Ther.* **5**, 755-766 (2006).
19. Yong, R.L. *et al.* Human Bone Marrow-Derived Mesenchymal Stem Cells for Intravascular Delivery of Oncolytic Adenovirus {Delta}24-RGD to Human Gliomas. *Cancer Res.* **69**, 8932-8940 (2009).
20. Hakkarainen, T. *et al.* Human mesenchymal stem cells lack tumor tropism but enhance the antitumor activity of oncolytic adenoviruses in orthotopic lung and breast tumors. *Hum. Gene Ther.* **18**, 627-641 (2007).
21. Qiao, J. *et al.* Purging metastases in lymphoid organs using a combination of antigen-nonspecific adoptive T cell therapy, oncolytic virotherapy and immunotherapy. *Nat. Med.* **14**, 37-44 (2008).
22. Butcher, E.C. & Picker, L.J. Lymphocyte homing and homeostasis. *Science* **272**, 60-66 (1996).
23. Gray, S.M. & Banerjee, N. Mechanisms of arthropod transmission of plant and animal viruses. *Microbiol. Mol. Biol. Rev.* **63**, 128-148 (1999).
24. Stojdl, D.F. *et al.* Exploiting tumor-specific defects in the interferon pathway with a previously unknown oncolytic virus. *Nat. Med.* **6**, 821-825 (2000).
25. Stojdl, D.F. *et al.* VSV strains with defects in their ability to shutdown innate immunity are potent systemic anti-cancer agents. *Cancer Cell* **4**, 263-275 (2003).
26. Yang, Y.J., Stoltz D.B., & Prevec, L. Growth of Vesicular Stomatitis Virus in a Continuous Culture line of *Antheraea eucalypti* Moth Cells. *J. Gen. Virol.* **5**, 473-483 (1969).
27. Mudd, J.A., Leavitt, R.W., Kingsbury, D.T., & Holland, J.J. Natural selection of mutants of vesicular stomatitis virus by cultured cells of *Drosophila melanogaster*. *J. Gen. Virol.* **20**, 341-351 (1973).
28. Breitbach, C.J. *et al.* Targeted inflammation during oncolytic virus therapy severely compromises tumor blood flow. *Mol. Ther.* **15**, 1686-1693 (2007).

29. Mastrangelo, M.J. *et al.* Intratumoral recombinant GM-CSF-encoding virus as gene therapy in patients with cutaneous melanoma. *Cancer Gene Ther.* **6**, 409-422 (1999).
30. Seet, B.T. *et al.* Poxviruses and immune evasion. *Annu. Rev. Immunol.* **21**, 377-423 (2003).
31. Symons, J.A., Alcami, A., & Smith, G.L. Vaccinia virus encodes a soluble type I interferon receptor of novel structure and broad species specificity. *Cell* **81**, 551-560 (1995).
32. Colamonici, O.R., Domanski, P., Sweitzer, S.M., Larner, A., & Buller, R.M. Vaccinia virus B18R gene encodes a type I interferon-binding protein that blocks interferon alpha transmembrane signaling. *J. Biol. Chem.* **270**, 15974-15978 (1995).
33. McCart, J.A. *et al.* Systemic cancer therapy with a tumor-selective vaccinia virus mutant lacking thymidine kinase and vaccinia growth factor genes. *Cancer Res.* **61**, 8751-8757 (2001).
34. LeBoeuf, F. & Bell, J.C. Unpublished data. 2009.
35. Kelly, K. *et al.* Reovirus-based therapy for cancer. *Expert. Opin. Biol. Ther.* **9**, 817-830 (2009).
36. Kim, J.H. *et al.* Systemic armed oncolytic and immunologic therapy for cancer with JX-594, a targeted poxvirus expressing GM-CSF. *Mol. Ther.* **14**, 361-370 (2006).
37. Willmon, C. *et al.* Cell carriers for oncolytic viruses: Fed Ex for cancer therapy. *Mol. Ther.* **17**, 1667-1676 (2009).
38. COOPER, P.D. Some characteristics of vesicular stomatitis virus growth-curves in tissue culture. *J. Gen. Microbiol.* **17**, 327-334 (1957).
39. Ikonomou, L., Schneider, Y.J., & Agathos, S.N. Insect cell culture for industrial production of recombinant proteins. *Appl. Microbiol. Biotechnol.* **62**, 1-20 (2003).
40. Schnell, M.J., Buonocore, L., Whitt, M.A., & Rose, J.K. The minimal conserved transcription stop-start signal promotes stable expression of a foreign gene in vesicular stomatitis virus. *J. Virol.* **70**, 2318-2323 (1996).

CHAPTER 4: DISCUSSION

The work described in this thesis has examined a novel cell carrier strategy for the systemic delivery of oncolytic viruses to tumors *in vivo*. Particular emphasis was placed on comparing this novel strategy to the administration of naked virions by intravenous injection, which has been the standard approach employed in all clinical trials of systemic virotherapy to date^{46-50, 94, 95}. In preclinical investigations, coating with various chemical carriers has also been explored as a strategy to enhance systemic oncolytic virus delivery⁹⁶⁻⁹⁸. Key points regarding the unique advantages and limitations of live cell carriers are discussed herein.

4.1 Targeting Virotherapeutic Delivery

The goal of systemic cancer therapy is to target micrometastatic tumor deposits growing within any organ of the body. However the quantity of intravenously-administered virions reaching disseminated tumors is limited by the reticuloendothelial system, which specializes in clearing microbes from the circulation. This problem has been particularly well-studied in murine systems with adenoviral agents, where it has been shown that greater than 99% of infused virus is rapidly cleared from the circulation within 30 minutes⁹⁷. Experimentally this problem can be alleviated by physically blocking blood flow into the liver during administration of the virus, resulting in increased delivery of virus to other organs⁹⁹. While this approach would be cumbersome to implement in humans, it has been shown that masking virus surface antigens can have a similar effect, and coating adenoviral virions with a covalently linked multivalent copolymer can dramatically increase plasma circulation time⁹⁷. However this approach may not be generally applicable to other oncolytic agents. For example, modification with covalently-linked polymers may interfere

with the membrane fusion step required for cellular entry by some enveloped viruses which are potent oncolytic agents such as VSV, measles and vaccinia.

Our studies with oncolytic VSV have also demonstrated the strong impact of reticuloendothelial uptake upon systemic virotherapy. We have found that the vast majority of injected virus is rapidly taken up by the liver and spleen within 5 minutes of intravenous injection¹⁰⁰. Consequently less than 0.001% of the administered dose will reach a murine tumor implanted in the hind flank¹⁰⁰. Similar to synthetic polymers, live cell carriers have the ability to mask viral antigen during delivery and thereby redirect tissue biodistribution. In the studies described here, we found that carriers derived from a variety of solid tumor cell lines accumulated exclusively in the lungs, and this became the primary site of virus delivery, rather than liver (Chapter 2). Consequently solid tumor cell carriers delivered oncolytic VSV to lung tumors with high efficiency. Similar results have been reported for mesenchymal stem cells carrying oncolytic adenoviruses^{101, 102}. The tissue restricted distribution of cell types derived from solid tissues would therefore appear to limit their utility for systemic delivery of oncolytic viruses to advanced metastatic disease.

In contrast, our *in vivo* studies show that hematogenous leukemia cell lines recirculate much more extensively than carriers of solid tissue origin and were able to traverse lung vessels to reach other organs. However blood cell carriers did not distribute uniformly, but preferentially delivered VSV to lymphoid organs (Chapter 2), consistent with the natural receptor-mediated trafficking patterns of these cell types¹⁰³. Thus interactions of mammalian cell carrier with host tissues may lead to off-target virus delivery. One solution to this problem would be to match the homing properties of the cell carrier to the location

of disease to be treated. For example, lymphocytes homing to lymph nodes might be used to deliver virus to lymph node metastasis¹⁰⁴. Practically, however, this approach would be difficult to apply to the treatment of advanced human disease, as micrometastatic growth is often not confined to a single organ and can be undetectable. Thus a better strategy may be to target carrier cell delivery based on general features of tumor cells themselves. For example, T cells targeting a model tumor antigen can home and deliver oncolytic virus to the tumor site in murine systems¹⁰⁵. However, tumor-antigen specific T cells are not available for the majority of the patient population. Ideally, carrier cells would be targeted to a specific but ubiquitous feature of tumor cells, tumor endothelium or tumor stromal cells to be widely effective across the heterogeneous spectrum of clinical disease. In this regard, insect cell carriers possess the unique advantage of lacking homing receptors that interact with mammalian tissues *in vivo*. These carriers displayed a much greater circulatory half-life than mammalian leukocytic carriers and effectively delivered oncolytic virus to distally-located tumor deposits (Chapter 3). Therefore insect cell carrier lines such as those described here are naturally de-targeted from non-tumor tissues and could be further modified to target delivery specifically to sites of disease growth (discussed further below).

In addition to systemic trafficking patterns, the timing of virus release is another crucial feature of OV carriers. Ideally, intravenously administered cell carriers would release virus only upon reaching metastatic tumor deposits, in order to maximize the effective therapeutic dose and minimize the potential for off-target toxicity. However, OVs undergo a time-sensitive growth cycle in mammalian carriers, and release of progeny virions occurs within a fixed period after the initial infection. In contrast, insect cell carriers propagated

VSV in a latent form until interacting directly with susceptible tumor cells (Chapter 3). Although further experimentation is required to determine the precise nature of this latency-reactivation behavior, it is clear from this work that full-length VSV genome copies are symmetrically partitioned in continuously dividing S2 cells, since a single infected carrier was sufficient to transmit fully infectious virus to mammalian cancer cells (Chapter 3). In preliminary electron microscopy studies we could not detect mature virions in infected S2 carriers (data not shown), suggesting that the VSV genome may persist as a naked RNP particle in these cells. This apparent inability of infected insect cells to form mature particles would also suggest that the virus is transmitted to tumor cells through a novel mechanism. Infected insect cells were seen to directly attach to the tumor cell surface (Chapter 3), which may allow for transfer of cytoplasmic RNPs containing the VSV genome. Viral glycoprotein expressed on the insect cell surface could bind to the tumor cell surface and trigger membrane fusion to facilitate this transfer. Clearly further studies are required to determine the form under which the VSV genome persists in insect cells, the copy number and the mechanism of vertical transmission. It will also be important to determine whether the VSV glycoprotein is indeed expressed on the insect cell surface, and what role it plays in attachment and transmission of virus to mammalian cells.

4.2 Evasion of Acquired Antiviral Immunity

In addition to uptake by off-target tissues, the efficacy of systemic virotherapy can be limited by the acquired immune response. Our studies show that high-titer neutralizing antiviral antibodies are naturally elicited during oncolytic VSV therapy in immunocompetent animals (Chapter 2). This leads to a long-lasting state of sterilizing immunity that is

sufficient to completely ablate systemic virus delivery and prevent tumor infection. Antibodies capable of neutralizing virus directly in the circulation, but not antiviral T cells, were found to be the crucial effectors of this phenomenon (Chapter 2). Similarly, other investigators have found that passively transferred human anti-sera are sufficient to ablate systemic delivery of oncolytic measles^{106, 107} and adenovirus^{108, 109}. These findings have significant consequences for human therapy in light of the fact that robust neutralizing antibody titers have been consistently elicited in patients receiving systemic virotherapy in clinical trials⁴⁶⁻⁵¹. It is likely that much of the naked virus administered to these patients would have been immediately neutralized in the bloodstream before having the opportunity to infect tumor cells. Improved methods for delivering oncolytic viruses are therefore urgently needed.

The studies described here provide the first report of successful intravenous oncolytic virus delivery in the face of high-titer neutralizing antibody. This was achieved by administering infected cells which trafficked to tumor beds through the circulation before releasing their viral cargo (Chapter 2). Consequently, multiple doses of oncolytic virus administered within carrier cells exhibited much greater therapeutic efficacy than when injected as naked virions (Chapter 2). Therefore, sequestration of oncolytic viruses within carriers to avoid neutralization during transit to tumor beds has the potential to improve their efficacy as systemic therapeutics. Ongoing work in the field is aimed at determining which types of cellular vehicles can be used to best exploit this ability in the clinic. Xenogeneic cell types such as insect cells have unique advantages and we show that they can deliver an initial dose of oncolytic virus to tumors in naïve mammalian hosts. However further work is

required to determine whether immunity develops against repeated administration of xenogeneic cells types, and if so, whether this immunity has any impact on systemic delivery. The possibility of multi-dosing with xenogeneic carriers would vastly expand the available repertoire of available cell lines whose diverse properties could be exploited for oncolytic virus delivery. Alternatively, patient-derived leukocytes offer a readily available source of autologous carriers should the expression of cellular xeno-antigens prove to limit multi-dose delivery.

4.3 Biosafety

Potential safety concerns are important to consider in the development of novel systemic cancer therapeutics. We did not observe any overt toxicity following systemic administration of cell carriers at the doses required for effective oncolytic virus delivery. Notably, this observation also extends to cell carriers of xenogeneic and invertebrate origin. However, *de novo* tumor growth was occasionally noted at the injection site following intravenous treatment with syngeneic tumor cell carriers, perhaps due to a small fraction which escaped *ex vivo* infection. The safety of systemically injecting live tumor cells for therapy is an obvious concern which might be addressed by lethally irradiating pre-infected carriers without compromising their ability to deliver oncolytic virus¹¹⁰. However the ideal solution might be to use insect cell carriers which are unable to proliferate or survive long-term in mammalian systems (Chapter 3). Intriguingly, sequestration of injected virus within carrier cells may help to alleviate some of the transient toxicities triggered by systemic administration of naked virus particles (ie fever, dehydration, lethargy). Although this hypothesis was not examined in the studies described here, others have shown that

excessive reticuloendothelial uptake of adenovirus particles can trigger these adverse effects. Cell carriers which effectively target virus delivery to tumor deposits and conceal viral antigen in transit may therefore help to mitigate the acute toxicity of these agents in patients.

4.4 Manufacturing

Manufacturing live therapeutic viruses of sufficient quantity and purity for use in human patients is a major challenge. Typically, oncolytic viruses are grown in cultured mammalian cells which undergo cytolysis as the virus is amplified. Cell supernatants or lysates containing live oncolytic virus are then collected and subjected to purification steps to remove medium or cellular components that might cause undesired effects upon administration to patients. The use of carrier cells would add extra complications to this process. Primary cells, if they were to be used as carriers would have to be isolated, purified and characterized. Carriers would then have to be infected *ex vivo* with large quantities of purified virus, and perhaps irradiated to ablate tumorigenicity. Mammalian cells carriers, being susceptible themselves to the cytolytic effects of their virotherapeutic cargoes, would be unstable and could only be administered to patients within hours of infection in the lab. Therefore clinical application of the mammalian carrier cell types investigated in preclinical studies to date may not be feasible.

In contrast, an insect cell carrier system would significantly streamline the process of oncolytic virus manufacturing and clinical delivery. As we have shown here, *Dipteran* cells carrying oncolytic virus can be stably propagated under minimal culture conditions (Chapter 3) that are highly amenable to large-scale production¹¹¹. We also find that insect cell carrier

lines retain oncolytic virus infectivity after cryopreservation, and therefore doses could be aliquoted and frozen on liquid nitrogen for storage or transport prior to therapeutic administration. Since infected insect cell carriers deliver oncolytic virus directly to tumor cells following intravenous injection, they could then be harvested from storage or culture and immediately administered to patients without any need for further purification of virus particles. A streamlined manufacturing and clinical delivery pipeline for systemically administered insect cell carriers could be readily standardized not only for use with viral therapeutics but any other biotherapeutic, or combination thereof, as discussed below.

4.5 A Programmable Cell Platform for Integrated Cancer Biotherapy

The vast potential of live cell carriers to be genetically reprogrammed is another unique advantage of this therapeutic approach. Cells possess a virtually unlimited capacity for the integration of multiple biotherapeutic transgenes, and unlike inert virions, have the ability to express the encoded gene products during systemic delivery and/or immediately upon arrival within the tumor microenvironment. Although infection would lead to a shutoff of cellular transgene expression in mammalian carriers, we have shown that insect cells carrying oncolytic virus remain viable and are therefore capable of simultaneously expressing additional biotherapeutic transgenes (Chapter 3). Therefore insect cell carriers could be modified to express surface proteins that cause them to be retained preferentially within tumor beds following systemic administration, for example those which bind to molecules exposed on the tumor neovasculature¹¹². Since these cells show little natural tropism for off-target mammalian tissues (Chapter 3) they provide an ideal starting point for engineering a tumor-targeted vehicle. Insect cells carrying oncolytic virus can also be

modified to constitutively secrete gene products upon arrival at the tumor site in order to enhance therapy. As an example, we have shown in this work that modification of insect cell carriers to secrete vaccinia-encoded immunomodulators upon arrival within the tumor microenvironment promotes the subsequent delivery of the oncolytic virus cargo (Chapter 3). These findings demonstrate the possibility of constructing sophisticated biotherapeutic systems consisting of multiple viruses and gene products integrated into a single cell carrier that can be delivered systemically to patients with metastatic disease. In our studies we have focused primarily on the delivery of viruses as a “proof of principle” but it is easy to imagine the establishment of stable insect cell lines expressing immune stimulating growth factors, monoclonal antibodies, imaging gene products, tumour antigens, suicide genes and/or targeting molecules along with viruses to create a sophisticated cancer killing machine.

4.6 Conclusions

This thesis has investigated the use of cellular carriers as a novel approach to overcome many of the challenges to systemic delivery of oncolytic viruses. Clinical testing is now required to establish the safety and feasibility of this approach. While mammalian cells have been exclusively used in preclinical studies to establish the potential of this approach, their use as carriers may be difficult to implement in the clinical setting. In contrast, persistently-infected insect cell carriers provide a platform that could be immediately tested in human patients. If established as a standardized therapeutic product, live insect cell carriers would serve as a useful chassis for the continued engineering of novel multi-gene/virus biotherapeutics for cancer.

REFERENCES

1. Parkin,D.M., Bray,F., Ferlay,J., & Pisani,P. Global cancer statistics, 2002. *CA Cancer J. Clin.* **55**, 74-108 (2005).
2. DeVita,V.T., Jr. & Chu,E. A history of cancer chemotherapy. *Cancer Res.* **68**, 8643-8653 (2008).
3. Chabner,B.A. & Roberts,T.G., Jr. Timeline: Chemotherapy and the war on cancer. *Nat. Rev. Cancer* **5**, 65-72 (2005).
4. Lecoq,H. [Discovery of the first virus, the tobacco mosaic virus: 1892 or 1898?]. *C. R. Acad. Sci. III* **324**, 929-933 (2001).
5. Kelly,E. & Russell,S.J. History of oncolytic viruses: genesis to genetic engineering. *Mol. Ther.* **15**, 651-659 (2007).
6. MOORE,A.E. Effects of viruses on tumors. *Annu. Rev. Microbiol.* **8**, 393-410 (1954).
7. Sinkovics,J. & Horvath,J. New developments in the virus therapy of cancer: a historical review. *Intervirology* **36**, 193-214 (1993).
8. Martuza,R.L., Malick,A., Markert,J.M., Ruffner,K.L., & Coen,D.M. Experimental therapy of human glioma by means of a genetically engineered virus mutant. *Science* **252**, 854-856 (1991).
9. Bischoff,J.R. *et al.* An adenovirus mutant that replicates selectively in p53-deficient human tumor cells. *Science* **274**, 373-376 (1996).
10. McCart,J.A. *et al.* Systemic cancer therapy with a tumor-selective vaccinia virus mutant lacking thymidine kinase and vaccinia growth factor genes. *Cancer Res.* **61**, 8751-8757 (2001).
11. Taylor,M.W., Cordell,B., Souhrada,M., & Prather,S. Viruses as an aid to cancer therapy: regression of solid and ascites tumors in rodents after treatment with bovine enterovirus. *Proc. Natl. Acad. Sci. U. S. A* **68**, 836-840 (1971).
12. Dupressoir,T., Vanacker,J.M., Cornelis,J.J., Duponchel,N., & Rommelaere,J. Inhibition by parvovirus H-1 of the formation of tumors in nude mice and colonies in vitro by transformed human mammary epithelial cells. *Cancer Res.* **49**, 3203-3208 (1989).
13. Duncan,M.R., Stanish,S.M., & Cox,D.C. Differential sensitivity of normal and transformed human cells to reovirus infection. *J. Virol.* **28**, 444-449 (1978).
14. Reichard,K.W. *et al.* Newcastle disease virus selectively kills human tumor cells. *J. Surg. Res.* **52**, 448-453 (1992).

15. Stojdl,D.F. *et al.* Exploiting tumor-specific defects in the interferon pathway with a previously unknown oncolytic virus. *Nat. Med.* **6**, 821-825 (2000).
16. Lun,X. *et al.* Myxoma virus is a novel oncolytic virus with significant antitumor activity against experimental human gliomas. *Cancer Res.* **65**, 9982-9990 (2005).
17. Bonjardim,C.A., Ferreira,P.C., & Kroon,E.G. Interferons: signaling, antiviral and viral evasion. *Immunol. Lett.* **122**, 1-11 (2009).
18. Belkowski,L.S. & Sen,G.C. Inhibition of vesicular stomatitis viral mRNA synthesis by interferons. *J. Virol.* **61**, 653-660 (1987).
19. Muller,U. *et al.* Functional role of type I and type II interferons in antiviral defense. *Science* **264**, 1918-1921 (1994).
20. Hwang,S.Y. *et al.* A null mutation in the gene encoding a type I interferon receptor component eliminates antiproliferative and antiviral responses to interferons alpha and beta and alters macrophage responses. *Proc. Natl. Acad. Sci. U. S. A* **92**, 11284-11288 (1995).
21. Einhorn,S. & Grander,D. Why do so many cancer patients fail to respond to interferon therapy? *J. Interferon Cytokine Res.* **16**, 275-281 (1996).
22. Wang,F. *et al.* Disruption of Erk-dependent type I interferon induction breaks the myxoma virus species barrier. *Nat. Immunol.* **5**, 1266-1274 (2004).
23. Grekova,S. *et al.* Activation of an antiviral response in normal but not transformed mouse cells: a new determinant of minute virus of mice oncotropism. *J. Virol.* **84**, 516-531 (2010).
24. Stojdl,D.F. *et al.* VSV strains with defects in their ability to shutdown innate immunity are potent systemic anti-cancer agents. *Cancer Cell* **4**, 263-275 (2003).
25. Strong,J.E., Coffey,M.C., Tang,D., Sabinin,P., & Lee,P.W. The molecular basis of viral oncolysis: usurpation of the Ras signaling pathway by reovirus. *EMBO J.* **17**, 3351-3362 (1998).
26. Markert,J.M., Malick,A., Coen,D.M., & Martuza,R.L. Reduction and elimination of encephalitis in an experimental glioma therapy model with attenuated herpes simplex mutants that retain susceptibility to acyclovir. *Neurosurgery* **32**, 597-603 (1993).
27. Randazzo,B.P. *et al.* Treatment of experimental intracranial murine melanoma with a neuroattenuated herpes simplex virus 1 mutant. *Virology* **211**, 94-101 (1995).
28. Bergmann,M. *et al.* A genetically engineered influenza A virus with ras-dependent oncolytic properties. *Cancer Res.* **61**, 8188-8193 (2001).
29. Garcia-Sastre,A. *et al.* Influenza A virus lacking the NS1 gene replicates in interferon-deficient systems. *Virology* **252**, 324-330 (1998).

30. Gromeier,M., Lachmann,S., Rosenfeld,M.R., Gutin,P.H., & Wimmer,E. Intergeneric poliovirus recombinants for the treatment of malignant glioma. *Proc. Natl. Acad. Sci. U. S. A* **97**, 6803-6808 (2000).
31. Takamizawa,J. *et al.* Reduced expression of the let-7 microRNAs in human lung cancers in association with shortened postoperative survival. *Cancer Res.* **64**, 3753-3756 (2004).
32. Edge,R.E. *et al.* A let-7 MicroRNA-sensitive vesicular stomatitis virus demonstrates tumor-specific replication. *Mol. Ther.* **16**, 1437-1443 (2008).
33. Kelly,E.J., Hadac,E.M., Greiner,S., & Russell,S.J. Engineering microRNA responsiveness to decrease virus pathogenicity. *Nat. Med.* **14**, 1278-1283 (2008).
34. Cawood,R. *et al.* Use of tissue-specific microRNA to control pathology of wild-type adenovirus without attenuation of its ability to kill cancer cells. *PLoS. Pathog.* **5**, e1000440 (2009).
35. Ikeda,K. *et al.* Oncolytic virus therapy of multiple tumors in the brain requires suppression of innate and elicited antiviral responses. *Nat. Med.* **5**, 881-887 (1999).
36. Wakimoto,H. *et al.* The complement response against an oncolytic virus is species-specific in its activation pathways. *Mol. Ther.* **5**, 275-282 (2002).
37. Jiang,H., Wang,Z., Serra,D., Frank,M.M., & Amalfitano,A. Recombinant adenovirus vectors activate the alternative complement pathway, leading to the binding of human complement protein C3 independent of anti-ad antibodies. *Mol. Ther.* **10**, 1140-1142 (2004).
38. Carlisle,R.C. *et al.* Human erythrocytes bind and inactivate type 5 adenovirus by presenting Coxsackie virus-adenovirus receptor and complement receptor 1. *Blood* **113**, 1909-1918 (2009).
39. Seiradake,E. *et al.* The cell adhesion molecule "CAR" and sialic acid on human erythrocytes influence adenovirus in vivo biodistribution. *PLoS. Pathog.* **5**, e1000277 (2009).
40. Worgall,S., Wolff,G., Falck-Pedersen,E., & Crystal,R.G. Innate immune mechanisms dominate elimination of adenoviral vectors following in vivo administration. *Hum. Gene Ther.* **8**, 37-44 (1997).
41. Ye,X., Jerebtsova,M., & Ray,P.E. Liver bypass significantly increases the transduction efficiency of recombinant adenoviral vectors in the lung, intestine, and kidney. *Hum. Gene Ther.* **11**, 621-627 (2000).
42. Kim,J.H. *et al.* Systemic armed oncolytic and immunologic therapy for cancer with JX-594, a targeted poxvirus expressing GM-CSF. *Mol. Ther.* **14**, 361-370 (2006).

43. Heise,C.C., Williams,A.M., Xue,S., Propst,M., & Kirn,D.H. Intravenous administration of ONYX-015, a selectively replicating adenovirus, induces antitumoral efficacy. *Cancer Res.* **59**, 2623-2628 (1999).
44. Hirasawa,K. *et al.* Systemic reovirus therapy of metastatic cancer in immune-competent mice. *Cancer Res.* **63**, 348-353 (2003).
45. Dingli,D. *et al.* Image-guided radiovirotherapy for multiple myeloma using a recombinant measles virus expressing the thyroidal sodium iodide symporter. *Blood* **103**, 1641-1646 (2004).
46. Hamid,O. *et al.* Phase II trial of intravenous CI-1042 in patients with metastatic colorectal cancer. *J. Clin. Oncol.* **21**, 1498-1504 (2003).
47. Freeman,A.I. *et al.* Phase I/II trial of intravenous NDV-HUJ oncolytic virus in recurrent glioblastoma multiforme. *Mol. Ther.* **13**, 221-228 (2006).
48. Nemunaitis,J. *et al.* Intravenous infusion of a replication-selective adenovirus (ONYX-015) in cancer patients: safety, feasibility and biological activity. *Gene Ther.* **8**, 746-759 (2001).
49. Small,E.J. *et al.* A phase I trial of intravenous CG7870, a replication-selective, prostate-specific antigen-targeted oncolytic adenovirus, for the treatment of hormone-refractory, metastatic prostate cancer. *Mol. Ther.* **14**, 107-117 (2006).
50. Vidal,L. *et al.* A phase I study of intravenous oncolytic reovirus type 3 Dearing in patients with advanced cancer. *Clin. Cancer Res.* **14**, 7127-7137 (2008).
51. White,C.L. *et al.* Characterization of the adaptive and innate immune response to intravenous oncolytic reovirus (Dearing type 3) during a phase I clinical trial. *Gene Ther.* **15**, 911-920 (2008).
52. Parato,K.A., Senger,D., Forsyth,P.A., & Bell,J.C. Recent progress in the battle between oncolytic viruses and tumours. *Nat. Rev. Cancer* **5**, 965-976 (2005).
53. Ikeda,K. *et al.* Oncolytic virus therapy of multiple tumors in the brain requires suppression of innate and elicited antiviral responses. *Nat. Med.* **5**, 881-887 (1999).
54. Wakimoto,H. *et al.* The complement response against an oncolytic virus is species-specific in its activation pathways. *Mol. Ther.* **5**, 275-282 (2002).
55. Worgall,S., Wolff,G., Falck-Pedersen,E., & Crystal,R.G. Innate immune mechanisms dominate elimination of adenoviral vectors following in vivo administration. *Hum. Gene Ther.* **8**, 37-44 (1997).
56. Ye,X., Jerebtsova,M., & Ray,P.E. Liver bypass significantly increases the transduction efficiency of recombinant adenoviral vectors in the lung, intestine, and kidney. *Hum. Gene Ther.* **11**, 621-627 (2000).

57. Hirasawa,K. *et al.* Systemic reovirus therapy of metastatic cancer in immune-competent mice. *Cancer Res.* **63**, 348-353 (2003).
58. Lang,S.I., Giese,N.A., Rommelaere,J., Dinsart,C., & Cornelis,J.J. Humoral immune responses against minute virus of mice vectors. *J. Gene Med.*(2006).
59. Chen,Y., Yu,D.C., Charlton,D., & Henderson,D.R. Pre-existent adenovirus antibody inhibits systemic toxicity and antitumor activity of CN706 in the nude mouse LNCaP xenograft model: implications and proposals for human therapy. *Hum. Gene Ther.* **11**, 1553-1567 (2000).
60. Tsai,V. *et al.* Impact of human neutralizing antibodies on antitumor efficacy of an oncolytic adenovirus in a murine model. *Clin. Cancer Res.* **10**, 7199-7206 (2004).
61. Stojdl,D.F. *et al.* VSV strains with defects in their ability to shutdown innate immunity are potent systemic anti-cancer agents. *Cancer Cell* **4**, 263-75 (2003).
62. Ebert,O., Harbaran,S., Shinozaki,K., & Woo,S.L. Systemic therapy of experimental breast cancer metastases by mutant vesicular stomatitis virus in immune-competent mice. *Cancer Gene Ther.*(2004).
63. Ahmed,M., Cramer,S.D., & Lyles,D.S. Sensitivity of prostate tumors to wild type and M protein mutant vesicular stomatitis viruses. *Virology* **330**, 34-49 (2004).
64. Obuchi,M., Fernandez,M., & Barber,G.N. Development of recombinant vesicular stomatitis viruses that exploit defects in host defense to augment specific oncolytic activity. *J. Virol.* **77**, 8843-8856 (2003).
65. Gobet,R., Cerny,A., Ruedi,E., Hengartner,H., & Zinkernagel,R.M. The role of antibodies in natural and acquired resistance of mice to vesicular stomatitis virus. *Exp Cell Biol* **56**, 175-80 (1988).
66. Garcia-Castro,J. *et al.* Tumor cells as cellular vehicles to deliver gene therapies to metastatic tumors. *Cancer Gene Ther.* **12**, 341-349 (2005).
67. Coukos,G. *et al.* Use of carrier cells to deliver a replication-selective herpes simplex virus-1 mutant for the intraperitoneal therapy of epithelial ovarian cancer. *Clin. Cancer Res.* **5**, 1523-1537 (1999).
68. Komarova,S., Kawakami,Y., Stoff-Khalili,M.A., Curiel,D.T., & Pereboeva,L. Mesenchymal progenitor cells as cellular vehicles for delivery of oncolytic adenoviruses. *Mol. Cancer Ther.* **5**, 755-766 (2006).
69. Thorne,S.H., Negrin,R.S., & Contag,C.H. Synergistic antitumor effects of immune cell-viral biotherapy. *Science* **311**, 1780-1784 (2006).
70. Raykov,Z., Balboni,G., Aprahamian,M., & Rommelaere,J. Carrier cell-mediated delivery of oncolytic parvoviruses for targeting metastases. *Int. J. Cancer* **109**, 742-749 (2004).

71. Jevremovic,D. *et al.* Use of blood outgrowth endothelial cells as virus-producing vectors for gene delivery to tumors. *Am. J. Physiol Heart Circ. Physiol* **287**, H494-H500 (2004).
72. Crittenden,M. *et al.* Pharmacologically regulated production of targeted retrovirus from T cells for systemic antitumor gene therapy. *Cancer Res.* **63**, 3173-3180 (2003).
73. Raykov,Z., Balboni,G., Aprahamian,M., & Rommelaere,J. Carrier cell-mediated delivery of oncolytic parvoviruses for targeting metastases. *Int. J. Cancer* **109**, 742-749 (2004).
74. Harrington,K. *et al.* Cells as vehicles for cancer gene therapy: the missing link between targeted vectors and systemic delivery? *Hum. Gene Ther.* **13**, 1263-1280 (2002).
75. Mineta,T., Rabkin,S.D., Yazaki,T., Hunter,W.D., & Martuza,R.L. Attenuated multi-mutated herpes simplex virus-1 for the treatment of malignant gliomas. *Nat. Med.* **1**, 938-943 (1995).
76. Bischoff,J.R. *et al.* An adenovirus mutant that replicates selectively in p53-deficient human tumor cells. *Science* **274**, 373-376 (1996).
77. Coffey,M.C., Strong,J.E., Forsyth,P.A., & Lee,P.W. Reovirus therapy of tumors with activated Ras pathway. *Science* **282**, 1332-1334 (1998).
78. Grote,D. *et al.* Live attenuated measles virus induces regression of human lymphoma xenografts in immunodeficient mice. *Blood* **97**, 3746-3754 (2001).
79. Schiedner,G. *et al.* A hemodynamic response to intravenous adenovirus vector particles is caused by systemic Kupffer cell-mediated activation of endothelial cells. *Hum. Gene Ther.* **14**, 1631-1641 (2003).
80. Hummel,J.L., Safroneeva,E., & Mossman,K.L. The role of ICP0-Null HSV-1 and interferon signaling defects in the effective treatment of breast adenocarcinoma. *Mol. Ther.* **12**, 1101-1110 (2005).
81. Plaksin,D. *et al.* Effective anti-metastatic melanoma vaccination with tumor cells transfected with MHC genes and/or infected with Newcastle disease virus (NDV). *Int. J. Cancer* **59**, 796-801 (1994).
82. Cole,C. *et al.* Tumor-targeted, systemic delivery of therapeutic viral vectors using hitchhiking on antigen-specific T cells. *Nat. Med.* **11**, 1073-1081 (2005).
83. Skalak,R. & Branemark,P.I. Deformation of red blood cells in capillaries. *Science* **164**, 717-719 (1969).
84. Stein,J.V. & Nombela-Arrieta,C. Chemokine control of lymphocyte trafficking: a general overview. *Immunology* **116**, 1-12 (2005).

85. Carlos,T.M. & Harlan,J.M. Leukocyte-endothelial adhesion molecules. *Blood* **84**, 2068-2101 (1994).
86. Fisher,K.D. *et al.* Polymer-coated adenovirus permits efficient retargeting and evades neutralising antibodies. *Gene Ther.* **8**, 341-348 (2001).
87. O'Riordan,C.R. *et al.* PEGylation of adenovirus with retention of infectivity and protection from neutralizing antibody in vitro and in vivo. *Hum. Gene Ther.* **10**, 1349-1358 (1999).
88. Chillon,M., Lee,J.H., Fasbender,A., & Welsh,M.J. Adenovirus complexed with polyethylene glycol and cationic lipid is shielded from neutralizing antibodies in vitro. *Gene Ther.* **5**, 995-1002 (1998).
89. Matthews,C., Jenkins,G., Hilfinger,J., & Davidson,B. Poly-L-lysine improves gene transfer with adenovirus formulated in PLGA microspheres. *Gene Ther.* **6**, 1558-1564 (1999).
90. Pearce,O.M. *et al.* Glycoviruses: chemical glycosylation retargets adenoviral gene transfer. *Angew. Chem. Int. Ed Engl.* **44**, 1057-1061 (2005).
91. Green,N.K. *et al.* Extended plasma circulation time and decreased toxicity of polymer-coated adenovirus. *Gene Ther.* **11**, 1256-1263 (2004).
92. Campbell,R.E. *et al.* A monomeric red fluorescent protein. *Proc. Natl. Acad. Sci. U. S. A* **99**, 7877-7882 (2002).
93. Naldini,L. *et al.* In vivo gene delivery and stable transduction of nondividing cells by a lentiviral vector. *Science* **272**, 263-267 (1996).
94. Pecora,A.L. *et al.* Phase I trial of intravenous administration of PV701, an oncolytic virus, in patients with advanced solid cancers. *J. Clin. Oncol.* **20**, 2251-2266 (2002).
95. Laurie,S.A. *et al.* A phase 1 clinical study of intravenous administration of PV701, an oncolytic virus, using two-step desensitization. *Clin. Cancer Res.* **12**, 2555-2562 (2006).
96. Doronin,K., Shashkova,E.V., May,S.M., Hofherr,S.E., & Barry,M.A. Chemical modification with high molecular weight polyethylene glycol reduces transduction of hepatocytes and increases efficacy of intravenously delivered oncolytic adenovirus. *Hum. Gene Ther.* **20**, 975-988 (2009).
97. Fisher,K.D. *et al.* Polymer-coated adenovirus permits efficient retargeting and evades neutralising antibodies. *Gene Ther.* **8**, 341-348 (2001).
98. Green,N.K. *et al.* Extended plasma circulation time and decreased toxicity of polymer-coated adenovirus. *Gene Ther.* **11**, 1256-1263 (2004).
99. Basu,S., Gerchman,Y., Collins,C.H., Arnold,F.H., & Weiss,R. A synthetic multicellular system for programmed pattern formation. *Nature* **434**, 1130-1134 (2005).

100. Breitbach,C.J. *et al.* Targeted inflammation during oncolytic virus therapy severely compromises tumor blood flow. *Mol. Ther.* **15**, 1686-1693 (2007).
101. Garcia-Castro,J. *et al.* Tumor cells as cellular vehicles to deliver gene therapies to metastatic tumors. *Cancer Gene Ther.* **12**, 341-349 (2005).
102. Hakkarainen,T. *et al.* Human mesenchymal stem cells lack tumor tropism but enhance the antitumor activity of oncolytic adenoviruses in orthotopic lung and breast tumors. *Hum. Gene Ther.* **18**, 627-641 (2007).
103. Butcher,E.C. & Picker,L.J. Lymphocyte homing and homeostasis. *Science* **272**, 60-66 (1996).
104. Qiao,J. *et al.* Purging metastases in lymphoid organs using a combination of antigen-nonspecific adoptive T cell therapy, oncolytic virotherapy and immunotherapy. *Nat. Med.* **14**, 37-44 (2008).
105. Cole,C. *et al.* Tumor-targeted, systemic delivery of therapeutic viral vectors using hitchhiking on antigen-specific T cells. *Nat. Med.* **11**, 1073-1081 (2005).
106. Iankov,I.D. *et al.* Infected cell carriers: a new strategy for systemic delivery of oncolytic measles viruses in cancer virotherapy. *Mol. Ther.* **15**, 114-122 (2007).
107. Ong,H.T., Hasegawa,K., Dietz,A.B., Russell,S.J., & Peng,K.W. Evaluation of T cells as carriers for systemic measles virotherapy in the presence of antiviral antibodies. *Gene Ther.* **14**, 324-333 (2007).
108. Tsai,V. *et al.* Impact of human neutralizing antibodies on antitumor efficacy of an oncolytic adenovirus in a murine model. *Clin. Cancer Res.* **10**, 7199-7206 (2004).
109. Chen,Y., Yu,D.C., Charlton,D., & Henderson,D.R. Pre-existent adenovirus antibody inhibits systemic toxicity and antitumor activity of CN706 in the nude mouse LNCaP xenograft model: implications and proposals for human therapy. *Hum. Gene Ther.* **11**, 1553-1567 (2000).
110. Coukos,G. *et al.* Use of carrier cells to deliver a replication-selective herpes simplex virus-1 mutant for the intraperitoneal therapy of epithelial ovarian cancer. *Clin. Cancer Res.* **5**, 1523-1537 (1999).
111. Ikonomou,L., Schneider,Y.J., & Agathos,S.N. Insect cell culture for industrial production of recombinant proteins. *Appl. Microbiol. Biotechnol.* **62**, 1-20 (2003).
112. Hallak,L.K., Merchan,J.R., Storgard,C.M., Loftus,J.C., & Russell,S.J. Targeted measles virus vector displaying echistatin infects endothelial cells via alpha(v)beta3 and leads to tumor regression. *Cancer Res.* **65**, 5292-5300 (2005).

APPENDICES

APPENDIX I. TAMING THE TROJAN HORSE: OPTIMIZING DYNAMIC CARRIER CELL/ONCOLYTIC VIRUS SYSTEMS FOR CANCER BIOTHERAPY

Contribution of Authors: AT Power wrote the review with feedback from JC Bell.

Published: Gene Therapy. 2008 May; 15(10):772-9.



REVIEW

Taming the Trojan horse: optimizing dynamic carrier cell/oncolytic virus systems for cancer biotherapy

AT Power and JC Bell

Centre for Cancer Therapeutics, Ottawa Health Research Institute, University of Ottawa, Ottawa, Ontario, Canada

Live cells offer unique advantages as vehicles for systemic oncolytic virus (OV) delivery. Recent studies from our laboratory and others have shown that virus-infected cells can serve as Trojan horse vehicles to evade antiviral mechanisms encountered in the bloodstream, prevent uptake by off-target tissues and act as microscale factories to produce OV upon arrival in tumor beds. However, to be employed effectively, OV-infected cells are best viewed as dynamic biological systems rather than static therapeutic agents. The time-dependent processes of infection and in vivo cell trafficking will inevitably vary depending on which particular OV is being delivered, as well as the type of carrier cells (CC) employed. Understanding these parameters with respect to each unique CC/OV combination will therefore be required in order to effectively evaluate and harness their potential in preclinical study. In the following review, we

discuss how early studies of OV delivery led us to investigate the use of cell carriers in our laboratory, and the approaches we are currently undertaking to compare the dynamics of different CC/OV systems. On the basis of these studies and others it is apparent that the success of any cell-based system for OV delivery rests upon the coordinated timing of three sequential phases—(1) ex vivo loading, (2) stealth delivery and (3) virus production at the tumor site. While at the current time, the timing of these processes are coupled to the natural cycle of infection and in vivo trafficking properties innate to each cell virus system, a quantitative delineation of their dynamics will lay the foundation for engineering CC/OV biotherapeutic systems that can be clinically deployed in a highly directed and controlled manner.

Gene Therapy (2008) 15, 772–779, doi:10.1038/gt.2008.40, published online 27 March 2008

Keywords: vesicular stomatitis virus, oncolytic virus, cancer therapeutics, immunity, cell-based delivery, biotherapeutics

Barriers to oncolytic virus delivery: lessons from the study of oncolytic vesicular stomatitis virus

A number of different oncolytic virotherapeutics have been developed to date, preclinical data regarding their unique mechanisms of tumor-specific replication, killing and potential to induce antitumor immunity have been reviewed previously,¹ as has the recent experience with some of these agents in clinical trials.² Work in our laboratory initially uncovered that innate immune-signaling pathways are defective in many types of cancer cells, rendering them particularly susceptible to infection and cytolysis by vesicular stomatitis virus (VSV).³ These findings prompted us to further investigate the oncolytic capacity of attenuated VSV strains in immunocompetent murine models.⁴ Although lasting disease remission could often be achieved following systemic administration, it was also apparent from these studies that there are unique challenges to achieving VSV delivery *in vivo*.

Innate barriers to systemic OV delivery

The circulatory system is an unwelcoming environment for any virus. However, it remains the best avenue for delivering therapeutics to undetectable or physically inaccessible sites of tumor metastasis. Understanding the impact of innate and acquired immune barriers to systemic OV delivery has therefore been an area of intense research in recent years. Our laboratory has focused on modeling the OV-host interactions that influence intravenous (i.v.) delivery of oncolytic VSV (AV1) in immunocompetent animals.^{4–6}

Early investigations in this system revealed that successful delivery to both lung and hind flank tumors could be achieved when acceptable therapeutic doses (at least 100-fold below maximum tolerated dose) were i.v. administered to naive animals.⁴ Viral titers, fluorescent transgene expression and immunohistochemical analysis independently confirmed successful delivery and amplification of virus within tumors.⁶ However, subsequent biodistribution experiments revealed that i.v. delivery was far from efficient—<0.001% of the administered virions were found to reach hind flank tumors, as the vast majority of the input dose was immediately taken up from the circulation by the liver and spleen.⁶ These organs also act as innate barriers to delivery in other OV systems, an effect generally attributable to phagocytic uptake by resident macrophages of the reticuloendothelial system.⁷

Correspondence: Dr JC Bell, Centre for Cancer Therapeutics, Ottawa Health Research Institute, University of Ottawa, 503 Smyth Road, Ottawa, Ontario, Canada K1H 8L6

E-mail: jbell@ohri.ca

Received 14 February 2008, accepted 16 February 2008, published online 27 March 2008

These studies revealed that although *iv* delivery of VSV was less than perfect even in naive animals, sufficient infectious virus could reach the tumor to initiate a robust infection and mediate a significant therapeutic response⁴ Thus innate barriers, while highly effective at clearing virus from the bloodstream, can ultimately be overwhelmed at VSV doses well within the practical limits of safety and manufacturing capacity

Adaptive barriers to systemic OV delivery

Unlike conventional therapeutics, the pharmacokinetic parameters of OV delivery change over time as treated animals mount an adaptive immune response Thus, having established that VSV could be delivered to tumors in naive animals, we were next interested in examining how adaptive defenses might affect repeat dosing regimens In this respect, the murine balb/c model has provided a useful model, as VSV infection induces a rapid and robust B- and T-cell response, leading to the formation of high-titer antiviral antibodies that play a crucial role in virus clearance^{8–10}

We found that the recombinant oncolytic strain of VSV developed in our laboratory (AV1) induced serum neutralizing antibodies with kinetics indistinguishable from the previously reported responses to wild-type strains⁵ VSV-neutralizing antibodies were detectable at least as early as 4 days following treatment with a single virus dose and reached peak levels (1/3200–1/6400) within 2–3 weeks, remaining at these elevated levels for at least several months Administration of repeated doses served to further boost antibody levels, leading to a two- to fourfold increase in plateau titers Consequently, we found that the evolution of this antibody response is a serious impediment to VSV delivery In contrast to the case of naive animals, VSV delivery was completely ablated in mice that had received a previous dose of the virus up to several months in advance, as we reproducibly found a lack of detectable virus transgene expression or viral titers in tumors⁵ Passive transfer experiments revealed that this adaptive state of sterilizing immunity to VSV treatment was mediated by serum antibodies, whereas adoptively transferred T cells had no impact⁵ Immune serum containing anti-VSV antibody was similarly potent *in vitro*, able to neutralize an entire therapeutic dose (approximately 10e8 PFUs (plaque-forming units)) at a 1/10 dilution (AT Power and JC Bell, unpublished data) Unlike the innate barriers discussed in the preceding section, it was not possible to saturate and overwhelm this induced antibody at sublethal virus doses *in vivo* (AT Power and JC Bell, unpublished data)

Thus antiviral antibodies are induced during treatment and intercept therapeutic virus even before it reaches the tumor Long-lived immunological memory is activated, leading to elevated antibody titers capable of mitigating *iv* delivery for months, if not years after the initiation of treatment These findings suggested that a carrier system capable of concealing viral antigen en route to the tumor site might be the best way to achieve consistent delivery of repeated OV doses in the face of evolving adaptive immunity

Carrier cells: Trojan horse vehicles for systemic OV delivery

Early *in vivo* experimentation with OVs had suggested that infected virus-producing cells could also mediate antitumor effects when administered in the place of naked virions^{3,11} This hinted that cellular carriers might be used as Trojan horse vehicles to shield OV from neutralization following systemic administration, and act as *in situ* virus factories once arriving at the tumor site Having established a reliable murine system to model OV therapy in the context of evolving host immunity,^{4,5} we were able to put this concept to the test We hypothesized that carrier cells (CCs), infected *ex vivo* and then infused *iv*, would enable escape from antiviral defenses if they could reach the tumor site during eclipse phase (prior to viral protein synthesis and virion release) and subsequently release progeny virions to infect surrounding cancer cells Early studies indicated that this was indeed the case, as we saw that infected cells delivered virus to murine lung tumors to establish a robust infection of the malignant tissue⁵ More importantly, cellular delivery and subsequent tumor infection was unaffected by the presence of circulating antiviral antibody at high titers that entirely neutralized delivery of naked virions⁵ These experiments provided exciting proof-of-concept that infected cells could indeed act as Trojan horse vehicles to smuggle an OV, such as VSV, past circulating antibody molecules into tumor beds

Similar studies by other groups have shown that cell carriers can also deliver oncolytic measles virus to tumors in the presence of virus-neutralizing antibody^{12,13} However, Ong *et al*¹² observed that this effect was antibody dose-dependent in their system, as tumor infection remained unattainable at higher concentrations of human neutralizing antibody even when carriers were used Failure to infect tumors at high antibody concentrations could have been a result of neutralization of carriers cells prematurely expressing viral surface proteins within the bloodstream, as the kinetics of measles antigen expression were not considered in this study It could also be a result of the general inefficiency of delivery with the particular cell type examined, as the primary T-cell carriers did not release progeny virus, but rather relied on direct cell contact to transfer infectivity by fusion with tumor cells Additionally, only 15% of virus-loaded T cells accumulated in the target tumor tissue in the model used for these experiments

In contrast, more efficient CC delivery may help to overcome antiviral immunity In the VSV system, we have observed robust antibody escape using highly virus-permissive carcinoma cell carriers,⁵ which are capable of producing upward of 100 progeny virions per cell (AT Power and JC Bell, unpublished data) Furthermore, these types of solid tumor-derived carriers accumulated primarily at the site of the target tumors (in the lungs) following *iv* administration in these experiments⁵

Comparing these studies highlights the fact that successful cell-based delivery of OV is highly dependent on the kinetics of virus replication, the *in vivo* trafficking properties of the CCs and the quantity of virions the cells can produce Numerous different CC/OV combinations are currently under investigation^{5,11–19} and in essence,

each represents a unique biotherapeutic system for which these time-dependent parameters must be considered to achieve optimal tumor delivery. In the remainder of this article, we discuss the main conditions that must in theory be met to achieve true Trojan horse OV delivery, and relate some of the lessons learned from our ongoing efforts to evaluate the properties of various established cell lines as VSV carriers.

Timing is of the essence: three critical phases for successful cell-based delivery of the OV payload

Ultimately the success or failure of any cellular OV delivery system rests on the proper coordination of three critical phases in both space and time, as illustrated in Figure 1. First, loading of the CCs is carried out *ex vivo*, second, delivery of cells to the tumor site is achieved via the circulation and third, release of virus must occur within the tumor bed. Once initiated, the timing of this sequence is inextricably linked to that of the OV life cycle within the particular cell type used for delivery. A detailed understanding the dynamics of these processes is therefore required to ensure that CCs reach the right place at the right time.

Phase I: *ex vivo* loading

Essentially the goal of the *ex vivo* loading phase is to productively infect as many CCs as possible in the shortest possible time. The reasoning for this is fairly straightforward; the more CCs infected, the greater the proportion of injected cells that will be capable of bringing virus to the tumor, and in turn the higher the potential oncolytic dose. Therefore cells must be exposed to virus for sufficient time for uptake to occur but no longer, as increasing the amount of time that passes before injection increases the likelihood that viral antigen expressed on the cell surface will be exposed to host antibodies during the stealth delivery phase (Figure 1; also see phase II below).

For each CC/OV system the efficiency of a given loading protocol is readily assessed by counting the proportion of cells that express viral protein during the first infection cycle following uptake. Flow cytometric analysis of viral transgene expression provides a useful tool for such analysis. In our studies, infection of adherent CC lines with VSV at an MOI (multiplicity of infection) of 10 PFUs per cell led to nearly 100% loading after a period of 1 h (AT Power and JC Bell, unpublished data). However, loading of non-adherent cell lines, necessary to study leukocyte carrier systems, appears to be less efficient. For example, suspension of Jurkat cell lines in 10 PFUs per cell of VSV (10^6 cells per ml) for the

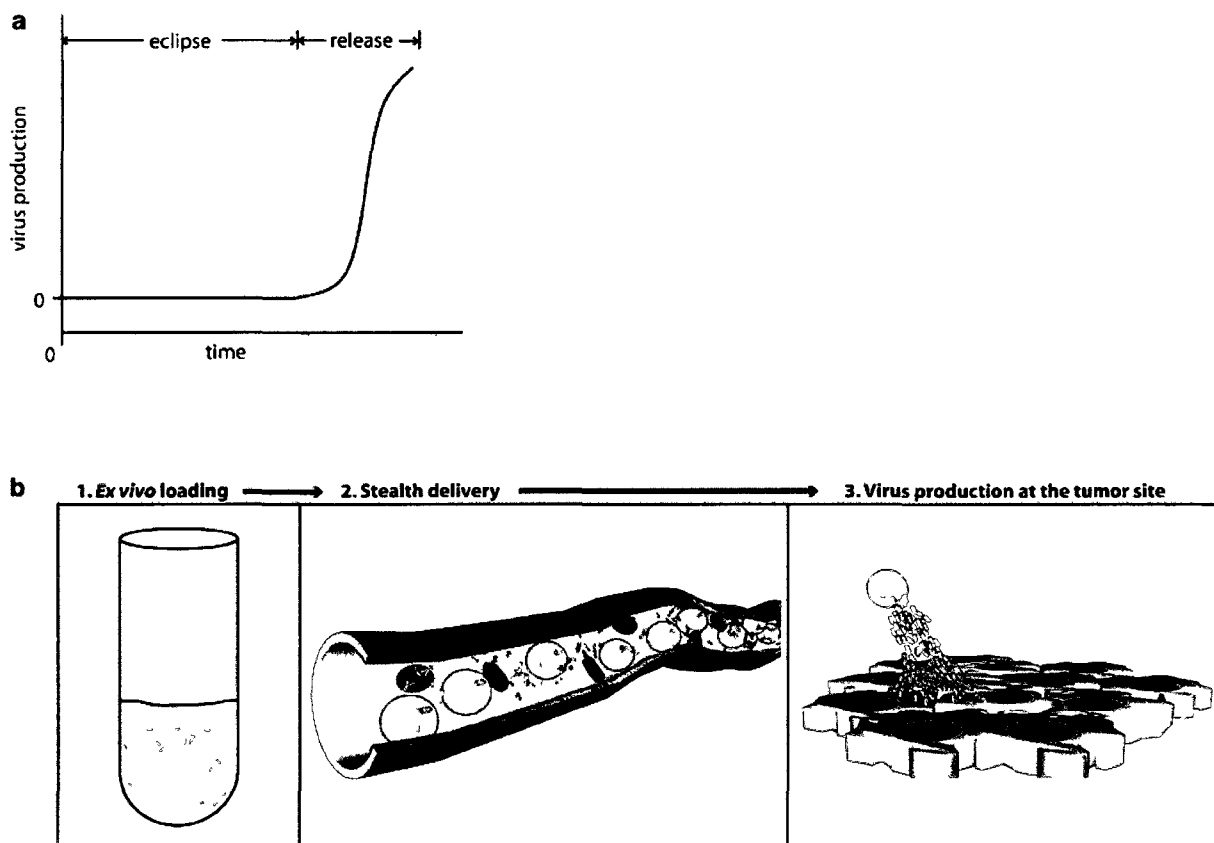


Figure 1 Three sequential phases are critical for carrier cell (CC)-based delivery of replicating oncolytic viruses (OV). (a) Typical kinetics of OV growth within permissive CCs. Following addition of virus at $t = 0$, cellular carriers undergo an eclipse period prior to the onset of viral protein synthesis, exponential amplification and release of progeny virions. (b) Three sequential phases of CC/OV delivery, mapped to their ideal timing within the viral growth cycle shown as in a).

same 1 h leads to uptake and infection of only 67% of the total cell population (Figure 2) Lengthening the loading phase or enhancing uptake by other means, such as centrifugation, may therefore be necessary to maximize loading of non-adherent leukocytic CCs In addition to variation between CC types, optimal uptake conditions are likely to vary between OV, for example, standard infection protocols for *Vaccinia virus* infection typically specify 2 h rather than the 1 h routinely used for VSV

While the optimizing the efficiency of virus uptake may seem of trivial importance with respect to therapy *in vivo*, it is in fact a crucial consideration for achieving effective immune evasion and tumor delivery Once they are injected into the circulation, premature expression of viral protein on the surface of CCs is likely to betray the presence of the OV payload hidden within, allowing antiviral antibodies to bind and target the Trojan horse vehicle for destruction by complement proteins, phagocytes or cytotoxic cells The length of this eclipse or latent period is therefore an important parameter to consider for each different CC/OV system In our initial immune evasion studies using carcinoma carriers to deliver VSV,⁵ *ex vivo* loading followed by western blotting analysis revealed minimal viral protein synthesis within the first 3 h of infection Therefore in subsequent experiments this data were used to guide the timing of loading, harvesting and administration of CCs to animals, and we found that cells injected into mice 2–3 h following infection could successfully avoid neutralization by antiviral antibodies⁵ As various other CC/OV systems are explored, therapeutically relevant measurement of antigen exposure kinetics could also be achieved by analyzing antiviral antibody binding to the CC surface by flow cytometry In summary, the timing of OV protein expression in infected CCs specifies the maximum allowable time for

ex vivo loading Determination of this crucial parameter therefore allows optimal CC loading and therapeutic administration to be achieved within a time window that will not compromise the stealth of these Trojan horse vehicles

Phase II: stealth delivery

This phase involves stealthy passage of OV-laden cells through the circulation and their arrival within tumor deposits (Figure 1) As for phase I, the timing of the oncolytic viral life cycle is a crucial determinant of the success of this phase To achieve true, 'direct-to-tumor' virus delivery requires that CCs accumulate in tumor beds before progeny virions are released Furthermore, to act as Trojan horse vehicles and successfully evade antiviral antibody, CCs should ideally reach the tumor site even before viral antigen is displayed on their surface To ensure that infected CCs arrive at their tumor destination on time, it is necessary to understand the kinetics of their dissemination following systemic administration

For example in the case of VSV, permissive cell types produce substantial amounts of viral protein by 6 h or less postinfection, so CCs will have ideally arrived at their destination before this time We have relied on bioluminescent imaging (BLI) to track the biodistribution of CCs in real time following *iv* administration to mice Using this approach we initially transduced several solid tumor cell lines with a lentivirus encoding *Renilla* luciferase and found that they exhibited similar biodistribution patterns—rapid accumulation and arrest in lung tissue within 30 min following tail-vein injection, where they remained for at least another 24–48 h⁵ In the same experiments, tumor-specific expression of a viral

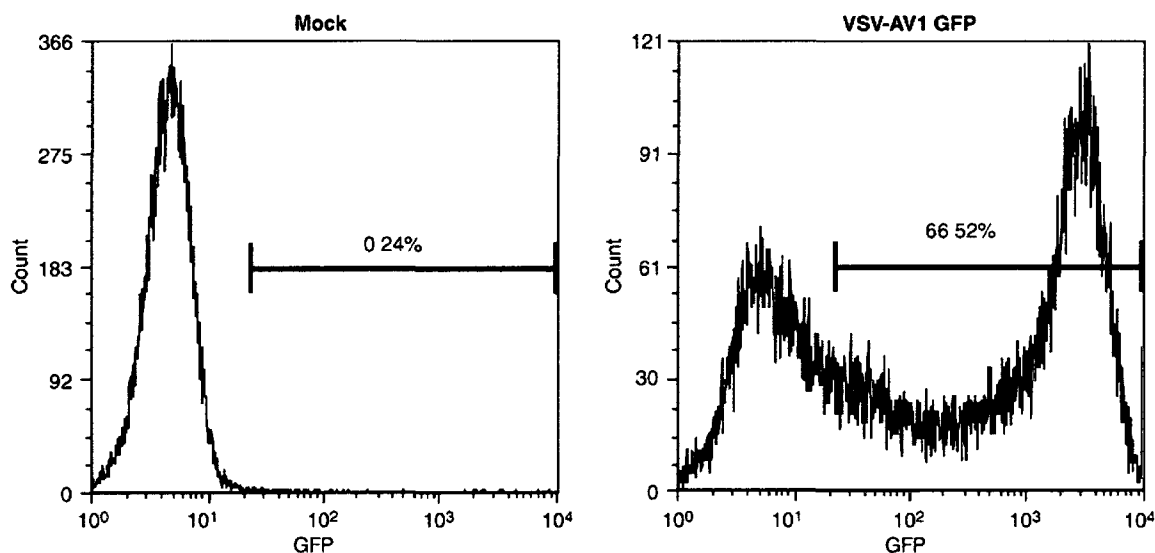


Figure 2 Assessing *ex vivo* loading of leukocytic carrier cells (CC) Jurkat human T cells were suspended in 10 PFUs (plaque forming units) per cell vesicular stomatitis virus (VSV) AV1-green fluorescent protein (GFP) for 1 h at a concentration of 10⁶ cells per ml Cells were then pelleted, washed twice with 10 ml phosphate-buffered saline, resuspended in 10 ml Dulbecco's modified Eagle's medium (DMEM)+10% fetal calf serum and incubated at 37 °C for an additional 7 h Mock or VSV AV1 GFP-infected cells were analyzed by flow cytometry and percentages of GFP-positive cells are shown on each histogram

by BLI, accumulated, like solid tumor lines, exclusively within lung tissue (Figure 3b). Therefore the ability to circulate through blood vessels may be a property of some, but not all types of leukocytic carriers.

In general, these examples demonstrate one important lesson learned from experiments to date—different CC lineages can exhibit quite distinct patterns of dissemination when injected into blood vessels. We are continuing to investigate these patterns using a large panel of different murine and human leukemia cell types to learn which variables—such as cell size or cell surface adhesion receptor expression profiles—determine innate CC tropisms. It would also be desirable to engineer CCs targeted specifically to the tumor microenvironment, which could be achieved by introducing cell surface proteins that bind receptors on neovasculature or the tumor cell surface such as those that have been designed to retarget the tropism of virotherapeutics previously.^{20–26}

Another issue that has been illuminated by our BLI studies is the clearance kinetics of histoincompatible CC lines. Although both allogeneic and xenogeneic (human) cell lines appear equally capable of delivering VSV to lung tumors in mice, bioluminescent signal from allogeneic lines persisted for up to 24–48 h (Figure 3a, Power *et al.*⁵), whereas xenogeneic carriers seem to be cleared more rapidly, within <8 h of administration to mice (Figure 3b, Power *et al.*⁵). These findings are consistent with known mechanisms of immunological rejection—activation of adaptive T-cell responses are required for allograft rejection, whereas xenografts can be targeted much more rapidly by innate circulating factors such as natural antibodies and complement proteins.²⁷ Although this clearance did not limit VSV delivery to tumors in the lung model we have examined, as OV release occurred before CCs were eliminated, if loaded with a slower-replicating OV virus or used to target tumor sites that take longer to access, rapidly cleared xenogenic cells might not have the opportunity to deliver their cargo to the tumor site. It also remains to be seen whether allo/xenogeneic carriers induce an adaptive response that might inhibit delivery with repeated dosing.

Although there is certainly more to learn, BLI has already provided valuable insight into the dynamics of CC delivery *in vivo*. Noninvasive molecular imaging technology should continue to be extremely useful as we seek to manipulate CC tropism to promote timely infiltration of tumor beds at diverse anatomical locations.

Phase III: virus production at the tumor site

Upon reaching the tumor bed, the role of each CC shifts from delivery vehicle to *in situ* OV factory (Figure 1). Depending on the CC/OV combination, each OV-infected cell may release a localized burst of up to hundreds of viral particles (as in production of VSV by permissive carrier lines). This unique ability offers the potential for significant dose amplification following delivery to the target tissue if cell types capable of high viral productivity are employed.

As for other parameters, the total quantity and kinetics of virus release is a unique property of each CC/OV combination. To evaluate candidate CC types, this variable is readily measured by loading the cells and following virus production *in vitro*. For the sake of comparing virus production between candidate carrier lines, it is straightforward to measure the average number of virions released per cell over time to construct classic one-step growth curves. Applying this analysis to some of the CC lines used to deliver oncolytic VSV in our laboratory, we have measured an average productivity on the order of 100–200 PFUs per cell following infection of permissive carcinoma cell lines of either human or murine origin (AT Power and JC Bell, unpublished data). In contrast, permissive leukemia cell lines grown in suspension culture have shown a trend toward lower productivity, on the order of 10–90 PFUs per cell, when infected at comparable MOIs (AT Power and JC Bell, unpublished data). However as discussed under the topic of cell loading, the efficiency of viral uptake also appears to be much diminished when cells are infected in suspension, since even at high MOIs (≥ 10 PFUs per cell) we have seen that *ex vivo* uptake is often submaximal (Figure 2, AT Power and JC Bell, unpublished data). Thus to accurately measure the average productivity of each candidate CC line, it is important to also determine the efficiency of uptake under the relevant infection conditions, which should ideally be as close as possible to 100%.

Despite the limitations of these studies to date, they also highlight differences between normal and transformed carriers. As discussed above, the activated primary T cells used as carriers as described by Ong *et al.*¹² produced no detectable measles virus progeny, despite showing synthesis of the green fluorescent protein (GFP) viral transgene. In a direct comparison, Iankov and co-workers also reported decreased oncolytic measles virus productivity in normal cell types compared to transformed cell lines.¹³ So although autologous primary cell carriers offer attractive benefits in terms of safety and immunological compatibility, special pharmacological or genetic manipulation may be necessary before they can be effectively used to produce OVs that have been engineered to replicate preferentially in transformed cells. In contrast, transformed cell lines generally produce large quantities of OV and are therefore immediately available as robust carriers for preclinical and clinical studies.

A final issue that may be relevant to future studies of CC populations is that of cell to cell variation in viral production capacity. Heterogeneous gene expression profiles within CC populations, for example due to variation in differentiation or cell cycle stage, could lead to differences in the quantity of progeny virions produced by each cell. It remains unknown whether such heterogeneity is characteristic of the types of CCs currently under study, as it is a rather cumbersome task to quantitate viral production by single cells of infected populations. Nonetheless such analysis is possible using basic virological techniques, and has indeed been used in the past to illuminate subpopulations of cultured cells with marked differences in viral productivity.²⁸ Cell to cell differences in viral productivity would have an impact on their utility as carriers *in vivo*, as each is likely to behave as an independent virus factory following

delivery to a particular region of the tumor. Depending on the source of any such heterogeneity, measures such as cell cycle synchronization or fluorescence-activated cell sorting might be used to ensure that each CC administered is capable of maximal virus production upon arrival at the tumor.

Prospects for the future: toward programming dynamic CC/OV systems

The above has outlined some of the important points to consider in evaluating and comparing the potential of different cell types as OV carriers. Currently, efforts in our laboratory are focused on applying this framework to compare a large panel of established cell lines of solid tissue and hematological origin. Taken together with the results of other studies (reviewed in Power and Bell¹⁹) that have examined cytokine-induced killer cells,¹⁴ primary leukocytes,^{12,13} mesenchymal stem cells^{15,16} and tumor antigen-specific T cells,²⁹ some of the key issues associated with the cell-based delivery approach are already beginning to become apparent. With respect to tumor targeting, for example, it is clear that many cell types are severely hampered by their inability to pass through capillary beds, causing accumulation within nontumor-bearing tissues.^{5,16} Several studies however have indicated that leukocytic carriers are better able to circulate,^{5,12,14} and therefore these cell types would seem the best platform for further efforts to refine the specificity of tumor targeting.

Ongoing study in this vein will allow the beneficial properties of diverse natural cell types to be exploited as systemic OV carriers, and will also delineate areas for further improvement. As our expertise in engineering biological systems grows, this knowledge could be used to move us closer toward reprogramming the natural trafficking and virus production dynamics of CC/OV systems so as to ensure efficient execution of each sequential stage of delivery (Figure 1). This avenue of research should therefore continue to be a fruitful one, as the CC approach opens up many new angles from which to attack the ultimate challenge of achieving controlled, reliable delivery of OVs to metastatic tumor deposits in humans.

References

- Parato KA, Senger D, Forsyth PA, Bell JC. Recent progress in the battle between oncolytic viruses and tumours. *Nat Rev Cancer* 2005, **5**: 965–976.
- Liu TC, Galanis E, Kirn D. Clinical trial results with oncolytic virotherapy: a century of promise, a decade of progress. *Nat Clin Pract Oncol* 2007, **4**: 101–117.
- Stojdl DF, Lichty B, Knowles S, Marus R, Atkins H, Sonenberg N *et al*. Exploiting tumor specific defects in the interferon pathway with a previously unknown oncolytic virus. *Nat Med* 2000, **6**: 821–825.
- Stojdl DF, Lichty BD, tenOever BR, Paterson JM, Power AT, Knowles S *et al*. VSV strains with defects in their ability to shutdown innate immunity are potent systemic anti-cancer agents. *Cancer Cell* 2003, **4**: 263–275.
- Power AT, Wang J, Falls TJ, Paterson JM, Parato KA, Lichty BD *et al*. Carrier cell based delivery of an oncolytic virus circumvents antiviral immunity. *Mol Ther* 2007, **15**: 123–130.
- Breitbach CJ, Paterson JM, Lemay CG, Falls TJ, McGuire A, Parato KA *et al*. Targeted inflammation during oncolytic virus therapy severely compromises tumor blood flow. *Mol Ther* 2007, **15**: 1686–1693.
- Fisher K. Striking out at disseminated metastases: the systemic delivery of oncolytic viruses. *Curr Opin Mol Ther* 2006, **8**: 301–313.
- Gobet R, Cerny A, Ruedi E, Hengartner H, Zinkernagel RM. The role of antibodies in natural and acquired resistance of mice to vesicular stomatitis virus. *Exp Cell Biol* 1988, **56**: 175–180.
- Leist TP, Cobbold SP, Waldmann H, Aguet M, Zinkernagel RM. Functional analysis of T lymphocyte subsets in antiviral host defense. *J Immunol* 1987, **138**: 2278–2281.
- Zinkernagel RM, Adler B, Holland JJ. Cell-mediated immunity to vesicular stomatitis virus infections in mice. *Exp Cell Biol* 1978, **46**: 53–70.
- Coukos G, Makrigiannakis A, Kang EH, Caparelli D, Benjamin I, Kaiser LR *et al*. Use of carrier cells to deliver a replication-selective herpes simplex virus 1 mutant for the intraperitoneal therapy of epithelial ovarian cancer. *Clin Cancer Res* 1999, **5**: 1523–1537.
- Ong HT, Hasegawa K, Dietz AB, Russell SJ, Peng KW. Evaluation of T cells as carriers for systemic measles virotherapy in the presence of antiviral antibodies. *Gene Therapy* 2007, **14**: 324–333.
- Iankov ID, Blechacz B, Liu C, Schmeckpeper JD, Tarara JE, Federspiel MJ *et al*. Infected cell carriers: a new strategy for systemic delivery of oncolytic measles viruses in cancer virotherapy. *Mol Ther* 2007, **15**: 114–122.
- Thorne SH, Negrin RS, Contag CH. Synergistic antitumor effects of immune cell-viral biotherapy. *Science* 2006, **311**: 1780–1784.
- Komarova S, Kawakami Y, Stoff Khalil MA, Curiel DT, Pereboeva L. Mesenchymal progenitor cells as cellular vehicles for delivery of oncolytic adenoviruses. *Mol Cancer Ther* 2006, **5**: 755–766.
- Hakkara T, Sarkoja M, Lehenkari P, Miettinen S, Ylikomi T, Suuronen R *et al*. Human mesenchymal stem cells lack tumor tropism but enhance the antitumor activity of oncolytic adenoviruses in orthotopic lung and breast tumors. *Hum Gene Ther* 2007, **18**: 627–641.
- Raykov Z, Balboni G, Aprahamian M, Rommelaere J. Carrier cell-mediated delivery of oncolytic parvoviruses for targeting metastases. *Int J Cancer* 2004, **109**: 742–749.
- Garcia Castro J, Martinez-Palacio J, Lillo R, Garcia-Sanchez F, Alemany R, Madero L *et al*. Tumor cells as cellular vehicles to deliver gene therapies to metastatic tumors. *Cancer Gene Ther* 2005, **12**: 341–349.
- Power AT, Bell JC. Cell-based delivery of oncolytic viruses: a new strategic alliance for a biological strike against cancer. *Mol Ther* 2007, **15**: 660–665.
- Bergman I, Whitaker-Dowling P, Gao Y, Griffin JA. Preferential targeting of vesicular stomatitis virus to breast cancer cells. *Virology* 2004, **330**: 24–33.
- Hallak LK, Merchan JR, Storgard CM, Loftus JC, Russell SJ. Targeted measles virus vector displaying echistatin infects endothelial cells via alpha(v)beta3 and leads to tumor regression. *Cancer Res* 2005, **65**: 5292–5300.
- Morizono K, Xie Y, Ringpis GE, Johnson M, Nassanian H, Lee B *et al*. Lentiviral vector retargeting to P-glycoprotein on metastatic melanoma through intravenous injection. *Nat Med* 2005, **11**: 346–352.
- Nakamura T, Peng KW, Harvey M, Greiner S, Lorimer IA, James CD *et al*. Rescue and propagation of fully retargeted oncolytic measles viruses. *Nat Biotechnol* 2005, **23**: 209–214.
- Buchteit AD, Kumar S, Grote DM, Lin Y, von MV, Cattaneo RB *et al*. An oncolytic measles virus engineered to enter cells through the CD20 antigen. *Mol Ther* 2003, **7**: 62–72.

- 25 Hammond AL, Plemper RK, Zhang J, Schneider U, Russell SJ, Cattaneo R Single-chain antibody displayed on a recombinant measles virus confers entry through the tumor-associated carcinoembryonic antigen *J Virol* 2001, **75** 2087–2096
- 26 Peng KW, Donovan KA, Schneider U, Cattaneo R, Lust JA, Russell SJ Oncolytic measles viruses displaying a single-chain antibody against CD38, a myeloma cell marker *Blood* 2003, **101** 2557–2562
- 27 Schuurman HJ, Pierson III RN Progress towards clinical xenotransplantation *Front Biosci* 2008, **13** 204–220
- 28 Huppert J, Gresland L, Lazar P Heterogeneity of chick embryo cells with regard to Newcastle disease virus multiplication *J Gen Virol* 1974, **23** 281–287
- 29 Cole C, Qiao J, Kottke T, Diaz RM, Ahmed A, Sanchez-Perez L *et al* Tumor-targeted, systemic delivery of therapeutic viral vectors using hitchhiking on antigen-specific T cells *Nat Med* 2005, **11** 1073–1081

**APPENDIX II. IN VIVO VIROTHERAPY AND REPORTER GENE IMAGING OF
MULTIPLE MYELOMA USING AN ATTENUATED VESICULAR STOMATITIS VIRUS
ENCODING THE SODIUM IODIDE SYMPORTER GENE**

Contribution of Authors: AT Power generated the recombinant VSV-NIS used in these studies.

Published: Blood. 2007 Oct 1; 110(7): 2342-50

Radioiodide imaging and radiovirotherapy of multiple myeloma using VSV(Δ 51)-NIS, an attenuated vesicular stomatitis virus encoding the sodium iodide symporter gene

Apollina Goel,¹ Stephanie K. Carlson,^{1,2} Kelly L. Classic,³ Suzanne Greiner,¹ Shruthi Naik,¹ Anthony T. Power,⁴ John C. Bell,⁴ and Stephen J. Russell¹

¹Molecular Medicine Program, ²Division of Radiation Oncology, Department of Radiology, ³Section of Safety, Mayo Clinic College of Medicine, Rochester, MN, and ⁴Ottawa Health Research Institute, University of Ottawa, Canada

Multiple myeloma is a radiosensitive malignancy that is currently incurable. Here, we generated a novel recombinant vesicular stomatitis virus [VSV(Δ 51)-NIS] that has a deletion of methionine 51 in the matrix protein and expresses the human sodium iodide symporter (NIS) gene. VSV(Δ 51)-NIS showed specific oncolytic activity against myeloma cell lines and primary myeloma cells and was able to replicate to high titers in myeloma cells in vitro. Iodide uptake assays showed accumulation of radioactive iodide in VSV(Δ 51)-NIS-in-

fectured myeloma cells that was specific to the function of the NIS transgene. In *bg/nd/* mice with established subcutaneous myeloma tumors, administration of VSV(Δ 51)-NIS resulted in high intratumoral virus replication and tumor regression. VSV-associated neurotoxicity was not observed. Intratumoral spread of the infection was monitored noninvasively by serial gamma camera imaging of ¹²³I-iodide biodistribution. Dosimetry calculations based on these images pointed to the feasibility of combination radiovirotherapy with VSV(Δ 51)-NIS plus ¹³¹I.

Immunocompetent mice with syngeneic 5TGM1 myeloma tumors (either subcutaneous or orthotopic) showed significant enhancements of tumor regression and survival when VSV(Δ 51)-NIS was combined with ¹³¹I. These results show that VSV(Δ 51)-NIS is a safe oncolytic agent with significant therapeutic potential in multiple myeloma. (Blood. 2007;110:2342-2350)

© 2007 by The American Society of Hematology

Introduction

Multiple myeloma is a malignancy of antibody-secreting plasma cells that reside predominantly in bone and bone marrow and secrete a monoclonal immunoglobulin.¹ The disease responds initially to alkylating agents, corticosteroids, and thalidomide, but eventually becomes refractory.² Multiple myeloma remains incurable causing more than 10 000 deaths each year in the United States.³ Although cultured myeloma cells are relatively resistant to radiotherapy in vitro,^{4,5} the malignancy is highly radiosensitive and radiation therapy is routinely used for palliation of pain, neurologic compromise, or structural instability from focal myeloma deposits. Efforts to use radiation as a systemic modality for definitive therapy of myeloma, however, have been problematic because of collateral toxicity to normal tissues especially the bone marrow progenitor cells.^{6,7} Developing novel therapies for multiple myeloma based on the targeted delivery of radioisotopes to sites of active disease may have important clinical implications for myeloma therapy.

Gene transfer using the thyroidal sodium iodide symporter (NIS) gene offers a novel strategy for delivery of radionuclides to disseminated cancer cells.⁸ NIS is a transmembrane protein in thyroid follicular cells that actively mediates iodide uptake to a concentration gradient more than 20 to 40-fold.⁹ Cloning the human NIS cDNA has aided in imaging and therapy of dedifferentiated thyroid cancer and nonthyroid cancers such as glioma, neuroblastoma, melanoma, multiple myeloma, and ovarian, breast, cervix, lung, liver, and colon carcinoma.¹⁰ Tissue-specific NIS

expression has been achieved in various cancer xenografts with minimal toxicity to normal organs by using promoters and enhancers from genes encoding immunoglobulins, prostate-specific antigen, probasin, and mucin-1.¹¹⁻¹⁶

Cancer therapy using oncolytic viruses (oncolytic virotherapy) requires agents that amplify efficiently through replication and spread causing rapid tumor lysis, yet are safe causing minimal toxicity to normal tissue enabling systemic inoculations to treat metastatic cancers.^{17,18} We previously engineered the NIS gene into a lymphotropic, replication-competent attenuated strain of measles virus (MV-NIS)¹⁹ that was subsequently used for oncolytic virotherapy of myeloma xenografts. Intratumoral spread of MV-NIS could be monitored noninvasively by radioiodine imaging and virus-resistant tumors were ablated after administration of ¹³¹I.²⁰ A phase I clinical trial to evaluate the targeting properties of MV-NIS in patients with recurrent or refractory myeloma is ongoing at our institution. Several RNA viruses other than measles virus, including reovirus, Newcastle disease virus, mumps virus, and vesicular stomatitis virus (VSV), are being developed as systemic oncolytic agents for cancer therapy.^{18,21} Each of these viruses has its own distinct cell-targeting mechanism and each one kills tumor cells by a different mechanism and with different kinetics. VSV is a negative-strand RNA virus classified under the family Rhabdoviridae, group vesiculoviruses, that has shown some promise as an antimyeloma agent in published preclinical studies.^{22,23} VSV(Δ 51) is an engineered mutant of VSV in which residue 51 of the matrix

Submitted January 3, 2007; accepted May 10, 2007. Prepublished online as *Blood* First Edition paper, May 21, 2007; DOI 10.1182/blood-2007-01-065573

The publication costs of this article were defrayed in part by page charge

payment. Therefore and solely to indicate this fact, this article is hereby marked "advertisement" in accordance with 18 USC section 1734.

© 2007 by The American Society of Hematology

protein is deleted such that the matrix protein can no longer block the nuclear export of interferon-coding mRNAs. VSV(Δ 51) therefore induces the expression of alpha/beta interferons (IFN- α/β), which prevent the infection from spreading in normal cells, but not in cancer cells.^{24,26}

In the present study, we generated and characterized a novel oncolytic virus, VSV(Δ 51)-NIS. The growth kinetics, oncolytic ability, and virus-encoded NIS transgene function were evaluated *in vitro* in myeloma cell lines and in primary samples from myeloma patients. *In vivo* studies used the 5TGM1 murine myeloma cell line, a variant of 5T33MM that originated spontaneously in aging C57BL/KaLwRij mice.²⁷ Both intratumoral and intravenous administrations of VSV(Δ 51)-NIS showed pronounced oncolytic activity in *bg/nd/xid* mice bearing subcutaneous 5TGM1 myeloma tumors. Intratumoral spread of the VSV(Δ 51)-NIS infection could be noninvasively and serially imaged by planar radioiodine scintigraphy and the data used for dosimetric calculations. In the syngeneic 5TGM1 model, regression of subcutaneous tumors was achieved in immunocompetent mice by intratumoral or intravenous administration of VSV(Δ 51)-NIS, and the potency of this treatment could be further enhanced by subsequent administration of iodine-131 (¹³¹I). Improved survival was also achieved in immunocompetent mice bearing orthotopic 5TGM1 myeloma tumors after radiovirotherapy. Based on its safety, oncolytic potency, and the feasibility of NIS-mediated radioiodine imaging and radiovirotherapy in multiple myeloma models, we believe that VSV(Δ 51)-NIS is a promising experimental agent for the treatment of this disease.

Materials and methods

Cells

Myeloma cell lines were obtained from the American Type Culture Collection (MPC-11, CCL-167, ATCC, Manassas, VA), or were from Dr Rafael Fonseca (JIN-3, MM1) or Dr Diane Jelinek (RPMI 8226, KAS 6/1) at the Mayo Clinic (Rochester, MN). These were grown in RPMI 1640 supplemented with heat-inactivated 10% fetal bovine serum, 100 U/mL penicillin, and 100 mg/mL streptomycin. KAS 6/1 cells were supplemented with interleukin-6 (IL-6, 1 ng/mL). The 5TGM1 murine myeloma cell line (Dr Babatunde O. Oyajobi, University of Texas Health Science Center at San Antonio, TX) was grown in Iscove-modified Dulbecco media with 10% fetal bovine serum and penicillin-streptomycin antibiotics. African green monkey kidney cells (CCL-81, Vero) and mouse bone marrow stromal cells (SR-4987, CRL-2028) from ATCC were maintained in Dulbecco-modified Eagle medium containing 10% fetal bovine serum. Normal human skin fibroblasts (GM-5659D) were from the Coriell Institute for Medical Research (Camden, NJ). Primary cells (CD138⁺ myeloma cells and CD138⁻ or normal bone marrow progenitor cells) were obtained from the bone marrow of patients with advanced myeloma disease.⁵ All tissue culture reagents were purchased from Gibco BRL (Rockville, MD).

Viruses

Polymerase chain amplification of human NIS has been described before.²⁰ VSV(Δ 51)-NIS was generated using the established method of reverse genetics.²⁸ Briefly, the VSV(Δ 51)-NIS genome was constructed by subcloning NIS cDNA into a plasmid encoding VSV(Δ 51) at *XhoI/NheI* restriction sites within an extra cistron between the G and L genes.²⁶ This plasmid was used to rescue a recombinant VSV(Δ 51)-NIS virus as described previously.²⁸ VSV(Δ 51)-green fluorescent protein (GFP) contains an extra cistron-encoding GFP inserted between the G and L sequences.²⁹ VSV-GFP (Indiana strain)²⁹ was provided by Dr Glen N. Barber, University of Miami School of Medicine, Miami, Florida.

For amplification of recombinant VSVs (rVSVs), Vero cells were plated at a density of 1.5×10^6 cells/flask. Cells were infected the next day at a multiplicity of infection (MOI) of 0.01 for 1 hour. Virus was then removed and cells were incubated at 37°C in a CO₂ incubator until complete virus-induced cytopathic effect were seen. Culture medium was harvested, subjected to low-speed centrifugation, and filtered through a 0.45- μ m filter. The supernatant was loaded on top of sucrose (10% w/v) and centrifuged at 70 000g for 2 hours to pellet the particles. For virus titration, Vero cells were grown on 96-well plates (7×10^3 cells/well/0.05 mL) and infected with 0.05 mL of serially diluted virus stock. Cells were incubated at 37°C in a CO₂ incubator. Tissue culture infectious dose (TCID₅₀) values were determined by the Spearman and Karber equation: $\text{Log}_{10}(\text{TCID}_{50}/\text{mL}) = L + d(s - 0.5) + \log_{10}(1/v)$ as described before.³⁰ Virus stocks were stored at -80°C.

In vitro cytotoxic activity

Cytotoxicity of VSV(Δ 51)-NIS on human and mouse myeloma cell lines was measured using the standard method of MTT [3-(4,5-dimethylthiazolyl)-2,-5-diphenyltetrazolium bromide] assay as described before.^{5,31} Briefly, cells were mock-infected or infected with VSV(Δ 51)-NIS (MOI = 1.0, 30 minutes at 37°C), unabsorbed virus was washed out, and cells were seeded into 96-well microplates at 10^4 cells per well in 0.1 mL medium. Plates were incubated for 24 or 48 hours, followed by the addition of 0.1 mL of MTT to each well. The mixture was incubated for 3 hours at 37°C. Formazan was extracted from the cells with 0.1 mL detergent and the color intensity was measured with a microplate enzyme-linked immunosorbent assay reader. Experiments were performed in triplicate. Results were recorded as percentage absorbance relative to untreated control cells and used to calculate cell death by VSV(Δ 51)-NIS.

In vitro ¹²⁵I uptake studies

Iodide uptake studies were performed as described before.²⁰ Cells (5TGM1 or Vero, 1.5×10^5 cells/well) were plated into 12-well plates. The next day, cells were washed and incubated in serum-free Dulbecco-modified Eagle medium with VSV(Δ 51)-NIS at an MOI of 1.0. After 30 minutes of incubation at 37°C, cells were washed and the medium was replaced with complete Iscove-modified Dulbecco media (5TGM1) or complete Dulbecco-modified Eagle medium (Vero) and incubated at 37°C for 48 hours before ¹²⁵I uptake. Cells were washed with Hanks balanced salt solution containing 10 mM HEPES [4-(2-hydroxyethyl)-1-piperazineethanesulfonic acid]. All wells, including the mock-infected wells, were incubated with an activity of 10^5 counts per minute (cpm) sodium-125 (Na¹²⁵) I/0.1 mL in 1 mL Hanks balanced salt solution containing HEPES. In controls, 100 μ M KClO₄ was added to inhibit NIS-mediated iodide influx. Plates were incubated at 37°C for 45 minutes and then transferred to ice to inhibit the efflux after removal of I⁻ from the medium. Cells were washed twice with ice-cold Hanks balanced salt solution containing HEPES buffer. Cells were lysed with 1 M NaOH and the activity in the lysis buffer was determined by gamma counting. All data points were measured in triplicate and displayed as means plus or minus the SEM.

In vivo experiments

Animal studies were approved by the Animal Care and Use Committee, Mayo Clinic. Beige/nude/X-linked immunodeficient (*bg/nd/xid*, NIH background) mice at 5 to 8 weeks of age were purchased from Harlan Sprague Dawley (Indianapolis, IN) and immunocompetent C57BL/KaLwRij mice (4- to 6-week-old) were purchased from Harlan CPB (Horst, The Netherlands). For subcutaneous engraftment mice were injected with 5×10^6 5TGM1 cells subcutaneously and blindly randomized to experimental and control groups. Serial caliper measurements of perpendicular diameters were used to calculate tumor volume using the following formula: (shortest diameter)² \times (longest diameter) \times 0.52. All VSV(Δ 51)-NIS treatment began after development of measurable tumors on day 7 (tumor measurements averaged 100 mm³). Two doses of VSV(Δ 51)-NIS were administered either intratumorally or intravenously on days 8 and 9 after cell implantation while the control group received phosphate-buffered saline (PBS, pH 7.4,

intratumorally) or VSV(Δ 51)-GFP (intratumorally). The virus dose was 5×10^7 TCID₅₀/mouse/dose/0.1 mL for bg/nu/xid and 2.5×10^8 TCID₅₀/mouse/dose/0.1 mL for C57BL/KaLwRij mice. In radiotherapy experiment, ¹³¹I (1 mCi/37 MBq) was administered intraperitoneally on day 10 after tumor implantation in specific groups. Mice were observed daily for signs of toxicity and weighed weekly. Animals were killed by CO₂ asphyxiation if the tumors became necrotic or grew to more than 10% of the mouse's weight. In the orthotopic 5TGM1 myeloma model, VSV(Δ 51)-NIS (2.5×10^8 TCID₅₀/mouse/dose/0.1 mL) was administered intravenously on days 12 and 13 after intravenous injection of 5×10^6 5TGM1 cells (myeloma burden is approximately 30% in bone marrow).³¹ ¹³¹I was administered intraperitoneally on day 14. Myeloma paraprotein (IgG2b) levels were measured on days 12 and 29 days, respectively, after cell engraftment as described before.³¹

In a separate experiment, bg/nu/xid mice (n = 6) were killed on days 1 and 3 after virus infusion into the tail vein, tumors were harvested aseptically, and weighed. Tumors were then mechanically minced using frosted glass slides. Cellular debris was removed by low speed centrifugation and virus titers were determined by limiting dilution on Vero cells. For toxicity studies, bg/nu/xid mice (n = 5/group) were injected with 0.2 mL PBS containing VSV-GFP, VSV(Δ 51)-NIS, or VSV(Δ 51)-GFP via tail vein injection. Mice were monitored for weight loss, liver or kidney damage, and signs of neurotoxicity such as huddling behavior, respiratory distress, and hind limb paralysis.

Histology and immunohistochemical staining

The bg/nu/xid mice were killed on days 1 and 4 (n = 4/group/time point) after virus administration, and their tumors were fixed in 4% formaldehyde overnight and paraffin embedded. Serial sections (4 μ m) were used for either hematoxylin and eosin staining or immunohistochemistry using polyclonal rabbit antibodies against VSV glycoprotein-G (provided by Dr John C. Bell, University of Ottawa, Canada). Other reagents were from a Vectastain antirabbit kit (Vector Laboratories, Burlingame, CA). Endogenous peroxidase activity was blocked by incubating with 3% H₂O₂ followed by blocking of nonspecific epitopes with normal goat serum. Sections were incubated with anti-VSV-G antibody (1:5000, 1 hour), followed by antirabbit biotinylated secondary antibody. The avidin biotinylated enzyme complex was added and the antigen was localized by incubation with 3,3'-diaminobenzidine. Sections were counterstained with hematoxylin.

¹²³I in vivo imaging studies

¹²³I animal imaging was performed on days 1 and 4 after VSV(Δ 51)-NIS infection using a high-resolution micro-single photon emission computed tomography/computed tomography system (X-SPECT, Gamma Medica Ideas, Northridge, CA). Because of the large sample sizes, planar imaging only was performed. Image acquisitions were obtained 3 hours after intraperitoneal injection of ¹²³I (5 mCi/185 MBq) using a low-energy, high resolution parallel-hole collimator with a 12.5-cm field of view. Image acquisition time was 5 minutes with a 159 KeV energy (window \pm 10%).

Quantitation of intratumoral radioisotope uptake was performed using a region of interest image analysis method previously described and validated.³² PMOD Biomedical Image Quantification and Kinetic Modeling Software (PMOD Technologies, Zurich, Switzerland) was used for image analysis. All planar images were adjusted for equal image intensity. Corresponding total intratumoral pixel counts were converted to activity using an equation derived from previously scanning a ¹²³I standard containing a known amount of radioactivity (data not shown). Background uptake was measured and corrected for by region-of-interest image analysis of the normal opposite flank tissue and subtracted from intratumoral activity measurements obtained by region-of-interest image analysis of the tumor uptake. Whole-body activity (injected dose) in each of the mice was determined by measuring activity in the syringe in a National Institute of Standards and Technology-calibrated dose calibrator before and after injection. Percent of injected dose (%ID) in the tumor was calculated by dividing intratumoral radioactivity (corrected for background) by whole-body activity (corrected for decay and time of imaging). The calculated radioiodine uptake in the VSV(Δ 51)-NIS-positive tumor is considered

specific for NIS gene expression. The %ID in groups receiving PBS and VSV(Δ 51)-NIS either intratumorally or intravenously were compared between days 1 and 4 to determine the optimum day for acquiring tumor-specific signal.

The absorbed radiation dose estimates in tumors were calculated by applying the Medical Internal Radiation Dose concept. For ¹²³I, Petrich et al³³ reported an effective half-life (which includes both the biologic turnover of iodine and physical radionuclide decay) of 6.5 hours. The biologic half-life (which represents the biologic turnover of iodine in the lesion) of radioactive iodine was thus calculated as 12.8 hours using the following equation: $1/T(\text{Effective}) = 1/T(\text{Physical}) + 1/T(\text{Biological})$. The effective half-life for ¹²³I was calculated as 12 hours. T(Physical) was taken as 13.2 hours and 192 hours for ¹²³I and ¹³¹I, respectively. The tumor dose (Gy/MBq) for ¹³¹I was calculated based on in vivo uptake data of ¹²³I. The radiation dose from ¹³¹I in a tumor was calculated as $\text{Dose} = C_0 \times 1.443 \times T(\text{Effective}) \times S$, where C_0 is the peak activity or count density, T(Effective) is the effective half-life (in hours), and S is the radiation dose per cumulated activity in the tissue.³⁴

Statistical analyses

The GraphPad Prism 4.0 program (GraphPad Software, San Diego, CA) was used for data handling, analysis, and graphic representation. Survival curves were plotted according to the Kaplan Meier method and survival function across treatment groups was compared using log rank test analyses.

Results

In vitro characterization of VSV(Δ 51)-NIS

VSV(Δ 51)-NIS was generated by cloning human NIS cDNA as an additional transcription unit between the G and L sequences of the VSV genome (Figure 1). The oncolytic activity of VSV(Δ 51)-NIS was ascertained in 6 different myeloma cell lines of human and mouse origin. Cells were either mock-infected or infected with VSV(Δ 51)-NIS at an MOI of 1.0, and cell viability was assessed by methyl-thiazol-tetrazolium (MTT) assay (Figure 2A). At 48 hours after infection, the percentage viability was less than 20% for all myeloma cell lines. Under similar conditions, normal mouse stromal cell line (SR-4987) and human skin fibroblasts showed minimal cell death with more than 80% cells alive at 48 hours after infection. Studies were extended to primary bone marrow samples from 3 myeloma patients. Each sample was sorted for CD138⁺ (myeloma cell) and CD138⁻ (normal cells) fraction, infected with VSV(Δ 51)-NIS at MOI of 1.0, and assayed at 48 hours after infection. Cell viability of mock-treated CD138⁺ and CD138⁻ cells was used to calculate percent cell viability at 48 hours after VSV(Δ 51)-NIS infection. Specific killing of CD138⁺ myeloma cells (78%-84%) was noted (Figure 2B), whereas the CD138⁻ cells were resistant to VSV(Δ 51)-NIS-mediated cytolysis. We conclude that VSV(Δ 51)-NIS efficiently and specifically replicates in and kills the myeloma cells.

One-step growth curves were performed to assess the growth kinetics and maximum virus yields of VSV(Δ 51)-NIS in 5TGM1 cells (Figure 2C). The growth curves were compared with those of VSV(Δ 51)-GFP.²⁶ At 24 hours, the progeny virus titers for VSV(Δ 51)-

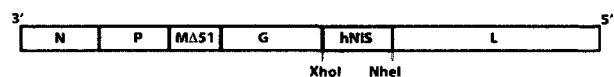


Figure 1. Schematic representation of VSV(Δ 51)-NIS. The genes in the VSV(Δ 51)-NIS cDNA are illustrated in 3' to 5' orientation. The hNIS cDNA was cloned downstream of G in the VSV(Δ 51) vector using XhoI and NheI restriction sites. N indicates nucleocapsid protein, P phosphoprotein, M, matrix protein, G, glycoprotein, and L polymerase protein.

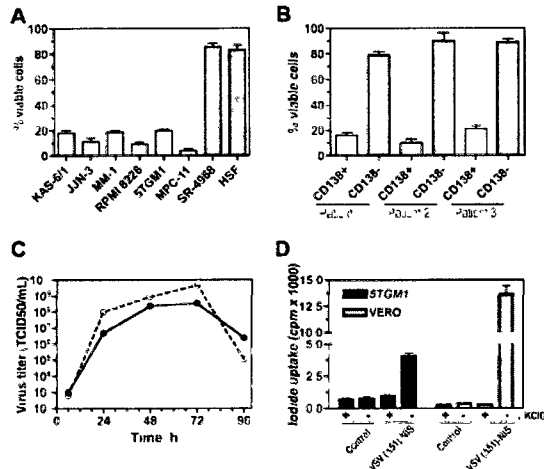


Figure 2. VSV(Δ 51)-NIS virus has in vitro antimyeloma activity and VSV(Δ 51)-NIS-infected cells can concentrate radioactive iodine. For cytotoxicity studies (A,B) cells were mock-infected or infected with VSV(Δ 51)-NIS (MOI = 1.0) for 30 minutes at 37°C and MTT assay was performed 48 hours after infection. Experiments were performed in triplicate and cell death is expressed as relative percentage viability compared with untreated control. Bars represent mean plus or minus a SEM. (A) Cytotoxicity of VSV(Δ 51)-NIS on myeloma cell lines (human and mouse), a mouse bone marrow stromal cell line (SR-4987), or human skin fibroblasts. (B) Specific cytotoxicity of VSV(Δ 51)-NIS on primary CD138-positive myeloma cells versus CD138-negative normal bone marrow progenitor cells. (C) One-step growth curves for VSV(Δ 51)-NIS (●) and VSV(Δ 51)-GFP (▲) in 5TGM1 cells. Cells were infected with VSV(Δ 51)-NIS (MOI = 1.0) for 30 minutes at 37°C, supernatants were harvested at various time points, and virus titers (TCID₅₀/mL) were determined on Vero cells. (D) In vitro Na¹²⁵I uptake in 5TGM1 or Vero cells infected with VSV(Δ 51)-NIS, with or without KClO₄. The data are presented as cpm per 10⁵ cells. Experiments were performed in triplicate (mean \pm SEM) and are representative of 3 independent experiments.

GFP and VSV(Δ 51)-NIS were 10⁸ and 5 \times 10⁶ TCID₅₀/mL, respectively. Both viruses showed maximum virus yields at 72 hours with titers for VSV(Δ 51)-GFP and VSV(Δ 51)-NIS of 4.7 \times 10⁹ and 3.5 \times 10⁸ TCID₅₀/mL, respectively. These data show that VSV(Δ 51)-NIS replicates slower than VSV(Δ 51)-GFP in 5TGM1 cells.

To study if the virally expressed NIS protein was functional in VSV(Δ 51)-NIS infected cells, in vitro iodide uptake assays were performed as described before.²⁰ Compared with mock-infected cells, iodide accumulation in 5TGM1 and Vero cells was 4.3-fold and 38.8-fold higher, respectively (Figure 2D). These uptake studies show proof of virus-driven NIS protein expression and its proper targeting to the plasma membrane.

In vivo characterization of VSV(Δ 51)-NIS

Immunocompromised mice engrafted with subcutaneous 5TGM1 myeloma tumors were treated with VSV(Δ 51)-NIS, then monitored for intratumoral virus replication and tumor response. On day 4 after intravenous or intratumoral administration of VSV(Δ 51)-NIS, strong VSV-G-specific immunoreactivity was seen in the tumors of virus-treated groups while the control tumors scored negative (Figure 3A). Both intratumoral and intravenous administration resulted in high viral titers in the subcutaneous tumors on days 1 and 3 after virus administration (Figure 3B). Interestingly, intratumoral administration of VSV(Δ 51)-NIS led to higher intratumoral viral titers on day 1 compared with day 3 (2.2 \times 10¹¹ and 2.7 \times 10¹⁰ TCID₅₀/mg on days 1 and 3, respectively). Conversely, for the group receiving intravenous VSV(Δ 51)-NIS, the viral titers were higher on day 3 (8.7 \times 10⁹ to 7.7 \times 10¹⁰ TCID₅₀/mg for days 1 and 3, respectively). For both intratumoral and intravenous groups, a 100-fold lower virus titer was observed by day 7 (data not shown).

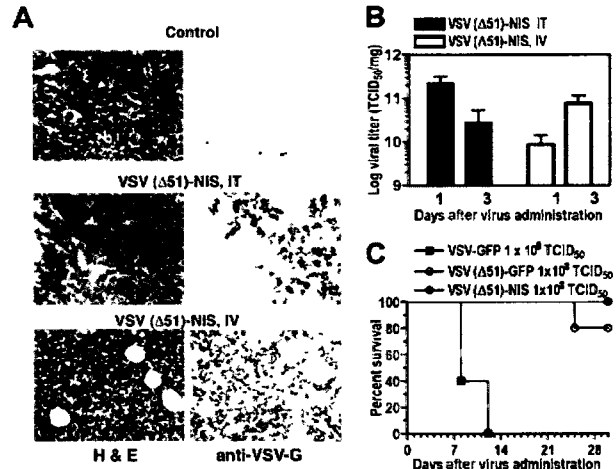


Figure 3. VSV(Δ 51)-NIS replicates in subcutaneous 5TGM1 tumors. (A) Histologic analysis and immunohistochemical staining for VSV-G antigen of representative sections of 5TGM1 myeloma tumors 4 days after initiation of therapy for groups receiving no virus or VSV(Δ 51)-NIS (IT or IV). Paraffin-embedded tissues were sectioned at 4- μ m thickness and incubated with polyclonal anti-VSV-G antibody, which was detected with biotinylated antirabbit secondary antibody and the avidin-biotin complexing system. Sections were counterstained with hematoxylin and viewed with an Olympus BX45 microscope (Olympus, Center Valley, PA) at 40 \times /0.9 NA magnification. (B) 5TGM1 tumors were treated with VSV(Δ 51)-NIS IT or IV, excised on days 1 and 3 after therapy, and viral titers determined by Vero cell titration. The data are expressed as log TCID₅₀/mg of tumor and are averaged for 3 tumors/time point. (C) Tumor-free bg/nu/xid mice received a single intravenous administration of 10⁸ TCID₅₀ of VSV-GFP, VSV(Δ 51)-NIS, or VSV(Δ 51)-GFP, and were monitored for toxicity and survival (n = 5/group). Experiments were performed in triplicate (mean \pm SEM).

To determine the safety of intravenous administration of VSV(Δ 51)-NIS in bg/nu/xid mice, toxicity studies were performed in animals (n = 5/group) treated with VSV-GFP, VSV(Δ 51)-GFP, or VSV(Δ 51)-NIS (2 doses of 5 \times 10⁷ TCID₅₀/dose). By day 12 after virus administration, all of the mice receiving VSV-GFP were dead, with signs characteristic of VSV-induced neurotoxicity.^{26,29,35} Mice receiving VSV(Δ 51)-NIS showed no signs of VSV-induced neurotoxicity even 2 months after virus treatment. In the VSV(Δ 51)-GFP group, one animal died on day 24 after virus administration for unknown reasons. A detailed necropsy was not performed but the brain was excised, homogenized, and incubated with Vero cells, and no virus-induced cytopathic effect was detected at 72 hours (data not shown). These toxicity data show that VSV(Δ 51)-NIS can be safely administered by the intravenous route even in immunocompromised bg/nu/xid mice at a dose of 10⁸ TCID₅₀ (Figure 3C).

To evaluate the potential of NIS as a reporter gene for noninvasive localization of virus infected cells, planar gamma camera scintigraphy was performed to determine the biodistribution of ¹²⁵I in VSV(Δ 51)-NIS treated bg/nu/xid mice. Whole-body images of the virus-treated animals showed definite iodide uptake by the VSV(Δ 51)-NIS infected tumors, whereas no iodine signal was seen in the tumors of control mice injected with PBS (Figure 4A) or with VSV(Δ 51)-GFP (data not shown). Quantitation of intratumoral radioisotope uptake showed that the percentage injected radioiodine dose (%ID) taken up by these tumors was 0, 4.1, or 7.0 for the control, intratumoral, and intravenous VSV(Δ 51)-NIS-treated mice, respectively (Figure 4A). Iodide accumulation was also seen in the thyroid and the stomach, organs known to express endogenous NIS, and in the bladder as a result of iodide excretion via the kidneys.

To determine whether analysis of planar gamma camera images could be used to monitor intratumoral virus propagation, mice were

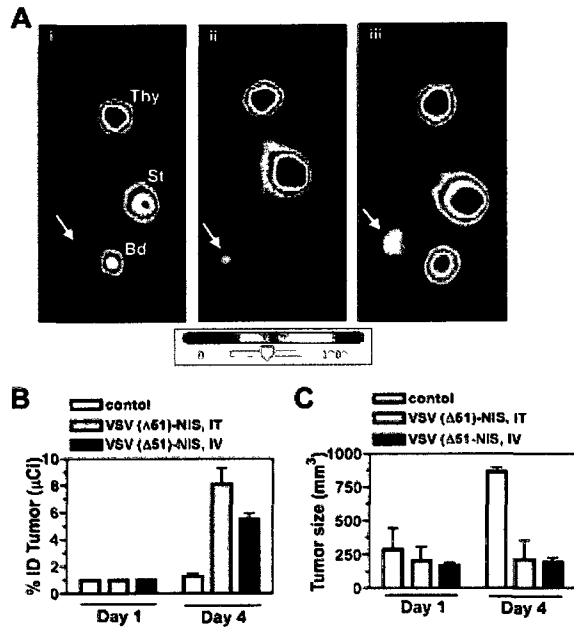


Figure 4. Imaging, dosimetric, and oncolytic activity of VSV(Δ51)-NIS. (A) Representative planar images of VSV(Δ51)-NIS-infected, tumor-bearing mice obtained 3 hours after intraperitoneal injection of ¹²³I 1 day after mock (PBS, intratumoral) or VSV(Δ51)-NIS injections (5×10^7 TCID₅₀/dose, 2 doses given days -1 and 0). Radioisotope uptake is seen in the salivary glands, thyroid gland (Thy), and stomach (St), with excreted radioisotope visible in the bladder (Bd). No increased uptake is seen in the subcutaneous flank tumor of (i) control mouse, whereas increased intratumoral radioisotope uptake is demonstrated in mice treated (ii) intratumorally or (iii) intravenously with VSV(Δ51)-NIS. Arrows indicate tumor locations. The color bar (image intensity scale) demonstrates the range of uptake intensities, with 100% representing the strongest signal in the image. Planar images were acquired using a Gamma Medica X-SPECT imaging system (Gamma Medica, Northridge, CA). Images were analyzed and processed using PMOD Biomedical Image Quantification and Kinetic Modeling software version 2.75 (PMOD Technologies) and Adobe Photoshop version 7.0 (Adobe Systems, San Jose, CA). (B) Serial planar images of subcutaneous myeloma tumors were acquired on days 1 and 4 after administration of VSV(Δ51)-NIS and %ID taken up by the tumor was calculated (n = 4/group). (C) The growth of subcutaneous myeloma tumors was tested by measuring tumor volumes on days 1 and 4 (n = 4/group). Bars indicate SE.

serially imaged on days 1 and 4 after VSV(Δ51)-NIS administration and tumor specific activity at each of these time points was calculated and expressed as %ID (Figure 4B). The %ID for all groups at day 0 was set to 1 and the fold-increase was calculated at day 4 (n = 4/group). On day 4, the fold-increase in %ID in the tumors of mice receiving VSV(Δ51)-NIS by intratumoral or intravenous routes was $8.1 (\pm 2.4)$ and $5.5 (\pm 0.9)$, respectively. The control group receiving PBS showed a nonsignificant change from 1 to $1.3 (\pm 0.4)$ in tumor radioiodine uptake. When tumor sizes were compared between the virus-treated and control groups, the average tumor sizes for the groups receiving VSV(Δ51)-NIS did not change significantly from day 1 to day 4. However, in the control group the untreated tumors tripled in size between days 1 and 4. (Figure 4C).

In vivo virotherapy of myeloma tumors with VSV(Δ51)-NIS

To evaluate the in vivo oncolytic potency of the VSV(Δ51)-NIS virus, bg/nu/xid mice bearing subcutaneous 5TGM1 tumors (n = 10/group) were given 2 doses of VSV(Δ51)-NIS (5×10^7 TCID₅₀/dose) by IT or IV injection, whereas control mice (n = 5) received PBS by the same route. In control mice, rapid tumor growth was observed whereas tumor growth was arrested in mice treated with VSV(Δ51)-NIS, IT or IV (Figure 5A). The average survival time for control animals receiving PBS was 22 days after tumor

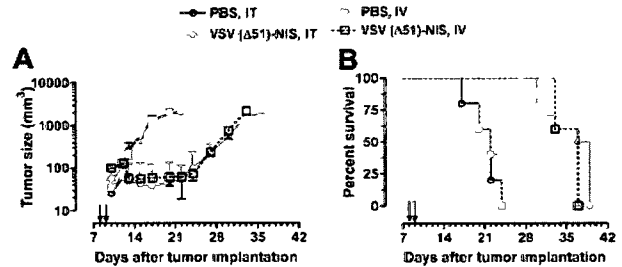


Figure 5. VSV(Δ51)-NIS controls the growth of myeloma tumors in bg/nu/xid mice. Mice bearing subcutaneous myeloma tumors (mean volume 100 mm³) were treated with VSV(Δ51)-NIS (2 doses of 5×10^7 TCID₅₀/dose) and monitored for (A) tumor growth. Points, mean tumor volumes (n = 10 for test groups and n = 5 for the control groups); bars indicate SE. (B) Kaplan-Meier survival curves of mice treated with saline or VSV(Δ51)-NIS (intratumorally or intravenously). Arrows indicate virus injections.

engraftment, whereas the average survival times for mice receiving VSV(Δ51)-NIS (intratumorally or intravenously) were 38 days (P < .001) or 37 days (P < .001), respectively. These studies show that, in the absence of a functional immune system, VSV(Δ51)-NIS has oncolytic activity against myeloma tumors in vivo.

Dosimetric calculations

To determine whether a therapeutic effect might be achieved by combining VSV(Δ51)-NIS with the radionuclide ¹³¹I, in vivo imaging studies with ¹²³I were performed and the data were used for dosimetry calculations (Table 1). Assuming a total ¹³¹I dose of 1 mCi, predicted tumor-absorbed doses were estimated to be $18.4 (\pm 5.9)$ Gy (n = 20, P = 0.03) and $11.6 (\pm 2.3)$ Gy (n = 20, P = .02), with VSV(Δ51)-NIS given IT or IV, respectively, on day 1 after virus administration. The predicted tumor absorbed dose for the control group was $4.2 (\pm 2.1)$ Gy. These results illustrated how ¹²³I biodistribution data can be used for dosimetric calculations to estimate potential tumor absorbed doses for radiovirotherapy studies and suggested that the administration of ¹³¹I could enhance the therapeutic efficacy of VSV(Δ51)-NIS therapy.

VSV(Δ51)-NIS for radiovirotherapy of subcutaneous and orthotopic myeloma in immunocompetent mice

To determine whether administration of ¹³¹I could enhance the therapeutic efficacy of VSV(Δ51)-NIS therapy, we used the syngeneic immunocompetent 5TGM1 murine myeloma model (Figure 6). For these experiments the total virus dose was increased from 10^8 TCID₅₀ to 5×10^8 TCID₅₀ because VSV particles can be rapidly inactivated by the host immune system.¹⁸

Initial studies were conducted in immunocompetent C57BL/KaLwRij mice bearing subcutaneous 5TGM1 tumors. The tumors

Table 1. Dosimetric calculations (MIRD) for ¹³¹I

	Intratumoral injections		Intravenous injections	
	PBS*	VSV (Δ51)-NIS†	PBS*	VSV (Δ51)-NIS†
Tumor volume, mm ³	180	170	190	120
Injected activity, MBq ¹²³ I	10.5	10.4	10.3	11.0
Tumor activity, MBq ¹²³ I	0.1	0.6	0.1	0.6
Tumor dose, Gy ¹³¹ I	4.2	18.4	4.1	11.6

Dosimetric calculations were based on imaging studies (with ¹²³I) performed on day 1 after virus administration in mice bearing subcutaneous 5TGM1 myeloma tumors. Mice were given PBS or VSV (Δ51)-NIS (5×10^7 TCID₅₀/dose, 2 doses given 24 hours apart) by intratumoral or intravenous routes.

MIRD indicates medical internal radiation dosimetry.

*N=10

†N=20.

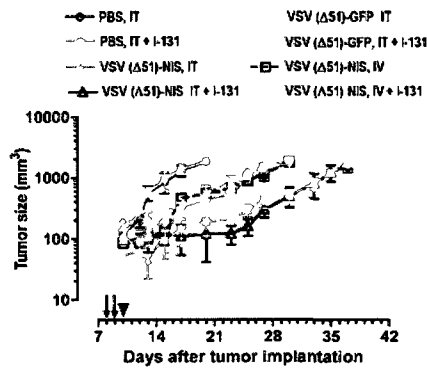


Figure 6. Radiovirotherapy of myeloma tumors in syngeneic, immunocompetent mice. C57BL/6/KaLwRij mice with established subcutaneous myeloma tumors were treated with VSV(Δ 51)-NIS or VSV(Δ 51)-GFP (2 doses of 2.5×10^8 TCID₅₀/dose) without or with ¹³¹I (1 mCi/mouse intraperitoneally 24 hours after virus administration) and tumor volumes are plotted against days after treatment. Arrows indicate virus injections; arrowhead, ¹³¹I injection; points, mean; bars, SE.

progressed rapidly in control mice (Figure 6, Table 2). With intratumoral and intravenous injections of VSV(Δ 51)-NIS or VSV(Δ 51)-GFP, tumor growth was suppressed until day 5 after therapy, after which the tumors grew rapidly. In mice receiving VSV(Δ 51)-NIS followed by a therapeutic dose of ¹³¹I, the growth of tumors was arrested until day 15 after therapy. ¹³¹I significantly enhanced the antitumor potency of VSV(Δ 51)-NIS but had no effect on the antitumor potency of VSV(Δ 51)-GFP. Tumor sizes were compared between the various groups on day 20 after tumor implantation (Table 2). Kaplan-Meier curves showed median survivals of animals treated intravenously with VSV(Δ 51)-NIS were prolonged significantly by the addition of ¹³¹I, from 28.5 to 35 days in the group that was treated intravenously ($P = .02$). These data show that VSV(Δ 51)-NIS is able to arrest tumor growth in immune competent mice and exhibits increased potency when combined with ¹³¹I.

We next evaluated the potential synergy of VSV(Δ 51)-NIS and ¹³¹I in immunocompetent C57BL/KaLwRij mice bearing orthotopic 5TGM1 tumors. Single-agent VSV(Δ 51)-NIS therapy prolonged survival from 30 to 33 days (Figure 7A). Radiovirotherapy prolonged the median survival to 38.5 days ($P = .001$, compared with ¹³¹I control ($P = .041$) compared with single-agent VSV(Δ 51)-NIS (Figure 7A). Serum paraprotein levels were measured to monitor myeloma progression in these mice (Figure 7B). On day 12 after myeloma engraftment, the paraprotein levels were comparable between groups ($n = 4$ /group) and ranged from 3.2 to 3.9 g/L (data not shown). On day 29, at which point most of the control mice injected with PBS or ¹³¹I showed terminal paraplegia, the IgG2b levels were $7.5 (\pm 0.9)$ g/L, $6.4 (\pm 0.5)$ g/L, and $4.9 (\pm 0.6)$

g/L, respectively, for the mice injected with PBS, VSV(Δ 51)-NIS, or VSV(Δ 51)-NIS plus ¹³¹I. Thus, the VSV(Δ 51)-NIS virus was able to inhibit myeloma progression *in vivo* and this inhibitory effect was more pronounced with ¹³¹I.

Discussion

Here we report for the first time a novel recombinant virus, VSV(Δ 51)-NIS, and demonstrate that it can be used for its oncolytic and imaging properties in multiple myeloma.

Pathogenic strains of VSV generally cause mild benign infections in humans.³⁶ However, similar to other RNA viruses, VSV shows neurotropism if given direct access to brain tissue. In immunodeficient mice, VSV infections are associated with fatal meningoencephalitis,³⁷ whereas immunocompetent mice can clear the virus before neurotoxicity is seen, at least at lower challenge doses. Efficient viral clearance is dependent on activation of innate and adaptive immune responses. Wild-type strains of VSV are poor inducers of IFN- α/β ³⁸ because the VSV matrix (M) protein blocks expression of interferon-stimulated genes by binding to a nuclear RNA export factor RAE1 (MRNP41).³⁹ VSVs carrying certain mutation(s) or a deletion in the M protein [eg, M51R,^{35,40} V221F, S226R, or Δ 51²⁶] cannot suppress the cellular interferon response, and therefore grow poorly in normal tissues showing greatly reduced neurotoxicity but little reduction in their tumor-killing ability.^{23,33,43} Other approaches to increase the therapeutic index of VSV include the generation of recombinant viruses engineered to express the mouse or human IFN- β genes²⁹ or prophylactic IFN- α treatment before challenge with wild-type VSV.^{41,42} Our *in vivo* studies show that 2 doses of VSV(Δ 51)-NIS (5×10^7 TCID₅₀/dose) are well tolerated by bg/nu/xid mice.

The concept of radiovirotherapy for multiple myeloma was originally established using a recombinant measles virus coding for NIS (MV-NIS),¹⁶ which is currently being evaluated in phase I clinical trials at Mayo Clinic. Compared with MV, VSV has a very rapid replication cycle time of 8 to 12 hours in permissive tumor cells.⁴³ *In vitro* studies using various cancer cell lines have shown complete killing by 48 to 96 hours after infection with VSV strains mutated in the matrix protein.^{26,35} Our *in vitro* studies show that VSV(Δ 51)-NIS has slower growth compared with VSV-GFP. This may allow a longer period of expression of the NIS transgene in the plasma membrane prior to virus-induced killing of the infected cells, thus enabling active concentration of iodide ions before the cell dies.⁴⁴

Because mouse cells lack MV receptors, *in vivo* studies of MV-NIS were conducted in SCID mice bearing human myeloma

Table 2. Average tumor volumes (day 20 after tumor implantation) in immunocompetent mice bearing subcutaneous 5TGM1 myeloma tumors after administration of recombinant VSV without or with ¹³¹I

Treatment	Mice/group	Average tumor volume, mm ³ plus or minus SD	95% CI of mean (mm ³)	
			Lower	Upper
PBS, intratumorally	4	1796.0 \pm 231.9	1427.0	2165
PBS, intratumorally + ¹³¹ I	4	1809.0 \pm 186.2	1512.1	2105.0
VSV (Δ 51)-NIS, IT intratumorally	6	421.3 \pm 100.2	316.2	526.4
VSV (Δ 51)-NIS, intratumorally + ¹³¹ I	6	129.0 \pm 63.3	62.6	195.4
VSV (Δ 51)-NIS, intravenously	6	558.0 \pm 114.2	438.1	677.9
VSV (Δ 51)-NIS, intravenously + ¹³¹ I	6	204.0 \pm 110.5	88.1	319.9
VSV (Δ 51)-GFP, intratumorally	4	494.5 \pm 166.2	230.1	758.9
VSV (Δ 51)-GFP, intratumorally + ¹³¹ I	4	524.5 \pm 156.5	275.4	773.6

Virus was administered on days 12 and 13 (intratumorally or intravenously) and ¹³¹I (1 mCi) was given intraperitoneally on day 14 after tumor-cell inoculation.

Table 3. Median survival of immunocompetent mice bearing subcutaneous myeloma tumors after administration of recombinant VSV without or with ¹³¹I

Treatment	Mice per group	Median survival, d	P compared with	
			PBS	Respective rVSV construct
PBS	4	20.0	—	—
PBS + ¹³¹ I	4	20.0	NS	—
VSV(Δ51)-NIS, intratumorally	6	30.0	0.02	213
VSV(Δ51)-NIS, intratumorally + ¹³¹ I	6	32.0	0.02	—
VSV(Δ51)-NIS, intravenously	6	28.5	0.02	018
VSV(Δ51)-NIS, intravenously + ¹³¹ I	6	35.0	0.02	—
VSV(Δ51)-GFP, intratumorally	4	28.5	0.1	NS
VSV(Δ51)-GFP, intratumorally + ¹³¹ I	4	28.5	0.1	—

rVSV was administered on days 12 and 13 after tumor cell inoculation. ¹³¹I was given intraperitoneally on day 14. Kaplan-Meier survival curves were drawn. NS indicates not significant. —, not applicable.

xenografts.²⁰ In contrast to MV receptors, VSV receptors are ubiquitously expressed on mouse and human cells. VSV(Δ51)-NIS was therefore studied in the murine 5TGM1 myeloma model. 5TGM1 provides a valuable orthotopic model of multiple myeloma, allowing the study of myeloma cell growth and survival in a normal murine bone marrow microenvironment.^{31,45,46} In addition to intratumoral injection, we studied systemic administration of VSV(Δ51)-NIS because myeloma is a disseminated malignancy and it is essential to develop therapeutic agents that can be administered systemically. Studies by other investigators have shown that systemic administration of VSV in mouse models can target both primary and metastatic tumors.^{26,29,35,47} Our *in vivo* studies show that intravenous administration of VSV(Δ51)-NIS resulted in infection and viral spread in subcutaneous myeloma tumors.

NIS imaging offers a convenient approach to noninvasively confirm correct localization of virus- or plasmid-encoded NIS gene expression before proceeding to ¹³¹I therapy.⁸ Numerous factors can influence NIS expression and hence the intensity of the NIS-mediated radioiodine image. Variable susceptibility of tumor cells to viral transduction and virus-mediated killing, variable rates of intratumoral virus propagation, variable tumor sizes and tumor injection techniques, and variable rates of tumor

regression are just a few of the factors that influence the image signal intensity after treatment with an oncolytic virus expressing NIS. We performed serial imaging on mice bearing subcutaneous myeloma tumors on days 1 and 4 after VSV(Δ51)-NIS administration. A specific signal was detected in the myeloma tumors after injection of VSV(Δ51)-NIS but not in the control groups, allowing us to attribute the tumor specific signal to virus-driven expression of the NIS gene.

Several preclinical studies have demonstrated ablative effects of ¹³¹I in tumor xenografts.^{12,15,48,53} Dosimetry calculations predicted that we would achieve cumulative radiation-absorbed doses to the VSV(Δ51)-NIS-infected myeloma tumors of approximately 11 to 18 Gy after a therapeutic dose of 1 mCi of ¹³¹I-iodide. Beta particle crossfire is an important mechanism contributing to the antitumor activity of intratumoral ¹³¹I. Each beta particle emitted by ¹³¹I deposits its energy within a local area of 2 to 3 mm from the point of decay such that a field of beta particle crossfire can exist only in a large tumor with multiple foci of radioiodine accumulation. Three-dimensional spheroids have been thus used with NIS radioiodide approach to assess therapeutic efficacy.^{54,55} Tumor deposits in orthotopic myeloma models are typically very small (up to 2-mm diameter) even when the disease is far advanced. For this reason we focused our studies initially on mice bearing subcutaneous myeloma tumors with diameters of approximately 5 mm. Because bg/nu/xid mice are hypersensitive to ionizing radiation and therefore unsuitable for radiovirotherapy studies, we used immunocompetent C57BL/6/KaLwRij mice bearing subcutaneous 5TGM1 tumors. The results obtained in this model demonstrated the superior potency of radiovirotherapy compared with single-agent VSV(Δ51)-NIS. Despite our reservations because of the small size of tumor deposits in orthotopic myeloma models, we next extended our radiovirotherapy studies to the 5TGM1 syngeneic orthotopic murine myeloma model.³¹ VSV(Δ51)-NIS alone did not significantly prolong survival in this model unless it was followed by treatment with ¹³¹I. Several studies have shown that VSV provokes the production of neutralizing antibodies, and we are conducting studies to determine whether this will lead to attenuated antitumor potency in this model.⁵⁶ We are also testing strategies to suppress the anti-VSV immune response and to evade it by delivering the VSV inside infected cell carriers.⁵⁷

In conclusion, we have generated and characterized a novel oncolytic VSV encoding the NIS gene. Our results show that this agent can be safely administered by the intravenous route and has strong oncolytic activity against myeloma tumors. The NIS transgene can be used to image VSV(Δ51)-NIS-infected myeloma tumors by planar scintigraphy. Therapeutic potency was enhanced by combining VSV(Δ51)-NIS with ¹³¹I in radiovirotherapy studies. VSV(Δ51)-NIS is a promising new experimental agent that should be further developed for the treatment of multiple myeloma.

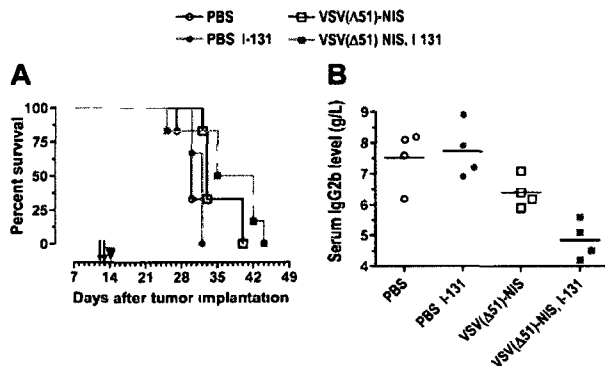


Figure 7. Radiovirotherapy of orthotopic myeloma tumors in syngeneic, immunocompetent mice. C57BL/6/KaLwRij mice with disseminated myeloma were treated with VSV(Δ51)-NIS (2 doses of 2.5 × 10⁸ TCID₅₀/dose) without or with ¹³¹I (1 mCi/mouse intraperitoneally 24 hours after virus administration). (A) Median survival of mice is shown as Kaplan-Meier plots. Arrows indicate virus injections and arrowhead indicate ¹³¹I injection. (B) Myeloma burden of various cohorts was determined by measuring serum IgG2b levels on day 29 after tumor engraftment (n = 4 per group; average values are shown by line).

Acknowledgments

The authors thank the Histology Core at Mayo Clinic, Scottsdale, AZ. The authors also acknowledge Tracy Decklever, Department of Radiology, Mayo Clinic, for helping in the acquisition of planar images.

This work was supported by grants from National Institutes of Health (NIH, CA100634-02 and HL66958-3P4). J.B. is supported by a Terry Fox Program Project grant, and A.P. is supported by an

Ontario Graduate Scholarship in Science and Technology (OGSST) studentship

Authorship

Contribution A G designed the study, conducted in vitro and in vivo experiments, analyzed the data, and wrote the manuscript S K C performed image analysis for calculating percent of injected dose of iodine-123 to the tumor K L C performed dosimetric analysis for iodine-131 S G contributed to animal experiments

S N conducted in vitro and in vivo experiments and assisted with analysis of data A T P constructed and rescued VSV-NIS virus J C B provided anti-VSV-G antibodies, oversaw generation of VSV-NIS virus, and provided expertise about VSV S J R conceptualized the study, oversaw in vivo studies, and cowrote the manuscript

Conflict-of-interest disclosure The authors declare no competing financial interests

Correspondence Stephen J Russell, Mayo Clinic, Guggenheim 1833, 200 First St SW, Rochester, MN 55905, e-mail sjr@mayo.edu

References

- Kyle RA Multiple myeloma: an odyssey of discovery. *Br J Haematol* 2000;111:1035-1044
- Kyle RA Current therapy of multiple myeloma. *Intern Med* 2002;41:175-180
- Jemal A, Murray T, Ward E, et al Cancer statistics, 2005. *CA Cancer J Clin* 2005;55:10-30
- Gluck S, Van Dyk J, Messner HA Radiosensitivity of human clonogenic myeloma cells and normal bone marrow precursors: effect of different dose rates and fractionation. *Int J Radiat Oncol Biol Phys* 1994;28:877-882
- Goel A, Dispenziani A, Greipp PR, Witzig TE, Mesa RA, Russell SJ PS-341-mediated selective targeting of multiple myeloma cells by synergistic increase in ionizing radiation induced apoptosis. *Exp Hematol* 2005;33:784-795
- Bjorkstrand B European Group for Blood and Marrow Transplantation Registry studies in multiple myeloma. *Semin Hematol* 2001;38:219-225
- Moreau P, Facon T, Attal M, et al Comparison of 200 mg/m² melphalan and 8 Gy total body irradiation plus 140 mg/m² melphalan as condition regimens for peripheral blood stem cell transplantation in patients with newly diagnosed multiple myeloma: final analysis of the Inter-groupe Francophone du Myelome 9502 randomized trial. *Blood* 2002;99:731-735
- Dingli D, Russell SJ, Morris JC, 3rd In vivo imaging and tumor therapy with the sodium iodide symporter. *J Cell Biochem* 2003;90:1079-1086
- Dai G, Levy O, Carrasco N Cloning and characterization of the thyroid iodide transporter. *Nature* 1996;379:458-460
- Chung JK Sodium iodide symporter: its role in nuclear medicine. *J Nucl Med* 2002;43:1188-1200
- Dingli D, Diaz RM, Bergert ER, O'Connor MK, Morris JC, Russell SJ Genetically targeted radiotherapy for multiple myeloma. *Blood* 2003;102:489-496
- Dwyer RM, Bergert ER, O'Connor MK, Gendler SJ, Morris JC In vivo radioiodide imaging and treatment of breast cancer xenografts after MUC1-driven expression of the sodium iodide symporter. *Clin Cancer Res* 2005;11:1483-1489
- Hart IR Tissue specific promoters in targeting systemically delivered gene therapy. *Semin Oncol* 1996;23:154-158
- Kakinuma H, Bergert ER, Spitzweg C, Chevillon JC, Lieber MM, Morris JC Probasin promoter (ARR(2)PB)-driven, prostate-specific expression of the human sodium iodide symporter (h-NIS) for targeted radioiodine therapy of prostate cancer. *Cancer Res* 2003;63:7840-7844
- Spitzweg C, O'Connor MK, Bergert ER, Tindall DJ, Young CY, Morris JC Treatment of prostate cancer by radioiodine therapy after tissue-specific expression of the sodium iodide symporter. *Cancer Res* 2000;60:6526-6530
- Spitzweg C, Zhang S, Bergert ER, et al Prostate-specific antigen (PSA) promoter-driven androgen-inducible expression of sodium iodide symporter in prostate cancer cell lines. *Cancer Res* 1999;59:2136-2141
- Bell JC, Lichty B, Stojdl D Getting oncolytic virus therapies off the ground. *Cancer Cell* 2003;4:7-11
- Parato KA, Senger D, Forsyth PA, Bell JC Recent progress in the battle between oncolytic viruses and tumours. *Nat Rev Cancer* 2005;5:965-976
- Peng KW, Ahmann GJ, Pham L, Greipp PR, Cattaneo R, Russell SJ Systemic therapy of myeloma xenografts by an attenuated measles virus. *Blood* 2001;98:2002-2007
- Dingli D, Peng KW, Harvey ME, et al Image-guided radiotherapy for multiple myeloma using a recombinant measles virus expressing the thyroidal sodium iodide symporter. *Blood* 2004;103:1641-1646
- Russell SJ RNA viruses as virotherapy agents. *Cancer Gene Ther* 2002;9:961-966
- Lichty BD, Power AT, Stojdl DF, Bell JC Vesicular stomatitis virus: re-inventing the bullet. *Trends Mol Med* 2004;10:210-216
- Lichty BD, Stojdl DF, Taylor RA, et al Vesicular stomatitis virus: a potential therapeutic virus for the treatment of hematologic malignancy. *Hum Gene Ther* 2004;15:821-831
- Balachandran S, Barber GN Vesicular stomatitis virus (VSV) therapy of tumors. *IUBMB Life* 2000;50:135-138
- Fernandez M, Porosnicu M, Markovic D, Barber GN Genetically engineered vesicular stomatitis virus in gene therapy application for treatment of malignant disease. *J Virol* 2002;76:895-904
- Stojdl DF, Lichty BD, tenOver BR, et al VSV strains with defects in their ability to shutdown innate immunity are potent systemic anti-cancer agents. *Cancer Cell* 2003;4:263-275
- Radl J Idiopathic paraproteinemia—a consequence of an age-related deficiency in the T immune system. Three-stage development—a hypothesis. *Clin Immunol Immunopathol* 1979;14:251-255
- Lawson ND, Stillman EA, Whitt MA, Rose JK Recombinant vesicular stomatitis viruses from DNA. *Proc Natl Acad Sci U S A* 1995;92:4477-4481
- Obuchi M, Fernandez M, Barber GN Development of recombinant vesicular stomatitis viruses that exploit defects in host defense to augment specific oncolytic activity. *J Virol* 2003;77:8843-8856
- Hadac EM, Peng KW, Nakamura T, Russell SJ Reengineering paramyxovirus tropism. *Virology* 2004;329:217-225
- Goel A, Dispenziani A, Geyer SM, Greiner S, Peng KW, Russell SJ Synergistic activity of the proteasome inhibitor PS-341 with non-myeloablative 153-Sm-EDTMP skeletal targeted radiotherapy in an orthotopic model of multiple myeloma. *Blood* 2006;107:4063-4070
- Carlson SK, Classic KL, Hadac EM, et al In vivo quantitation of intratumoral radioisotope uptake using micro-single photon emission computed tomography/computed tomography. *Mol Imaging Biol* 2006;8:324-332
- Petrich T, Helmeke HJ, Meyer GJ, Knapp WH, Potter E Establishment of radioactive astatine and iodine uptake in cancer cell lines expressing the human sodium/iodide symporter. *Eur J Nucl Med Mol Imaging* 2002;29:842-854
- Reynolds JC Percent 131I uptake and post-therapy 131I scans: their role in the management of thyroid cancer. *Thyroid* 1997;7:281-284
- Ebert O, Harbaran S, Shinozaki K, Woo SL Systemic therapy of experimental breast cancer metastases by mutant vesicular stomatitis virus in immune-competent mice. *Cancer Gene Ther* 2005;12:350-358
- Letchworth GJ, Rodriguez LL, Delcarrera J Vesicular stomatitis. *Vet J* 1999;157:239-260
- Huneycutt BS, Bi Z, Aoki CJ, Reiss CS Central neuropathogenesis of vesicular stomatitis virus infection of immunodeficient mice. *J Virol* 1993;67:6698-6706
- Marcus PI, Rodriguez LL, Sekellick MJ Interferon induction as a quasispecies marker of vesicular stomatitis virus populations. *J Virol* 1998;72:542-549
- Fania PA, Chakraborty P, Levay A, et al VSV disrupts the Rae1/mmp41 mRNA nuclear export pathway. *Mol Cell* 2005;17:93-102
- Desforges M, Charron J, Berard S, et al Different host-cell shutoff strategies related to the matrix protein lead to persistence of vesicular stomatitis virus mutants on fibroblast cells. *Virus Res* 2001;76:87-102
- Stojdl DF, Lichty B, Knowles S, et al Exploring tumor-specific defects in the interferon pathway with a previously unknown oncolytic virus. *Nat Med* 2000;6:821-825
- Shinozaki K, Ebert O, Sunawinata A, Thung SN, Woo SL Prophylactic alpha interferon treatment increases the therapeutic index of oncolytic vesicular stomatitis virus virotherapy for advanced hepatocellular carcinoma in immune-competent rats. *J Virol* 2005;79:13705-13713
- Rose JKA, W, M A Rhabdoviridae: the viruses and their replication. Philadelphia: Lippincott Williams and Wilkins, 2001
- Eskandari S, Loo DD, Dai G, Levy O, Wright EM, Carrasco N Thyroid Na⁺/I⁻ symporter: Mechanism, stoichiometry, and specificity. *J Biol Chem* 1997;272:27230-27238
- Dallas SL, Garrett IR, Oyajobi BO, et al Ibandronate reduces osteolytic lesions but not tumor burden in a murine model of myeloma bone disease. *Blood* 1999;93:1697-1706
- Turner JH, Clannngbold PG, Manning LS, O'Donoghue HL, Berger JD, Glancy RJ Radiopharmaceutical therapy of 5T33 murine myeloma by sequential treatment with samarium-153 ethylenediaminetetraacetic acid methylene phosphonate, melphalan, and bone marrow transplantation. *J Natl Cancer Inst* 1993;85:1508-1513
- Balachandran S, Porosnicu M, Barber GN Oncolytic activity of vesicular stomatitis virus is effective against tumors exhibiting aberrant p53, Ras,

- or myc function and involves the induction of apoptosis *J Virol* 2001,75:3474-3479
- 48 Nakamoto Y, Saga T, Misaki T, et al Establishment and characterization of a breast cancer cell line expressing Na⁺/I⁻ symporters for radioiodide concentrator gene therapy *J Nucl Med* 2000,41:1898-1904
- 49 Boland A, Ricard M, Opolon P, et al Adenovirus-mediated transfer of the thyroid sodium/iodide symporter gene into tumors for a targeted radiotherapy *Cancer Res* 2000,60:3484-3492
- 50 Spitzweg C, Dietz AB, O'Connor MK, et al In vivo sodium iodide symporter gene therapy of prostate cancer *Gene Ther* 2001,8:1524-1531
- 51 Cho JY, Shen DH, Yang W, et al In vivo imaging and radioiodine therapy following sodium iodide symporter gene transfer in animal model of intracerebral gliomas *Gene Ther* 2002,9:1139-1145
- 52 Dwyer RM, Bergert ER, O'Connor M K, Gendler SJ, Morns JC Adenovirus-mediated and targeted expression of the sodium-iodide symporter permits in vivo radioiodide imaging and therapy of pancreatic tumors *Hum Gene Ther* 2006,17:661-668
- 53 Dwyer RM, Bergert ER, O'Connor MK, Gendler SJ, Morns JC Sodium iodide symporter-mediated radioiodide imaging and therapy of ovarian tumor xenografts in mice *Gene Ther* 2006,13:60-66
- 54 Mitrofanova E, Hagan C, Qi J, Seregina T, Link C, Jr Sodium iodide symporter/radioactive iodine system has more efficient antitumor effect in three-dimensional spheroids *Anticancer Res* 2003,23:2397-2404
- 55 Mitrofanova E, Unfer R, Vahanian N, Link C Rat sodium iodide symporter allows using lower dose of ¹³¹I for cancer therapy *Gene Ther* 2006,13:1052-1056
- 56 Barber GN Vesicular stomatitis virus as an oncolytic vector *Viral Immunol* 2004,17:516-527
- 57 Power AT, Wang J, Falls TJ, et al Carrier cell-based delivery of an oncolytic virus circumvents antiviral immunity *Mol Ther* 2007,15:123-130

**APPENDIX III. CELL-BASED DELIVERY OF ONCOLYTIC VIRUSES: A NEW
STRATEGIC ALLIANCE FOR A BIOLOGICAL STRIKE AGAINST CANCER**

Contribution of Authors: AT Power wrote the review with feedback from JC Bell.

Published: Molecular Therapy 2007 Apr;15(4):660-5.

Cell-based Delivery of Oncolytic Viruses: A New Strategic Alliance for a Biological Strike Against Cancer

Anthony T Power¹ and John C Bell¹

¹Department of Biochemistry, Microbiology and Immunology, University of Ottawa, Centre for Cancer Therapeutics, Ottawa Health Research Institute Ottawa Hospital, Ottawa, Ontario, Canada

Recent years have seen tremendous advances in the development of exquisitely targeted replicating virotherapeutics that can safely destroy malignant cells. Despite this promise, clinical advancement of this powerful and unique approach has been hindered by vulnerability to host defenses and inefficient systemic delivery. However, it now appears that delivery of oncolytic viruses within carrier cells may offer one solution to this critical problem. In this review, we compare the advantages and limitations of the numerous cell lineages that have been investigated as delivery platforms for viral therapeutics, and discuss examples showing how combined cell-virus biotherapeutics can be used to achieve synergistic gains in antitumor activity. Finally, we highlight avenues for future preclinical research that might be taken in order to refine cell-virus biotherapeutics in preparation for human trials.

Received 7 November 2006, accepted 7 December 2006, advance online publication 30 January 2007 doi 10.1038/mt.sj.6300098

INTRODUCTION

The idea of using viruses for the treatment of human cancer was suggested as early as 1912 by DePace, only 14 years after the first virus was discovered¹. His curiosity aroused by a case of cervical tumor regression following vaccination against rabies virus, DePace² at that time undertook the first recorded clinical trial of virotherapy, inoculating eight more cancer patients with the vaccine. Nearly 100 years later, advances in molecular biology and virology have, for the first time, made it possible to harness these highly effective cellular parasites to destroy malignant cells. Many natural viruses have now been engineered or selected to create replicating oncolytic therapeutics that precisely target genetic defects arising during tumor development or unique features of the tumor microenvironment (reviewed in ref. 3). Administration of these viruses can safely induce tumor regression in a variety of models of human cancer through both direct oncolysis and stimulation of antitumor immune activity. By inserting molecular reporters into viral genomes, key aspects of virotherapy such as delivery and intratumoral replication are readily monitored *in vivo*, permitting tremendous advances in our understanding of the complex dynamics of this approach⁴⁻⁷. These promising advances have led to the hope that oncolytic viruses might be infused into the circulatory system to "seek and destroy" metastatic deposits in patients with advanced and otherwise incurable disease. However, the host immune system remains a critical obstacle to systemic administration of virotherapeutics⁷⁻¹⁴.

The primary approach to systemic therapy thus far has been to inject naked purified virions into the bloodstream of tumor-bearing hosts. However, many oncolytic viruses that are effective when administered intratumorally are highly vulnerable to host defense mechanisms that survey the circulation for pathogens, including complement proteins, antibodies, and the reticulo-endothelial system. It has been well documented that complement proteins compromise the oncolytic activity of herpes simplex virus vectors,^{8,9} and also neutralize the infectivity of retroviral therapeutics¹⁵. Pre-existing or therapy-induced neutralizing antibodies also severely compromise or ablate the systemic antitumor efficacy of adenovirus,^{10,11} vesicular stomatitis virus,⁷ herpes simplex virus,⁸ measles virus,¹⁶ reovirus,¹³ and parvovirus¹⁴ platforms. In the case of adenovirus, adhesion to human erythrocytes appears to be another significant factor contributing to therapeutic inactivation¹⁷. Extensive investigation of adenoviral therapeutics in murine models has also revealed that liver uptake is a major impediment to systemic delivery, where the majority of virus is rapidly removed from the circulation by resident Kupffer macrophages following intravenous infusion^{18,19}. Macrophage-reticuloendothelial uptake appears to be a theme common to other oncolytic viruses, as we have also observed accumulation of most vesicular stomatitis virus virions within the liver and spleen following systemic administration (JC Bell and J Paterson, unpublished results).

As, thus far, the naked virion approach to systemic administration has failed to breach this multifaceted defense

Correspondence: John C Bell, Department of Biochemistry, Microbiology and Immunology, University of Ottawa, Centre for Cancer Therapeutics, Ottawa Health Research Institute, Ottawa Hospital, 503 Smyth Road, Ottawa, Ontario, Canada K1H 1C4. E-mail: jbell@ohri.ca

system, it seems clear that alternative delivery approaches must be developed before maximal efficacy can be achieved in the clinic. To this end, it has been hypothesized that the body's cells might be used as a "trojan horse" delivery vehicle, if first infected *in vitro*, injected systemically and then carried to tumor beds to release oncolytic virus. Indeed, cells are attractive as stealth carriers, as they are the natural hosts for virus, but are generally ignored by the immune system until the onset of antigen expression at the later stages of infection. A variety of cell types have now been studied as carriers to smuggle oncolytic viruses to tumors. As these cells exhibit different characteristics and many possess therapeutic activity in their own right, the type chosen for virus delivery will likely to have important repercussions on the efficacy of treatment. In the following, we discuss the lessons learned from work to date examining cells as virotherapeutic vehicles.

PRIMARY T LYMPHOCYTES

T lymphocytes normally use the circulatory system to travel between lymphatic organs and sites of foreign antigen expression, and thus tumor-targeted T cells would seem a logical carrier for systemic virus delivery. A variety of methods have been established that permit tumor-specific T cells to be isolated from patients or engineered to express transgenic T-cell receptors for specific tumor-associated antigens.²⁰ Cells generated in this way recognize tumor antigens presented in the context of major histocompatibility complex molecules and are therefore cytotoxic effectors that home to tumors and exhibit therapeutic activity in their own right.²¹ In a screen for potential oncolytic measles virus carrier cells, Ong *et al*¹² examined freshly isolated human peripheral blood lymphocytes and found that only a minority (predominantly T cells) were susceptible to viral infection. In order to facilitate further study of this population as carriers, the proportion of T cells infected could be doubled from roughly 20 to 40% when the cells were first activated with interleukin-2 and phytohemagglutinin. Interestingly, however, the viral replication cycle appeared to be abortive even when T cells had been preactivated, as they expressed virally encoded GFP, but failed to develop characteristic cytopathic effects or release infectious virions. Despite their failure to produce free virions, infected T cells could, however, transfer measles virus infection to tumor cells via cell-cell fusion. This "heterofusion" process led to successful delivery and tumor infection when the infected T cells were administered to mice by intravenous injection. In a separate study, Cole *et al*²² successfully employed T cells to achieve systemic delivery of tumor-targeted retroviral therapeutics, albeit through quite a different strategy. Murine CD8⁺ T cells proved refractory to infection with retroviral particles, although the latter could efficiently and reversibly adhere to the cellular surface until subsequent "hand-off" when T cells were cocultured with target cells. Release of virus was enhanced both by exposure to the heparanase-rich tumor cell surface, as well as upregulation of heparanase, upon activation of the carrier T cells, providing an additional level of tumor specific targeting. In proof-of-principle experiments, the authors used CD8⁺ T cells specific for a particular tumor model to convincingly demonstrate that retroviral particles could "hitch-

hike" on the surface of tumor-homing effector cells before being handed off to malignant cells upon arrival in the tumor bed. Not surprisingly, intravenous administration of retrovirus-loaded effector T cells to mice with established metastases led to much greater efficacy than was achievable with either therapeutic alone. These findings indicate that the complementary properties of cellular and viral therapeutics may be combined for a synergistic, multipronged attack on tumors by arming tumolytic effector cells with a secondary, self-propagating weapon in the form of an oncolytic virus. This study also demonstrates that combined biotherapeutic strategies can dramatically enhance tumor specificity, as multiple targeting mechanisms can be built into both the therapeutic virus and the carrier cell.

CYTOKINE-INDUCED KILLER CELLS

As an alternative to antitumor T cells, cytokine induced killer (CIK) cells are another potential dual-purpose effector/carrier. CIK cells are obtained by *in vitro* treatment of human peripheral blood lymphocytes or murine splenocytes with interferon- γ , interleukin-2, and a T-cell receptor crosslinking antibody.^{23,24} The resultant CD8⁺, natural killer-T effector cells mediate NKG2D-dependent, non-major histocompatibility complex-restricted lysis of a variety of transformed cell types²⁵ and traffic to tumors *in vivo*.²⁶ Without any further manipulation, Thorne *et al*²⁷ have found that these cells support infection with an oncolytic strain of vaccinia virus. Importantly, CIK cells were able to produce high titers of virus, comparable to those generated by transformed cells, although viral release was delayed by several days. In theory, such replication kinetics could benefit viral delivery, allowing sufficient time for infected CIK cells to traffic to tumors before releasing their oncolytic payload. Indeed, systemically administered CIK cells have been shown to take up to 72 h to traffic to tumors,²⁶ roughly the same time frame at which vaccinia production was seen to peak in CIK cells. Using non-invasive imaging techniques, infected CIK cells were seen to deliver vaccinia to tumors following intravenous administration in mice and displayed powerful antitumor efficacy in several disease models. These findings demonstrate that like effector T cells, CIK cells can be loaded with virotherapeutics to achieve synergistic gains in antitumor activity. However, as CIK cell activity is not restricted to specific tumor antigens, it may be much easier to apply this type of biotherapeutic carrier to treat a wider range of patients and tumor types in the clinic.²⁵

PROGENITOR CELLS AS VIRUS CARRIERS

Mesenchymal progenitor cells are readily obtained from the bone marrow stroma, and can be cultured continuously under minimal growth conditions.²⁸ Their ability to engraft in tumors following intravenous injection²⁹ suggests that they may be suitable as systemic carriers for oncolytic virus. Studies to date have established that mesenchymal progenitor cells support the replication of oncolytic adenovirus and can transfer infectivity to tumors when injected directly,³⁰ although it is not yet clear whether these cells can mediate effective systemic delivery.

Circulating endothelial cells are thought to contribute to tumor neovasculature,³¹ and are therefore another cell type

whose tumor-homing abilities might be exploited. Outgrowth endothelial cells may be amenable to use as therapeutic carriers because they are readily isolated from peripheral blood samples, grow rapidly in culture, and can be maintained for at least 30 population doublings³²⁻³⁵. Their potential as virotherapeutic carriers has been investigated and, notably, outgrowth endothelial cells supported infection with non-replicating retroviral and adenoviral vectors and were able to deliver retrovirus to tumors upon systemic administration³⁶. If they prove susceptible to infection with replicating therapeutics, outgrowth endothelial cells might also be suitable vehicles for oncolytic viruses.

IMMORTALIZED CELL LINES

The ease with which transformed cells can be propagated and infected with oncolytic virus makes them an attractive vector with which to explore cell-based delivery. Early studies examining the administration of herpes simplex virus-infected teratocarcinoma cells were the first to show *in vivo* delivery to tumors³⁷. Subsequently, delivery of adenovirus to lung metastases in human carcinoma cells provided the first true demonstration of systemic oncolytic virus delivery using carrier cells, albeit in immunocompromised mice³⁸. A variety of transformed cell lineages have now been shown to mediate delivery of oncolytic parvovirus,³⁹ measles virus,¹⁶ and vesicular stomatitis virus⁷ in immune-competent as well as immune-deficient animals. Interestingly, non-invasive imaging studies have shown that cell carriers derived from a variety of solid tumor types accumulate entirely within the lungs of both tumor-bearing and tumor-free mice following intravenous administration (AT Power and JC Bell, unpublished results)⁷. These findings are consistent with previous reports showing that large-diameter solid tumor cells passively arrest within the first microcapillary bed encountered in the circulation⁴⁰ and therefore their potential as vehicles for systemic delivery may be somewhat limited. In contrast, both transformed and normal cells of hematopoietic lineages appear to show more disseminated distribution following intravenous injection and can deliver virus to other anatomical locations beside the lungs^{7, 12, 16, 27}. Given their natural residence within the circulatory system, it is perhaps not surprising that blood cells would exhibit size, deformability, and surface adhesion properties that facilitate passage through the circulatory system, making them ideal virus carriers for systemic delivery.

Perhaps the key theoretical advantage of using transformed cells for delivery is their ability to support high levels of viral replication and to release large quantities of virus within tumor beds. In a direct comparison, measles virus infection and *in vivo* delivery were indeed significantly more efficient when transformed human monocytes were used as carriers versus untransformed peripheral blood mononuclear cells or outgrowth endothelial cells¹⁶.

In order to use transformed cells as therapeutic carriers in human patients, it will be critical to ensure that uninfected cells cannot establish *de novo* metastatic growth following systemic administration. This could be accomplished by γ -irradiation of tumor cells before administration, which ablates tumorigenicity, but preserves metabolic activity. Indeed, it has been demon-

strated in several clinical trials that modified tumor vaccines consisting of both autologous and allogeneic cells are able to maintain transgene expression, but do not give rise to tumors if first irradiated before intradermal injection into patients⁴¹⁻⁴⁴. As γ -irradiation of cells does not appear to affect oncolytic virus production,^{37, 39} this may also be an effective way to ablate the tumorigenicity of systemically administered viral carriers. Alternatively, histoincompatible allogeneic or xenogeneic cells might be ideal carriers, because they can deliver oncolytic virus to tumor beds^{7, 39} before being cleared by the recipient's immune system, and have been well tolerated when given intratumorally to patients in clinical trials^{45, 46}. Genetically engineering carrier cells to express inducible suicide programs could be another potential way to ensure safety. Clinical precedence demonstrating the feasibility of this strategy has been established in studies where retroviral producer cells were safely administered and delivered the suicide gene thymidine kinase to brain tumors, suggesting that this approach would also be suitable for oncolytic virus delivery in human patients⁴⁷. Given that the appropriate safeguards are taken, immortalized cell lines may provide a highly robust carrier platform with the ability to release a targeted burst of any given oncolytic virus upon delivery to tumor sites.

IMMUNE EVASION WITH CELL-BASED ONCOLYTIC VIRUS DELIVERY: THE "TROJAN HORSE" APPROACH TO BIOTHERAPY

Although cellular delivery of virotherapies has been investigated for nearly a decade with the implicit notion of using this strategy for immune evasion, only very recently have data emerged concerning its efficacy in the context of host immunity. This is due in large part to the fact that many of the original oncolytic therapeutics were based on human viruses whose weak infectivity in murine tissues made it difficult to model immune responses in existing cancer models. Vesicular stomatitis virus is one oncolytic agent that induces a robust immune response upon administration to mice and therefore offers the opportunity to study virotherapy in the context of naturally evolving immunity. In this system, neutralizing antibody responses are elicited within the first week of therapy and completely ablate delivery of repeat systemic doses of naked virions⁷. In contrast, carcinoma cells administered during the eclipse phase of infection were able to conceal viral antigen from circulating antibodies during delivery and subsequently release virus upon delivery to tumor beds. As a result, the efficacy of a systemic multiple-dose treatment regimen in an immune-competent tumor model was dramatically increased when virus was administered within carrier cells rather than as naked virions⁷. Cells can also be used to evade anti-viral immune responses with other oncolytic viruses, Iankov *et al*¹⁶ have shown that an immortalized monocyte cell line can deliver measles virus to tumors despite the presence of high-titer human antibodies passively transferred to mice. Although these results are promising, further work is now required to determine whether consecutive administrations of virus-laden cells elicit immunity and whether these repeated doses continue to achieve tumor delivery, as this will be an important goal of any multi-dose

treatment regimen to be employed in a clinical setting. In order to predict the clinical potential of this and any other novel delivery strategy, it will be critical in future studies to expand this analysis using a quantitative approach. As demonstrated by Ong *et al.*,¹² one way this can be achieved is by using non-invasive molecular imaging technology to quantitate viral transgene expression in tumors of mice passively immunized with varying levels of neutralizing antibody. Applying this approach to examine measles virus delivery, they have demonstrated that the extent of tumor infection is dependent on the quantity of neutralizing antibody present, whether the therapeutic is administered as naked virions or within infected T cells.¹² However, their analysis also revealed quantitative differences between these two strategies, as cell-based delivery was effective over a range of antibody titers that mitigated infection with naked virions. Future studies employing and refining methods of quantitative *in vivo* assessment of viral and carrier-cell platforms will be critical in order to properly evaluate and compare their utility. Models describing relationships between key parameters such as antibody titers and tumor infection can then be constructed based on this experimental data, potentially providing mechanistic insight and clinically relevant predictions.

Approached from a quantitative perspective, future studies within both animal models and human patients will undoubtedly reveal a great deal more about how the complex interactions between cell-delivered virotherapeutics and the host immune system influence tumor infection and growth dynamics.

AWAKENING THE IMMUNE SYSTEM TO TUMORS CELL-VIRUS SYNERGY?

In addition to eradicating pre-existing tumors, cancer biotherapies have the capacity to induce protective immunity against disease recurrence. Although administration of oncolytic viruses elicits anti-viral immunity that compromises efficacy, beneficial antitumor immunity can also be stimulated.⁴⁸⁻⁵¹ Similarly, irradiated, cytokine-expressing cancer cells or antigen-presenting immune cells can be used to vaccinate experimental animals against tumor challenge and administration to human patients have been investigated.⁵²⁻⁵⁴ Combining these two approaches, by arming an already immunogenic cell-based therapeutic with an oncolytic virus, could therefore lead to synergistic enhancement of antitumor responses. Indeed, viral infection is known to activate a concerted cellular response involving the activation of hundreds of immunostimulatory genes, including those involved

Table 1 Summary of cell lineages studied as carriers for systemic delivery of oncolytic viruses

Cellular delivery platform	Advantages	Limitations
<i>Primary leukocytes</i>		
Tumor specific CD8 ⁺ T cells ¹⁹	Home to tumor antigens Specific activation/virus release at tumor site Specifically cytotoxic to tumor cells	Laborious isolation from patient samples required Typically refractory to viral infection <i>in vitro</i> hitchhiking applies to retroviruses but may not be useful for other viruses
Activated T cells ^{10,16}	Increased efficiency of infection in comparison to unstimulated T cells	Collection of primary leukocytes and lengthy activation procedure necessary Infection efficiency and viral titers produced remain low in comparison to transformed cells
CIKs ²⁴	Home to tumor sites Support infection and release high titers of oncolytic virus (<i>i.e.</i> , vaccinia) Cytotoxic against a broad spectrum of tumor types	Requires collection of primary leukocytes and <i>in vitro</i> expansion using a defined combination of cytokines May not support infection with all oncolytic viruses
<i>Immortal cell lines</i>		
Solid tumor lineage (<i>i.e.</i> , carcinoma) ^{34,36}	Ease of manipulation and propagation <i>in vitro</i> Cell lines supporting replication and high titer production of any desired OV are available May stimulate antitumor immunity	Proliferative capacity must be ablated to prevent seeding <i>de novo</i> metastatic growth Large diameter causes arrest in narrow blood vessels
Hematological lineage (<i>i.e.</i> , leukemia) ^{7,16}	Capable of dissemination throughout the circulatory system	Proliferative capacity must be ablated to prevent seeding <i>de novo</i> metastatic growth
Xenogeneic/allogeneic ⁷	Rejection by recipient's immune system prevents survival of injected cells	Host versus graft immune response may cause adverse effects and prevent continued delivery
<i>Progenitor cells</i>		
Blood outgrowth endothelial cells ^{16,33}	Can engraft into tumor neovasculature for targeted delivery Can be propagated <i>in vitro</i> over numerous population doublings	Cells are non immortal, periodic re-isolation from clinical samples is required Ability to support infection with replicating therapeutics remains untested
Mesenchymal stem cells ²⁷	Can engraft into tumor stroma for targeted delivery	Periodic re-isolation from clinical samples is required Capacity for systemic delivery remains untested

CIK, cytokine-induced killer cell, OV oncolytic virus. The advantages and limitations of each cell type as a therapeutic delivery platform are listed, preclinical studies examining their potential as oncolytic virus carriers are cited adjacent to each cell type.

in chemotaxis, inflammation, T-cell regulation and antigen presentation,^{6,55,56} which would likely boost their potency as vaccines. In support of this idea, administration of autologous tumor cells infected with Newcastle disease virus elicits a significant antitumor immune response in the B16.F10 murine melanoma model, whereas treatment with non-infected irradiated cells affords no therapeutic benefit.⁵⁷ Thus, oncolytic viruses concealed within cells for systemic delivery may, coincidentally, act as adjuvants to potentiate the immunostimulatory properties of the cellular carriers themselves.

CELL VIRUS PARTNERSHIP: THE FUTURE OF CANCER BIOTHERAPY?

Nearly 100 years after the first virus was administered to a human patient in the effort to cure cancer, tremendous successes have been achieved in creating potent replicating virotherapeutics exquisitely designed to target malignant cells. The fusion of oncolytic virus and cell-based approaches into a single biotherapeutic modality has now opened the door to promising new areas of preclinical and clinical investigation. Having established the capacity of cells to systemically deliver virus to tumor deposits and evade circulating antibodies, murine models, and non-invasive imaging techniques now offer the opportunity to refine the targeting of cellular vehicles. As discussed above, early results suggest that all cell lineages are not equally capable of widespread dissemination to target more advanced metastatic disease. Therefore hematological cells that more readily navigate the circulation may provide the best platform for therapeutic delivery. Engineering cells to express surface molecules that bind the tumor cell surface or neovasculature, such as those previously used to retarget the tropism of virotherapeutics,⁵⁸⁻⁶⁵ could help to promote accumulation of infected carrier cells within tumor beds to further enhance the efficiency of delivery. Genetic manipulation could also be used to overcome the limitations of primary effector cells as viral carriers. Gene knockdown of the key upstream components of the innate antiviral defense might enhance their ability to support viral replication and therefore the robustness of viral delivery. Engineering of immortalized leukocyte progenitors has been accomplished in order to generate myeloid cells continuously *in vitro*;⁶⁶ a similar approach might be adapted to generate a renewable source of antitumor effector cells and dispense with the laborious isolation and culture procedures required to obtain these cells for therapy. Alternatively, readily available tumor cell lines also offer advantages as oncolytic virus carriers; future exploration of their potential for systemic therapy in a clinical setting should be quite feasible provided appropriate measures are taken to first abrogate their proliferative capacity. Further preclinical study of the issues described here should pave the way for intelligently designed clinical trials investigating the safety and efficacy of this promising new partnership between cellular and viral biotherapeutics (Table 1).

REFERENCES

- Lecoq, H (2001) Discovery of the first virus, the tobacco mosaic virus 1892 or 1898? *C R Acad Sci III* **324** 929-933
- DePace, N (1912) Sulla scomparsa di un enorme vegetante del collo dell'utero senza cura chirurgica cancro *La Ginecologia* **9** 82-88
- Parato, KA, Senger, D, Forsyth, PA and Bell, JC (2005) Recent progress in the battle between oncolytic viruses and tumours *Nat Rev Cancer* **5** 965-976
- Yu, YA, Shabahang, S, Timiryasova, TM, Zhang, Q, Beltz, R and Gentschev, I *et al* (2004) Visualization of tumors and metastases in live animals with bacteria and vaccinia virus encoding light-emitting proteins *Nat Biotechnol* **22** 313-320
- Phuong, LK, Allen, C, Peng, KW, Giannini, C, Greiner, S and TenEyck, CJ *et al* (2003) Use of a vaccine strain of measles virus genetically engineered to produce carcinoembryonic antigen as a novel therapeutic agent against glioblastoma multiforme *Cancer Res* **63** 2462-2469
- Stojdl, DF, Lichty, BD, tenOever, BR, Paterson, JM, Power, AT and Knowles, S *et al* (2003) VSV strains with defects in their ability to shutdown innate immunity are potent systemic anti-cancer agents *Cancer Cell* **4** 263-275
- Power, AT, Wang, J, Falls, TJ, Paterson, JM, Parato, KA and Lichty, BD *et al* Cell-based delivery of an oncolytic virus circumvents anti-viral immunity *Mol Ther* **15** 123-130
- Ikeda, K, Ichikawa, T, Wakimoto, H, Silver, JS, Deisboeck, TS and Finkelstein, D *et al* (1999) Oncolytic virus therapy of multiple tumors in the brain requires suppression of innate and elicited antiviral responses *Nat Med* **5** 881-887
- Wakimoto, H, Ikeda, K, Abe, T, Ichikawa, T, Hochberg, FH and Ezekowitz, RA (2002) The complement response against an oncolytic virus is species-specific in its activation pathways *Mol Ther* **5** 275-282
- Chen, Y, Yu, DC, Charlton, D and Henderson, DR (2000) Pre-existent adenovirus antibody inhibits systemic toxicity and antitumor activity of CN706 in the nude mouse LNCaP xenograft model: implications and proposals for human therapy *Hum Gene Ther* **11** 1553-1567
- Tsai, V, Johnson, DE, Rahman, A, Wen, SF, LaFace, D and Philopena, J *et al* (2004) Impact of human neutralizing antibodies on antitumor efficacy of an oncolytic adenovirus in a murine model *Clin Cancer Res* **10** 7199-7206
- Ong, HT, Hasegawa, K, Dietz, AB, Russell, SJ and Peng, KW (2006) Evaluation of T cells as carriers for systemic measles virotherapy in the presence of antiviral antibodies *Gene Ther*, advance online publication, 19 October 2006
- Hirasawa, K, Nishikawa, SG, Norman, KL, Coffey, MC, Thompson, BG and Yoon, CS *et al* (2003) Systemic reovirus therapy of metastatic cancer in immune-competent mice *Cancer Res* **63** 348-353
- Lang, SI, Giese, NA, Rommelaere, J, Dinsart, C and Cornelis, JJ (2006) Humoral immune responses against minute virus of mice vectors *J Gene Med* **8** 1141-1150
- Takeuchi, Y, Cosset, FL, Lachmann, PJ, Okada, H, Weiss, RA and Collins, MK (1994) Type C retrovirus inactivation by human complement is determined by both the viral genome and the producer cell *J Virol* **68** 8001-8007
- Iankov, I, Blechacz, B, Liu, C, Schmeckpeper, JD, Tarara, JE and Federspiel, MJ *et al* Infected cell carriers—a new strategy for systemic delivery of oncolytic measles viruses in cancer virotherapy *Mol Ther* **15** 114-122
- Lyons, M, Onion, D, Green, NK, Aslan, K, Rajaratnam, R and Bazan, Peregrino, M *et al* (2006) Adenovirus type 5 interactions with human blood cells may compromise systemic delivery *Mol Ther* **14** 118-128
- Worgall, S, Wolff, G, Falck-Pedersen, E and Crystal, RG (1997) Innate immune mechanisms dominate elimination of adenoviral vectors following *in vivo* administration *Hum Gene Ther* **8** 37-44
- Ye, X, Jerebtsova, M and Ray, PE (2000) Liver bypass significantly increases the transduction efficiency of recombinant adenoviral vectors in the lung, intestine, and kidney *Hum Gene Ther* **11** 621-627
- Dudley, ME and Rosenberg, SA (2003) Adoptive-cell-transfer therapy for the treatment of patients with cancer *Nat Rev Cancer* **3** 666-675
- Yee, C, Riddell, SR and Greenberg, PD (2001) *In vivo* tracking of tumor-specific T cells *Curr Opin Immunol* **13** 141-146
- Cole, C, Qiao, J, Kottke, T, Diaz, RM, Ahmed, A and Sanchez Perez, L *et al* (2005) Tumor-targeted, systemic delivery of therapeutic viral vectors using hitchhiking on antigen-specific T cells *Nat Med* **11** 1073-1081
- Lu, PH and Negrin, RS (1994) A novel population of expanded human CD3+CD56+ cells derived from T cells with potent *in vivo* antitumor activity in mice with severe combined immunodeficiency *J Immunol* **153** 1687-1696
- Baker, J, Verners, MR, Ito, M, Shizuru, JA and Negrin, RS (2001) Expansion of cytolytic CD8(+) natural killer T cells with limited capacity for graft-versus-host disease induction due to interferon gamma production *Blood* **97** 2923-2931
- Verners, MR, Karami, M, Baker, J, Jayaswal, A and Negrin, RS (2004) Role of NKG2D signaling in the cytotoxicity of activated and expanded CD8+ T cells *Blood* **103** 3065-3072
- Edinger, M, Cao, YA, Verners, MR, Bachmann, MH, Contag, CH and Negrin, RS *et al* (2003) Revealing lymphoma growth and the efficacy of immune cell therapies using *in vivo* bioluminescence imaging *Blood* **101** 640-648
- Thorne, SH, Negrin, RS and Contag, CH (2006) Synergistic antitumor effects of immune cell-viral biotherapy *Science* **311** 1780-1784
- Prockop, DJ (1997) Marrow stromal cells as stem cells for nonhematopoietic tissues *Science* **276** 71-74
- Studený, M, Marini, FC, Dembinski, JL, Zompetta, C, Cabreira Hansen, M and Bekele, BN *et al* (2004) Mesenchymal stem cells: potential precursors for tumor stroma and targeted-delivery vehicles for anticancer agents *J Natl Cancer Inst* **96** 1593-1603
- Komarova, S, Kawakami, Y, Stoff-Khalili, MA, Curiel, DT and Pereboeva, L (2006) Mesenchymal progenitor cells as cellular vehicles for delivery of oncolytic adenoviruses *Mol Cancer Ther* **5** 755-766
- Lyden, D, Hattori, K, Dias, S, Costa, C, Blaikie, P and Butros, L *et al* (2001) Impaired recruitment of bone-marrow-derived endothelial and hematopoietic precursor cells blocks tumor angiogenesis and growth *Nat Med* **7** 1194-1201
- Gehling, UM, Ergun, S, Schumacher, U, Wagener, C, Pantel, K and Otte, M *et al* (2000) *In vitro* differentiation of endothelial cells from AC133-positive progenitor cells *Blood* **95** 3106-3112
- Lin, Y, Weisdorf, DJ, Solovey, A and Hebbel, RP (2000) Origins of circulating endothelial cells and endothelial outgrowth from blood *J Clin Invest* **105** 71-77

- 34 Peichev, M, Naiyer, AJ, Pereira, D, Zhu, Z, Lane, WJ and Williams, M *et al* (2000) Expression of VEGFR-2 and AC133 by circulating human CD34(+) cells identifies a population of functional endothelial precursors *Blood* **95** 952-958
- 35 Quirici, N, Soligo, D, Caneva, L, Servida, F, Bossolasco, P and Deliliers, GL (2001) Differentiation and expansion of endothelial cells from human bone marrow CD133(+) cells *Br J Haematol* **115** 186-194
- 36 Jevremovic, D, Gulati, R, Hennig, I, Diaz, RM, Cole, C and Kleppe, L *et al* (2004) Use of blood outgrowth endothelial cells as virus-producing vectors for gene delivery to tumors *Am J Physiol Heart Circ Physiol* **287** H494-H500
- 37 Coukos, G, Makrigiannakis, A, Kang, EH, Caparelli, D, Benjamin, I and Kaiser, LR *et al* (1999) Use of carrier cells to deliver a replication-selective herpes simplex virus-1 mutant for the intraperitoneal therapy of epithelial ovarian cancer *Clin Cancer Res* **5** 1523-1537
- 38 Garcia-Castro, J, Martinez-Palacio, J, Lillo, R, Garcia-Sanchez, F, Alemany, R and Madero, L *et al* (2005) Tumor cells as cellular vehicles to deliver gene therapies to metastatic tumors *Cancer Gene Ther* **12** 341-349
- 39 Raykov, Z, Balboni, G, Aprahamian, M and Rommelaere, J (2004) Carrier cell-mediated delivery of oncolytic parvoviruses for targeting metastases *Int J Cancer* **109** 742-749
- 40 Chambers, AF, Groom, AC and MacDonald, IC (2002) Dissemination and growth of cancer cells in metastatic sites *Nat Rev Cancer* **2** 563-572
- 41 Raetz, LE, Cassileth, PA, Schlesselman, JJ, Sridhar, K, Padmanabhan, S and Fisher, EZ *et al* (2004) Allogeneic vaccination with a B7.1 HLA-A gene-modified adenocarcinoma cell line in patients with advanced non-small-cell lung cancer *J Clin Oncol* **22** 2800-2807
- 42 Nemunaitis, J, Jahan, T, Ross, H, Serman, D, Richards, D and Fox, B *et al* (2006) Phase 1/2 trial of autologous tumor mixed with an allogeneic GVAX vaccine in advanced-stage non-small-cell lung cancer *Cancer Gene Ther* **13** 555-562
- 43 Bowman, LC, Grossmann, M, Rill, D, Brown, M, Zhong, WY and Alexander, B *et al* (1998) Interleukin-2 gene-modified allogeneic tumor cells for treatment of relapsed neuroblastoma *Hum Gene Ther* **9** 1303-1311
- 44 Bowman, L, Grossmann, M, Rill, D, Brown, M, Zhong, WY and Alexander, B *et al* (1998) IL-2 adenovector-transduced autologous tumor cells induce antitumor immune responses in patients with neuroblastoma *Blood* **92** 1941-1949
- 45 Tartour, E, Mehtali, M, Sastre-Garau, X, Joyeux, I, Mathiot, C and Pleau, JM *et al* (2000) Phase I clinical trial with IL-2-transfected xenogeneic cells administered in subcutaneous metastatic tumours: clinical and immunological findings *Br J Cancer* **83** 1454-1461
- 46 Rochlitz, C, Dreno, B, Jantschke, P, Cavalli, F, Squiban, P and Acres, B *et al* (2002) Immunotherapy of metastatic melanoma by intratumoral injections of Vero cells producing human IL-2: phase II randomized study comparing two dose levels *Cancer Gene Ther* **9** 289-295
- 47 Ram, Z, Culver, KW, Oshiro, EM, Viola, JJ, DeVroom, HL and Otto, E *et al* (1997) Therapy of malignant brain tumors by intratumoral implantation of retroviral vector-producing cells *Nat Med* **3** 1354-1361
- 48 Hallden, G, Hill, R, Wang, Y, Anand, A, Liu, TC and Lemoine, NR *et al* (2003) Novel immunocompetent murine tumor models for the assessment of replication-competent oncolytic adenovirus efficacy *Mol Ther* **8** 412-424
- 49 Kim, JH, Oh, JY, Park, BH, Lee, DE, Kim, JS and Park, HE *et al* (2006) Systemic armed oncolytic and immunologic therapy for cancer with JX-594, a targeted poxvirus expressing GM-CSF *Mol Ther* **14** 361-370
- 50 Hummel, JL, Safroneeva, E and Mossman, KL (2005) The role of ICP0-Null HSV-1 and interferon signaling defects in the effective treatment of breast adenocarcinoma *Mol Ther* **12** 1101-1110
- 51 Todo, T, Rabkin, SD, Sundaresan, P, Wu, A, Meehan, KR and Herscovitz, HB *et al* (1999) Systemic antitumor immunity in experimental brain tumor therapy using a multmutated, replication-competent herpes simplex virus *Hum Gene Ther* **10** 2741-2755
- 52 Saigaller, ML and Lodge, PA (1998) Use of cellular and cytokine adjuvants in the immunotherapy of cancer *J Surg Oncol* **68** 122-138
- 53 Gilboa, E (1996) Immunotherapy of cancer with genetically modified tumor vaccines *Semin Oncol* **23** 101-107
- 54 Pardoll, DM (1995) Paracrine cytokine adjuvants in cancer immunotherapy *Annu Rev Immunol* **13** 399-415
- 55 Huang, Q, Liu, D, Majewski, P, Schulte, LC, Korn, JM and Young, RA *et al* (2001) The plasticity of dendritic cell responses to pathogens and their components *Science* **294** 870-875
- 56 Der, SD, Zhou, A, Williams, BR and Silverman, RH (1998) Identification of genes differentially regulated by interferon alpha, beta, or gamma using oligonucleotide arrays *Proc Natl Acad Sci USA* **95** 15623-15628
- 57 Plaksin, D, Porgador, A, Vada, E, Feldman, M, Schirmacher, V and Eisenbach, L (1994) Effective anti-metastatic melanoma vaccination with tumor cells transfected with MHC genes and/or infected with Newcastle disease virus (NDV) *Int J Cancer* **59** 796-801
- 58 Hallak, LK, Merchan, JR, Storgard, CM, Loftus, JC and Russell, SJ (2005) Targeted measles virus vector displaying echistatin infects endothelial cells via alpha(v)beta3 and leads to tumor regression *Cancer Res* **65** 5292-5300
- 59 Bergman, I, Whitaker-Dowling, P, Gao, Y and Griffin, JA (2004) Preferential targeting of vesicular stomatitis virus to breast cancer cells *Virology* **330** 24-33
- 60 Morizono, K, Xie, Y, Ringpis, GE, Johnson, M, Nassanian, H and Lee, B *et al* (2005) Lentiviral vector retargeting to P-glycoprotein on metastatic melanoma through intravenous injection *Nat Med* **11** 346-352
- 61 Hasegawa, K, Nakamura, T, Harvey, M, Ikeda, Y, Oberg, A and Figini, M *et al* (2006) The use of a tropism-modified measles virus in folate receptor targeted virotherapy of ovarian cancer *Clin Cancer Res* **12** (Part 1) 6170-6178
- 62 Nakamura, T, Peng, KW, Harvey, M, Greiner, S, Lorimer, IA and James, CD *et al* (2005) Rescue and propagation of fully retargeted oncolytic measles viruses *Nat Biotechnol* **23** 209-214
- 63 Bucheit, AD, Kumar, S, Grote, DM, Lin, Y, von Messling, V and Cattaneo, RB *et al* (2003) An oncolytic measles virus engineered to enter cells through the CD20 antigen *Mol Ther* **7** 62-72
- 64 Hammond, AL, Plemper, RK, Zhang, J, Schneider, U, Russell, SJ and Cattaneo, R (2001) Single-chain antibody displayed on a recombinant measles virus confers entry through the tumor-associated carcinoembryonic antigen *J Virol* **75** 2087-2096
- 65 Peng, KW, Donovan, KA, Schneider, U, Cattaneo, R, Lust, JA and Russell, SJ (2003) Oncolytic measles viruses displaying a single-chain antibody against CD38, a myeloma cell marker *Blood* **101** 2557-2562
- 66 Wang, GC, Calvo, KR, Pasillas, MP, Sykes, DB, Hacker, H and Kamps, MP (2006) Quantitative production of macrophages or neutrophils *ex vivo* using conditional Hoxb8 *Nat Methods* **3** 287-293

APPENDIX IV. EFFECTS OF INTRAVENOUSLY ADMINISTERED RECOMBINANT VESICULAR STOMATITIS VIRUS (VSV(DELTA M51)) ON MULTIFOCAL AND INVASIVE GLIOMAS

Contribution of Authors: AT Power generated the VSV Δ 51 recombinant virus used in these studies. AT Power extracted RNA from brain tumor samples and performed RT-PCR of the matrix gene to sequence verify the stability of the matrix gene deletion during growth of the recombinant virus *in vivo*.

Published: J Natl Cancer Inst. 2006 Nov 1;98(21):1546-57

Effects of Intravenously Administered Recombinant Vesicular Stomatitis Virus (VSV Δ M51) on Multifocal and Invasive Gliomas

XueQing Lun, Donna L. Senger, Tommy Alain, Andra Oprea, Kelley Parato, Dave Stojdl, Brian Lichty, Anthony Power, Randal N. Johnston, Mark Hamilton, Ian Parney, John C. Bell, Peter A. Forsyth

Background: An ideal virus for the treatment of cancer should have effective delivery into multiple sites within the tumor, evade immune responses, produce rapid viral replication, spread within the tumor, and infect multiple tumors. Vesicular stomatitis virus (VSV) has been shown to be an effective oncolytic virus in a variety of tumor models, and mutations in the matrix (M) protein enhance VSV's effectiveness in animal models. **Methods:** We evaluated the susceptibility of 14 glioma cell lines to infection and killing by mutant strain VSV Δ M51, which contains a single-amino acid deletion in the M protein. We also examined the activity and safety of this strain against the U87 and U118 experimental models of human malignant glioma in nude mice and analyzed the distribution of the virus in the brains of U87 tumor-bearing mice using fluorescence labeling. Finally, we examined the effect of VSV Δ M51 on 15 primary human gliomas cultured from surgical specimens. All statistical tests were two-sided. **Results:** All 14 glioma cell lines were susceptible to VSV Δ M51 infection and killing. Intratumoral administration of VSV Δ M51 produced marked regression of malignant gliomas in nude mice. When administered systemically, live VSV Δ M51 virus, as compared with dead virus, statistically significantly prolonged survival of mice with unilateral U87 tumors (median survival: 113 versus 46 days, $P = .0001$) and bilateral U87 tumors (median survival: 73 versus 46 days, $P = .0025$). VSV Δ M51 infected multifocal gliomas, invasive glioma cells that migrated beyond the main glioma, and all 15 primary human gliomas. There was no evidence of toxicity. **Conclusions:** Systemically delivered VSV Δ M51 was an effective and safe oncolytic agent against laboratory models of multifocal and invasive malignant gliomas, the most challenging clinical manifestations of this disease. [J Natl Cancer Inst 2006;98:1546–57]

Human malignant glioma is one of the most common primary central nervous system tumors in adults. The ability to treat

patients with malignant gliomas remains poor. Despite dramatic improvements in neuroimaging and neurosurgical techniques, the prognosis of patients with malignant glioma has not improved substantially during the past 30 years (1). The most aggressive treatment available for patients with malignant glioma is surgical resection followed first by conventional radiotherapy administered with concomitant chemotherapy and then by adjuvant chemotherapy (2). Despite successful initial treatment of patients with malignant glioma, the median survival of patients with glioblastoma multiforme thus treated is just over 1 year (2), and virtually all patients die of recurrent disease (3–5).

Malignant gliomas are diffuse, highly invasive, and often multifocal. The core tumor is surrounded by a penumbra of invasive tumor cells that are detectable several centimeters away from the main tumor mass. These locally invasive glioma cells, which are often found at the margins of the tumor resection, are the most common site of malignant glioma recurrence. In addition, these invasive glioma cells activate several cellular signaling pathways that render them more

Affiliations of authors Departments of Oncology, Clinical Neurosciences, and Biochemistry and Molecular Biology, Tom Baker Cancer Centre (XL, DLS, TA, AO, RNJ, IP, PAF), Clark H. Smith Integrative Brain Tumor Research Center (XL, DLS, TA, AO, MH, IP, PAF), Department of Neurosurgery (MH), University of Calgary, AB, Canada; Ottawa Regional Cancer Centre Research Laboratories, Ottawa, ON, Canada (KP, AP, JCB), Apoptosis Research Center, Children's Hospital of Eastern Ontario, Ottawa, ON, Canada (DS), Centre for Gene Therapeutics, Department of Pathology and Molecular Medicine, McMaster University, Hamilton, ON, Canada (BL)

Correspondence to Peter A Forsyth, MD, Clark H Smith Integrative Brain Tumor Research Center, Rm 372A, Heritage Medical Research Building, 3330 Hospital Dr NW, Calgary, AB T2N 4N1, Canada (e-mail pforssyth@ucalgary.ca)

See "Notes" following "References"

DOI 10.1093/jnci/djj413

© 2006 The Author(s)

This is an Open Access article distributed under the terms of the Creative Commons Attribution Non-Commercial License (<http://creativecommons.org/licenses/by-nc/2.0/uk/>), which permits unrestricted non-commercial use, distribution, and reproduction in any medium, provided the original work is properly cited

resistant to conventional chemotherapies than their noninvasive counterparts (6). Therefore, malignant glioma must be considered as a cerebral disease that requires treatment not only of a single, main tumor mass but also of invasive cells and multiple tumor foci.

Recently, several oncolytic viruses have shown promising results in preclinical models of brain tumors. These viruses include reovirus (7–9), recombinant herpes simplex virus (10–14), Newcastle disease virus (15–17), recombinant poliovirus (18,19), myxoma virus (20), modified adenovirus (21–23), and wild-type vesicular stomatitis virus (VSV) (24–28). Despite impressive preclinical data, there are potential limitations to the use of these viruses in patients, such as inadequate distribution and/or delivery and insufficient levels of gene transfer or virus replication (29–32). Indeed, no dramatic results have been reported in the small number of early clinical trials in humans using oncolytic viruses against malignant glioma (15,16,33–36). Case reports of long-term survivors (35) and a patient with a complete response (17) have been described, and a clinical trial in patients with recurrent malignant gliomas treated with reovirus has been completed (37), but a final report has not been published.

Oncolytic viruses exploit a number of genetic defects in tumor cells (38–42). A common genetic defect occurring during tumor evolution is diminished responsiveness to interferon (43,44). This common defect reflects the important role of interferon-regulated pathways in the control of normal growth and apoptosis. Interferon is also a key mediator of the individual cell's innate antiviral response. When tumor cells acquire mutations that allow them to escape interferon-mediated growth control pathways (e.g., those controlling proliferation or apoptosis), the tumor cells simultaneously compromise their innate viral responses, permitting a lethal viral infection within the tumor cell. In addition, tumor cells may have defects in signaling pathways such as the Myc, Ras, or p53 pathways that render them susceptible to VSV replication (26,28,45). Thus, tumor cells undergo growth and proliferation at the expense of losing their resistance to viral infection, and a lethal oncolytic infection occurs.

We and others have found that wild-type VSV is a potent oncolytic virus in a number of tumor cell types, including gliomas (24,28,43–45) but is lethal to animals that have not been treated with interferon (43). Hence, we used a VSV mutant called VSV Δ M51. VSV Δ M51 has a single amino acid deletion of methionine-51 (M51) of the matrix (M) protein. One of the functions of the M protein is to block the nuclear to cytoplasmic transport of interferon-beta mRNA, thereby circumventing the cellular interferon response. The deletion of methionine-51 from the M protein of VSV Δ M51 abolishes this block and restores interferon-mediated responses in normal cells. This mutant theoretically has an improved therapeutic value (that is, safer but retaining the same efficacy) compared with wild-type VSV because it induces a marked interferon response in normal cells but retains its full oncolytic effect against tumor cells both *in vitro* and *in vivo* (43).

During the past several years of oncolytic virus development, it has become apparent that insufficient viral delivery can be a key limitation in the treatment of brain tumors (29,38,40,43). Direct inoculation of virus into a tumor may be advantageous in the treatment of localized tumor, but focal necrosis, tissue planes, and high intratumoral pressure will still limit viral distribution. Intravascular administration is an attractive alternative and may allow for multiple administrations over a long period of time. Although

an intact blood–brain barrier will affect delivery to the normal brain, the blood–tumor barrier is somewhat permeable and may provide a potential advantage over direct intratumoral inoculation in delivery to multifocal tumors and invasive tumor cells. In addition, intravascular injection is simpler, less expensive, and less invasive clinically than direct local delivery. A number of preclinical studies have shown that virus treatments can be delivered to brain tumors via intracarotid delivery (46–50), but only two studies have shown intravenous delivery of an oncolytic virus for the treatment of brain tumors (51,52). The systemic/vascular delivery of VSV mutants has previously been shown to be effective in animal models of cancer, including those that had already widely metastasized (43,53) or were multifocal (54).

In this study, we investigated the effects of intravenous delivery of VSV Δ M51 for the treatment of brain tumors. We carried out a detailed evaluation of the oncolytic properties of VSV Δ M51 *in vitro*, *in vivo*, and *ex vivo* in human malignant glioma surgical specimens. We also compared the effects of VSV Δ M51 to those of another oncolytic virus, reovirus. Reovirus has activity against experimental models of malignant glioma, but a small number of glioma cell lines are highly resistant to infection and killing by this virus (8,9).

MATERIALS AND METHODS

Cell Lines

Fourteen human glioma cell lines (U87, U118, U251, U343, U373, U563, SF126, SF188, SNB19, UC12, UC13, UC14, RG2, and 9L) and murine NIH3T3 and L929 fibroblast cells were purchased from the American Type Culture Collection (ATCC, Manassas, VA). HS68 human foreskin fibroblast cells were a gift from Karl Riabowol (University of Calgary, Canada). All cells were propagated in Dulbecco's modified Eagle medium/F12 (DMEM/F12, Hybri-care, ATCC, Manassas, VA) containing 10% fetal bovine serum (FBS) at 37 °C in a humidified, 5% CO₂ incubator. Each cell line was tested regularly for mycoplasma contamination.

Transfection of Glioma Cells With Red Fluorescent Protein

FuGene transfection reagent (Roche Diagnostic Co, Indianapolis, IN) and an expression plasmid containing red fluorescent protein (RFP) (Clontech, Palo Alto, CA) were used for transfection of a glioma cell line (U87) with RFP, as previously described (7). Briefly, FuGene transfection reagent and RFP DNA vector were incubated together for 30 minutes at room temperature in serum-free media. The DNA mixture was applied to U87 cells for 4 hours at 37 °C in serum-free media. FBS was then added to a final concentration of 10%. Cells were grown at 37 °C and 5% CO₂, and the culture medium was changed daily. After 4 days, transfected cells were selected for G418 antibiotic resistance (400 µg/mL) and identified by fluorescent microscopy. RFP expression was found in more than 95% of cells as determined by fluorescence-activated cell sorting; this method confirmed the purity of the U87-RFP-expressing cells.

Viruses and Cell Infection

VSV Δ M51 is derived from the Indiana serotype of VSV and is propagated in Vero cells (African green monkey kidney cells)

VSV Δ M51 has a single amino acid deletion of methionine-51 of the M protein and contains an extra cistron that encodes green fluorescent protein (GFP) inserted between the G and L sequences. This recombinant genome was used to generate a replication-competent, GFP-expressing VSV clone (43). Dead virus was prepared by exposing live virus to ultraviolet (UV) irradiation for 1 hour. Reovirus serotype 3 (strain Dearing or T3D) was grown in L929 mouse fibroblast cells and purified as previously described (55), it was similarly UV inactivated to generate dead virus. Tumor or normal cells grown to 50%–60% confluence in 96-well plates were infected in 50 μ L of serum-free medium and incubated for 1 hour at 4 °C for reovirus or 37 °C for VSV Δ M51. Medium (150 μ L) was then added to each well, and cells were returned to 37 °C at 5% CO₂ for use in subsequent experiments.

3-(4,5-Dimethylthiazol-2-yl)-2,5-Diphenyl-2H-Tetrazolium Bromide Assay

Viability of tumor or normal cells infected as above with different doses (multiplicity of infection [MOI] = 0, 1, and 10) of VSV Δ M51 or reovirus-T3D was measured 24 hours (VSV Δ M51) and 72 hours (reovirus) after infection by 3-(4,5-dimethylthiazol-2-yl)-2,5-diphenyl-2H-tetrazolium bromide (MTT) assay, as previously described (55). Briefly, cells were incubated with MTT (1 mg/mL) at 37 °C and 5% CO₂ for 1 hour and lysed with dimethyl sulfoxide, and the absorbance was read with an ultra microplate reader (Bio-Tek Instruments, Inc, Burlington, VT).

Assays to Measure Cytopathic Effect of VSV Δ M51 or Reovirus Infection

All glioma and normal cell lines were seeded at 5 \times 10⁴ cells per well in six-well plates and incubated at 37 °C in 5% CO₂ overnight. After infection with live or dead VSV Δ M51 at an MOI of 1 or 10 for 24–72 hours, the cells were examined using a Zeiss inverted microscope (Axiovert 200M) mounted with a Carl Zeiss camera (AxioCam MRc, Carl Zeiss Inc, Thornwood, NY) to obtain both phase contrast and fluorescent images (using a fluorescein isothiocyanate filter to visualize virus-encoded GFP).

Western Blot to Detect Viral Proteins

All cell lines were seeded at 5 \times 10⁴ cells per well in six-well plates and incubated at 37 °C in 5% CO₂ overnight. Cells were then treated with either dead or live VSV Δ M51 virus at an MOI of 1. Twenty-four hours after infection, the cells were collected by scraping and were lysed in 500 μ L of lysis buffer (20 mM Tris pH 8.0, 136 mM NaCl, 10% glycerol, 1% NP40, 0.02% leupeptin, 0.5% aprotinin, and 1.5% sodium orthovanadate) for 20 minutes. Cellular debris was removed by low-speed centrifugation (1000g for 10 minutes) at 4 °C. Protein concentration of cell lysates was determined using the BCA protein assay kit (BioLynx, Inc, Brockville, ON, Canada). Supernatants were frozen at –80 °C for long-term storage. For electrophoresis, equal amounts of protein were separated on 7.5% sodium dodecyl sulfate–polyacrylamide gels and transferred to nitrocellulose membranes. Membranes were incubated with polyclonal anti-VSV antibody (1:1000) overnight at 4 °C, washed three times with 1 \times Tris buffered saline, and incubated for 1 hour with horseradish peroxidase (HRP)–conjugated secondary antibody (1:3000 dilution,

Biosciences, Amersham, Piscataway, NJ) at room temperature (John C Bell, unpublished). Antibody binding was detected using an enhanced chemiluminescence reagent (Biosciences, Amersham) according to the manufacturer's instructions.

Mice

CD-1 nude mice (female, 6–8 weeks old) were purchased from Charles River Canada, Constant, PQ, Canada. Three to four mice were caged together in each vivarium with a 12-hour light/dark schedule at 22 \pm 1 °C and a relative humidity of 50 \pm 5%. Food and water were available ad libitum. In all experiments, mice were killed by cervical dislocation when they had difficulty ambulating, feeding, or grooming or had lost at least 20% of their body weight. All animal procedures were reviewed and approved by the University of Calgary Animal Care Committee.

In Vivo Oncolysis in Subcutaneous Tumor Model

Female CD-1 nude mice (n = 21) were each implanted with 1 \times 10⁶ U87 (n = 11) or U118 (n = 10) malignant glioma cells on the right flank to establish subcutaneous tumors. Tumor size (length \times width) was measured daily using calipers. When palpable tumors reached approximately 25 mm², mice were treated intratumorally with live or dead VSV Δ M51 virus (three injections of VSV Δ M51 1 \times 10⁷ plaque-forming units [PFU] at 2-day intervals) (8). Tumor size was then measured until sacrifice was indicated.

Determination of the Toxicity of the Intracerebral Administration of VSV Δ M51 in Nude Mice

Female CD-1 nude mice (n = 8) were injected intracerebrally with either dead or live VSV Δ M51 (5 \times 10², 1 \times 10³, 1 \times 10⁴ PFU per mouse, two mice per dose) at a depth of 3 mm under guidance of a stereotactic frame (Kopf Instruments, Tujunga, CA), as described previously (7,20,56). Briefly, virus was injected intracerebrally into the right putamen. A 0.5-mm burr hole was made 1.5–2 mm right of the midline and 0.5–1 mm posterior to the coronal suture through a scalp incision. Stereotactic injection used a 5- μ L syringe (Hamilton Co, Reno, NV) with a 30-gauge needle, inserted through the burr hole to a depth of 3 mm, mounted on a Kopf stereotactic apparatus (Kopf Instruments). After 10 seconds, the needle was withdrawn and the incision was sutured. Mice were followed daily for toxic effects. After the mice were killed, their brains, lungs, kidneys, hearts, and livers were removed, fixed in 10% formalin, embedded in paraffin, and sectioned with a microtome. Sections were stained with hematoxylin and eosin for histologic analysis, analyzed for VSV antigens by immunohistochemistry, or analyzed for the presence of DNA fragments by terminal transferase deoxyuridine triphosphate nick-end labeling (TUNEL) assay.

Immunohistochemistry to Detect VSV Antigens

Frozen sections of mouse brain and major organs (heart, liver, lung, and kidney) were fixed in 4% paraformaldehyde for 20 minutes and washed three times in phosphate-buffered saline (PBS). Sections were then exposed to primary polyclonal rabbit anti-VSV antibody at a 1:3000 dilution in PBS containing 2%

bovine serum albumin, for 24 hours at 4 °C Biotinylated anti-rabbit IgG (Vector Laboratories, Burlingame, CA) was used as the secondary antibody Sections were then incubated with avidin conjugated to HRP (Vectastain ABC immunohistochemistry kit, Vector Laboratories), and staining was visualized by addition of the DAB (3,3'-diaminobenzidine) substrate To visualize VSV antigens, sections were mounted and viewed with a Zeiss inverted microscope (Axiovert 200M) and a Carl Zeiss camera (AxioCam MRc) to obtain both phase contrast and fluorescent images

TUNEL Assay

The presence of fragmented DNA was analyzed with the TUNEL technique using the ApopTag plus fluorescein in situ apoptosis detection kit (Chemicon, Inc, Temecula, CA) according to the manufacturer's instructions Briefly, paraffin-embedded brain sections were dewaxed in xylene, rehydrated in an ethanol gradient, and treated with proteinase K (Invitrogen, Carlsbad, CA, 20 µg/mL in PBS) for 20 minutes at room temperature Sections were washed in PBS, incubated with reaction mixture including terminal deoxynucleotidyl transferase and fluorescein-dUTP for 1 hour at 37 °C, washed in PBS, incubated with the antidigoxigenin conjugate for 30 minutes at 37 °C, and then counterstained with 4'-6-diamidino-2-phenylindole

Sequencing of M Protein in VSV Δ M51

At 48 hours after intracerebral injections of 1×10^4 PFU of VSV Δ M51, mice were killed by cervical dislocation and their brains were homogenized in PBS (pH 7.2) Virus was amplified by a single passage of brain homogenate on Vero cells for 24 hours Virions were purified from the Vero cell supernatant by passage through a 0.2-µm filter followed by centrifugation at 30 000g for 90 minutes The virus pellet was resuspended in PBS, and genomic RNA was extracted by sequential addition of Trizol (Invitrogen) and chloroform (57), except that rather than lysing and extracting RNA from the cells, we extracted it from purified VSV particles Samples were then centrifuged at 10 000g for 10 minutes, and the aqueous phase was removed and washed on an RNeasy spin column (Qiagen, Mississauga, Ontario, Canada) per the manufacturer's instructions The RNA product was used as a template in a random hexamer-primed reaction using Superscript II reverse transcriptase to generate single-stranded viral cDNA From this cDNA template, specific primers (sense ACGAATTCAAATTAGGGATCGCACCACC, antisense ACGGATCCCCTGATACTCGGGTTGACCT) were used in the polymerase chain reaction to amplify a 377-bp fragment spanning bases 61–438 of the VSV M gene This product was purified on an agarose gel and sequenced directly from the above sense primer using an Applied Biosystems 3730 DNA Analyzer (Ottawa Genomics Innovation Centre)

Determination of the Appropriate VSV Δ M51 Dose for Intravenous Administration in Nude Mice

Female CD-1 nude mice ($n = 24$) received intravenous injection of dead or live virus (at doses of 5×10^7 , 5×10^8 , 1×10^9 , or 5×10^9 PFU per mouse) via the tail vein Mice were followed for up to 60 days, and their body weights were recorded every other day After the mice were killed by cervical dislocation, their

brains and major organs (liver, lung, heart, and kidney) were saved either for virus recovery assays in liquid nitrogen or pathologic analysis in formalin as described above For the *in vivo* therapeutic experiments, we selected a dose that was one dose level below the dose at which 50% of the mice died, we refer to this dose as the maximum tolerated

Virus Recovery Assays

Mice were killed by cervical dislocation, and saline was immediately infused into the left ventricle of the heart Tissues were extracted and then homogenized in liquid nitrogen using a Pellet Pestles Kit (VWR International, Edmonton, Alberta, Canada) followed by repeated freeze-thawing to release virus from the cells Supernatants were used for plaque titration on Vero cells as previously described (58) Briefly, Vero cells were plated in six-well plates and infected with serial dilutions of sample supernatant Forty-eight hours after incubation at 37 °C in 5% CO₂, cells were overlaid with 2× MEM (Mediatech, Herndon, VA) and 2× Noble agar (Difco Laboratories, Detroit, MI) containing 0.2 mL neutral red (Sigma Chemical, Oakville, Ontario, Canada) Virus plaques were counted, and PFU were calculated by the number of plaques multiplied by the dilution factor

Survival Studies in an Orthotopic Human Glioma Model of Nude Mice

To investigate the antitumor efficacy of VSV Δ M51 in mice, an orthotopic unilateral glioma animal model was established with the human glioma cell line U87 The stereotactic techniques used to implant glioma cells in the right putamen have been described previously (7,20) Briefly, female CD-1 nude mice ($n = 13$) were anesthetized, and U87 glioma cells (1×10^5 cells per mouse) were implanted under the guidance of a stereotactic frame, as described above After 15 days, mice were injected intravenously via the tail vein with multiple doses of live ($n = 8$) or dead ($n = 5$) virus (5×10^8 PFU per mouse every 2 days, for a total of three injections) Mice were monitored every other day for survival After the mice were killed, their brains and major organs were prepared as described above for histologic analysis, immunohistochemical analysis of VSV antigen, and TUNEL assay to assess apoptosis

Survival was also assessed in mice with bilateral brain tumors To prepare these mice, we implanted U87 cells (5×10^4 cells per mouse per side in both sides of the brain) in CD-1 nude mice ($n = 11$) After 11 days, mice were injected intravenously, via the tail vein, with live ($n = 6$) or dead ($n = 5$) virus (5×10^8 PFU per mouse) every other day for three injections and every 5 days for another three injections for a total of six injections Survival was followed, and organs were analyzed as above

VSV Δ M51 Viral Distribution Studies

To determine if VSV Δ M51 targets multifocal gliomas in the brain, we established a dual tumor model using U87 tumor cells Cells were implanted by stereotactic techniques as described above in CD-1 nude mice ($n = 18$) After 15 days, each mouse was injected intravenously, via the tail vein, with a single dose of VSV Δ M51 (5×10^8 PFU per mouse) Mice were killed at the following time points after virus injection (three mice at each time

point) 0 hour, 10 hours, 24 hours, 72 hours, 7 days, and 15 days After sacrifice by cervical dislocation, a whole brain picture was taken with a Leica MZ-FLIII fluorescence stereomicroscope using a standard GFP filter set (6,20) Photoshop 6.0 (Adobe) was used to process the images After imaging, the brain and other major organs were removed and frozen in liquid nitrogen for virus recovery assays

To determine the ability of VSV Δ M51 to target invasive cells, we implanted U87-RFP cells (3×10^5 per mouse) into the brains of mice ($n = 6$) to generate tumors After 15 days, we injected VSV Δ M51 (5×10^8 PFU per mouse) intravenously, via the tail vein, into tumor-bearing mice After 72 hours, mice were perfused with 5 mL of saline and killed by cervical dislocation The brains were removed and embedded in OCT embedding medium RFP-expressing tumors and GFP-labeled viruses were visualized in frozen brain sections by a Zeiss inverted microscope (Axiovert 200M) with a fluorescent GFP or rhodamine filter set (20) Immunohistochemical staining of VSV antigen was performed on tissue sections A Carl Zeiss camera (AxioCam MRc) was used to obtain both phase contrast and fluorescent images of the tumor cell-expressed RFP and the virus-expressed GFP

Primary Human Glioma Culture

Short-term cultures were established from patient samples of human gliomas ($n = 15$) obtained following brain tumor surgery at the Foothills Hospital (Calgary), this study was approved by the Conjoint Medical Ethics Committee Briefly, each patient specimen was split in two pieces, one portion of the specimen was fixed in 10% formalin and the other portion of the specimen was used for short-term cultures The tumor tissue that was used to establish short-term cultures was washed several times in sterile saline, transferred to a 35-mm tissue culture dish, cut into small pieces (approximately 0.5–1 mm in diameter), and dissociated with trypsin (0.25%) and 50 μ g/mL deoxyribonuclease (Roche Diagnostics, Laval, PQ, Canada) for 30 minutes at 37 °C After filtering and washing with DMEM/F12 (containing 20% FBS), cells were resuspended in 20% FBS in DMEM/F12 and plated (at 10 000–100 000 cells per well) in 96-well plates Cells were infected the following day with VSV Δ M51 virus, both live and UV inactivated, at MOIs of 0.1, 1, and 10 Cell viability was measured 72 hours later by MTT and cytopathic effect assays [as above and in (20)]

Primary Tumor Immunocytochemistry for Glial Fibrillary Acid Protein Expression

Primary tumor cells obtained from surgical specimens were grown in eight-well chamber slides (50 000–200 000 cells per well) and fixed for 15 minutes in 4% paraformaldehyde Cells were then blocked with 10% goat serum and 0.1% Triton X-100 in PBS for 30 minutes Primary antibody (glial fibrillary acidic protein [GFAP] monoclonal antibody 1:1000, Chemicon, Inc) was then added After 24 hours at 4 °C, cells were washed with PBS and then incubated with anti-mouse IgG-Cy3 (Vector Laboratories) for 1 hour Sections were mounted with Geltol mounting medium (Fisher scientific Co, Pittsburgh, PA) and viewed with a Zeiss microscope (Axiovert 200M), and pictures were taken with a Zeiss inverted microscope and a Carl Zeiss camera (AxioCam MRc)

Statistical Analyses

Statistical Analysis Software (SAS Institute, Inc, Cary, NC) and GraphPad Prism (version 4, GraphPad Software Inc, San Diego, CA) were used for statistical analyses Survival curves were generated by the Kaplan–Meier method The log-rank test and two-way analysis of variance (ANOVA) were used to compare the effect of different forms of treatment (live virus versus dead virus) and the time since administration on tumor size All reported *P* values were two-sided and were considered to be statistically significant at $P < 0.05$

RESULTS

Susceptibility of Human Malignant Glioma Cell Lines to Infection and Killing by VSV Δ M51

Fourteen malignant glioma cell lines were tested for susceptibility to infection and killing by VSV Δ M51 and reovirus T3D by cytopathic effect and MTT assays (representative examples in Fig 1) All 14 cell lines were susceptible to infection and killing by VSV Δ M51, whereas only 12 (85%) of the lines were susceptible to infection and killing by reovirus (U118 and U343 were resistant) In contrast, neither of the normal cell lines tested (HS68 and NIH3T3) was killed by VSV Δ M51 or reovirus Cells were infected with either 1 MOI of VSV Δ M51 or 10 MOI of reovirus, complete cell death was observed in all glioma cell lines 48 hours after infection with VSV Δ M51 (Fig 1, A) but not until 144 hours after infection with reovirus (Fig 1, B) Untreated cells and cells treated with UV-inactivated (dead) virus did not exhibit any cytopathic effect at any time point assessed

The MTT viability assay confirmed the results from the cytopathic effect assays (Fig 1, C) VSV Δ M51 produced more rapid glioma cell killing and at a lower (1 MOI, 24 hours) MOI than reovirus T3D (10 MOI, 72 hours) (Fig 1, C) Extensive cell killing was found in all glioma cell lines in the presence of VSV Δ M51 The normal cell lines NIH3T3 and HS68 were not susceptible to either reovirus or VSV Δ M51 (Fig 1, C) To ensure that cell killing following treatment with VSV Δ M51 was due to viral infection rather than a nonspecific effect, viral protein production was assessed by western blotting All glioma lines exhibited viral protein production 24 hours after infection, in accordance with their susceptibility to killing by VSV (Fig 1, D), whereas no viral protein production was seen in normal cell lines (Fig 1, D)

Effects of Intratumoral Administration of VSV Δ M51 on a Glioma Cell Line Resistant to Infection by Reovirus

We next investigated if VSV Δ M51 would infect and kill a cell line resistant to reovirus in a subcutaneous tumor in CD-1 nude mice We treated mice bearing subcutaneous human malignant glioma xenografts of U87 (susceptible to reovirus) and of U118 (resistant to reovirus) These cells were implanted in the hind flanks of mice, which were treated intratumorally with live or dead virus after palpable tumors had formed (1×10^7 PFU per mouse, every other day, for a period of 6 days) We observed statistically significant inhibition of tumor growth in the live virus-treated mice compared with the dead virus-treated control mice bearing either U87 (ANOVA, $P < 0.001$) (Fig 2, A) or U118 (two-way ANOVA, $P < 0.001$) tumors (Fig 2, B)

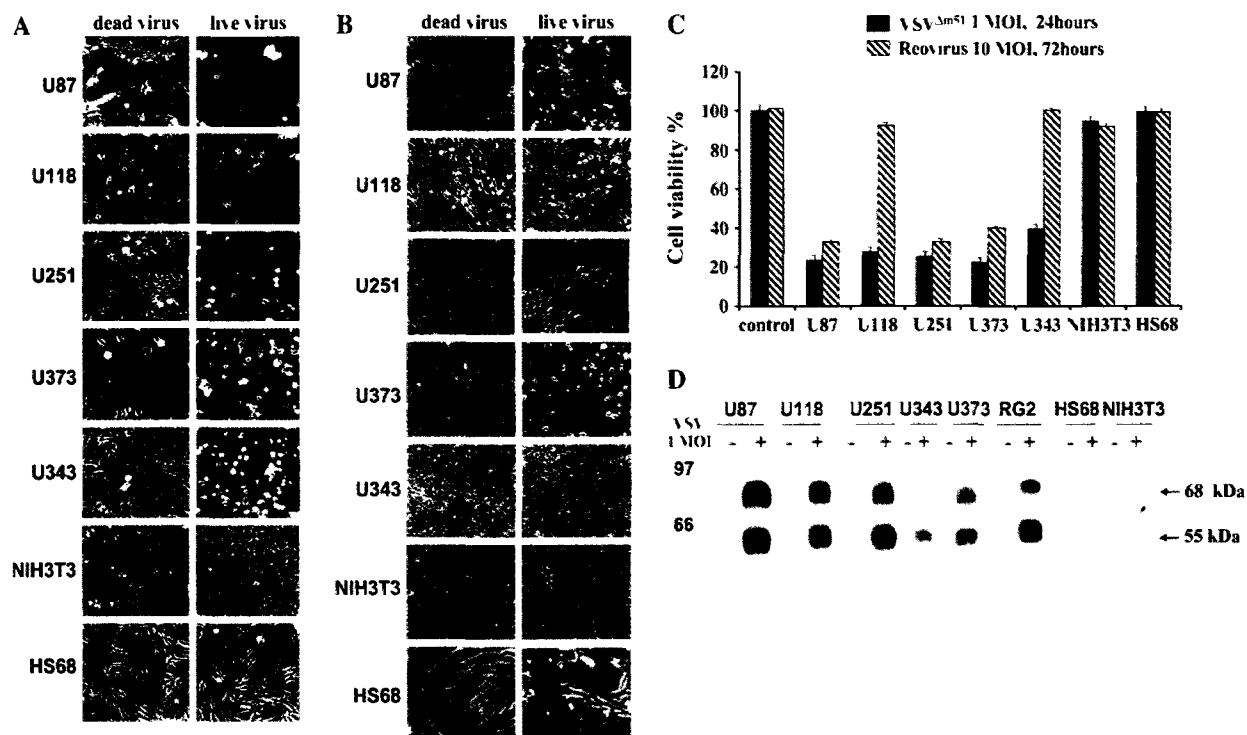


Fig. 1. Effects of vesicular stomatitis virus strain $\Delta M51$ ($VSV^{\Delta M51}$) and reovirus T3D in vitro on established human malignant glioma cell lines. **A)** Cytopathic effects on glioma (U87, U118, U251, U373, U343) and normal (NIH3T3, HS68) cell lines of dead and live $VSV^{\Delta M51}$ at multiplicity of infection (MOI) - 1, 48 hours after infection (magnification $\times 100$). **B)** Cytopathic effects on the same cell lines of dead and live reovirus at 10 MOI, 144 hours after infection, when the

full cytopathic effect of reovirus was produced (magnification $\times 100$). **C)** 3-(4,5-Dimethylthiazol-2-yl)-2,5-diphenyl-2H-tetrazolium bromide assay comparing the effects of $VSV^{\Delta M51}$ or reovirus on the viability of glioma cell lines (U87, U118, U251, U373, U343) and normal cell lines (NIH3T3, HS68), ultraviolet-inactivated viruses were used as a negative control. **D)** Detection of VSV proteins by western blot after infection of glioma cell lines with $VSV^{\Delta M51}$.

Toxicity of Intracerebrally Administered $VSV^{\Delta M51}$ in CD-1 Nude Mice

We evaluated the toxicity of $VSV^{\Delta M51}$ in vivo when administered intracerebrally. A single intracerebral administration of $VSV^{\Delta M51}$ was lethal, even at a dose as low as 5×10^2 PFU per mouse (Fig 3, A). This experiment was repeated three times with similar results (data not shown). Following intracerebral administration we found a diffuse meningoencephalitis, a marked tropism for neurons, and neuronal apoptosis. This was severe in the hippocampus (Fig 3, B) and brain stem (data not shown), and the affected areas were positive for VSV antigen expression and TUNEL staining (Fig 3, B).

We were surprised that the mutant $VSV^{\Delta M51}$, which was engineered to enhance the antiviral responses in normal cells, retained substantial neurotoxicity when administered intracerebrally. To exclude the possibility that the $VSV^{\Delta M51}$ had reverted to wild-type VSV (i.e., lost the mutation in the M protein), we sequenced the M protein of virus collected from mice after intracerebral administration. We confirmed that the virus cultured from the brains retained the mutation in the M protein and had not reverted to wild-type VSV.

Safety Evaluation of Intravenous Administration of $VSV^{\Delta M51}$ in Nude Mice

We next evaluated the toxicity and maximum tolerated dose of $VSV^{\Delta M51}$ administered intravenously. The mice tolerated

much higher doses of intravenously than intracerebrally administered $VSV^{\Delta M51}$. All mice ($n = 4$ per group) administered intravenously, via the tail vein, with doses of $\leq 1 \times 10^9$ PFU survived and appeared normal for up to 60 days (Fig 4, A), when we terminated the experiment by killing all mice that were still alive. At a dose of 5×10^9 PFU (the highest dose we were technically capable of preparing), however, only 50% (two of four) of the mice survived for 60 days (Fig 4, A). A transient and not statistically significant weight loss was observed 3–11 days after intravenous virus administration in surviving mice of both the 5×10^9 PFU and the 1×10^9 PFU groups (Fig 4, B). Control mice treated with dead virus appeared normal. Hence, 1×10^9 PFU was the maximum tolerated dose when administered intravenously, and we used one dose level below this dose for all subsequent therapeutic experiments.

The histology of major organs (brain, liver, lung, kidney, and heart) of mice treated with a dose of 5×10^8 PFU was normal, and there was no histologic evidence of apoptosis by TUNEL assay (data not shown). In addition, we detected no viral antigen expression in liver, lung, kidney, or heart by immunohistochemistry, although in the brain there was minor VSV antigen staining within the meninges or ventricle at 24 and 72 hours after intravenous administration of virus (data not shown). Similar results were obtained by virus recovery assay. Virus was detected in the brain (but not in any other organs) only beginning 4 hours after intravenous administration, peaking at 24 hours, and declining thereafter (data not shown).

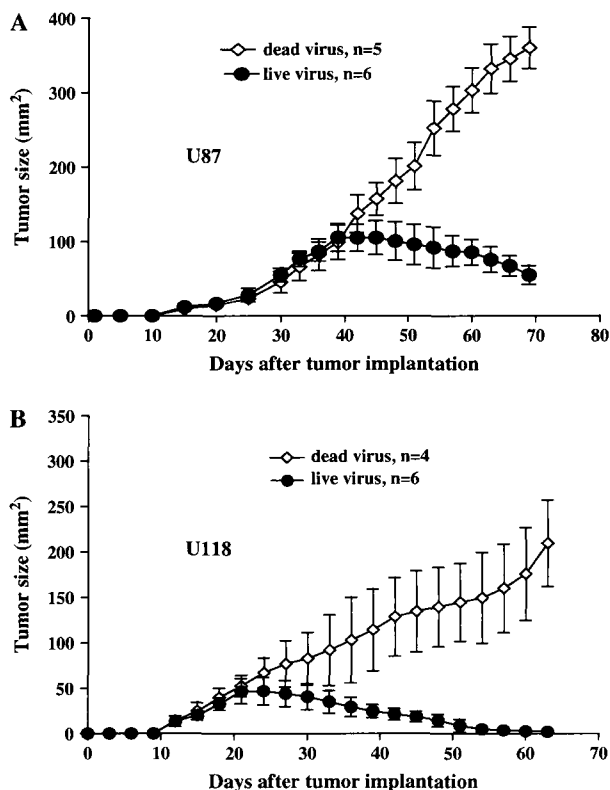


Fig. 2. Effects of vesicular stomatitis virus strain $\Delta M51$ ($VSV^{\Delta M51}$) on growth of reovirus-susceptible (U87) and reovirus-resistant (U118) glioma in a subcutaneous model of malignant gliomas in CD-1 nude mice. Mice bearing subcutaneous glioma implants were treated intratumorally with live or dead $VSV^{\Delta M51}$ virus when a palpable tumor reached approximately 25 mm², tumor size (length \times width) was measured using a caliper. **A**) U87-derived gliomas, live virus (closed circles, $n = 6$) versus dead virus (open diamonds, $n = 5$) **B**) U118-derived gliomas, live virus (closed circles, $n = 6$) versus dead virus (open diamonds, $n = 4$). Results shown are the means and 95% confidence intervals of the tumor size.

Survival Following Systemic Intravenous Administration of $VSV^{\Delta M51}$ in CD-1 Nude U87 Tumor-Bearing Mice

We evaluated the effect of $VSV^{\Delta M51}$ delivered intravenously to mice with unilateral or bilateral brain tumors. Unilateral or bilateral U87 glioma orthotopic xenograft models were established by intracerebral inoculation of U87 cells into the brains of CD-1 nude mice. Mice were treated intravenously with multiple doses of $VSV^{\Delta M51}$ either 15 days (for unilateral tumors) or 11 days (for bilateral tumors) after tumor implantation. Mice with unilateral tumors treated with live virus survived statistically significantly longer (mean = 113 days, 95% CI = 96 to 130 days) than those treated with dead virus (mean = 46 days, 95% CI = 39 to 53 days, log-rank test, $P = .0001$) (Fig. 5, A). All mice eventually died from recurrent tumors between 35 and 140 days after tumor implantation. Similar, although less dramatic, results were found in mice harboring bilateral U87 human malignant gliomas. The median survival of dead versus live virus-treated mice was 46 versus 73 days, respectively (difference = 27 days, 95% CI = 38 to 54 days, and 95% CI = 62 to 84 days, respectively, log-rank test, $P = .0025$; Fig. 5, B). Similar results were obtained when these experiments were repeated (data not shown).

Histologic analysis showed that all live virus- and dead virus-treated mice died from a large tumor in the brain, with some live

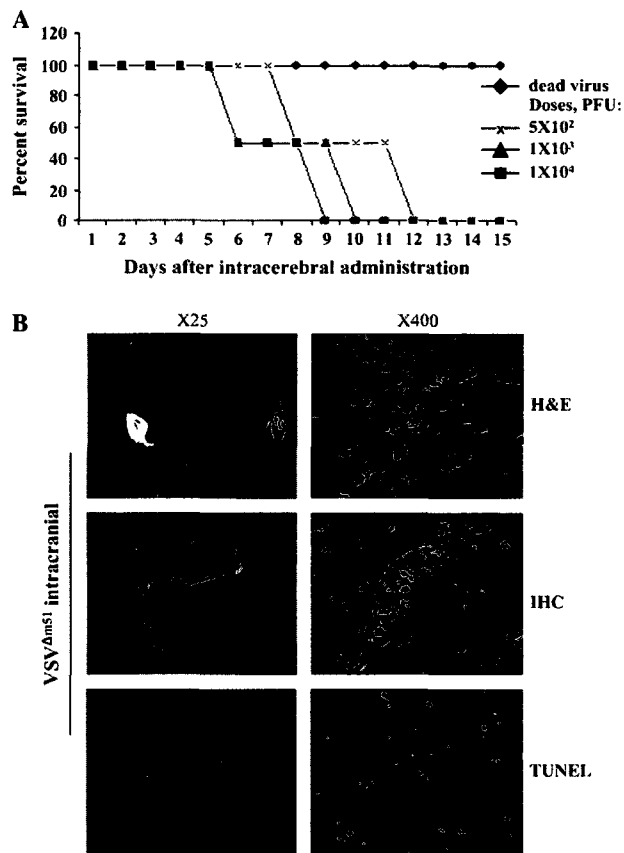


Fig. 3. Determination of the maximum tolerated intracerebral dose of vesicular stomatitis virus strain $\Delta M51$ ($VSV^{\Delta M51}$). **A**) Intracerebral administration. Normal CD-1 nude mice received a single administration of either ultraviolet-inactivated (dead virus) $VSV^{\Delta M51}$ or live $VSV^{\Delta M51}$ at doses of 5×10^2 , 1×10^3 , or 1×10^4 plaque-forming units (PFU) per mouse, two mice per dose. Mice were monitored for a period of 20 days. **B**) Neurotoxicity in mouse brain treated with $VSV^{\Delta M51}$ (1×10^4 PFU per mouse) administered intracerebrally (magnification $\times 25$ and $\times 400$). Representative images show mouse brain stained for hematoxylin and eosin (H&E) (top row), by immunohistochemistry (IHC) for VSV antigen (middle row), and by terminal transferase deoxyuridine triphosphate nick-end labeling (TUNEL) assay (bottom row). Right column is a higher-magnification view of the hippocampus region of the brain.

virus-treated mice having slightly larger ventricles than dead virus-treated mice (data not shown). There was no histologically evident change in the hippocampus region of the brain, immunohistochemical staining evidence of viral infection of the hippocampus, or evidence of apoptosis by TUNEL staining of the hippocampus (Fig. 5, C).

Infection of Multifocal Gliomas and Invasive Tumor Cells With Intravenous $VSV^{\Delta M51}$

Having shown that intravenous $VSV^{\Delta M51}$ prolonged survival of mice bearing gliomas, we evaluated whether a productive infection occurred in the tumors and characterized the distribution of infection in the tumor margin and invasive glioma cells. Mice ($n = 18$) were implanted in both brain hemispheres with U87 cells and were administered a single intravenous dose of 5×10^8 PFU per mouse GFP-labeled $VSV^{\Delta M51}$ 15 days after tumor implantation. Mice were killed at multiple time points (three mice per time point), and their brains were examined in detail.

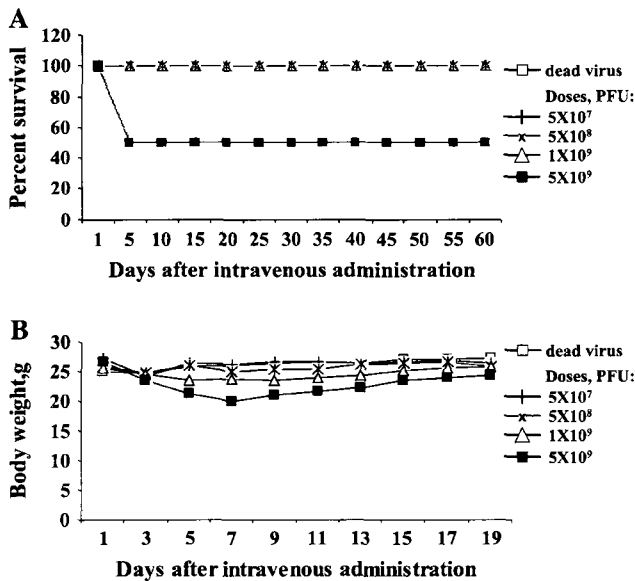


Fig. 4. Safety and toxicity evaluation of vesicular stomatitis virus strain $\Delta M51$ ($VSV^{\Delta M51}$) when administered intravenously to nude mice. **A)** Intravenous administration of $VSV^{\Delta M51}$ in CD-1 nude mice at doses of 5×10^7 , 5×10^8 , 1×10^9 , or 5×10^9 plaque-forming units (PFU) per mouse ($n = 4$ per group). Mice were given a single injection of dead or live $VSV^{\Delta M51}$ intravenously, via the tail vein, and monitored for 60 days. **B)** Mean body weight over time of mice intravenously administered $VSV^{\Delta M51}$.

GFP-expressing virus, as visualized by fluorescence microscopy, was confined to the tumor, with no expression elsewhere in the normal brain, lung, kidney, liver, or heart. Viral expression of GFP began 10 hours after infection, increased up to 72 hours, decreased slightly by day 7, and was undetectable by 15 days after viral administration (Fig. 6, A). The viral titers from the tumor tissues, as determined by virus recovery assays (Fig. 6, B), confirmed that a productive viral infection occurred in these tissues and that the infection had a similar temporal profile to the results based on fluorescence microscopy. No evidence of replicating virus was found in non-tumor-containing brain tissue (data not shown) or dead virus-treated brains (data not shown).

To determine whether $VSV^{\Delta M51}$ infects invasive glioma cells that have migrated beyond the main glioma mass, we inoculated U87 cells that had been transfected with an expression plasmid containing RFP into the brains of six CD-1 nude mice. Fifteen days after implantation, a single intravenous dose of $VSV^{\Delta M51}$ was administered, and (based on the in vivo viral distribution results above) the mice were killed 72 hours later. We then examined the sections of the brain using fluorescence microscopy and immunohistochemistry. We found that viral GFP colocalized with the tumoral RFP using fluorescence microscopy and colocalization of VSV proteins and tumor cells by immunohistochemistry (Fig. 6, C). In addition, viral GFP expression colocalized with isolated invasive tumor cells at the margins of the tumor (Fig. 6, C).

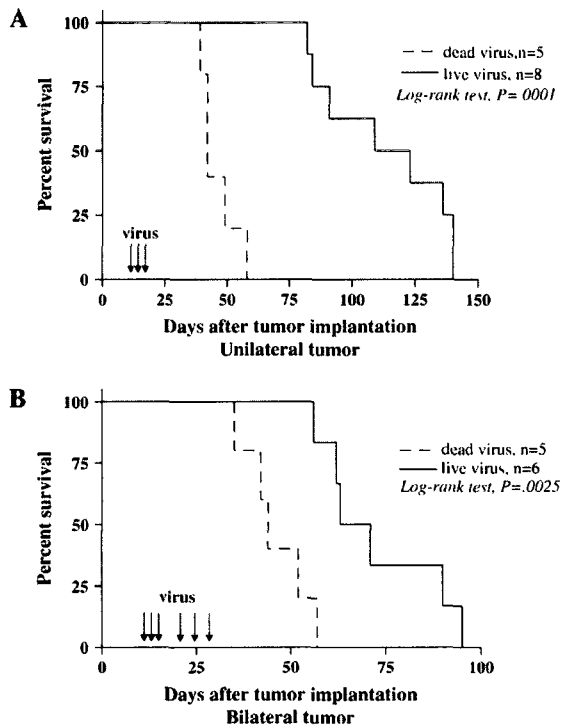
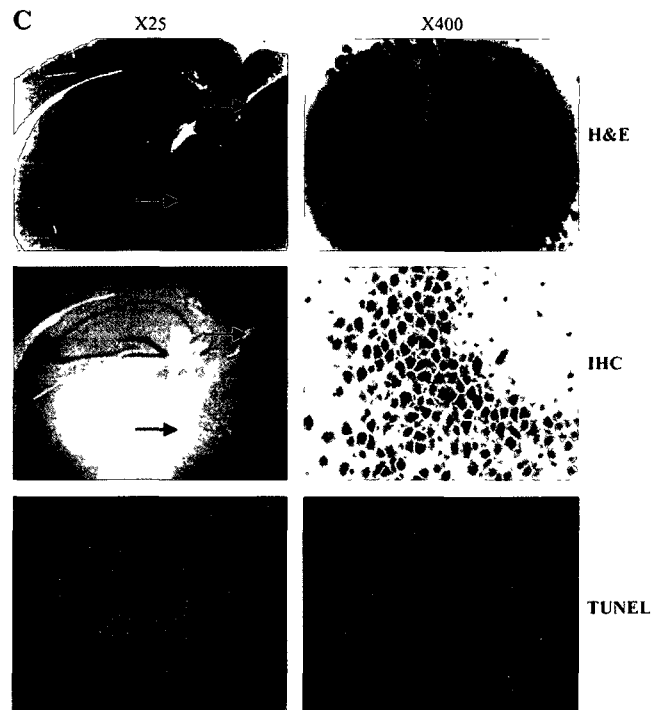


Fig. 5. Systemic administration of vesicular stomatitis virus strain $\Delta M51$ ($VSV^{\Delta M51}$) and survival of nude mice with unilateral and bilateral U87 cell-derived brain tumors. **A)** Unilateral tumor model. Kaplan-Meier survival analysis of mice implanted with U87 cells (1×10^5 cells per mouse) and treated with either dead ($n = 5$) or live ($n = 8$) virus every 2 days for a total of three doses. One intravenous injection contained 5×10^8 plaque-forming units (PFU) per mouse. All P values are two-sided. **B)** Bilateral tumor model. Kaplan-Meier survival analysis of mice implanted with U87 cells (5×10^4 cells per mouse per side) and injected with either dead ($n = 5$) or live ($n = 6$) virus (5×10^8 PFU per



mouse three times every 2 days followed by three times every 5 days for a total of six injections. All P values are two-sided. **Arrows** in **(A)** and **(B)** indicate virus injections. **C)** Representative photomicrographs of a whole brain slice from a live virus-treated mouse (magnification: **left**, $\times 25$; **right**, $\times 400$). **Top row** of panels shows hematoxylin and eosin staining (H&E) of the hippocampus region, **middle row** of panels shows immunohistochemical (IHC) staining of the VSV antigen in the hippocampus region, and **bottom row** of panels shows terminal transferase deoxyuridine triphosphate nick-end labeling (TUNEL) assay of the hippocampus. Adjacent brain sections were used. **Arrows** indicate the tumor.

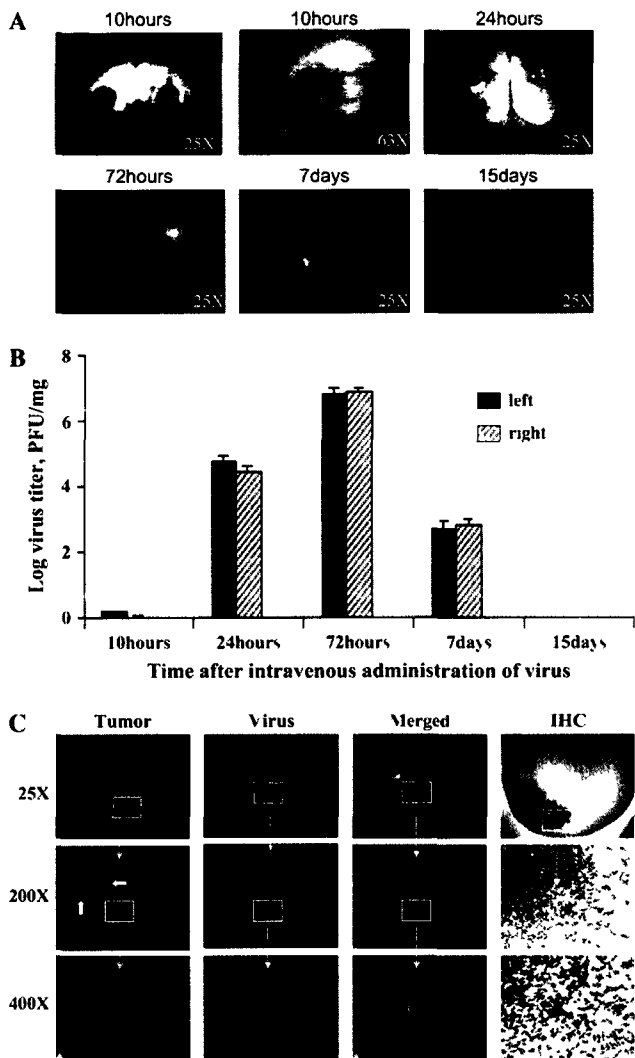


Fig. 6. Distribution of intravenously administered vesicular stomatitis virus strain $\Delta M51$ ($VSV^{\Delta M51}$) expressing green fluorescent protein (GFP) in multifocal gliomas and invasive tumor cells. Mice bearing intracerebral bilateral U87 tumors were treated intravenously with live or dead $VSV^{\Delta M51}$ virus. Mice were killed at several timepoints, and localization of tumor and virus was assessed. **A)** Photomicrograph of GFP-expressing virus in bilateral tumors. Arrows indicate GFP-virus expression. **B)** Titer of virus present in the bilateral tumors ($n = 3$ mice per time point). Tumors on each side of the brain were harvested for virus extraction, and the samples were analyzed by virus recovery assay. The error bars indicate upper 95% confidence intervals. **C)** Localization of $VSV^{\Delta M51}$ expression in experimental invasive gliomas using fluorescence microscopy and immunohistochemistry (IHC). VSV antigen staining. Mice bearing U87-RFP-labeled tumors were injected intravenously, via the tail vein, with a single dose of $VSV^{\Delta M51}$ and were killed 72 hours later. Left three panels of the top row show fluorescent images of a representative RFP-labeled tumor and GFP virus expression in frozen sections (magnification $\times 25$), left three panels of the center and bottom rows show representative GFP virus targeting the invasive RFP-glioma cells (rows show increasing magnification of the same section: top row, $\times 25$, center row, $\times 200$, bottom row, $\times 400$). White arrows indicate the edge of the tumor. Merged refers to a superimposed image of tumor and virus (third column). IHC of $VSV^{\Delta M51}$ protein on consecutive sections (right column) confirms the presence of viral proteins in the invasive glioma cells (brown staining, magnification, top to bottom: $\times 25$, $\times 200$, $\times 400$).

Infection and Killing by $VSV^{\Delta M51}$ of Primary Human Malignant Gliomas Cultured From Surgical Specimens

We next determined whether the *in vitro* cell line results would also apply to glioma samples from patients. Accordingly, we

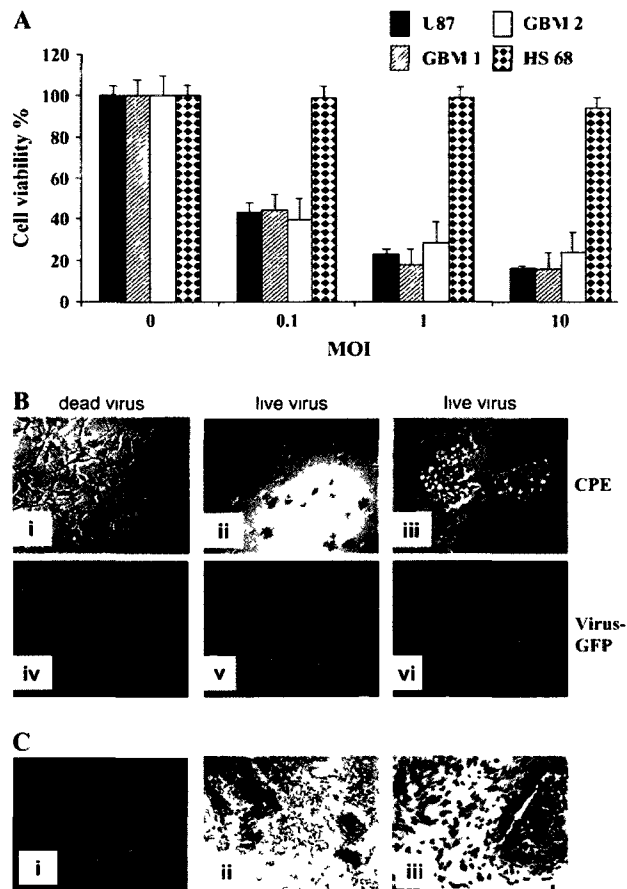


Fig. 7. Effect of vesicular stomatitis virus strain $\Delta M51$ ($VSV^{\Delta M51}$) on human primary tumor samples. **A)** The viability of the glioma samples was measured by the 3-(4,5-dimethylthiazol-2-yl)-2,5-diphenyl-2H-tetrazolium bromide assay, 72 hours after infection with $VSV^{\Delta M51}$ (0, 1, 10 multiplicity of infection). Error bars indicate 95% confidence intervals of three independent experiments performed in triplicate. Samples of dissociated tumor cells from a surgical sample of glioma were plated and 24 hours later infected with either live or dead virus. U87 malignant glioma and HS68 (nontransformed human fibroblasts) were used as positive and negative controls for $VSV^{\Delta M51}$ susceptibility. **B)** Virus infectivity and cell killing were confirmed by assessing the cytopathic effect (CPE) and virus green fluorescent protein (GFP) expression, shown are phase contrast (upper panel) and fluorescent GFP (lower panel) images from a representative human glioblastoma taken 24 hours after infection (magnification: ii and v, $\times 100$, iii and vi, $\times 400$). Dead virus was used as a negative control (i and iv, $\times 100$). **C)** Glial fibrillary acidic protein (i) and hematoxylin and eosin staining (ii and iii) of the same sample as above (magnification: i, $\times 400$, ii, $\times 100$, iii, $\times 400$).

tested whether $VSV^{\Delta M51}$ could infect and kill short-term glioma cultures derived from glioma surgical specimens. We examined the susceptibility to $VSV^{\Delta M51}$ of 15 *ex vivo* brain tumor surgical specimens derived from four glioblastomas, five oligodendrogliomas, five astrocytomas, and one gliosarcoma. All specimens tested (15/15) were killed by $VSV^{\Delta M51}$ infection (Fig 7, A) and to a degree that was similar to infection and killing of U87. A widespread cytopathic effect and viral GFP expression was seen in live virus-treated glioma cells (Fig 7, B-ii, iii, v, vi). In contrast, short-term cultures treated with dead virus showed no cytopathic effect or viral GFP expression (Fig 7, B-i, iv). GFAP staining confirmed the glial lineage of the astrocytic specimens (e.g., a glioblastoma) (Fig 7, C-i), which was also apparent morphologically using hematoxylin and eosin staining (Fig 7, C-ii, iii).

DISCUSSION

We found that an attenuated VSV mutant, designated VSV Δ M51, infected and killed all malignant glioma cell lines tested and did not infect normal cells *in vitro*. When administered intravenously to CD-1 nude mice bearing human gliomas, VSV Δ M51 dramatically prolonged their survival and infected both multifocal gliomas and invasive glioma cells. The invasive and multifocal natures of glioma are major clinical challenges in treating this disease.

An ideal oncolytic virus for cancer should have several characteristics (38,42,59). It should have effective delivery into multiple sites within the tumor, evade innate and acquired immune responses, produce rapid viral replication, spread within the tumor, and infect multifocal tumors. It should also be “engineerable” so that it can be modified to, for example, improve its efficacy or tumor targeting. This is precisely what we found using the attenuated live virus we constructed (VSV Δ M51). Its efficacy was maintained and the antiviral responses were enhanced in normal cells, thereby improving its therapeutic index (43). In addition, we found that VSV Δ M51 infects both multifocal gliomas and invasive glioma cells. Conventional therapies such as surgery and radiotherapy are ineffective in treating invasive glioma cells because these cells may have become more resistant to these therapies than the tumor cells in the main tumor mass by adopting a number of cellular characteristics (e.g., increasing expression of survival pathways, decreasing expression of apoptotic programs, reduced proliferation, etc.) (60). Hence, VSV Δ M51 may represent an effective treatment for these chemotherapy-resistant tumor cells.

We compared the effectiveness and toxicities of VSV Δ M51 to reovirus in this study on the basis of our previous work (8,9,55). We found that VSV Δ M51 was superior in several ways to reovirus for treating gliomas. VSV Δ M51 killed all glioma lines we tested (including two that were resistant to reovirus), was effective *in vivo* when administered systemically, infected invasive glioma cells, and killed multifocal gliomas. By contrast, reovirus did not cause regression of bilateral gliomas in an immunocompetent rat glioma model (55). However, reovirus is superior to VSV Δ M51 in many other ways. When administered intratumorally, reovirus “cures” experimental gliomas in the majority of glioma-bearing mice (i.e., mice survived until the experiment was arbitrarily terminated 90 days after tumor implantation, often without histologic evidence of residual tumor) (8), whereas we found that intravenous VSV Δ M51 did not cure any mice. Finally, unlike VSV Δ M51, reovirus is benign when administered intracerebrally in adult nude mice (8) or immunocompetent rats (55). Comparisons between oncolytic viruses of putative efficacy or toxicities in animal models at present are very limited (61). Definitive conclusions regarding efficacy or toxicity await the testing of these oncolytic viruses in clinical trials in malignant glioma patients.

Our study has several limitations. First, we have not yet evaluated VSV Δ M51 in immunocompetent models of gliomas. Such evaluation is important because immune responses (partially ablated in the immunocompromised mice we used here) may limit delivery of the virus to the tumor when administered intravenously. Immune responses may also limit the distribution of the virus within the tumor. Second, the precise mechanism by which intravenous VSV Δ M51 accesses the invasive glioma cells, which in many cases appear to be single cells, is unknown. The

main tumor mass of U87 is highly vascularized and has a “leaky” blood–brain barrier, which would allow intravenously delivered virus access to the main tumor mass (62,63). In contrast, invasive glioma cells are not believed to be extensively vascularized (64) and would therefore have limited contact with systemically delivered virus. We assume that higher pressure within the tumor mass (65) and high concentrations of virus within the tumor, under pressure, may move the virus out along tracts of white matter. Because these invasive cells may be in a hypoxic environment, it should be noted that VSV is able to infect and kill hypoxic glioma cells both *in vitro* and *in vivo* (24). Alternatively, peritumoral increases in neovascularity and tissue edema can increase the permeability of the blood–brain barrier (66,67), allowing the virus to leak out into the perivascular interstitium around the vessels. Third, all the glioma-bearing mice ultimately died from recurrent tumor. We are now exploring strategies to understand the causes of treatment failure with the goal of improving its efficacy (e.g., using live imaging of viral delivery, improving blood–brain barrier breakdown and intra-arterial delivery, etc.).

REFERENCES

- (1) Scott JN, Rewcastle NB, Brasher PM, Fulton D, Mackinnon JA, Hamilton M, et al Which glioblastoma multiforme patient will become a long-term survivor? A population-based study *Ann Neurol* 1999;46 183–8
- (2) Stupp R, Mason WP, van den Bent MJ, Weller M, Fisher B, Taphoorn MJ, et al Radiotherapy plus concomitant and adjuvant temozolomide for glioblastoma *N Engl J Med* 2005;352 987–96
- (3) Fisher PG, Buffer PA Malignant gliomas in 2005 where to GO from here? *JAMA* 2005;293 615–7
- (4) Ohgaki H, Kleihues P Epidemiology and etiology of gliomas *Acta Neuropathol (Berl)* 2005;109 93–108
- (5) Castro MG, Cowen R, Williamson IK, David A, Jimenez-Dalmaroni MJ, Yuan X, et al Current and future strategies for the treatment of malignant brain tumors *Pharmacol Ther* 2003;98 71–108
- (6) Giese A, Bjerkvig R, Berens ME, Westphal M Cost of migration invasion of malignant gliomas and implications for treatment *J Clin Oncol* 2003;21 1624–36.
- (7) Yang WQ, Senger D, Muzik H, Shi ZQ, Johnson D, Brasher PM, et al Reovirus prolongs survival and reduces the frequency of spinal and leptomeningeal metastases from medulloblastoma *Cancer Res* 2003;63 3162–72.
- (8) Wilcox ME, Yang WQ, Senger D, Rewcastle NB, Morris DG, Brasher PM, et al Reovirus as an oncolytic agent against experimental human malignant gliomas *J Natl Cancer Inst* 2001;93 903–12
- (9) Coffey MC, Strong JE, Forsyth PA, Lee PW Reovirus therapy of tumors with activated Ras pathway *Science* 1998;282 1332–4.
- (10) Todo T, Rabkin SD, Sundaresan P, Wu A, Meehan KR, Herscovitz HB, et al Systemic antitumor immunity in experimental brain tumor therapy using a multmutated, replication-competent herpes simplex virus. *Hum Gene Ther* 1999;10 2741–55
- (11) Mineta T, Rabkin D, Yazaki T, Hunter WD, Martuza RL Attenuated multmutated herpes simplex virus-1 for the treatment of malignant gliomas *Nat Med* 1995;1 938–43
- (12) Yazaki T, Manz HJ, Rabkin SD, Martuza RL Treatment of human malignant meningiomas by G207, a replication-competent multmutated herpes simplex virus 1 *Cancer Res* 1995;55 4752–6
- (13) Mineta T, Rabkin SD, Martuza RL Treatment of malignant gliomas using ganciclovir-hypersensitive, ribonucleotide reductase-deficient herpes simplex viral mutant *Cancer Res* 1994;54 3963–6
- (14) Martuza RL, Malick A, Markert JM, Ruffner KL, Coen DM Experimental therapy of human glioma by means of a genetically engineered virus mutant *Science* 1994;262 854–6
- (15) Csatory LK, Gosztonyi G, Szeberenyi J, Fabian Z, Liszka V, Bodey B, et al MTH-68/H oncolytic viral treatment in human high-grade gliomas *J Neurooncol* 2004;67 83–93

- (16) Csatory LK, Bakacs T Use of Newcastle disease virus vaccine (MTH-68/H) in a patient with high-grade glioblastoma *JAMA* 2000,283 2107
- (17) Freeman AI, Zakay-Rones Z, Gomori JM, Linetsky E, Rasooly L, Greenbaum E, et al Phase I/II trial of intravenous NDV-HUJ oncolytic virus in recurrent glioblastoma multiforme *Mol Ther* 2005,13 221-8
- (18) Gromeier M, Lachmann S, Rosenfeld MR, Gutin PH, Wimmer E Intergenic poliovirus recombinants for the treatment of malignant glioma *Proc Natl Acad Sci U S A* 2000,97 6803-8
- (19) Ochiai H, Moore SA, Archer GE, Okamura T, Chewning TA, Marks JR, et al Treatment of intracerebral neoplasia and neoplastic meningitis with regional delivery of oncolytic recombinant poliovirus *Clin Cancer Res* 2004,10 4831-8
- (20) Lun XQ, Yang WQ, Alain T, Shi ZQ, Muzik H, Barrett JW, et al Myxoma virus is a novel oncolytic virus with significant antitumor activity against experimental human gliomas *Cancer Res* 2005,65 9982-90
- (21) Chioocca EA, Abbed KM, Tatter S, Louis DN, Hochberg F, Kracher J, et al A phase I open-label, dose-escalation, multi-institutional trial of injection with an E1B-attenuated adenovirus, ONYX-015, into the peritumoral region of recurrent malignant gliomas, in the adjuvant setting *Mol Ther* 2004,10 958-66
- (22) Jiang H, Conrad C, Fueyo J, Gomez-Manzano C, Liu TJ Oncolytic adenoviruses for malignant glioma therapy *Front Biosci* 2003,8 d577-88
- (23) Georger B, Grill J, Opolon P, Morizet J, Aubert G, Terrier-Lacombe MJ, et al Oncolytic activity of the E1B-55 kDa-deleted adenovirus ONYX-015 is independent of cellular p53 status in human malignant glioma xenografts *Cancer Res* 2002,62 764-72
- (24) Connor JH, Naczki C, Koumenis C, Lyles DS Replication and cytopathic effect of oncolytic vesicular stomatitis virus in hypoxic tumor cells in vitro and in vivo *J Virol* 2004,78 8960-70
- (25) Porosnicu M, Mian A, Barber GN The oncolytic effect of recombinant vesicular stomatitis virus is enhanced by expression of the fusion cytosine deaminase/uracil phosphoribosyltransferase suicide gene *Cancer Res* 2003,63 8366-76
- (26) Balachandran S, Porosnicu M, Barber GN Oncolytic activity of vesicular stomatitis virus is effective against tumors exhibiting aberrant p53, Ras, or Myc function and involves the induction of apoptosis *J Virol* 2001,75 3474-9
- (27) Lee H, Song JJ, Kim E, Yun CO, Choi J, Lee B, et al Efficient gene transfer of VSV-G pseudotyped retroviral vector to human brain tumor *Gene Ther* 2001,8 268-73
- (28) Balachandran S, Barber GN Vesicular stomatitis virus (VSV) therapy of tumors *IUBMB Life* 2000,50 135-8
- (29) Lang FF, Bruner JM, Fuller GN, Aldape K, Prados MD, Chang S, et al Phase I trial of adenovirus-mediated p53 gene therapy for recurrent glioma: biological and clinical results *J Clin Oncol* 2003,21 2508-18
- (30) Hermiston TW, Kuhn I Armed therapeutic viruses: strategies and challenges to arming oncolytic viruses with therapeutic genes *Cancer Gene Ther* 2002,9 1022-35
- (31) Green NK, Seymour LW Adenoviral vectors: systemic delivery and tumor targeting *Cancer Gene Ther* 2002,9 1036-42
- (32) Yamamoto S, Yoshida Y, Aoyagi M, Ohno K, Hirakawa K, Hamada H Reduced transduction efficiency of adenoviral vectors expressing human p53 gene by repeated transduction into glioma cells in vitro *Clin Cancer Res* 2002,8 913-21
- (33) Harrow S, Papanastassiou V, Harland J, Mabbs R, Petty R, Fraser M, et al HSV1716 injection into the brain adjacent to tumor following surgical resection of high-grade glioma: safety data and long-term survival *Gene Ther* 2004,11 1648-58
- (34) Papanastassiou V, Rampling R, Fraser M, Petty R, Hadley D, Nicoll J, et al The potential for efficacy of the modified (ICP 34 5(-)) herpes simplex virus HSV1716 following intratumoral injection into human malignant glioma: a proof of principle study *Gene Ther* 2002,9 398-406
- (35) Markert JM, Medlock MD, Rabkin SD, Gillespie GY, Todo T, Hunter WD, et al Conditionally replicating herpes simplex virus mutant, G207 for the treatment of malignant glioma: results of a phase I trial *Gene Ther* 2000,7 867-74
- (36) Rampling R, Cruickshank G, Papanastassiou V, Nicoll J, Hadley D, Brennan D, et al Toxicity evaluation of replication-competent herpes simplex virus (ICP 34 5 null mutant 1716) in patients with recurrent malignant glioma *Gene Ther* 2000,7 859-66
- (37) Forsyth PA, Roldan G, George D, Wallace C, Morris DG, Cairncross J, et al A phase I trial of intratumoral (i.t.) administration of reovirus in patients with histologically confirmed recurrent malignant gliomas (MGs) *J Clin Oncol ASCO Proc* 2006,24 18S (June 20 Supplement), Abstract 1563
- (38) Parato K, Senger D, Forsyth PA, Bell JC Recent progress in the battle between oncolytic viruses and tumors *Nat Rev Cancer* 2005,5 965-76
- (39) Barber GN Vesicular stomatitis virus as an oncolytic vector *Viral Immunol* 2004,17 516-27
- (40) Bell JC, Lichty B, Stojdl D Getting oncolytic virus therapies off the ground *Cancer Cell* 2003,4 7-11
- (41) Gromeier M, Wimmer E Viruses for the treatment of malignant glioma *Curr Opin Mol Ther* 2001,3 503-8
- (42) Kim D, Martuza RL, Zwiebel J Replication-selective virotherapy for cancer: biological principles, risk management and future directions *Nat Med* 2001,7 781-7
- (43) Stojdl DF, Lichty BD, TenOever BR, Paterson JM, Power AT, Knowles S, et al VSV strains with defects in their ability to shutdown innate immunity is potent systemic anti-cancer agents *Cancer Cell* 2003,4 263-75
- (44) Stojdl DF, Lichty B, Knowles S, Marus R, Atkins H, Sonenberg N, et al Exploiting tumor-specific defects in the interferon pathway with a previously unknown oncolytic virus *Nat Med* 2000,6 821-5
- (45) Balachandran S, Barber GN Defective translational control facilitates vesicular stomatitis virus oncolysis *Cancer Cell* 2004,5 51-65
- (46) Liu R, Varghese S, Rabkin SD Oncolytic herpes simplex virus vector therapy of breast cancer in C3(1)/SV40 T-antigen transgenic mice *Cancer Res* 2005,65 1532-40
- (47) Abe T, Wakimoto H, Bookstein R, Maneval DC, Chioocca EA, Basilion JP Intra-arterial delivery of p53-containing adenoviral vector into experimental brain tumors *Cancer Gene Ther* 2002,9 228-35
- (48) Ikeda K, Wakimoto H, Ichikawa T, Jung S, Hochberg FH, Louis DN, et al Complement depletion facilitates the infection of multiple brain tumors by an intravascular, replication-conditional herpes simplex virus mutant *J Virol* 2000,74 4765-75
- (49) Schellingerhout D, Rainov NG, Breakefield XO, Weissleder R Quantitation of HSV mass distribution in a rodent brain tumor model *Gene Ther* 2000,7 1648-55
- (50) Ikeda K, Ichikawa T, Wakimoto H, Silver JS, Deisboeck TS, Finkelstein D, et al Oncolytic virus therapy of multiple tumors in the brain requires suppression of innate and elicited antiviral responses *Nat Med* 1999,5 881-7
- (51) Zhan JH, Gao Y, Wang W, Shen A, Aspelund A, Young M, et al Tumor-specific intravenous gene delivery using oncolytic adenoviruses *Cancer Gene Ther* 2005,12 19-25
- (52) LeMay DR, Kittaka M, Gordon EM, Gray B, Stuns MF, McComb JG, et al Intravenous RMP-7 increases delivery of ganciclovir into rat brain tumors and enhances the effects of herpes simplex virus thymidine kinase gene therapy *Hum Gene Ther* 1998,9 989-95
- (53) Ebert O, Harbaran S, Shinozaki K, Woo SL Systemic therapy of experimental breast cancer metastases by mutant vesicular stomatitis virus in immune-competent mice *Cancer Gene Ther* 2005,12 350-8
- (54) Shinozaki K, Ebert O, Woo SL Treatment of multi-focal colorectal carcinoma metastatic to the liver of immune-competent and syngeneic rats by hepatic artery infusion of oncolytic vesicular stomatitis virus *Int J Cancer* 2005,114 659-64
- (55) Yang WQ, Lun XQ, Palmer CA, Wilcox ME, Muzik H, Shi ZQ, et al Efficacy and safety evaluation of human reovirus type 3 in immunocompetent animals: racine and nonhuman primates *Clin Cancer Res* 2004,10 8561-76
- (56) Yang WQ, Senger DL, Lun XQ, Muzik H, Shi ZQ, Dyck RH, et al Reovirus as an experimental therapeutic for brain and leptomeningeal metastases from breast cancer *Gene Ther* 2004,11 1579-89
- (57) Chomczynski P, Sacchi N Single-step method of RNA isolation by acid guanidinium thiocyanate-phenol-chloroform extraction *Anal Biochem* 1987, 162 156-9
- (58) Cave DR, Hendrickson FM, Huang AS Defective interfering virus particles modulate virulence *J Virol* 1985,55 366-73
- (59) Wein LM, Wu JT, Kim DH Validation and analysis of a mathematical model of a replication-competent oncolytic virus for cancer treatment: implications for virus design and delivery *Cancer Res* 2003,63 1317-24
- (60) Joy AM, Beaudry CE, Tran NL, Ponce FA, Holz DR, Demuth T, et al Migrating glioma cells activate the PI3-K pathway and display decreased susceptibility to apoptosis *J Cell Sci* 2003,116 4409-17

- (61) Wollmann G, Tattersall P, van den Pol AN Targeting human glioblastoma cells: comparison of nine viruses with oncolytic potential *J Virol* 2005,79 6005–22
- (62) Yuan F, Salehi HA, Boucher Y, Vasthare US, Tuma RF, Jain RK Vascular permeability and microcirculation of gliomas and mammary carcinomas transplanted in rat and mouse cranial windows *Cancer Res* 1994,54 4564–8
- (63) Kragh M, Quistorff B, Lund EL, Kristjansen PE Quantitative estimates of vascularity in solid tumors by non-invasive near-infrared spectroscopy *Neoplasia* 2001,3 324–30
- (64) Stewart PA, Hayakawa K, Farrell CL, Del Maestro RF Quantitative study of microvessel ultrastructure in human peritumoral brain tissue: Evidence for a blood-brain barrier defect *J Neurosurg* 1987,67 697–705
- (65) Helmlinger G, Yuan F, Dellian M, Jain RK Interstitial pH and pO₂ gradients in solid tumors in vivo: high-resolution measurements reveal a lack of correlation *Nat Med* 1997,3 177–82
- (66) Jain RK 1995 Whitaker lecture: delivery of molecules, particles, and cells to solid tumors *Ann Biomed Eng* 1996,24 457–73
- (67) Yuan F, Chen Y, Dellian M, Safabakhsh N, Ferrara N, Jain RK Time-dependent vascular regression and permeability changes in established

human tumor xenografts induced by an anti-vascular endothelial growth factor/vascular permeability factor antibody *Proc Natl Acad Sci U S A* 1996, 93 14765–70

NOTES

This work was funded by the National Cancer Institute of Canada with funds raised by the Canadian Cancer Society (D Stojdl and P A Forsyth), a Program Project Grant from the Terry Fox Foundation (J C Bell and P A Forsyth), and the Clark Smith Integrative Brain Tumor Research Center (P A Forsyth and D L Senger). T Alain is funded by the Alberta Heritage Foundation for Medical Research and a fellowship by the Canadian Institutes of Health Research. The sponsors had no role in the design, analysis, writing, or decision to submit the study for publication.

Funding to pay the Open Access publication charges for this article was provided by the Clark Smith Integrative Brain Tumor Center.

Manuscript received December 16, 2005, revised August 18, 2006, accepted September 8, 2006.

APPENDIX V.: VESICULAR STOMATITIS VIRUS: RE-INVENTING THE BULLET

Contribution of Authors: AT Power generated all figures and the table summarizing VSV recombinants (and researched literature cited therein).

Published: Trends Mol Med. 2004 May;10(5):210-6.

Vesicular stomatitis virus: re-inventing the bullet

Brian D. Lichty¹, Anthony T. Power^{1,2}, David F. Stojdl¹ and John C. Bell^{1,2}

¹Ottawa Regional Cancer Centre Research Laboratories, 503 Smyth Road, Ottawa, Ontario K1H 1C4, Canada

²Department of Biochemistry, Microbiology and Immunology, University of Ottawa, Ontario K1H 8M5, Canada

As our understanding of the molecular aspects of human disease increases, it is becoming possible to create designer therapeutics that are exquisitely targeted and have greater efficacy and fewer side effects. One class of targeted biological agents that has benefited from recent advances in molecular biology is designer viruses. Vesicular stomatitis virus (VSV) is normally relatively innocuous but can be engineered to target cancer cells or to stimulate immunity against diseases such as AIDS or influenza. Strains of VSV that induce or direct the production of interferon are superior to wild-type strains of the virus for inducing oncolysis. These strains might also make better vaccine vectors. In this review, some of the features that make VSV an excellent platform for the development of a range of viral therapeutics are discussed.

Many viruses are being developed as clinical tools for the treatment or prevention of human disease. A relative newcomer for this application is the vesicular stomatitis virus (VSV), which has had an important role in our increasing understanding of both innate and acquired immunity, as well as virology in general. Although VSV has been used extensively as a laboratory tool for probing aspects of cellular physiology, it was only during the last decade that its potential as a therapeutic has been appreciated. VSV is a clinically important vaccine vector but, more recently, it has attracted attention as an oncolytic virus. Several naturally occurring or recombinant strains of VSV have been developed as potential therapeutic vectors (Table 1). Vaccine vectors have been engineered to express foreign viral proteins designed either to elicit a specific immune response or to be more attenuated than the wild-type protein. The oncolytic strains have been selected and designed for tumor targeting and engineered to express marker proteins or suicide genes. Historically, vaccine vectors and oncolytic viruses have been based on human DNA viruses. RNA viruses are now being considered and offer several advantages, including rapid and robust growth, which aids the production and amplification of dose. The use of animal viruses, such as VSV, also avoids the problems associated with pre-existing immunity to the therapeutic vector in the patient. Recent findings demonstrated that strains of VSV that induce or direct the expression of

interferon are an important advancement in the development of RNA-virus-based therapeutics.

VSV epidemiology

VSV is an arthropod-borne virus that primarily affects rodents, cattle, swine and horses, but can also infect humans and other species. It is thought that VSV is spread between hoofed animals and rodents via insect vectors [1]. The two prevalent serotypes in the Americas are New Jersey (VSV-NJ) and Indiana (VSV-Ind), with VSV-NJ representing the agriculturally relevant pathogen. VSV produces an acute disease in cattle, horses and swine. The disease is characterized by vesiculation and ulceration of the oral cavity, feet and teats and, although relatively harmless, it mimics the early symptoms caused by a notorious veterinary pathogen of horses and cattle, foot-and-mouth-disease virus (reviewed in [2]). Although high transmission rates to farm animals are seen in regions where VSV-NJ is endemic, clinical disease rates are low [3]. In regions endemic for VSV, seropositivity for antibodies against VSV-Ind is common, but most clinical disease is caused by VSV-NJ. Arthropod vectors, such as sandflies, black flies and mosquitoes, have been found to either harbor VSV-Ind or be able, in the laboratory, to transmit VSV and probably participate in the spread of the virus between animals and, possibly, from animals to humans [1]. Naturally occurring human infections with VSV are rare. However, cases of VSV infection have been reported in individuals exposed to infected livestock and in researchers exposed within laboratory environments. Most VSV infections are asymptomatic in humans, although mild flu-like symptoms have been reported in some individuals. A single case of encephalitis in a 3-year-old boy has been reported, which was potentially associated with VSV-Ind infection, (reviewed in [4]).

The occurrence of antibodies against VSV in the general human population is extremely low, except in those regions where it is endemic, such as Georgia, USA (VSV-NJ) and Central America (VSV-Ind and VSV-NJ). Seropositivity is occasionally reported in individuals with a high risk of exposure, for example, in laboratory personnel who work with the virus, as well as veterinarians and farm workers exposed to infected livestock. During epizootics, those individuals with the highest risk of exposure to VSV infection show ~20% seroconversion rate [4]. The lack of antibodies against VSV in the general population and the extremely rare incidence of adverse

Table 1 The growing arsenal of VSV-based therapeutics for use against infectious and malignant disease^a

VSV application	Features	Refs
Vaccine vectors		
VSV-HA	Insertion of influenza hemagglutinin gene into VSV genome hemagglutinin antigen is expressed in VSV infected cells and on viral surface	[27]
VSV ΔG-HA	Improved influenza vector attenuating deletion of VSV glycoprotein increases safety and prevents stimulation of VSV specific humoral immunity	[4]
VSV-GagEnv	Insertion of HIV <i>Gag</i> and <i>Env</i> genes into VSV genome VSV infected cells express Env and Gag proteins to induce HIV specific CD8 ⁺ CTL and neutralizing antibody responses	[29 32]
VSV-MV H	Insertion of measles virus hemagglutinin gene into VSV genome elicits protective MV specific neutralizing antibody despite the presence of circulating maternal antibody	[28]
VSV ΔG-RSV F	Insertion of respiratory syncytial virus fusion gene into VSV genome RSV fusion antigen is expressed in VSV infected cells and on viral surface attenuated by deletion of VSV G	[31]
VSV-HCV C/E1/E2	Insertion of Hep C gene encoding contiguous C/E1/E2 proteins HepC antigens are expressed in VSV infected cells	[33]
VSV rearranged genome	Rearrangement of genes generates a stably attenuated vector	[2]
Natural oncolytic strains		
WtVSV ⁹	High sensitivity to anti viral interferons selective replication and cytotoxicity in tumor cells exhibiting compromised interferon response	[35 37 40]
VSV AV1 or VSV AV2	Highly attenuated replication in normal cells but conserved tumor killing enhanced therapeutic index	[16]
Recombinant oncolytic strains		
wtVSV-GFP	Expression of green fluorescent protein transgene	[16 39 48]
VSV-Δ51M	Deletion of Met 51 of matrix protein highly attenuated replication in normal cells but conserved tumor killing enhanced therapeutic index	[16]
Oncolytic VSVs expressing immunostimulatory cytokines		
VSV-IL 4	Expresses IL 4 gene enhanced therapeutic index	[36]
VSV-IFN β	Expresses IFN β gene enhanced therapeutic index	[45]
Oncolytic VSVs expressing a suicide gene		
VSV-TK	Expresses thymidine kinase gene killing of infected and bystander cells with gancyclovir treatment	[36]
VSV-CD/UPRT	Expresses cytosine deaminase (CD)/uracil phosphoribosyltransferase gene killing of infected and bystander cells with 5 fluorocytosine treatment	[41]
Receptor targeted VSVs		
VSV-CD4	Expresses CD4 and can infect cells expressing HIV gp120	[43 44]
VSV-Sindbis ZZ glycoproteins	VSV pseudotype coated with a Sindbis virus glycoprotein/protein A fusion targeting to tumor specific antigens when co administered with a monoclonal antibody	[42]

^aAbbreviations AV attenuated virus CD/UPRT cytosine deaminase (CD)/uracil phosphoribosyltransferase CTL cytotoxic T lymphocyte G glycoprotein HA hemagglutinin HCV C/E1/E2 hepatitis C virus capsid/envelop 1/envelop 2 IFN interferon IL interleukin MV H measles virus hemagglutinin RSU F respiratory syncytial virus fusion TK thymidine kinase VSV vesicular stomatitis virus Wt wild type

outcomes following human infection are important prerequisites for its potential as a candidate therapeutic virus

VSV is an RNA virus

Current DNA-based therapeutic viruses replicate and transcribe their genomes in the nucleus of the infected cell, where they displace components of the host-cell transcriptional machinery. Although this feature can be exploited to target specific cell or tissue types, in some situations it has the disadvantage of causing mutations following virus integration into the host genome. VSV, however, has an RNA genome and replicates entirely in the cytoplasm. Its compact 11-kilobase (kb) genome is a single RNA strand of negative polarity (i.e. it cannot be directly translated) that is completely coated by the viral nucleoprotein. During infection, VSV synthesizes five subgenomic mRNAs that encode its five distinct proteins (Figure 1) [5]. The nucleoprotein, in conjunction with the phosphoprotein, the large polymerase protein and specific host proteins, is responsible for both viral transcription and replication. Furthermore, a glycoprotein is necessary for viral binding

to target cells, and the multi-functional matrix protein, which consists of 229 amino acids, has a crucial role in virus assembly, budding, cellular apoptosis and disruption of the host-cell innate-immunity programs [6].

VSV has a broad tissue tropism

The glycoprotein of VSV serves both to bind the surface of the host cell and to fuse viral and cellular membranes, enabling the release of the viral genome and replicase into the cytoplasm. The glycoprotein binds to phosphatidylserine, a near-universal component of cell surface membranes, enabling VSV to infect virtually all animal cells. This extensive tissue tropism, therefore, enables VSV to be used as an anti-cancer agent in all types of tumors, although normal tissues can also be infected. Following attachment to the cell surface, the virus enters by endocytosis and, after a subsequent drop in endosomal pH, the glycoprotein catalyzes the fusion of viral and cellular membranes, releasing the viral ribonucleoprotein (RNP) into the cytoplasm (Figure 2). The RNA dependent RNA-polymerase complex (nucleoprotein, phosphoprotein and large polymerase protein) of the virus is then able to

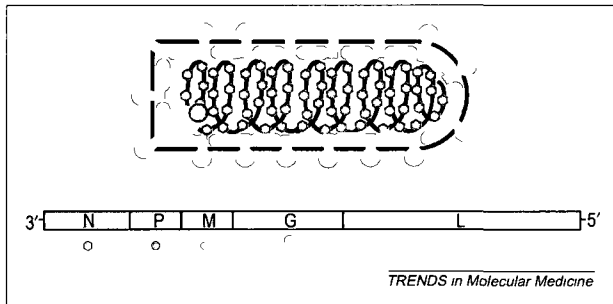


Figure 1 The vesicular stomatitis virus (VSV) genome and virus particle structure. The negative sense, single-stranded RNA genome of VSV consists of five genes that encode the five major viral proteins: the nucleoprotein (N), the phosphoprotein (P), the matrix protein (M), the glycoprotein (G) and the large polymerase protein (L). Transcription of viral genes proceeds from the 3' to 5' end of the genome (5' to 3' on the anti-genome template), beginning with the N gene. Viral mRNA-expression levels decrease as each subsequent gene is transcribed, owing to the viral polymerase falling off and incomplete re-initiation at the intergenic regions. The five viral proteins are assembled into a bullet shaped virus particle that is enveloped in a phospholipid bilayer and coated with the protruding transmembrane glycoprotein.

transcribe the viral genes. The polymerase stutters at each intergenic region during polyadenylation of the transcript before advancing to transcribe the next gene. Because re-initiation does not always occur, there is a gradation of transcript production across the genome, such that nucleoprotein is more abundant than phosphoprotein, which is more abundant than the matrix protein, and so on (reviewed in [6]). The viral polymerase complex also produces the positive-strand RNA from which additional copies of the negative-strand genome are made and packaged for progeny virus production.

Matrix protein: the 'brains' of the virus

One of the smallest gene products encoded by the VSV genome, the matrix protein, has some of the most crucial and diversified roles in the control of VSV replication and pathogenesis (Figure 3), and a thorough understanding of this protein will aid in the design of improved VSV-based therapeutic vectors. For example, matrix protein partially regulates the transcription of VSV genes by the virally encoded RNA-dependent RNA polymerase [7,8]. It appears that, late in infection, accumulated matrix protein catalyzes the generation of inactive RNP cores, preparing them for packaging into virions. Concomitant with this activity, VSV usurps the same endosomal-membrane fission machinery that is used by retroviruses, flaviviruses and, probably, many additional enveloped viruses to facilitate virus budding. Matrix protein has a role in this activity through a so-called 'late domain' found at the N-terminus of the protein. This late domain contains an essential PPPY motif that mediates the interaction with the cellular enzyme Nedd4, an ubiquitin ligase implicated in the budding of other enveloped viruses [9,10]. Matrix protein also contains a PSAP motif that, in other viruses (HIV and Ebola virus), binds to the cellular protein TSG101, aiding viral budding [11].

In addition to its role in budding, matrix protein has a crucial role in the early phases of viral infection, helping VSV to avoid the cellular antiviral programs. This appears to be accomplished by two activities: the interruption of

cellular transcription programs and the blockade of mRNA export from the nucleus. In both mechanisms, the role of matrix protein is to block the expression of antiviral gene products (such as interferon β), enabling the virus to replicate unabated. This inhibition of cellular transcription by matrix protein has been demonstrated in several ways. For example, when an expression-plasmid encoding matrix protein is transfected into a cell, there is profound inhibition of the transcription of host genes and co-transfected plasmids, whether transcribed by RNA polymerase I, II or III [12]. It has recently been recognized that the matrix protein of VSV (and other vesiculoviruses) blocks nucleocytoplasmic transport [13–15]. It now appears that VSV uses this block in mRNA transport to thwart host innate immune mechanisms [16]. This inhibition appears to involve an interaction between matrix protein and cellular Nup98, one of the nucleoporins present at the nuclear pore [13]. Interestingly, Nup98 is an interferon-responsive gene, and pretreatment of cells with interferon increases Nup98 expression and reduces the ability of VSV matrix protein to inhibit nucleocytoplasmic transport [17]. This suggests that cells have evolved this mechanism to defend themselves against viruses that use this strategy to prevent the establishment of an anti-viral state. Mutations in matrix protein that abolish the ability of the protein to block host-cell transcription also restore nucleocytoplasmic transport, suggesting that these two activities of the matrix protein are not mutually exclusive.

Although these studies establish a role for the matrix protein in the nuclear compartment and at the inner surface of the plasma membrane, it is also known to reside in the cellular cytoplasm, where it might disrupt cell-signaling pathways and the cytoskeleton. For example, Terstegen *et al.* have reported that VSV matrix protein is able to abrogate STAT signaling in response to IL-6 stimulation, and this might have a role in the attenuation of inflammatory responses to VSV infection [18].

Infection of susceptible host cells with VSV leads to cell rounding and, ultimately, to cell death displaying the hallmarks of apoptosis. This response is largely owing to the effects of matrix protein, because transfection of cells with a matrix-protein expression construct leads to this response *in vitro* [19]. The induction of apoptosis by matrix protein probably results from the blockade of host-cell gene expression, because mutations to the matrix protein that abrogate this blockade also reduce its cytotoxicity in most cells [20,21]. Given the crucial role that the matrix protein has for viral replication, it has become a focal point of attempts to engineer improved therapeutic VSV strains.

The ability to use reverse genetics to manipulate the genomes of the negative-stranded RNA viruses has greatly improved the understanding of these viruses and has increased their potential use as therapeutic tools. VSV recombinants can be recovered from DNA copies following the transfection of expression plasmids into mammalian cells, and foreign genes can be expressed from multiple sites within the genome [22–26]. Recombinant VSV genomes can accommodate at least 4.5 kb of foreign RNA and the new genes can be expressed at high levels from at least two additional mRNAs [26]. It is now relatively easy

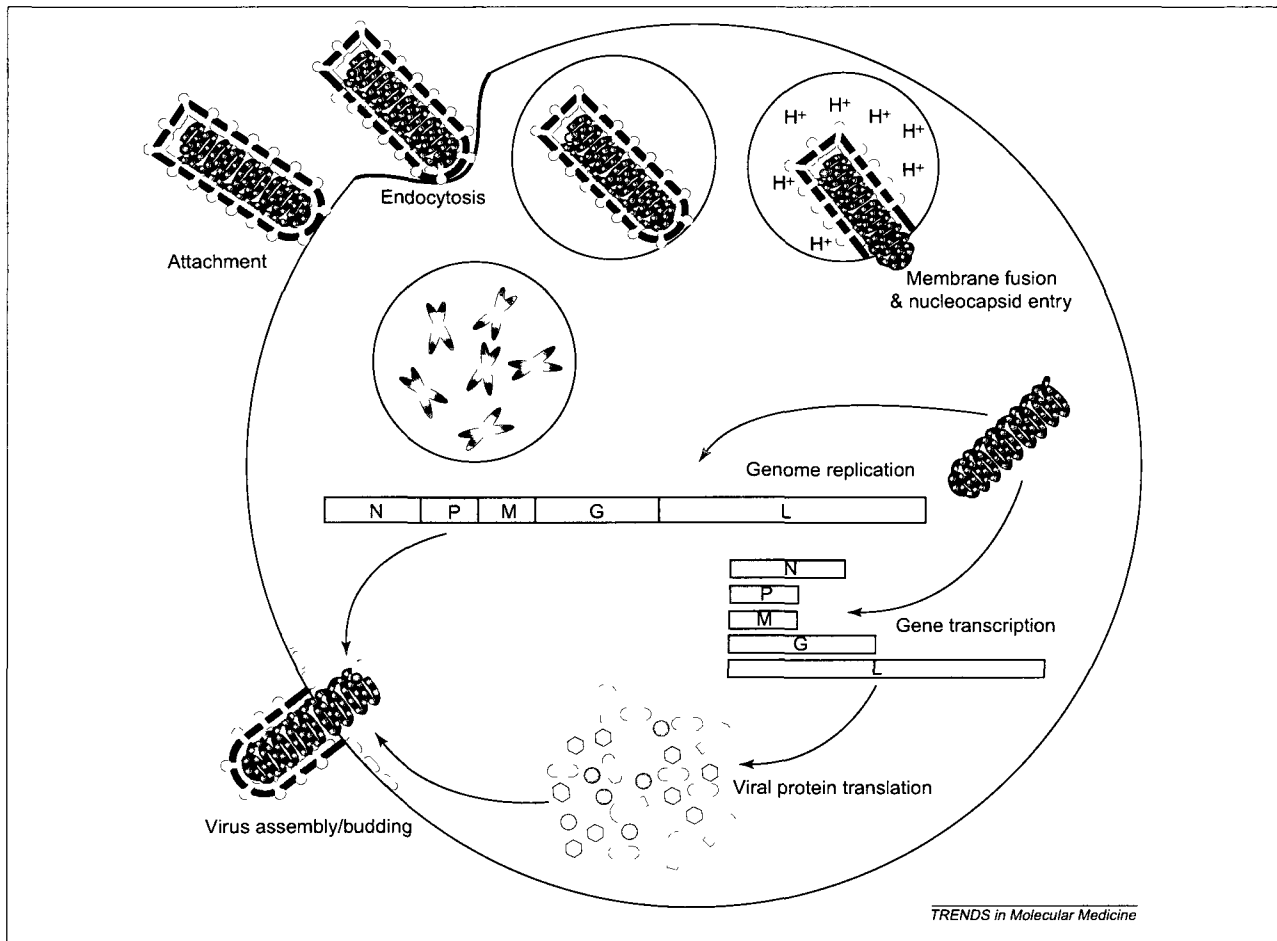


Figure 2. The vesicular stomatitis virus (VSV) replication cycle. Attachment of viral particles to the host cell is mediated by the glycoprotein of VSV. Attached particles are engulfed by endocytosis and enter the cellular endosomal trafficking pathway. As late endosomes are acidified, the drop in endosomal pH triggers a conformational change in the glycoprotein that mediates fusion between the viral envelope and the endosomal membrane. The viral nucleocapsid is then able to escape into the cytoplasm and initiate viral replication. The viral polymerase first transcribes the individual mRNAs for each viral gene, which are then translated by host ribosomes to yield functional viral proteins. At later stages of infection, the viral polymerase switches from transcription to replication and synthesizes copies of the negative-sense VSV genome through positive-strand intermediates. Finally, viral proteins and genomic RNA are assembled into complete virus particles and the virus exits the cell by budding through the plasma membrane.

to generate novel VSV vectors expressing an antigen of interest or bearing a particular mutation in a viral gene.

VSV as a vaccine vector

Vaccines that are based on live, attenuated VSV strains are not only highly effective in animal models but are also particularly attractive because they can be administered via a mucosal route, without the need for injection [27]. For example, a single intranasal vaccination with a live, attenuated VSV-recombinant expressing an influenza-virus hemagglutinin protein completely protects mice against a lethal challenge with influenza virus [4,27]. Another VSV recombinant, expressing the measles virus hemagglutinin, induced protective immunity in cotton rats against a measles challenge following a single intranasal vaccination [28]. To further attenuate VSV-based vaccine vectors, deletion of the gene that encodes the glycoprotein from the genome created a replication-incompetent vector [4]. Another creative strategy for VSV attenuation has been developed. The genes of all

VSV strains are arranged in a specific order that favors the expression of genes in a gradient from the nucleoprotein gene to the large polymerase gene (Figure 2); manipulating the genome by scrambling the order of the genes has created strains that are much less virulent than the parental strains [2]. Because VSV has a negative-stranded RNA genome that is unable to undergo natural recombination or reassortment, these scrambled genomes are fixed and can only be artificially created. Initial studies in mice established that VSV-HIV recombinants expressing the envelope glycoprotein of HIV could induce an HIV-neutralizing antibody. This was accomplished by boosting with a second VSV-HIV recombinant in which the VSV glycoprotein was substituted to avoid the neutralizing antibody that could be generated against the glycoprotein from the initial vector [29]. Several recombinant VSV vaccine vectors have now been reported, including vectors expressing antigens from HIV, influenza, hepatitis C, respiratory syncytial and measles viruses [28,30–33]. It is expected that interferon-inducing mutants of VSV will be

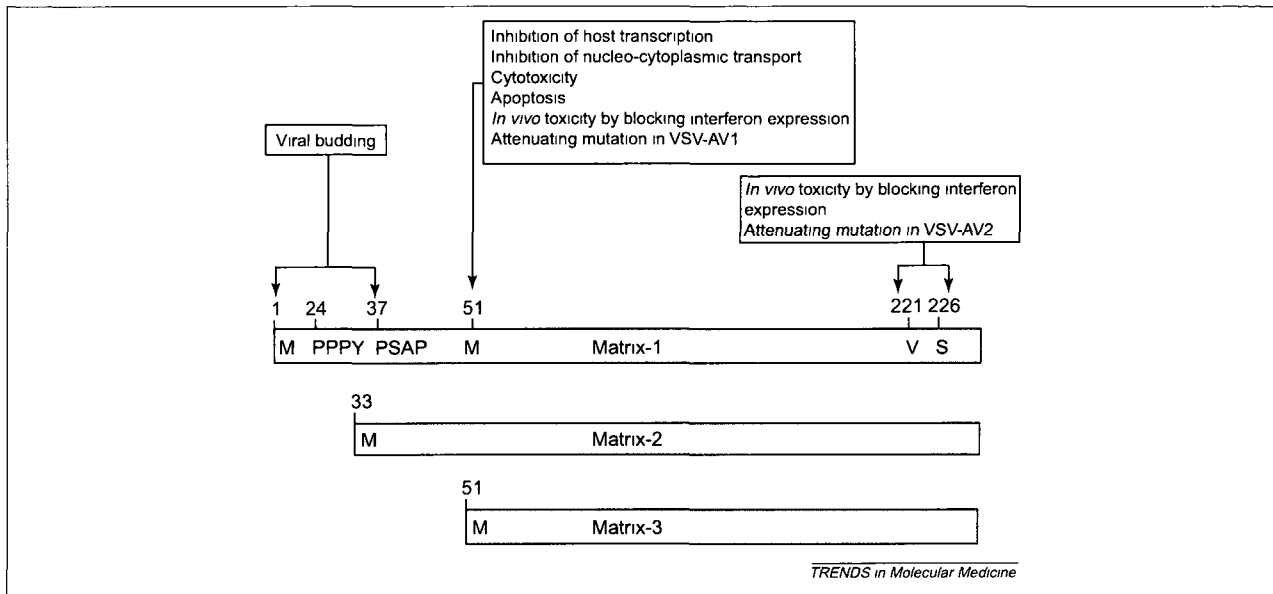


Figure 3 Crucial regions of the multifunctional vesicular stomatitis virus (VSV) matrix protein. The VSV matrix gene encodes three polypeptides. Translation of matrix mRNA from the first ATG start codon yields the full-length protein matrix-1, whereas initiation at Met33 or Met51 yields two truncated versions of the protein, matrix-2 and matrix-3. Important amino acid residues or motifs are shown, as are associated functions or phenotypes.

excellent vaccine vector platforms, because the wide range of antiviral cytokines induced by these strains should act as a natural adjuvant for the induction of immunity.

VSV as an oncolytic virus

In the majority of patients, tumors are either non-responsive to interferon treatment or they develop resistance [34]. This, and other observations, led to the hypothesis that tumor cells could be targeted for selective infection and destruction by a virus that was sensitive to the antiviral properties of interferon [35]. VSV is exquisitely sensitive to these antiviral properties and it was reasoned that VSV might have specific oncolytic properties; although being able to replicate in and kill tumor cells, it would be unable to infect normal cells. A laboratory strain of VSV-Ind can productively infect and kill many tumor cell lines *in vitro*, but growth is attenuated in normal, primary cultured cells, a difference that is dramatically enhanced in the presence of interferon [16,35,36]. This natural preference of the virus for transformed cells can also be seen *in vivo*, where VSV will preferentially target and replicate in tumors implanted in rodents [16,35–39]. The ability of VSV to infect malignant cells because of an impairment of the interferon response in these cells has also been demonstrated for primary cells from patients [40].

Building a better oncolytic VSV

It is possible to modify the VSV genome and several groups have pursued strategies to enhance the oncolytic properties of VSV. For example, the herpes-virus genes that encode thymidine kinase [36] and cytosine deaminase [41] have been added to the VSV genome in an attempt to increase tumor killing and further improve the safety of the virus by making virally infected cells sensitive to the drug gancyclovir. An alternative method was the addition

of a cDNA encoding IL-4 to VSV [36], with the hope of augmenting tumor killing through the stimulation of the immune system. Both of these strategies seem to have a positive effect on VSV-induced oncolysis in experimental animal models without compromising the tumor specificity of the virus.

Recently, Bergman *et al.* created a novel VSV vector that was targeted specifically to cells expressing the Her2/neu oncogene product [42]. Using this approach, they replaced the VSV glycoprotein with a mutant Sindbis-virus glycoprotein and the Fc-binding motif from *Staphylococcus aureus* protein A. The virus was then coated with monoclonal antibodies against HER2/neu and specifically directed to infect cells overexpressing the HER2/neu gene, including human breast cancer cells. Because the HER2/neu gene product is crucial to the transformed state of certain tumor cells, it is unlikely to be lost during tumor evolution. In an interesting twist on this approach, it was demonstrated that the expression of CD4 on the surface of VSV could specifically target the virus to infect cells expressing the HIV gp120 protein, raising the possibility of eliminating chronic viral infections by using an acute viral infection [43,44].

Because VSV can specifically kill cells that are unresponsive to interferon, a recombinant VSV strain that expressed the interferon- β cDNA was created, with the belief that this virus would have attenuated growth in normal cells but should still grow well in tumor cells [45]. Stojdl *et al.* have used a different strategy to exploit the lack of interferon responsiveness of certain tumor cells, using natural interferon-inducing VSV mutants [called attenuated virus 1 (AV1) and AV2], which were originally identified by the reduced plaque size on cells able to produce and respond to interferon [46]. AV1 and AV2 produce large plaques on cells with interferon defects, such as tumor cells. Mutations to the matrix protein render

these viruses interfere with and prevent the matrix protein from blocking nucleocytoplasmic transport and inhibiting host-cell transcription. Wild type and mutant strains of VSV are both able to induce the expression of the gene encoding interferon- β but the mutant viruses fail to block the export and translation of the interferon message [16]. These viruses are significantly attenuated *in vivo* by the induction of interferon following infection, but are still able to infect and kill tumor cells both *in vitro* and *in vivo*. The induction of interferon and other antiviral genes by these viruses generates a 'cytokine cloud' that protects the host not only from the mutant virus, but also from any wild-type virus present in the inoculum (Figure 4) [16]. This strategy for viral attenuation reduces the risk posed by reverted or mutated viruses that might arise during preparation of the therapeutic virus. In addition, this strategy produces an efficacious oncolytic virus, which is less toxic than a recombinant virus that is engineered to express interferon, because the expression levels of interferon can be controlled by the host. These viruses are attenuated through a loss of function mutation that can be only corrected in a limited number of ways, whereas exogenous genes added to therapeutic viruses can be inactivated by a great variety of mutations, potentially eliminating the useful properties supplied by that gene. To further enhance the stability of AV1 and AV2, amino acid deletions have been engineered that should make reversion to the wild-type VSV strains unlikely.

Advantages of VSV as a therapeutic virus

Many groups have suggested that RNA viruses, such as VSV, might prove to be superior to DNA viruses for oncolytic applications [47], for a variety of reasons. For example, VSV is a rapidly growing virus that can be produced to very high titers in bioreactors or in well-characterized mammalian cell lines. It has been estimated that one liter of culture supernatant could yield sufficient VSV to vaccinate one billion people [32]. This is a crucial issue in the production of viral therapeutics. Furthermore, VSV is a relatively innocuous virus that, even in its most virulent state, causes mild disease in ruminants and humans. In North America, at least, it is unlikely that humans have come into contact with VSV and so will not have pre-existing immunity to it. VSV replicates quickly and might be able to mediate a significant (or even a complete) response before the patient develops an acquired immunity to the virus (which might limit the effectiveness of subsequent treatments). Furthermore, the interferon-inducing mutants described might serve as adjuvants for the development of effective anti-tumor immune responses by inducing the expression of multiple mediators of the immune system.

Concluding remarks

Viral therapeutics have the promise of becoming biological agents that function at the cellular level for the treatment of human diseases. VSV has been an important basic research tool for many years, but is now approaching entry into the clinical realm. Because we know a great deal about the molecular biology and epidemiology of this virus, it is possible to engineer new strains that would function as safe and effective vaccines or, alternatively, as killers of

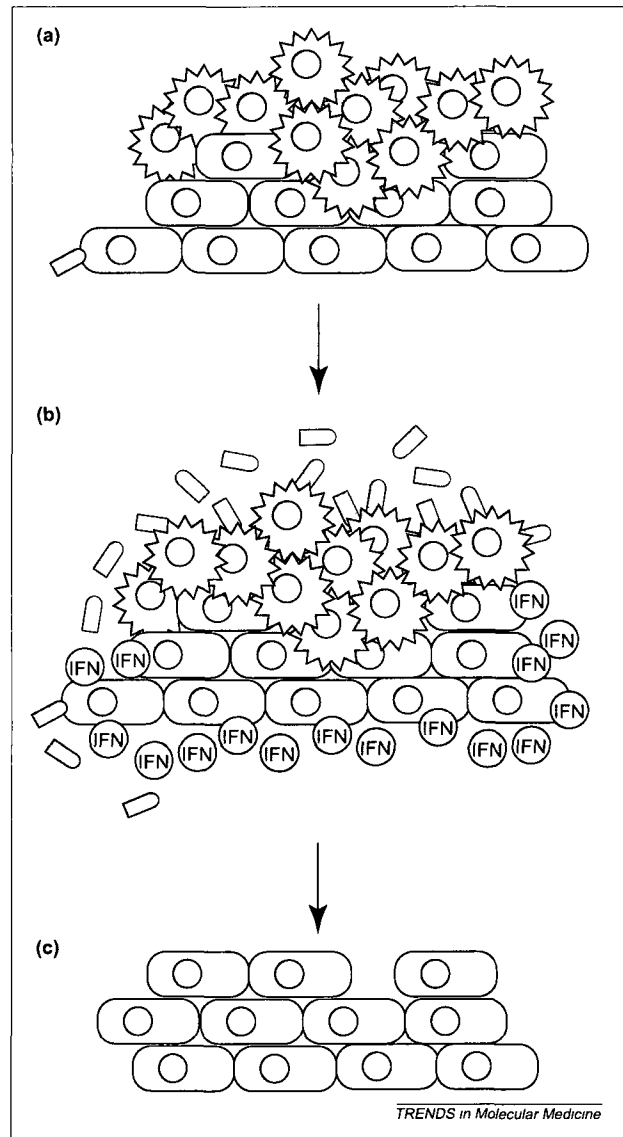


Figure 4 Induction of a cytokine cloud by attenuated vesicular stomatitis viruses (VSVs) protects normal cells from viral infection, whereas cancer cells are eliminated (a) Infection of normal cells (depicted as pale-orange, lozenge shaped cells) by interferon-inducing mutants of VSV (green bullets) enables these 'sentinel cells' (green) to respond by expressing and producing several cytokines, including type I interferons (b) This generates a 'cytokine cloud' in the infected host that establishes an anti-viral state in neighboring cells, thus protecting them from infection by VSV. Many malignant cells (depicted as spiked cells, blue when uninfected, green when VSV infected) are non-responsive to interferon and continue to remain susceptible to infection and killing by VSV, despite the presence of these cytokines. The cytokine cloud generated by these viruses can also protect the host from co-administered wild-type virus, thereby reducing the risk associated with reverted clones [16] (c) Malignant cells are killed as a result of the viral infection; normal cells are unharmed. When used for vaccination, these vectors will induce an array of cytokines that can act as natural adjuvants

diseased cells. However, despite all that is known about the replication and epidemiology of natural VSV infections, a new field of research focusing on how to deliver pharmaceutical viruses, how they interact with the host, the effects of the immune system, the measures of efficacy and the impact of virus shedding on the environment now needs to be addressed. There have been several significant

advances made in the past five years that have moved VSV-based therapeutics closer to reality. Over the next few years, the pre-clinical testing that is required to allow the use of VSV in clinical applications, for use against infectious disease and malignancy, should be completed.

References

- Mead, D G *et al* (2000) Transmission of vesicular stomatitis virus from infected to noninfected black flies co-feeding on nonviremic deer mice *Science* 287, 485–487
- Flanagan, E B *et al* (2001) Rearrangement of the genes of vesicular stomatitis virus eliminates clinical disease in the natural host: new strategy for vaccine development *J Virol* 75, 6107–6114
- Stallknecht, D E (2000) VSV–NJ on Ossabaw Island, Georgia: The truth is out there *Ann New York Acad Sci* 916, 431–436
- Roberts, A *et al* (1999) Attenuated vesicular stomatitis viruses as vaccine vectors *J Virol* 73, 3723–3732
- Wagner, R R and Rose, J K (1996) Rhabdoviridae: the viruses and their replication. In *Fields Virology* (Fields, B N and Knipe, D M, eds), pp 1121–1136, Lippincott-Raven
- Barr, J N *et al* (2002) Transcriptional control of the RNA-dependent RNA polymerase of vesicular stomatitis virus *Biochim Biophys Acta* 1577, 337–353
- Clinton, G M *et al* (1978) The matrix (M) protein of vesicular stomatitis virus regulates transcription *Cell* 15, 1455–1462
- Carroll, A R and Wagner, R R (1979) Role of the membrane (M) protein in endogenous inhibition of *in vitro* transcription by vesicular stomatitis virus *J Virol* 29, 134–142
- Jayakar, H R *et al* (2000) Mutations in the PPPY motif of vesicular stomatitis virus matrix protein reduce virus budding by inhibiting a late step in virion release *J Virol* 74, 9818–9827
- Harty, R N *et al* (2001) Rhabdoviruses and the cellular ubiquitin-proteasome system: a budding interaction *J Virol* 75, 10623–10629
- Martin-Serrano, J *et al* (2001) HIV-1 and Ebola virus encode small peptide motifs that recruit Tsg101 to sites of particle assembly to facilitate egress *Nat Med* 7, 1313–1319
- Black, B L and Lyles, D S (1992) Vesicular stomatitis virus matrix protein inhibits host cell-directed transcription of target genes *in vivo* *J Virol* 66, 4058–4064
- von Kobbe, C *et al* (2000) Vesicular stomatitis virus matrix protein inhibits host cell gene expression by targeting the nucleoporin Nup98 *Mol Cell* 6, 1243–1252
- Petersen, J M *et al* (2000) The matrix protein of vesicular stomatitis virus inhibits nucleocytoplasmic transport when it is in the nucleus and associated with nuclear pore complexes *Mol Cell Biol* 20, 8590–8601
- Petersen, J M *et al* (2001) Multiple vesiculoviral matrix proteins inhibit both nuclear export and import *Proc Natl Acad Sci U S A* 98, 8590–8595
- Stöjdl, D F *et al* (2003) VSV strains with defects in their ability to shutdown innate immunity are potent systemic anti-cancer agents *Cancer Cell* 4, 263–275
- Enninga, J *et al* (2002) Role of nucleoporin induction in releasing an mRNA nuclear export block *Science* 295, 1523–1525
- Terstegen, L *et al* (2001) The vesicular stomatitis virus matrix protein inhibits glycoprotein 130-dependent STAT activation *J Immunol* 167, 5209–5216
- Blondel, D *et al* (1990) Role of matrix protein in cytopathogenesis of vesicular stomatitis virus *J Virol* 64, 1716–1725
- Kopecky, S A *et al* (2001) Matrix protein and another viral component contribute to induction of apoptosis in cells infected with vesicular stomatitis virus *J Virol* 75, 12169–12181
- Kopecky, S A and Lyles, D S (2003) Contrasting effects of matrix protein on apoptosis in HeLa and BHK cells infected with vesicular stomatitis virus are due to inhibition of host gene expression *J Virol* 77, 4658–4669
- Lawson, N D *et al* (1995) Recombinant vesicular stomatitis viruses from DNA *Proc Natl Acad Sci U S A* 92, 4477–4481
- Schnell, M J *et al* (1996) The minimal conserved transcription start signal promotes stable expression of a foreign gene in vesicular stomatitis virus *J Virol* 70, 2318–2323
- Schnell, M J *et al* (1996) Foreign glycoproteins expressed from recombinant vesicular stomatitis viruses are incorporated efficiently into virus particles *Proc Natl Acad Sci U S A* 93, 11359–11365
- Kretzschmar, E *et al* (1997) High-efficiency incorporation of functional influenza virus glycoproteins into recombinant vesicular stomatitis viruses *J Virol* 71, 5982–5989
- Haglund, K *et al* (2000) Expression of human immunodeficiency virus type 1 Gag protein precursor and envelope proteins from a vesicular stomatitis virus recombinant: high-level production of virus-like particles containing HIV envelope *Virology* 268, 112–121
- Roberts, A *et al* (1998) Vaccination with a recombinant vesicular stomatitis virus expressing an influenza virus hemagglutinin provides complete protection from influenza virus challenge *J Virol* 72, 4704–4711
- Schlereth, B *et al* (2000) Successful vaccine induced seroconversion by single-dose immunization in the presence of measles virus-specific maternal antibodies *J Virol* 74, 4652–4657
- Rose, N F *et al* (2000) Glycoprotein exchange vectors based on vesicular stomatitis virus allow effective boosting and generation of neutralizing antibodies to a primary isolate of human immunodeficiency virus type 1 *J Virol* 74, 10903–10910
- Kahn, J S *et al* (1999) Recombinant vesicular stomatitis virus expressing respiratory syncytial virus (RSV) glycoproteins: RSV fusion protein can mediate infection and cell fusion *Virology* 254, 81–91
- Kahn, J S *et al* (2001) Replication-competent or attenuated, nonpropagating vesicular stomatitis viruses expressing respiratory syncytial virus (RSV) antigens protect mice against RSV challenge *J Virol* 75, 11079–11087
- Rose, N F *et al* (2001) An effective AIDS vaccine based on live attenuated vesicular stomatitis virus recombinants *Cell* 106, 539–549
- Ezelle, H J *et al* (2002) Generation of hepatitis C virus-like particles by use of a recombinant vesicular stomatitis virus vector *J Virol* 76, 12325–12334
- Grander, D and Einhorn, S (1998) Interferon and malignant disease—how does it work and why doesn't it always? *Acta Oncol* 37, 331–338
- Stöjdl, D F *et al* (2000) Exploiting tumor-specific defects in the interferon pathway with a previously unknown oncolytic virus *Nat Med* 6, 821–825
- Fernandez, M *et al* (2002) Genetically engineered vesicular stomatitis virus in gene therapy: application for treatment of malignant disease *J Virol* 76, 895–904
- Balachandran, S and Barber, G N (2000) Vesicular stomatitis virus (VSV) therapy of tumors *IUBMB Life* 50, 135–138
- Balachandran, S *et al* (2001) Oncolytic activity of vesicular stomatitis virus is effective against tumors exhibiting aberrant p53, Ras, or myc function and involves the induction of apoptosis *J Virol* 75, 3474–3479
- Ebert, O *et al* (2003) Oncolytic vesicular stomatitis virus for treatment of orthotopic hepatocellular carcinoma in immune-competent rats *Cancer Res* 63, 3605–3611
- Dummer, R *et al* (2001) Interferon resistance of cutaneous T-cell lymphoma-derived clonal T-helper 2 cells allows selective viral replication *Blood* 97, 523–527
- Porosnicu, M *et al* (2003) The oncolytic effect of recombinant vesicular stomatitis virus is enhanced by expression of the fusion cytosine deaminase/uracil phosphoribosyltransferase suicide gene *Cancer Res* 63, 8366–8376
- Bergman, I *et al* (2003) Vesicular stomatitis virus expressing a chimeric Sindbis glycoprotein containing an Fc antibody binding domain targets to Her2/neu overexpressing breast cancer cells *Virology* 316, 337–347
- Schubert, M *et al* (1992) Insertion of the human immunodeficiency virus CD4 receptor into the envelope of vesicular stomatitis virus particles *J Virol* 66, 1579–1589
- Schnell, M J *et al* (1997) Construction of a novel virus that targets HIV-1-infected cells and controls HIV-1 infection *Cell* 90, 849–857
- Obuchi, M *et al* (2003) Development of recombinant vesicular stomatitis viruses that exploit defects in host defense to augment specific oncolytic activity *J Virol* 77, 8843–8856
- Francoeur, A M *et al* (1987) The isolation of interferon-inducing mutants of vesicular stomatitis virus with altered viral P function for the inhibition of total protein synthesis *Virology* 160, 236–245
- Giedlin, M A *et al* (2003) Vesicular stomatitis virus: an exciting new therapeutic oncolytic virus candidate for cancer or just another chapter from Field's *Virology*? *Cancer Cell* 4, 241–243
- Huang, T G *et al* (2003) Oncolysis of hepatic metastasis of colorectal cancer by recombinant vesicular stomatitis virus in immune-competent mice *Mol Ther* 8, 434–440

**APPENDIX VI.: VSV STRAINS WITH DEFECTS IN THEIR ABILITY TO SHUTDOWN
INNATE IMMUNITY ARE POTENT SYSTEMIC ANTI-CANCER AGENTS**

Contribution of Authors: AT Power performed molecular cloning to generate the recombinant VSV Δ 51 used in these studies. AT Power and J. Paterson performed *in vivo* imaging of infected tumors.

Published: Cancer Cell. 2003 Oct;4(4):263-75.

VSV strains with defects in their ability to shutdown innate immunity are potent systemic anti-cancer agents

David F. Stojdl,¹ Brian D. Lichty,¹ Benjamin R. tenOever,² Jennifer M. Paterson,^{1,6} Anthony T. Power,^{1,6} Shane Knowles,¹ Ricardo Marius,¹ Jennifer Reynard,¹ Laurent Poliquin,³ Harold Atkins,¹ Earl G. Brown,⁶ Russell K. Durbin,⁴ Joan E. Durbin,⁴ John Hiscott,^{2,5} and John C. Bell^{1,6*}

¹Ottawa Regional Cancer Centre Research Laboratories 501 Smyth Road, Ottawa, Ontario, Canada K1H 8L6

²Terry Fox Molecular Oncology Group Lady Davis Institute for Medical Research McGill University, Montreal Quebec Canada

³Department of Biological Sciences Université du Québec a Montréal, P O Box 8888 Station Centre-ville Quebec, H3C 3P8 Montreal Canada

⁴Children's Research Institute, Children's Hospital, Columbus Department of Pediatrics College of Medicine and Public Health, The Ohio State University Columbus, Ohio 43205

⁵Departments of Microbiology and Immunobiology, Medicine, McGill University, Montreal, Quebec, Canada H3T 1E2

⁶Department of Biochemistry Microbiology and Immunology, University of Ottawa, 451 Smyth Road Ottawa Ontario Canada K1H 8M5

*Correspondence John.bell@orcc.on.ca

Summary

Ideally, an oncolytic virus will replicate preferentially in malignant cells, have the ability to treat disseminated metastases, and ultimately be cleared by the patient. Here we present evidence that the attenuated vesicular stomatitis strains, AV1 and AV2, embody all of these traits. We uncover the mechanism by which these mutants are selectively attenuated in interferon-responsive cells while remaining highly lytic in 80% of human tumor cell lines tested. AV1 and AV2 were tested in a xenograft model of human ovarian cancer and in an immune competent mouse model of metastatic colon cancer. While highly attenuated for growth in normal mice, both AV1 and AV2 effected complete and durable cures in the majority of treated animals when delivered systemically.

Introduction

Over the last decade, a variety of replicating oncolytic viruses have been selected or engineered to be therapeutics that exploit genetic defects unique to tumor cells (reviewed in Bell et al., 2002; Gromeier and Wimmer, 2001; Hawkins et al., 2002; Kruyt and Curiel, 2002; Norman et al., 2000). One genetic defect frequently arising during tumor evolution, is diminished interferon (IFN) responsiveness (Bello et al., 1994; Linge et al., 1995; Lu et al., 2000; Matin et al., 2001; Sun et al., 1998; Wong et al., 1997). This reflects the important role that interferon-regulated pathways play in the control of normal cell growth and apoptosis. Interferon is also a key mediator of the individual cell's antiviral response and thus tumor cells, which acquire mutations allowing them to escape interferon-mediated growth control programs, will simultaneously compromise their innate antiviral response. We hypothesized that viruses whose replication is inhibited by interferon should grow well in tumor but not normal cells. We and others have found that vesicular stomatitis virus (VSV), whose growth is strongly inhibited by interferon, is a

potent oncolytic virus (Balachandran and Barber, 2000; Stojdl et al., 2000b). In fact, while VSV infections are uniformly fatal to nude mice (Huneycutt et al., 1993; Stojdl et al., 2000b), we found that prophylactic interferon treatment can rescue even immunocompromised animals while preserving virus-mediated oncolysis. We reasoned that a virus that both induces the production of interferon and is susceptible to its antiviral effects would be a superior therapeutic. Here we describe two naturally occurring VSV variants that possess both these properties. The VSV variants retain oncolytic activity in vitro and in a variety of in vivo models but because of their potent induction of interferon have a vastly improved therapeutic index over their wild-type (WT) counterpart.

Results

Attenuation of VSV in vivo is dependent upon intact interferon signaling pathways

Two variants of VSV that produce small plaques on interferon-responsive cells (herein referred to as AV1 and AV2) were found

SIGNIFICANCE

A key limitation to the application of viruses as cancer therapeutics is the possibility of uncontrolled virus growth in normal tissues, potentially leading to treatment complications or disease. Here, we describe novel, oncolytic variants of vesicular stomatitis virus (VSV) that not only have potent anti-tumor activity in vivo, but establish an anti-viral state that protects against the toxicity associated with infection of healthy cells. Our work has uncovered the mechanism that virulent VSV strains use to defeat host antiviral defences, furthering our understanding of early IFN signaling in response to a viral invader. These findings have directed us toward the development of improved VSV-based oncolytic viruses and are generally applicable to a wide range of viral based therapeutics.

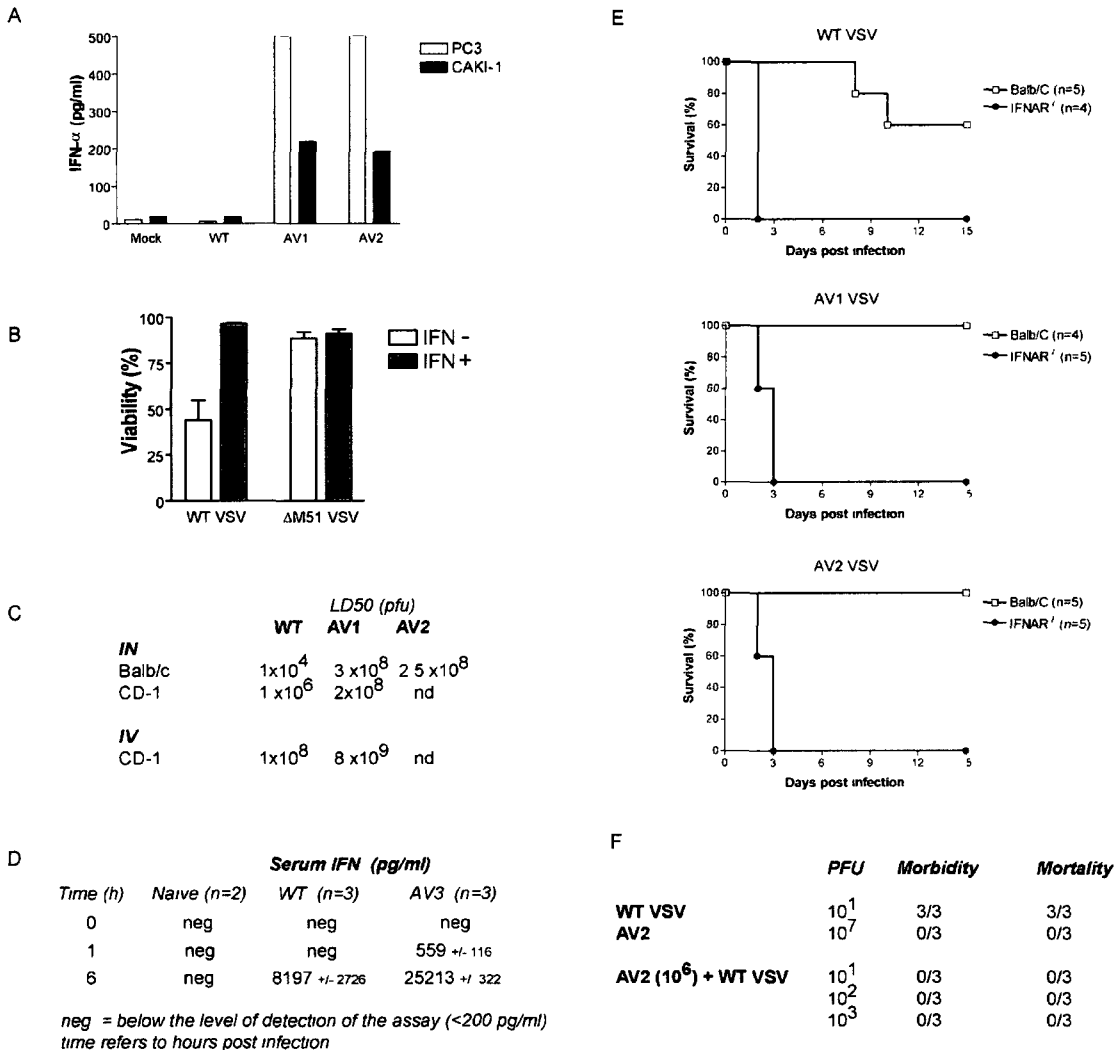


Figure 1. Decreased in vivo toxicity of AV1 and AV2 is mediated by interferon

A: Human prostate carcinoma cells (PC3) and human renal carcinomas cells (CAKI-1) were either mock infected or infected with wild-type (WT), AV1, or AV2 strains of VSV. Culture media were assayed by ELISA to detect human IFN- α production 48 hr post-infection.

B: Exogenous interferon is required to protect MEFs from WT GFP but not from AV3 GFP. Balb/C MEFs were pretreated with 0 or 30 U/ml universal type I interferon for 16 hr and then infected with WT GFP VSV or AV3 GFP at an MOI of 0.1. Twenty-four hours later, cell viability was measured by MTS assay.

C: In vivo toxicity of WT versus mutant VSV strains by route and mouse strain. IN = intranasal, IV = intravenous, nd = not determined.

D: AV3 induces IFN- α quicker and to a greater degree than WT VSV in vivo. Groups of mice were either mock infected or infected with WT GFP or AV3 GFP, and their serum IFN- α levels were assayed at the indicated times post-infection.

E: Balb/C and Balb/C *IFNAR*^{-/-} mice were infected intranasally with WT VSV, AV1, or AV2 virus and monitored for morbidity.

F: AV2 can protect mice against lethal WT VSV infection. *PKR*^{-/-} mice were infected intranasally at various doses with either WT, AV2, or both and monitored for morbidity or mortality. Values denote number of mice per group.

to induce from twenty to fifty times more interferon α (IFN- α) than WT VSV following infection of epithelial cell lines (Figure 1A). Sequencing of the variants revealed that they differed from the wild-type strain in their M proteins with a single amino acid substitution in the case of AV1 (M51R) and two amino acids (V221F and S226R) in AV2. A third variant was created to be a mimetic of AV1 by complete deletion of methionine 51 (Δ M51 or AV3) and found to have biological properties indistinguishable from AV1 and AV2. As expected (Stojdl et al., 2000b), primary mouse embryonic fibroblasts are protected against WT VSV infec-

tion only in the presence of exogenously added interferon whereas MEFs (mouse embryonic fibroblasts) are refractory to infection by the interferon inducing mutant AV3 (Figure 1B).

In animals, the role of the interferons in protecting against virus infection and the mechanisms underlying their induction are more complex than in the simple tissue culture systems described above (Barchet et al., 2002; Levy, 2002). Nevertheless, we show in the following that the AV strains are more potent interferon inducers and have reduced toxicity in mice in a strictly interferon-dependent fashion. For example, mice

infected intravenously can tolerate some 80 times more AV1 virus than WT VSV, and AV3 induced a more rapid and robust production of interferon than WT VSV (Figures 1C and 1D). The critical role that interferon signaling plays in the protection of mice from infection by AV1 and AV2 was verified using interferon receptor knockout (*INFAR*^{-/-}) animals. The LD₅₀ of AV1 and AV2 when delivered intranasally to Balb/C (*INFAR*^{+/+}) mice was determined to be 10,000 times greater than WT VSV delivered by the same route (Figure 1C). Similar results were seen in CD-1 mice (WT = 1 × 10⁶; AV1 = 2 × 10⁸ pfu). However, in the absence of a functional interferon receptor, AV1 and AV2 were as toxic as wild-type virus, indicating that the attenuation of AV1 and AV2 growth in vivo is dependent upon an intact interferon system (Figure 1E).

The AV1 and AV2 variants protect mice from infection by WT VSV

Mice that lack the double-stranded RNA-dependent kinase (PKR) gene are known to be exquisitely sensitive to infection by wild-type vesicular stomatitis virus, although PKR^{-/-} fibroblasts can be protected by prophylactic treatment with interferon (Balachandran et al., 2000). Since AV1 and AV2 strongly induce interferon production during the course of a natural infection, we tested whether PKR^{-/-} mice would be resistant to infection by these viruses. Indeed we found that while <10 pfu of wild-type VSV can kill PKR^{-/-} mice (Figure 1F), doses greater than 10⁷ pfu of AV1 and AV2 were well tolerated by PKR^{-/-} animals. More strikingly, when coinfecting with AV2, the LD₁₀₀ of wild-type VSV was dramatically increased in PKR^{-/-} animals. Indeed, doses 100 times greater than the LD₁₀₀ for WT VSV were well tolerated when coinfecting with AV2 (Figure 1F). Given that PKR^{-/-} fibroblasts can be protected from WT VSV infection by prophylactic interferon administration (Balachandran et al., 2000), that the AV variants induce interferon, and that AV variants are toxic in mice that lack a functional interferon receptor, we believe that the protective effect of AV2 on PKR^{-/-} mice is most easily explained by the ability of these viruses to strongly induce interferon production in the infected animal.

Wild-type, AV1 and AV2 viruses trigger antiviral responses in infected cells

We used microarray and Western blot analysis over a time-course of virus infection to allow us to detect early signaling events triggered by WT and AV variants that lead to the transcriptional activation of antiviral genes. Others have established that an early response to virus infection is the phosphorylation and activation of the latent transcription factor IRF-3 (Sato et al., 1998b). It appears that WT, AV1 and AV2 viruses trigger IRF-3 phosphorylation with similar kinetics (Figure 2A). Following phosphorylation, IRF-3 assembles together with CBP/300 and, along with other transcription factors (e.g., NFκB and c-JUN/ATF-2), initiates the transcription of a number of antiviral gene products (Wathelet et al., 1998). As shown in Table 1, microarray analysis revealed that a large number of genes were dramatically induced 3 hr post-infection with all three viruses. Many of these genes are known to be activated by virus infection (Nakaya et al., 2001), including several that are directly regulated following activation of the latent transcription factors IRF-3, NFκB, and c-JUN/ATF-2 (Genin et al., 2000). We validated the microarray data by performing RT-PCR analysis on a sampling of gene products (Figure 2B).

In Figures 2C–2E, we present a model in which virus infection leads to waves of transcriptional events that are sequential and interdependent. For example, genes that we refer to herein as primary response genes were induced 3–6 hr post-infection by all three viruses (Figures 2B and 2C). On the other hand, secondary response genes that require the production of IFN-β protein and the autocrine activation of the JAK/STAT pathway (Figure 2D) were differentially induced by the wild-type and attenuated viruses (see IRF-7 in Figures 2A and 2D). As a consequence of the impaired IRF-7 production in WT VSV-infected cells, tertiary response gene products like the IFN-α transcripts were not induced in wild-type VSV-infected cells (Figure 2E). These results indicate that all three viruses trigger activation of IRF-3 and the subsequent transcription of a cohort of genes that we call primary response genes. We hypothesized that the M protein encoded by wild-type VSV disables the host cell's antiviral response by disrupting subsequent activation of secondary and tertiary response genes.

VSV M protein blocks the nuclear export of interferon-β mRNA

It has been suggested that VSV M protein either blocks the transcription of the *IFN-β* gene (Ahmed et al., 2003, Ferran and Lucas-Lenard, 1997), inhibits the nuclear export of mRNAs (Her et al., 1997, von Kobbe et al., 2000), or interferes with JAK/STAT signaling (Terstegen et al., 2001). Our transcript profiling studies would be consistent with either of the latter two mechanisms, however, we have been unable to show any impairment in the induction of the JAK/STAT pathway by exogenous interferon in infected cells (data not shown). On the other hand, when we used microarray or RT-PCR analysis to compare and contrast transcripts in nuclear and cytoplasmic fractions, we found clear differences between wild-type and attenuated virus-infected cells (Figure 3A). Importantly, *IFN-β* mRNA although induced in nuclear fractions by all three viruses was not found in the cytoplasmic pool of mRNAs in WT infected cells. Furthermore, IFN-β was undetectable in culture media from cells infected with WT VSV, while copious amounts of the cytokine were produced from cells infected with either AV1 or AV2 (Figure 3B). Two additional experiments help shed light upon how WT VSV subverts the interferon signaling pathway. First, cells were infected with either WT or AV3 VSV, and at 22 hr post-infection, IFN-α production in tissue culture supernatant was measured. WT VSV does not induce the production of IFN-α while AV3 is a potent inducer (Figure 3C). The induction of IFN-α by AV3 was dependent upon prior production of IFN-β as inclusion of neutralizing anti-IFN-β antibody to infected cultures inhibited IFN-α production from these cells (Figure 3C). Second, we constructed a wild-type VSV that expresses a constitutively active version of IRF-7. This virus has an attenuated phenotype and induces the expression of *IFN-α* genes within 4 hr post-infection, even in the presence of wild-type VSV M protein (Figure 2D). In total, these results are consistent with the idea that wild-type VSV triggers a primary antiviral response, but through coordinate expression of viral gene products blunts secondary and tertiary responses by blocking nuclear export of critical antiviral mRNAs.

AV1 and AV2 retain their ability to kill tumor cells in vitro and in vivo

To assess the oncolytic properties of the attenuated VSV strains, the NCI human tumor cell panel (60 cell lines from a spectrum

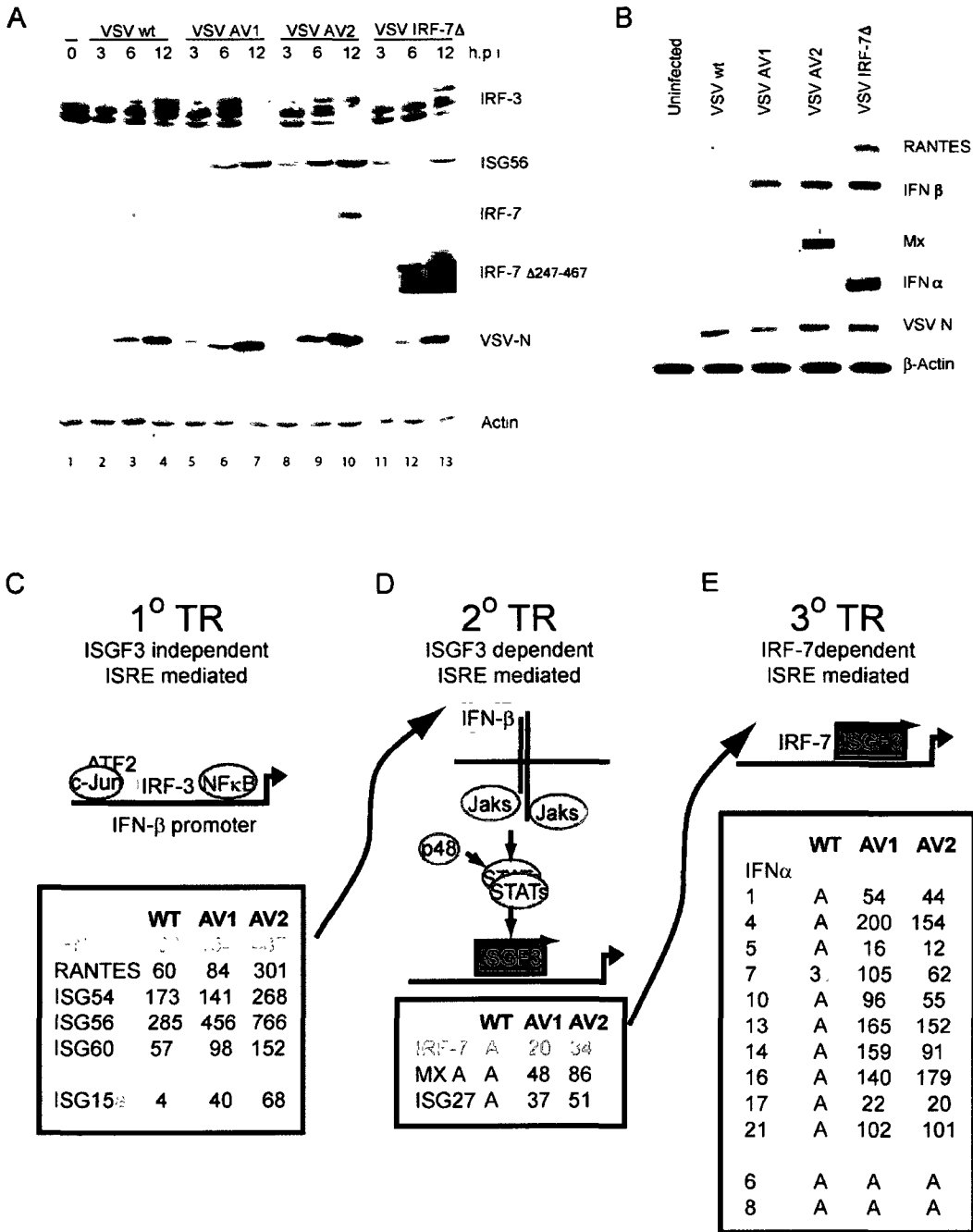


Figure 2. The secondary transcriptional response is inhibited by WT VSV but not AV1 or AV2

A: Western blot analysis showed similar kinetics of IRF-3 activation between WT and mutant VSVs; however, ISG56 (primary response) protein expression was severely impaired in WT infected cells. IRF-7 protein is detected only in AV1- and AV2-infected cells. IRF-7Δ appears to be able to induce the expression of endogenous IRF-7.

B: RT-PCR data at 4 hr post-infection of A549 cells showed primary response genes RANTES and IFN-β induced to similar levels in WT and mutant VSV-infected cells while upregulation of MX1 (secondary response) was impaired in WT infected cells.

C: Primary response to viral infection is mediated by IRF-3, cJUN/ATF-2, and NFκB (shown here forming part of the enhancosome complex at the IFN-β promoter). Microarray data indicate primary transcriptional response genes robustly upregulated in both WT and mutant virus-infected cells. (α: ISG15 is known to require ISGF3 for full induction). Values represent fold induction over mock infected.

D: IFN-β is then translated and secreted to stimulate, in an autocrine fashion, JAK/STAT signaling to form ISGF3 complexes in the nucleus, which mediates the induction of genes of the secondary transcriptional response. While cells infected with AV1 or AV2 show robust upregulation of these genes, WT infected cells show no expression at all (A = absent).

E: Without the consequent expression of IRF-7 in cells infected with WT VSV, the tertiary transcriptional wave, which includes almost all IFN-α genes, cannot take place (b: IFN-α7 is marginally detected by the array in WT samples). In contrast, AV1- and AV2-infected cells efficiently induce the expression of IFN-α genes.

Table 1. Microarray analysis of the transcriptional response to VSV infection over time

Accession #	Common name	WT			AV1			AV2		
		Hours post infection			Hours post infection			Hours post infection		
		3	6	12	3	6	12	3	6	12
Primary transcriptional response										
NM_000201.1	CD54	2.3	A	A	3.3	3.0	33.6	2.7	5.4	56.8
NM_016323.1	CEB1	2.0	21.2	204.4	1.6	38.0	279.3	1.9	73.6	490.5
U83981	GADD34	10.8	57.5	95.0	3.1	48.8	422.7	5.5	159.0	686.7
NM_002176.1	IFN beta	4.2	103.2	488.6	3.2	154.5	1531.6	3.6	487.3	2157.9
NM_000600.1	IL6	7.3	19.1	38.2	3.8	44.7	171.6	7.4	120.3	238.7
BE888744	ISG54	19.5	173.1	804.5	4.7	141.0	721.9	11.4	268.4	1357.8
NM_001548.1	ISG56	32.3	285.9	855.2	20.0	456.8	1411.7	39.8	766.0	1992.1
NM_001549.1	ISG60	7.6	57.5	238.0	4.1	97.7	288.6	7.0	151.6	457.7
AF063612.1	OASL	6.6	71.8	222.0	3.4	81.9	388.9	5.7	172.0	776.9
NM_021127.1	PMAIP1	5.2	22.1	58.6	2.1	17.3	87.5	4.3	34.3	169.8
NM_002852.1	PTX3	5.9	3.1	A	6.4	11.7	114.0	4.9	29.9	117.6
AF332558.1	PUMA	10.6	A	A	A	38.7	211.6	9.8	77.8	428.0
NM_002985.1	RANTES	3.4	60.1	945.0	2.6	84.9	1796.7	4.1	301.8	3916.1
AY029180.1	SUPAR	3.7	9.8	14.7	2.4	10.5	40.5	2.8	27.7	46.3
NM_006290.1	TNFAIP3	2.8	6.3	15.5	2.7	13.8	83.5	3.1	30.5	152.8
Secondary transcriptional response										
NM_030641.1	APOL6	A	A	A	A	15.3	40.8	A	25.2	37.3
AF323540.1	APOLL	1.8	A	A	1.0	11.3	25.7	2.2	10.7	34.5
U84487	CX3C chemokine precursor	2.0	2.5	2.5	1.7	7.0	45.1	2.3	14.1	65.9
BC002666.1	GBP1	A	A	4.2	A	35.9	171.6	1.4	66.2	249.2
NM_006018.1	HM74	A	A	A	2.2	29.1	72.5	A	66.4	45.4
NM_031212.1	hmrs3/4	A	A	A	2.5	4.2	21.3	A	10.1	18.3
NM_005531.1	IFI16	A	A	A	2.4	12.8	38.1	2.8	18.9	46.2
NM_005532.1	IFI27	A	A	21.9	A	36.6	281.0	A	51.0	295.4
NM_004509.1	IFI41	A	A	A	A	10.0	22.8	1.3	11.9	18.1
NM_022873.1	IFI 6-16	0.9	2.5	2.2	0.7	7.0	15.6	1.1	9.6	15.7
NM_003641.1	IFITM1	1.9	A	A	1.2	8.5	67.1	1.9	14.3	42.1
AA749101	IFITM1	1.2	3.1	2.3	1.0	6.6	40.9	1.2	9.5	32.6
NM_000882.1	IL12A	1.6	A	A	A	4.9	13.7	A	6.5	28.8
M15329.1	IL1A	nd	A	A	A	8.3	79.4	A	27.0	287.6
NM_004030.1	IRF7	1.4	A	A	A	19.9	109.9	2.2	33.7	144.3
NM_006084.1	IRF9	A	A	1.2	1.6	6.5	11.2	1.5	7.8	17.4
BC001356.1	ISG35	1.1	A	A	1.0	5.8	23.2	1.4	7.1	20.2
AF280094.1	ISG75	1.3	1.8	2.2	1.5	10.3	16.2	1.2	12.5	13.8
AF280094.1	ISG75	0.9	1.7	A	1.2	7.5	10.8	1.5	9.5	11.1
U17496.1	LMP7	A	A	A	A	7.6	15.3	0.9	10.0	10.4
NM_006417.1	MTAP44	A	A	23.3	A	10.8	82.7	A	18.0	133.9
NM_002462.1	MX A	A	A	27.6	A	48.1	261.9	A	85.7	232.9
AB014515	NEDD4 BP1	A	A	9.2	2.0	4.0	13.1	1.5	4.5	19.5
NM_002759.1	PKR	0.5	0.9	2.0	0.8	4.3	15.2	1.0	6.6	9.6
NM_021105.1	PLSCR1	1.4	1.7	A	2.2	5.0	24.9	2.1	4.9	15.1
NM_017912.1	putative Ub ligase	A	A	19.1	A	9.6	26.3	A	12.5	24.8
BF939675	SECTM1	A	A	A	A	20.7	93.8	A	24.8	33.9
BC004395.1	Similar to apolipoprotein L	A	A	A	A	11.7	17.2	A	14.6	21.3
NM_003141.1	SSA1	A	A	A	1.2	5.9	11.2	1.4	7.9	11.1
AA083478	STAF50	nd	A	nd	1.7	8.5	96.3	nd	16.7	56.1
NM_005419.1	STAT2	1.1	A	A	1.3	3.0	9.1	1.1	4.3	9.1
NM_003810.1	TRAIL	A	A	A	A	22.4	135.4	0.7	37.3	88.6
NM_020119.1	ZAP	A	A	19.4	0.9	4.6	79.9	A	11.4	133.8
Tertiary transcriptional response										
M12350.1	IFN 27	A	A	A	nd	nd	102.3	nd	A	101.4
NM_024013.1	IFNA1	nd	A	A	nd	2.2	53.6	nd	A	44.0
NM_002171.1	IFNA10	A	A	A	A	A	96.2	A	A	55.1
NM_006900.2	IFNA13	A	A	A	A	A	165.4	nd	A	152.1
NM_002172.1	IFNA14	A	A	A	A	A	159.0	A	4.4	91.1
NM_002173.1	IFNA16	1.0	A	1.8	1.1	0.9	139.9	0.7	3.3	95.7
M38289.1	IFNA17	A	A	A	A	A	21.5	A	A	19.8
NM_002169.1	IFNA5	1.0	A	A	0.9	A	16.4	0.9	A	11.6
NM_021057.1	IFNA7	A	A	3.5	A	A	105.0	A	3.4	61.7

Data represented as fold change compared to mock infected samples. All samples are from nuclear fractions of infected cells. A = Absent (no detectable mRNA) nd = no data. bold genes represent "archetypal genes" see text for explanation.

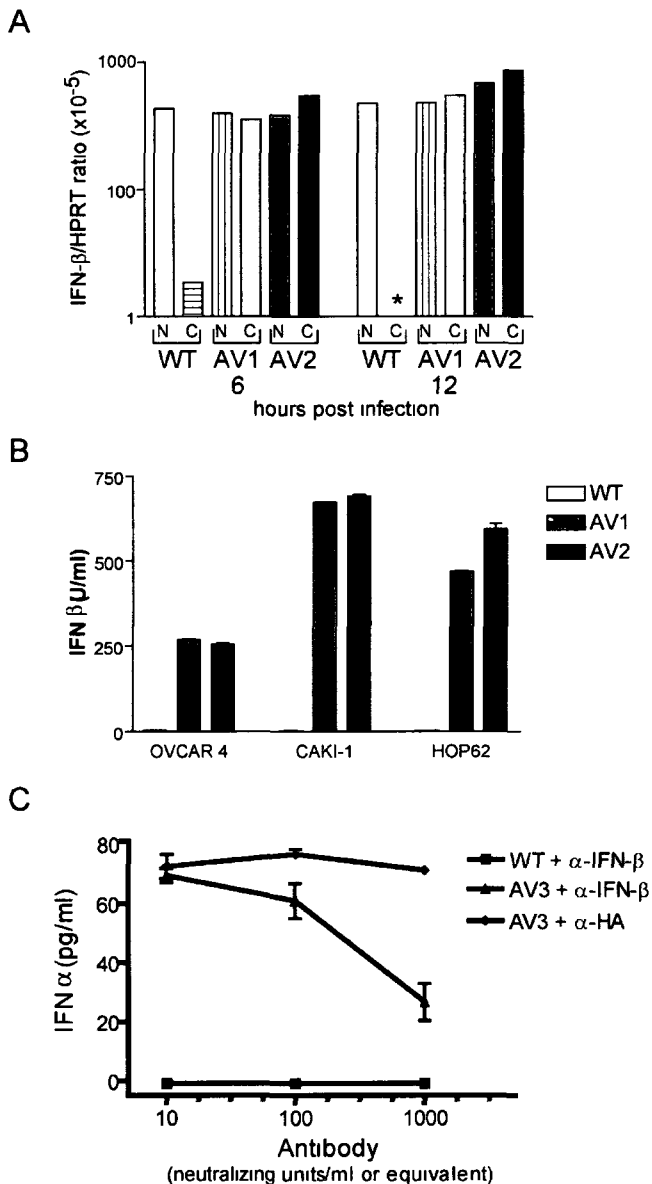


Figure 3 WT VSV inhibits IFN β mRNA nuclear/cytoplasmic transport and blocks IFN α production

A IFN β mRNAs are severely depleted in cytoplasmic fractions from WT VSV infected cells as determined by quantitative RT-PCR. Nuclear (N) and cytoplasmic (C) total RNA fractions from cells infected with WT, AV1, or AV2 VSV were assayed for IFN β mRNA normalized to HPRT mRNA from the same sample. * indicates no IFN β mRNA detected.

B Cells infected with either WT or mutant VSV strains were assayed by ELISA for IFN β production. AV1 and AV2 infected cells and not WT VSV infected cells produce secreted IFN β .

C Blocking IFN β inhibits the production of IFN α . OVCAR 4 cells were infected with mutant VSV in the presence of neutralizing antibody to IFN β or an irrelevant antibody and subsequently assayed by ELISA for IFN α production.

of malignancies) was challenged with either WT, AV1, or AV2 viruses and assayed for metabolic cell death 48 hr later. It is clear from Table 2A that WT VSV is able to infect and kill a wide range of cancer cell types, and furthermore, the majority of cancer cell lines tested demonstrated impaired responses to either IFN- α or IFN- β (Table 2B). AV1 and AV2 were as effective at killing these interferon nonresponsive tumor cell lines as WT VSV.

We previously reported the successful treatment of subcutaneous xenograft tumors in nude mice with WT VSV; however, in these experiments, exogenous interferon was required to protect the animals from succumbing to viral infection. Our results with the NCI cell panel suggest that AV1 and AV2 should efficiently kill tumor cells with little toxicity in mouse models even in the absence of interferon treatment, and therefore we conducted an extensive analysis of the *in vivo* oncolytic properties of the AV variants. In a first series of experiments, human ovarian carcinoma cells were injected into the peritoneal cavity of CD-1 nude mice and allowed to grow for 12 days. Mice (14/15) receiving UV-inactivated virus developed ascites by day 15 post-treatment. In contrast, three doses of AV2 delivered into the peritoneal cavity provided durable cures in 70% of the mice (Figure 4A). Remarkably, while a single therapeutic dose of WT VSV is uniformly lethal to nude mice (Stojdl et al., 2000b), none of the animals treated with three doses of AV2 exhibited even symptoms of virus infection.

Systemic treatment in immune-competent mouse models

Earlier preclinical, clinical, and mathematical modeling studies (Wein et al., 2003) predict that greatest anti-tumor efficacy is achieved when the delivered virus is distributed diffusely throughout the tumor (e.g., through tumor vasculature). Given that certain oncolytic viruses are rapidly inactivated in blood or inhibited by physical barriers (Ikeda et al., 2000; Wakimoto et al., 2002, 2003; Yoon et al., 2001), we felt it was important to determine the minimum VSV doses required to achieve effective delivery of VSV into tumor sites. For these studies, we engineered a VSV strain to express GFP during productive infections and examined subcutaneous tumors 24 hr after intravenous virus administration. Virus doses in the range of 10^8 – 10^9 pfu per mouse gave optimum tumor delivery (Figure 5). In other experiments and those shown below, we found that virus administered in this dose range also provided maximum therapeutic benefit to tumor-bearing animals. For example, subcutaneous tumors were established by injecting CT26 colon carcinoma cells into the hind flank of syngeneic Balb/c mice. Once tumors became palpable (approximately 10 mm³), virus was administered via tail vein injection. Twelve days post-treatment, mice receiving UV-inactivated VSV reached endpoint with an average tumor size of 750 mm³. In contrast, a single treatment with AV2 showed significant efficacy, delaying the time to endpoint by almost 3-fold (34 days). Of the eight animals in this treatment group, seven were considered partial responders while only one mouse did not respond to the treatment (data not shown). When multiple doses of AV1 or AV2 were given intravenously, the efficacy of the treatments was markedly increased (Figure 4B). With the exception of one animal, all tumors responded to treatment with AV1, with 3/6 mice showing complete tumor regression. Two of these mice showed complete regressions as early as day 8 and 9, respectively, post-infection. Two of the re-

Table 2A Mutant VSV strains are highly lytic on members of the NCI 60 panel of cancer cell lines

	WT		AV1		AV2	
		MOI		MOI		MOI
Leukemia	67% (4/6)*	0.13	nd		60% (3/5)	0.02
NSC lung carcinoma	78% (7/9)	0.02	60% (3/5)	0.001	75% (6/8)	0.19
Colon carcinoma	86% (6/7)	0.037	100% (5/5)	0.001	100% (6/6)	0.017
CNS	80% (4/5)	0.02	50% (1/2)	0.6	60% (3/5)	0.38
Melanoma	75% (6/8)	0.1	100% (2/2)	0.15	63% (5/8)	0.25
Ovarian carcinoma	100% (6/6)	0.3	67% (2/3)	0.0005	60% (3/5)	0.14
Renal carcinoma	88% (7/8)	0.24	100% (3/3)	0.14	100% (7/7)	0.48
Prostate	100% (2/2)	0.06	100% (2/2)	0.035	100% (2/2)	0.04
Breast	83% (5/6)	0.009	75% (3/4)	0.005	60% (3/5)	0.12
All cell lines tested	82% (47/57)	0.11	80% (21/26)	0.07	75% (38/51)	0.20

*Percent of NCI 60 panel cell lines by tumor type deemed highly sensitive to virus infection () denote the number of highly susceptible cell lines out of the number of cell lines tested. Cell line deemed highly susceptible if the $EC_{50} \leq$ MOI of 1 following a 48 hr infection. MOI represents average EC_{50} (MOI) of susceptible cell lines. nd = not determined.

maining animals showed partial responses, delaying tumor progression by almost 2-fold compared to controls. All eight AV2-infected mice responded well to treatment with five of eight developing durable tumor regressions. In fact, no sign of tumor regrowth was evident even 7 months post-treatment. Furthermore, these mice failed to produce tumors when rechallenged with CT26 cells 7 months post-treatment, with no trace of detectable virus, perhaps indicating that host-mediated immunity to the tumor had developed. All forms of intravenous treatment were well tolerated by the mice, with no mortalities occurring and minimal signs of morbidity. Infected mice had mild to medium piloerection, mild dehydration, and some transient body weight loss following the initial treatment (Figure 4C). These symptoms were only observed after the initial infection, and all subsequent doses failed to elicit any signs of infection.

Systemic administration of AV1 and AV2 is effective against disseminated disease

CT-26 cells, when injected into the tail vein, seed tumors throughout the mouse, although predominantly within the lungs. We examined the lungs of four mice 16 days after tumor cell injection and four days after treatment with UV-inactivated virus (Figure 4D). These lungs were three times their normal mass due to their tumor burden. In contrast, tumor-bearing littermates receiving a single intravenous or intranasal dose of AV2 4 days

prior to the time of sacrifice had lungs with normal mass and few obvious tumor nodules (Figure 4D). Consistent with this result, viral gene expression could be detected within 24 hr of a single intravenous dose of GFP-expressing AV3 in all tumor nodules, with little or no detectable expression in normal lung tissue (Figure 4D, inset).

Figure 4E shows the survival plots of mice seeded with lung tumors and then treated intranasally with UV-inactivated virus, AV1 or AV2. The mean time to death (MTD) of animals treated with UV-inactivated virus was approximately 20 days. However, mice treated with either AV1 or AV2 were completely protected. This experiment demonstrates the remarkable ability of AV1 and AV2 to produce durable cures in an aggressive, disseminated, immune-competent tumor model.

Discussion

A key difference between the attenuated viruses described here and previously reported oncolytic versions of VSV is the inability of mutant M proteins of the AV viruses to block interferon production in infected cells. VSV M is a multifunctional protein required for several key viral functions including budding (Jayakar et al., 2000), virion assembly (Newcomb et al., 1982), cytopathic effect (Blondel et al., 1990), and inhibition of host gene expression (Lyles et al., 1996). The latter property has been attributed to the ability of M to block host RNA polymerase activity (Ahmed et al., 2003; Yuan et al., 2001) or to inhibit the nuclear transport of both proteins and mRNAs into and out of the host nucleus (Her et al., 1997; von Kobbe et al., 2000). The results presented here using virus infection are consistent with blocks in nuclear transport being the major mechanism by which wild-type VSV strains mitigate host antiviral response. Our analysis of infected cell transcripts provided little evidence to support a role for M protein in inhibiting host cell transcription but rather shows that VSV infection triggers an IRF-3-mediated stimulation of antiviral genes followed by an M protein-mediated block of transport of primary response transcripts from infected cell nuclei. Particularly germane to this study is the work from Dahlberg's group (Petersen et al., 2000) and others (von Kobbe et al., 2000) that has shown, by transfection studies, that M protein can associate with nuclear pore proteins and effect a block in mRNA export possibly through an association with the

Table 2B The majority of cell lines in the NCI 60 cell panel show IFN defects

	Type I IFN defects
Leukemia	100% (6/6)*
NSC Lung carcinoma	71% (5/7)
Colon carcinoma	100% (7/7)
CNS	75% (3/4)
Melanoma	85% (6/7)
Ovarian carcinoma	67% (4/6)
Renal carcinoma	75% (6/8)
Prostate	100% (2/2)
Breast	60% (3/5)
All cell lines tested	81% (42/52)

*Denotes the number of cells in each group which were unresponsive to either IFN α or IFN β pre-treatment. Cell line deemed unresponsive if IFN pre-treatment was unable to significantly affect (<10 fold) the EC_{50} of cells infected with WT VSV for 48 hr.

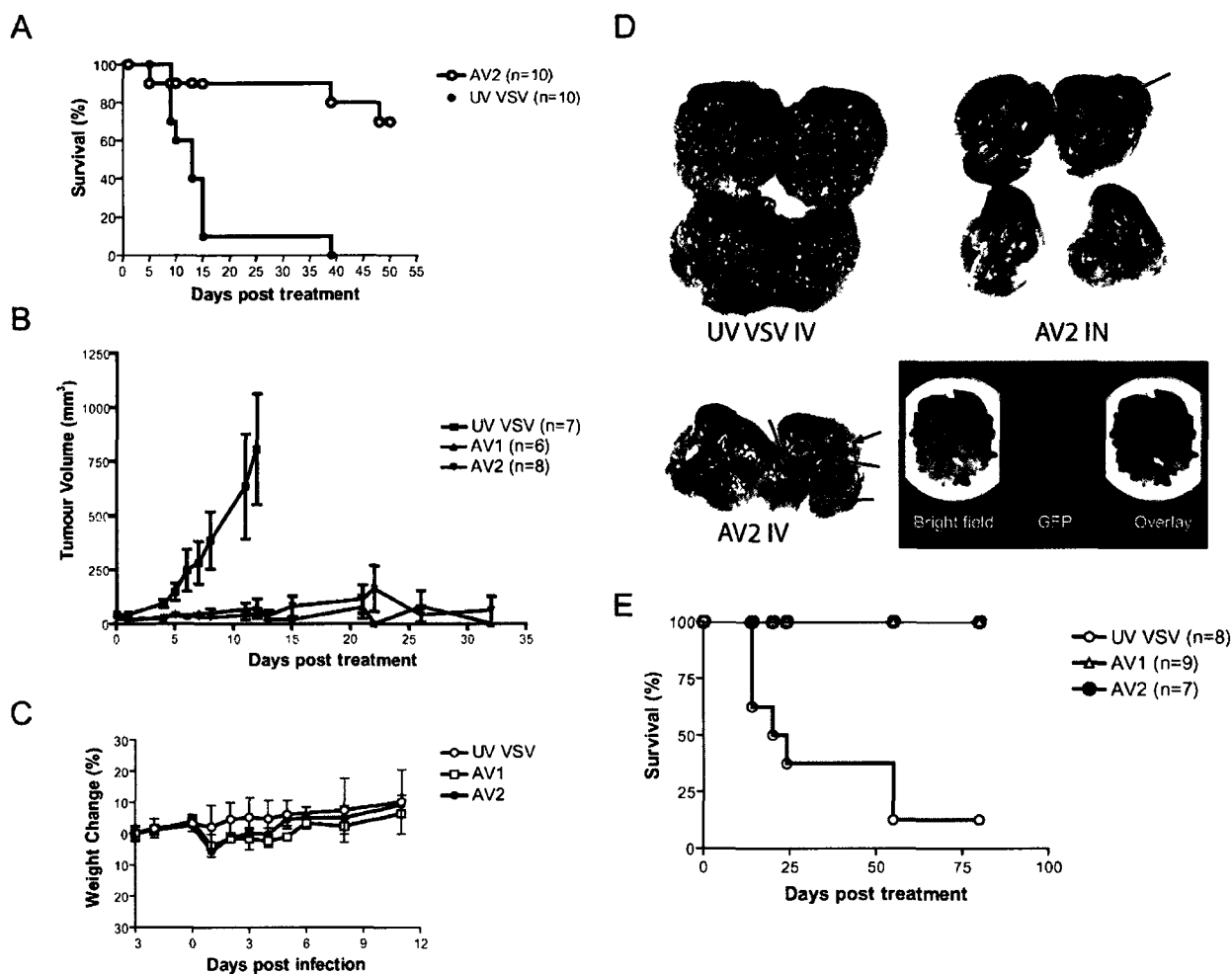


Figure 4. AV strains are efficacious in mouse tumor models

A: AV2 is effective in treating human ovarian tumor xenografts. 1×10^6 human ES-2 ovarian carcinoma cells were injected into the intraperitoneal cavity of CD-1 nude mice. Twelve days later, animals were treated by intraperitoneal injection every other day with either AV2 or UV-inactivated AV2 (1×10^8 pfu/dose, three doses total). Animals were assessed for morbidity and mortality and euthanized following the appearance of moderate ascites formation. "n" denotes number of animals per group.

B: Intravenous treatment of subcutaneous tumors. Tumors were established in the hind flank of Balb/C mice by injecting 1×10^6 CT26 cells. When tumors reached approximately 10 mm^3 , mice were treated every other day for 10 days (six doses total) with an intravenous injection of 5×10^8 pfu of the indicated virus. Control mice received six doses of 5×10^8 pfu equivalents of UV-inactivated AV2 VSV. Tumors were measured daily to calculate tumor volumes and animals were euthanized when tumors reached approximately 750 mm^3 . Error bars denote SEM.

C: Mouse weights measured daily, for each treated group, for the 3 days before treatment to day 11 post-treatment. Error bars denote SEM.

D: Treatment of disseminated lung tumors. Lung tumors were established by injecting 3×10^5 CT26 cells into the tail vein of Balb/C mice. On day 12, mice were treated as follows: UVAV2 IV = 1 dose intravenously (5×10^8 pfu equivalents), AV2 IV = 1 dose AV2 intravenously (5×10^8 pfu), AV2 IN = 1 dose of AV2 intranasally (5×10^7 pfu). Four days after treatment, all mice were sacrificed and their lungs were removed (hearts are visible for scale). Arrows indicate residual tumors. Inset: mice bearing CT-26 lung tumors were infected with AV3 GFP, and the lungs were removed and visualized as indicated.

E: Lung tumors were established as described above. On day 12, mice received 5×10^7 pfu of AV1 or AV2 by intranasal instillation every other day for 2 weeks (six doses total). "n" denotes number of mice in treatment group.

interferon-inducible cellular gene product Nup98. Indeed others have suggested that overexpression of Nup98 following interferon treatment may be sufficient to overcome an M-induced block of mRNA export. Interestingly, when we compared transcript levels in nuclear and cytoplasmic fractions following virus infection, we detected that nuclear export defects were more pronounced on some transcripts than others (D.F.S. and J.C.B., data not shown), which may reflect that the M-induced block may be specific for a subset of transcripts. It is interesting to

note that in yeast, specific mRNA export factors (Yra1 and Mex67) have been shown to be responsible for the transport of different groups of transcripts (Hieronymus and Silver, 2003). Yra1 exports transcripts depending upon their rate of transcription whereas the Mex67 export protein does not discriminate on this basis (Hieronymus and Silver, 2003). Perhaps M protein in conjunction with Nup98 is targeting a specific set of proteins involved in the regulation of export of a subset of nuclear transcripts.

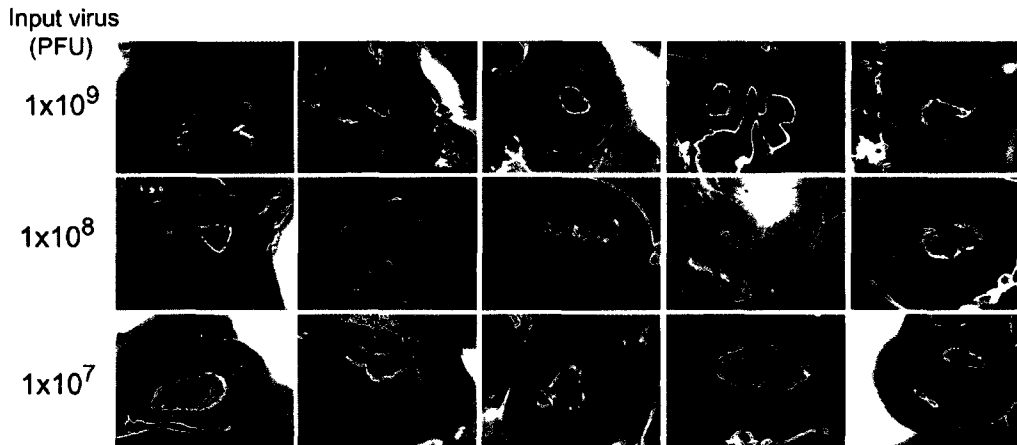


Figure 5 Threshold dose required for systemic delivery to subcutaneous tumors

Balb/C mice bearing CT26 subcutaneous tumors were treated with AV3 GFP intravenously at the indicated dose. At 24 hr tumors were examined for fluorescence under a dissecting microscope. Tumors are shown in black and white, overlaid with fluorescent image.

It appears that host cell antiviral programs are initiated by activation of the latent transcription factors NF κ B, c-JUN/ATF2, and IRF-3. Upon viral entry into the host cell, the transcription factors c-JUN and IRF-3 are phosphorylated by JNK and a recently identified virally activated kinase (Sharma et al., 2003), while NF κ B is released from its inhibitor I κ B through the action of upstream IKK(s) (DiDonato et al., 1997). The activated transcription factors translocate to the nucleus and coordinately form an enhancer complex at the *IFN*- β promoter, leading to *IFN*- β induction (Wathelet et al., 1998). Here we refer to this as the primary transcriptional response to virus infection. We and others (Levy, 2002; Sato et al., 1998a) postulate that a secondary transcriptional wave (or positive feedback loop; Levy, 2002) is triggered by the *IFN*- β -dependent induction of a variety of interferon-stimulated genes. The data presented here with wild-type M protein help to delineate the distinction between these primary and secondary transcriptional events as well as identify several novel viral response genes (*GADD34*, *PUMA*). Following infection with viruses harboring mutant M proteins, it becomes clear that autocrine stimulation of the JAK/STAT signaling pathway by *IFN*- β leads to the production of secondary response genes like *IRF-7*, which in turn are critical for the tertiary induction of *IFN*- α genes (Morin et al., 2002). Indeed the M protein block of secondary and tertiary transcripts can be overcome by expressing a constitutively active version of *IRF-7* (from a viral promoter) even in the presence of wild-type M protein. While our cell culture studies clearly delineate the role of VSV M in blunting the positive feedback loop that is dependent upon production of *IFN*- β and a functional interferon receptor, WT VSV infection still is capable of inducing interferon in intact animals (albeit more slowly and to lower levels). Others have shown that in virus-infected animals, an *IFN*- β -independent, systemic induction of interferon can occur in certain dendritic cell subsets; however, it is the local *IFN*- β -dependent production of interferon that is critical in determining the magnitude and ultimate success of an interferon-mediated antiviral response (Barchet et al., 2002). We show that the amount of interferon and the timing of its production in WT VSV-infected animals are

not sufficient to protect against lethal infections. The results presented here and elsewhere (Barchet et al., 2002) are consistent with the idea that the rapid and robust local stimulation of interferon by AV strains in mice successfully attenuates virus replication in normal tissues (even of WT VSV, see Figure 1F). Our data indicates that defects in interferon signaling frequently occur during tumor evolution, with a majority of the cell lines in the NCI panel having an impaired response. Accumulating data have indicated that interferon is a multifunctional cytokine that can coordinately regulate cell growth, apoptosis, and antiviral pathways. Perhaps during tumor evolution, the selection for relentless growth and loss of apoptosis outstrips the occasional need for antiviral activity.

Kirn and colleagues argue that several factors are important in tumor killing by oncolytic virus therapeutics, including the effective delivery to multiple sites within the tumor, evasion of acquired and innate immunity, and rapid virus growth and spread (Wein et al., 2003). We have found that intravenous administration of VSV is an effective means of delivering virus to multiple sites within the tumor, and because of its broad tissue tropism and short replicative cycle, VSV can rapidly grow and spread within the tumor. These same traits, however, can be a lethal combination if virus growth in normal tissues is unchecked (Figures 1B and 1C). The attenuated viruses described here provide the best of both worlds; they grow rapidly in a broad spectrum of tumor cells but, because of their ability to trigger antiviral responses in normal cells, may be exceptionally safe to the treated animal.

One concern about the use of oncolytic virus therapeutics is the idea that a virulent strain could arise during virus propagation in a tumor. It is of interest to note, however, that it has proven impossible to date to select for VSV variants that are resistant to the antiviral effects of interferon (Novella et al., 1996), and we have shown that *IFN*-inducing mutants protect the host against infection with WT VSV (Figure 1F). Others have found that M mutations of the type described here cannot be complemented by mutations in other parts of M or other VSV genes (Coulon et al., 1990). In other words, only true revertants that

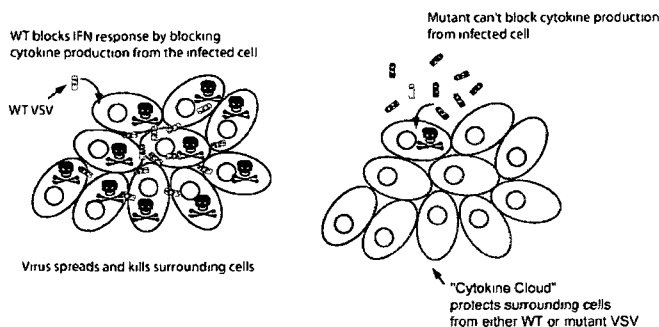


Figure 6 Model depicting how mutant VSV strains protect against virus spread

A WT VSV blocks IFN production from infected cells. Uninfected cells are not protected from virus spread.
B VSV strains defective in blocking nuclear/cytoplasmic mRNA export potently induce a "cytokine cloud" of antiviral cytokines (e.g., IFNs) protecting neighboring cells from virus spread.

convert arginine 51 back to methionine 51 can restore mutant M back to the wild-type phenotype. One of the viruses we have used in this work is a complete deletion of methionine 51, making the possibility of reversion to wild-type, even following several rounds of replication, remote. We speculate that in any population of interferon-responsive viruses where the majority of particles are potent inducers of interferon, it is unlikely that a wild-type variant could rise to dominance. The resulting "cytokine cloud" produced by infection with the IFN-inducing virus would protect the normal tissues of the host from the more virulent WT strain (Figure 6). Tumor killing would, however, be unaffected, as we have shown the majority of malignancies to be defective in responding to such a "cytokine cloud." We suggest that oncolytic viruses that trigger but do not disable antiviral responses will have a significantly improved therapeutic index over viruses that lack this property.

Experimental procedures

Viruses

The Indiana serotype of VSV was used throughout this study and was propagated in Vero cells T1026R (Desforges et al., 2001) and TP3 (Desforges et al., 2001), herein referred to as AV1 and AV2, respectively, were shown in this study and elsewhere to be IFN-inducing mutants of the HR strain of wild-type VSV Indiana (Francoeur et al., 1987). WT GFP and AV3 GFP are recombinant viruses rescued from plasmids described below. The rescue procedure has been described in detail elsewhere (Lawson et al., 1995).

Constructs and viral rescue

Creation of the constitutively active IRF-7 Δ (IRF-7 Δ 247–467) has been previously described elsewhere (Lin et al., 2000). IRF-7 Δ 247–467 was amplified by PCR using a forward primer to the Flag epitope with an additional 5' VSV cap signal and an Xho1 linker (ATCGCTCGAGAACAGATGACTA CAAAGACGATGACGACAAG), together with a specific IRF-7 reverse primer containing a VSV poly A signal and an Nhe1 linker (ATCGGCTAGCAGTTTTT TTCAGGGATCCAGCTCTAGGTGG GCTGC). The PCR fragment was then cloned into the Xho1 and Nhe1 sites of the rVSV replicon vector pVSV-XN2 (provided by John Rose). Recovery of rVSV has been previously described (Lawson et al., 1995).

AV3 GFP is a recombinant virus with a deletion of methionine 51 in the M protein, as well as an extra cistron-encoding green fluorescent protein (GFP) inserted between the G and L sequences. Using T4 RNA ligase, an oligonucleotide containing a consensus T7 polymerase sequence was li-

gated to the single-stranded RNA genome of the HR strain of VSV. Reverse transcription coupled PCR was used to clone the entire genome as fragments into the pBluescript II SK+ vector (Stratagene). The PCR primers were designed in such a manner as to introduce unique restriction endonuclease sites between each of the five viral cistrons. Ligation of these fragments resulted in the construction of a full-length positive sense copy of the HR VSV genome with a T7 promoter sequence at the 5' end of this anti-genome. Two overlapping oligonucleotides were synthesized to correspond to the hepatitis delta virus ribozyme sequence such that an Xho1 site was introduced at the 3' terminus of the ribozyme to facilitate further cloning. These oligos were annealed and extended using Klenow to form a blunt-ended double-stranded DNA fragment. A 300 bp fragment from the 3' terminus of the anti-genome was PCR amplified and blunt end cloned to the ribozyme fragment. This fragment was subsequently cloned into the full-length genome construct described above via an internal AflIII site in the 3' terminus of the viral genome, and the Xho1 site engineered into the ribozyme fragment. Finally, the T7 terminator sequence was cloned into this vector using the flanking Xho1 and BssHII sites. This plasmid was designated pDSV1. To generate AV3VSV, we removed a Xho1/KpnI fragment spanning a region from within the P gene to within the G gene of pDSV1, replacing a similar fragment from within pXN, yielding the plasmid pXNDG. This facilitated the exchange of the M cistron from pXNDG, with one previously mutated by deleting the codon for methionine at position 51 in the amino acid sequence using directed mutagenesis (Quickchange XL, Stratagene). Subsequently, the GFP coding sequence was removed from pEGFP (Clontech) by digesting with Xho1 and Xba1 and ligated into Xho1 and Nhe1 sites downstream of the additional stop/start sequence in the pXNDG vector.

WT GFP VSV was constructed by inserting the coding region of GFP from pEGFP (Clontech) between the Xho1 and Nhe1 sites in the pXN vector (provided by John Rose).

IFN ELISA

Interferon- α levels were measured using a Human Interferon-Alpha ELISA kit (PBL Biomedical) per manufacturer's directions. Various cell lines were infected with either WT VSV or AV1 or AV2 VSVs at an MOI of 10. One hundred microliters of culture medium was collected at 48 hr post-infection and incubated in a 96-well microtiter plate along with standards supplied by manufacturer. IFN- β production was measured at 10 hr post-infection using a human IFN- β detection kit (TFB INC, Tokyo, Japan). Samples were processed as per manufacturer's instructions and then read on a DYNEX plate reader at primary wavelength of 450 nm with a reference wavelength of 630 nm.

A variation of the above assay was used to determine the impact of IFN- β on IFN- α production. Briefly, 24-well plates of OVCAR-4 cells were either mock infected or infected with WT GFP VSV or AV3 GFP VSV at an MOI of 5 for 30 min. These wells were then washed with PBS and fed with OptiMEM (Invitrogen) or OptiMEM supplemented with various concentrations of antibody as indicated. To neutralize IFN- β in the media, an anti-IFN- β antibody was used (AHC4024, Biosource International), and as a nonspecific control, an anti-HA antibody was used (sc-805, Santa Cruz). Twenty-two hours post-infection, 100 μ l of media from each well was assayed for IFN- α production using a Human IFN- α ELISA (PBL Biomedical) kit as described.

Mouse serum IFN- α levels were assayed using a mouse Interferon-Alpha ELISA kit (PBL Biomedical). Balb/C females (10 weeks old, Charles River) were injected intravenously with either PBS or 1×10^8 pfu of WT GFP or AV3 GFP diluted in PBS. At the indicated times post-infection, blood was collected from the saphenous vein of each mouse into heparinized tubes and centrifuged to obtain serum. For each sample, 5 μ l of serum was diluted in 95 μ l of PBS and assayed as per manufacturer's instructions.

Determination of in vivo toxicity of VSV mutant viruses

Eight- to ten-week-old female mice (strains as indicated, Charles River) were divided into groups of five and infected with dilutions of virus from 1×10^{10} pfu to 1×10^2 pfu by the indicated route. Animals were monitored for weight loss, dehydration, piloerection, huddling behavior, respiratory distress, and hind limb paralysis. Mice showing moderate to severe morbidity were euthanized as per good laboratory practices prescribed by the CCAS. Lethal dose 50 values were calculated by the Karber-Spearman method.

Four-week-old Balb/C mice or Balb/C interferon- α receptor knockout

mice (IFNAR^{-/-}) (Steinhoff et al., 1995) were infected intranasally with 10⁴ pfu of either WT VSV, AV1, or AV2. Mice were monitored for signs of morbidity and were euthanized upon signs of severe respiratory distress.

Determination of in vivo toxicity of mixed samples of WT and mutant VSV strains

Groups of three mice were infected by intranasal instillation with either WT, AV2, or mixtures of these strains as indicated. Mice were monitored for signs of morbidity and were euthanized upon signs of severe respiratory distress or hind limb paralysis.

MTS assay

In each experiment, the test cell line was seeded into 96-well plates at 3 × 10⁴ cells/well in growth medium (DMEM-F12-HAM + 10% FBS; Invitrogen). Following overnight incubation (37°C, 5% CO₂), media were removed by aspiration and to each well was added 20 μl of virus-containing media (α-MEM, no serum) ranging in 10-fold increments from 3 × 10⁶ pfu/well to 3 pfu/well or negative control media containing no virus. Each virus dose tested was done in replicates of six. After a 60 min incubation to allow virus attachment, 80 μl of growth medium was added to each well, and the plates were incubated for another 48 hr. Cell viability was measured using the CellTiter 96 AQueous MTS reagent (Promega).

To assay for IFN defects, cell lines were pretreated with either 5 units/ml of IFN-α (Schering) or IFN-β (PBL Biomedical) for 12 hr and then challenged with a range of doses of WT VSV as described above. A standard MTS assay was performed and the results compared from nonpretreated cells.

Microarray

OVCAR4 cells either mock treated or infected with WT and AV strains were harvested in PBS, pelleted, and resuspended in 250 μl of resuspension buffer (10 mM Tris [pH 7.4], 15 mM NaCl, 12.5 mM MgCl₂). Six hundred microliters of Lysis buffer (25 mM Tris [pH 7.4], 15 mM NaCl, 12.5 mM MgCl₂, 5% sucrose, and 1% NP-40) was added and the lysates were incubated at 4°C for 10 min with occasional vortexing. Nuclei were collected by centrifugation at 1000 × g for 3 min. The supernatant (cytoplasmic fraction) was collected and frozen at -80°C while the pellet (nuclear fraction) was washed once with 250 μl of lysis buffer and frozen. Total RNA was isolated from both nuclear and cytoplasmic fractions using the Qiagen RNeasy kit (as per manufacturer's instructions; Qiagen) followed by LiCl precipitation to concentrate each sample. Twenty micrograms of each RNA sample was processed according to manufacturer's standard protocol (Affymetrix) and hybridized to an Affymetrix HGA133u A chip. Each chip was scaled to 1500, normalized to the 100 normalization control genes present on each chip, then all nuclear samples were normalized to the mock nuclear sample on a per gene basis, while the cytoplasmic fractions were normalized to the corresponding mock cytoplasmic sample. Data were analyzed using GeneSpring software (SiliconGenetics).

Western blotting

OVCAR4 cells were grown in RPMI (Wisent) supplemented with 10% fetal bovine serum (Wisent). 1 × 10⁷ cells were plated in 10 cm dishes the day prior to infection. For infection, the media were removed and replaced with RPMI alone prior to the addition of 5 × 10⁷ pfu per VSV viral strain. One hour after virus addition, media were removed and replaced with RPMI supplemented with 10% FBS for the remaining duration of the experiment. Cells were lysed in standard NP-40 lysis buffer, and 75 μg of whole-cell extract was run on SDS-polyacrylamide gel and blotted with the following antibodies as indicated: IRF-7 (sc-9083; Santa Cruz), IRF-3 (sc-9082, Santa Cruz), ISG56 (a gift from Ganes Sen), VSV-N (polyclonal directed against the full-length Indiana N protein), and Actin (sc-8432; Santa Cruz).

Quantitative PCR of Interferon-β mRNA

Nuclear and cytoplasmic total RNA from infected or mock-infected OVCAR4 cells was isolated as per manufacturer's instruction (RNeasy; Qiagen). Four micrograms of total RNA was DNase treated and reverse transcribed. Quantitative PCR was performed in triplicate to amplify IFN-β and HPRT targets from each using Roche Lightcycler technology (Roche Diagnostics). Crossing points were converted to absolute quantities based on standard curves generated for each target amplicon. IFN-β signal was subsequently normalized to HPRT as HPRT levels are unchanged during the course of these

infections (data not shown). Primers used to amplify IFN-β were sense 5'-TTGTGCTTCTCCACTACAGC-3', antisense 5'-CTGTAAGTCTGTTAATGAAG-3' and HPRT primers were sense 5'-TGACACTGGCAAAACAA TGCA-3', antisense 5'-GGTCCTTTTCACCAGCAAGCT-3'.

RT-PCR of interferon-α and interferon-stimulated genes

A549 cells cultured in F12K medium supplemented with 10% FBS were infected with WT or AV strains (MOI 10). RNA was extracted 4 hr post-infection using Trizol (Invitrogen) according to the manufacturer's instructions. One microgram of RNA was reverse transcribed with Oligo dT primers and 5% of RT was used as template in a Taq PCR. Primers used were as follows. Mx forward primer 5'-TTTGTGTTCCGAAGTGGAC-3' and reverse primer 5'-TTTCTTCAGTTTCAGCACCAG-3'; VSV N forward primer 5'-ATGTCTGTTACAGTCAAGAGAATC-3' and reverse primer 5'-TCATTTGTCAAATTCGACTTAGCATA-3', RANTES forward primer 5'-TACACCAGTGCAAGTGCTCCAACCCAG-3' and reverse primer 5'-GTCTCGAACTCCTGACCTCAAGTGATCC-3', β-actin forward primer 5'-ACAATGAGCTGCTGGTGGCT-3' and reverse primer 5'-GATGGGCACAGTGGTGGTA-3'.

Ovarian xenograft cancer model in athymic mice

Approximately 1 × 10⁶ ES-2 human ovarian carcinoma cells were injected into the peritoneal cavity of CD-1 athymic mice (Charles River). Ascites development is generally observed by day 15 after cell injection. On days 12, 14, and 16, mice were treated with 1 × 10⁶ AV2 virus or 1 × 10⁶ pfu equivalent of UV-inactivated AV2 VSV by intraperitoneal injection. Mice were monitored for morbidity and euthanized upon development of ascites.

Subcutaneous tumor model

To establish subcutaneous tumors, 8- to 10-week-old Balb/C female mice (Charles River) were shaved on the right flank and injected with 1 × 10⁶ CT26 colon carcinoma cells (Kashtan et al., 1992) syngeneic for Balb/C mice. These tumors were allowed to develop until they reached approximately 10 mm³, at which time virus treatments were initiated. Groups of animals received 1 of 6 doses of the indicated virus every other day for 2 weeks. Each dose of 5 × 10⁶ pfu was administered by tail vein infection. Tumors were measured daily and volumes calculated using the formula 1/2(L*W*H). Mice were weighed daily and monitored for weight loss, dehydration, piloerection, huddling behavior, respiratory distress, and hind limb paralysis. Animals were euthanized when their tumor burden reached end point (750 mm³).

Lung model

Lung tumors were established in 8- to 10-week-old female Balb/C mice (Charles River) by tail vein injection of 3 × 10⁵ CT26 cells (Specht et al., 1997). On days 10, 12, 14, 17, 19, and 21, groups of mice received 5 × 10⁷ pfu of the indicated virus by intranasal instillation as described elsewhere (Stojdl et al., 2000a). Mice were weighed daily and monitored for weight loss, dehydration, piloerection, huddling behavior, respiratory distress, and hind limb paralysis. Animals were euthanized at the onset of respiratory distress and their lungs examined to confirm tumor development.

Visualization of GFP-expressing VSV strains in vivo

Female Balb/c mice (Charles River) were injected with 3 × 10⁵ CT26 cells via the vein to initiate pulmonary metastases. On day 17, mice were injected intravenously with 2.5 × 10⁶ pfu AV3 GFP VSV. Hind limb tumors were seeded by subcutaneous injection with 3 × 10⁵ CT26 cells. When tumors reached a volume of approximately 400 mm³, mice were injected intravenously with 2.5 × 10⁶ pfu of AV3 GFP VSV. At the indicated times, mice were euthanized and tumors examined using a Leica MZFLIII microscope with a standard GFP filter set. Pictures were captured with a Nikon Coolpix 100 camera. Overlaid images were generated using Adobe Photoshop 7.0.

Acknowledgments

B.D.L. is a recipient of a fellowship from the National Cancer Institute of Canada (NCIC). This work was funded by grants from the NCIC and the Canadian Institutes of Health Research awarded to J.C.B. Funding for portions of this work was also provided by Wellstat Biologics Corporation. J.C.B. is Senior Scientist of Cancer Care Ontario. We thank John Rose for plasmids required to produce recombinant VSVs and Ken Garson for critical reading of the manuscript.

Received April 15, 2003
 Revised July 31, 2003
 Published October 20, 2003

References

- Ahmed, M., McKenzie, M.O., Puckett, S., Hojnacki, M., Poliquin, L., and Lyles, D.S. (2003). Ability of the matrix protein of vesicular stomatitis virus to suppress beta interferon gene expression is genetically correlated with the inhibition of host RNA and protein synthesis. *J. Virol.* **77**, 4646–4657.
- Balachandran, S., and Barber, G.N. (2000). Vesicular stomatitis virus (VSV) therapy of tumors. *IUBMB Life* **50**, 135–138.
- Balachandran, S., Roberts, P.C., Brown, L.E., Truong, H., Pattnaik, A.K., Archer, D.R., and Barber, G.N. (2000). Essential role for the dsRNA-dependent protein kinase PKR in innate immunity to viral infection. *Immunity* **13**, 129–141.
- Barchet, W., Cella, M., Odermatt, B., Asselin-Paturel, C., Colonna, M., and Kalinke, U. (2002). Virus-induced interferon alpha production by a dendritic cell subset in the absence of feedback signaling in vivo. *J. Exp. Med.* **195**, 507–516.
- Bell, J.C., Garson, K.A., Lichty, B.D., and Stojdl, D.F. (2002). Oncolytic viruses: programmable tumour hunters. *Curr. Gene Ther.* **2**, 243–254.
- Bello, M.J., de Campos, J.M., Kusak, M.E., Vaquero, J., Sarasa, J.L., Pestana, A., and Rey, J.A. (1994). Molecular analysis of genomic abnormalities in human gliomas. *Cancer Genet. Cytogenet.* **73**, 122–129.
- Blondel, D., Harmison, G.G., and Schubert, M. (1990). Role of matrix protein in cytopathogenesis of vesicular stomatitis virus. *J. Virol.* **64**, 1716–1725.
- Coulon, P., Deutsch, V., Lafay, F., Martinet-Edelist, C., Wyers, F., Herman, R.C., and Flamand, A. (1990). Genetic evidence for multiple functions of the matrix protein of vesicular stomatitis virus. *J. Gen. Virol.* **71**, 991–996.
- Desforges, M., Charron, J., Berard, S., Beausoleil, S., Stojdl, D.F., Despars, G., Laverdiere, B., Bell, J.C., Talbot, P.J., Stanners, C.P., and Poliquin, L. (2001). Different host-cell shutoff strategies related to the matrix protein lead to persistence of vesicular stomatitis virus mutants on fibroblast cells. *Virus Res.* **76**, 87–102.
- DiDonato, J.A., Hayakawa, M., Rothwarf, D.M., Zandi, E., and Karin, M. (1997). A cytokine-responsive I κ B kinase that activates the transcription factor NF- κ B. *Nature* **388**, 548–554.
- Ferran, M.C., and Lucas-Lenard, J.M. (1997). The vesicular stomatitis virus matrix protein inhibits transcription from the human beta interferon promoter. *J. Virol.* **71**, 371–377.
- Francoeur, A.M., Poliquin, L., and Stanners, C.P. (1987). The isolation of interferon-inducing mutants of vesicular stomatitis virus with altered viral P function for the inhibition of total protein synthesis. *Virology* **160**, 236–245.
- Genin, P., Algarte, M., Roof, P., Lin, R., and Hiscott, J. (2000). Regulation of RANTES chemokine gene expression requires cooperativity between NF- κ B and IFN-regulatory factor transcription factors. *J. Immunol.* **164**, 5352–5361.
- Gromeier, M., and Wimmer, E. (2001). Viruses for the treatment of malignant glioma. *Curr. Opin. Mol. Ther.* **3**, 503–508.
- Hawkins, L.K., Lemoine, N.R., and Kirn, D. (2002). Oncolytic biotechnology: a novel therapeutic platform. *Lancet Oncol.* **3**, 17–26.
- Her, L.S., Lund, E., and Dahlberg, J.E. (1997). Inhibition of Ran guanosine triphosphatase-dependent nuclear transport by the matrix protein of vesicular stomatitis virus. *Science* **276**, 1845–1848.
- Hieronymus, H., and Silver, P.A. (2003). Genome-wide analysis of RNA-protein interactions illustrates specificity of the mRNA export machinery. *Nat. Genet.* **33**, 155–161.
- Huneycutt, B.S., Bi, Z., Aoki, C.J., and Reiss, C.S. (1993). Central neuropathogenesis of vesicular stomatitis virus infection of immunodeficient mice. *J. Virol.* **67**, 6698–6706.
- Ikedo, K., Wakimoto, H., Ichikawa, T., Jung, S., Hochberg, F.H., Louis, D.N., and Chiocca, E.A. (2000). Complement depletion facilitates the infection of multiple brain tumors by an intravascular, replication-conditional herpes simplex virus mutant. *J. Virol.* **74**, 4765–4775.
- Jayakar, H.R., Murti, K.G., and Whitt, M.A. (2000). Mutations in the PPPY motif of vesicular stomatitis virus matrix protein reduce virus budding by inhibiting a late step in virion release. *J. Virol.* **74**, 9818–9827.
- Kashtan, H., Rabau, M., Mullen, J.B., Wong, A.H., Roder, J.C., Shpitz, B., Stern, H.S., and Gallinger, S. (1992). Intra-rectal injection of tumour cells: a novel animal model of rectal cancer. *Surg. Oncol.* **1**, 251–256.
- Kruyt, F.A., and Curiel, D.T. (2002). Toward a new generation of conditionally replicating adenoviruses: pairing tumor selectivity with maximal oncolysis. *Hum. Gene Ther.* **13**, 485–495.
- Lawson, N.D., Stillman, E.A., Whitt, M.A., and Rose, J.K. (1995). Recombinant vesicular stomatitis viruses from DNA. *Proc. Natl. Acad. Sci. USA* **92**, 4477–4481.
- Levy, D.E. (2002). Whence interferon? Variety in the production of interferon in response to viral infection. *J. Exp. Med.* **195**, F15–F18.
- Lin, R., Mamane, Y., and Hiscott, J. (2000). Multiple regulatory domains control IRF-7 activity in response to virus infection. *J. Biol. Chem.* **275**, 34320–34327.
- Linge, C., Gewert, D., Rossmann, C., Bishop, J.A., and Crowe, J.S. (1995). Interferon system defects in human malignant melanoma. *Cancer Res.* **55**, 4099–4104.
- Lu, R., Au, W.C., Yeow, W.S., Hageman, N., and Pritha, P.M. (2000). Regulation of the promoter activity of interferon regulatory factor-7 gene. Activation by interferon and silencing by hypermethylation. *J. Biol. Chem.* **275**, 31805–31812.
- Lyles, D.S., McKenzie, M.O., Ahmed, M., and Woolwine, S.C. (1996). Potency of wild-type and temperature-sensitive vesicular stomatitis virus matrix protein in the inhibition of host-directed gene expression. *Virology* **225**, 172–180.
- Matin, S.F., Rackley, R.R., Sadhukhan, P.C., Kim, M.S., Novick, A.C., and Bandyopadhyay, S.K. (2001). Impaired alpha-interferon signaling in transitional cell carcinoma: lack of p48 expression in 5637 cells. *Cancer Res.* **61**, 2261–2266.
- Morin, P., Braganca, J., Bandu, M.T., Lin, R., Hiscott, J., Doly, J., and Civas, A. (2002). Preferential binding sites for interferon regulatory factors 3 and 7 involved in interferon-A gene transcription. *J. Mol. Biol.* **316**, 1009–1022.
- Nakaya, T., Sato, M., Hata, N., Asagiri, M., Suemori, H., Noguchi, S., Tanaka, N., and Taniguchi, T. (2001). Gene induction pathways mediated by distinct IRFs during viral infection. *Biochem. Biophys. Res. Commun.* **283**, 1150–1156.
- Newcomb, W.W., Tobin, G.J., McGowan, J.J., and Brown, J.C. (1982). In vitro reassembly of vesicular stomatitis virus skeletons. *J. Virol.* **41**, 1055–1062.
- Norman, K.L., Farassati, F., and Lee, P.W. (2001). Oncolytic viruses and cancer therapy. *Cytokine Growth Factor Rev.* **12**, 271–282.
- Novella, I.S., Cilnis, M., Elena, S.F., Kohn, J., Moya, A., Domingo, E., and Holland, J.J. (1996). Large-population passages of vesicular stomatitis virus in interferon-treated cells select variants of only limited resistance. *J. Virol.* **70**, 6414–6417.
- Petersen, J.M., Her, L.S., Varvel, V., Lund, E., and Dahlberg, J.E. (2000). The matrix protein of vesicular stomatitis virus inhibits nucleocytoplasmic transport when it is in the nucleus and associated with nuclear pore complexes. *Mol. Cell. Biol.* **20**, 8590–8601.
- Sato, M., Hata, N., Asagiri, M., Nakaya, T., Taniguchi, T., and Tanaka, N. (1998a). Positive feedback regulation of type I IFN genes by the IFN-inducible transcription factor IRF-7. *FEBS Lett.* **441**, 106–110.
- Sato, M., Tanaka, N., Hata, N., Oda, E., and Taniguchi, T. (1998b). Involvement of the IRF family transcription factor IRF-3 in virus-induced activation of the IFN-beta gene. *FEBS Lett.* **425**, 112–116.
- Sharma, S., tenOever, B.R., Grandvaux, N., Zhou, G.P., Lin, R., and Hiscott, J. (2003). Triggering the interferon antiviral response through an IKK-related pathway. *Science* **300**, 1148–1151.

- Specht, J.M., Wang, G., Do, M.T., Lam, J.S., Royal, R.E., Reeves, M.E., Rosenberg, S.A., and Hwu, P. (1997). Dendritic cells retrovirally transduced with a model antigen gene are therapeutically effective against established pulmonary metastases. *J. Exp. Med.* *186*, 1213–1221.
- Steinhoff, U., Muller, U., Schertler, A., Hengartner, H., Aguet, M., and Zinkernagel, R.M. (1995). Antiviral protection by vesicular stomatitis virus-specific antibodies in alpha/beta interferon receptor-deficient mice. *J. Virol.* *69*, 2153–2158.
- Stojdl, D.F., Abraham, N., Knowles, S., Marius, R., Brasey, A., Lichty, B.D., Brown, E.G., Sonenberg, N., and Bell, J.C. (2000a). The murine double-stranded RNA-dependent protein kinase PKR is required for resistance to vesicular stomatitis virus. *J. Virol.* *74*, 9580–9585.
- Stojdl, D.F., Lichty, B., Knowles, S., Marius, R., Atkins, H., Sonenberg, N., and Bell, J.C. (2000b). Exploiting tumor-specific defects in the interferon pathway with a previously unknown oncolytic virus. *Nat. Med.* *6*, 821–825.
- Sun, W.H., Pabon, C., Alsayed, Y., Huang, P.P., Jandeska, S., Uddin, S., Platanias, L.C., and Rosen, S.T. (1998). Interferon-alpha resistance in a cutaneous T-cell lymphoma cell line is associated with lack of STAT1 expression. *Blood* *91*, 570–576.
- Terstegen, L., Gatsios, P., Ludwig, S., Pleschka, S., Jahnen-Dechent, W., Heinrich, P.C., and Graeve, L. (2001). The vesicular stomatitis virus matrix protein inhibits glycoprotein 130-dependent STAT activation. *J. Immunol.* *167*, 5209–5216.
- von Kobbe, C., van Deursen, J.M., Rodrigues, J.P., Sitterlin, D., Bach, A., Wu, X., Wilm, M., Carmo-Fonseca, M., and Izaurralde, E. (2000). Vesicular stomatitis virus matrix protein inhibits host cell gene expression by targeting the nucleoporin Nup98. *Mol. Cell* *6*, 1243–1252.
- Wakimoto, H., Ikeda, K., Abe, T., Ichikawa, T., Hochberg, F.H., Ezekowitz, R.A., Pasternack, M.S., and Chiocca, E.A. (2002). The complement response against an oncolytic virus is species-specific in its activation pathways. *Mol. Ther.* *5*, 275–282.
- Wakimoto, H., Johnson, P.R., Knipe, D.M., and Chiocca, E.A. (2003). Effects of innate immunity on herpes simplex virus and its ability to kill tumor cells. *Gene Ther.* *10*, 983–990.
- Wathelet, M.G., Lin, C.H., Parekh, B.S., Ronco, L.V., Howley, P.M., and Maniatis, T. (1998). Virus infection induces the assembly of coordinately activated transcription factors on the IFN-beta enhancer in vivo. *Mol. Cell* *1*, 507–518.
- Wein, L.M., Wu, J.T., and Kirn, D.H. (2003). Validation and analysis of a mathematical model of a replication-competent oncolytic virus for cancer treatment: implications for virus design and delivery. *Cancer Res.* *63*, 1317–1324.
- Wong, L.H., Krauer, K.G., Hatzinisiriou, I., Estcourt, M.J., Hersey, P., Tam, N.D., Edmondson, S., Devenish, R.J., and Ralph, S.J. (1997). Interferon-resistant human melanoma cells are deficient in ISGF3 components, STAT1, STAT2, and p48-ISGF3gamma. *J. Biol. Chem.* *272*, 28779–28785.
- Yoon, S.K., Armentano, D., Wands, J.R., and Mohr, L. (2001). Adenovirus-mediated gene transfer to orthotopic hepatocellular carcinomas in athymic nude mice. *Cancer Gene Ther.* *8*, 573–579.
- Yuan, H., Puckett, S., and Lyles, D.S. (2001). Inhibition of host transcription by vesicular stomatitis virus involves a novel mechanism that is independent of phosphorylation of TATA-binding protein (TBP) or association of TBP with TBP-associated factor subunits. *J. Virol.* *75*, 4453–4458.

CURRICULUM VITAE

ANTHONY T. POWER

PhD Candidate
Centre for Cancer Therapeutics
University of Ottawa Hospital Research Institute

EDUCATION

2002-Present	Ph.D. Biochemistry University of Ottawa "Systemic Delivery of Oncolytic Virotherapies" Thesis Supervisor: Dr. John Bell
1998-2002	B.Sc. (Honors) Biochemistry, <i>Cum Laude</i> University of Ottawa

PEER-REVIEWED PUBLICATIONS

Power A.T., and Bell J.C. (2008) **Taming the Trojan Horse: Optimizing Dynamic Carrier Cell/Oncolytic Virus Systems for Cancer Biotherapy.** *Gene Therapy*. **15**: 772.

Goel, A., Carlson, S.K., Classic, K.L., Greiner, S., **Power, A.T.**, Bell, J.C., and Russell, S.J. (2007) **In Vivo Virotherapy and Reporter Gene Imaging of Multiple Myeloma Using an Attenuated Vesicular Stomatitis Virus Encoding the Sodium Iodide Symporter Gene.** *Blood*. **110**: 2342.

Power, A.T. and J.C. Bell, (2007) **Cell-based Delivery of Oncolytic Viruses: A New Strategic Alliance for a Biological Strike Against Cancer.** *Mol Ther*. **15**: 660-665.

Power, A.T., J. Wang, T.J. Falls, J.M. Paterson, K.A. Parato, B.D. Lichty, *et al.*, (2007) **Carrier Cell-based Delivery of an Oncolytic Virus Circumvents Antiviral Immunity.** *Mol Ther*. **15**: 123-30.

Lun, X., D.L. Senger, T. Alain, A. Oprea, K. Parato, D. Stojdl, B. Lichty, **A. Power**, *et al.*, (2006) **Effects of intravenously administered recombinant vesicular stomatitis virus (VSV(deltaM51)) on multifocal and invasive gliomas.** *J Natl Cancer Inst*. **98**: 1546-57.

PEER-REVIEWED PUBLICATIONS (cont'd)

Lichty, B.D., **A.T. Power**, D.F. Stojdl, and J.C. Bell, (2004) **Vesicular stomatitis virus: re-inventing the bullet.** *Trends Mol Med.* **10**: 210-6.

Stojdl, D.F., B.D. Lichty, B.R. tenOever, J.M. Paterson, **A.T. Power**, S. Knowles, *et al.*, (2003) **VSV strains with defects in their ability to shutdown innate immunity are potent systemic anti-cancer agents.** *Cancer Cell.* **4**: 263-75.

PATENTS

Power, A.T. and Bell, J.C. **"Disparate Suicide Carrier Cells For Tumor Targeting of Promiscuous Oncolytic Viruses"**. International Patent Application CT/CA2007/001268.

AWARDS

- | | |
|------------------|--|
| 2005-2008 | Ontario Graduate Scholar in Science and Technology (Doctoral Fellowship) |
| 2009 | Second Place, University of Ottawa Biochemistry Graduate Poster Day |
| 2007 | Travel Award, Synthetic Biology 3.0 Conference (Selected Abstract) |
| 2007 | Travel Award, Fourth Annual Conference on Oncolytic Viruses as Cancer Therapeutics (Selected Abstract) |
| 2006 | First Place Oral Doctoral Seminar, University of Ottawa Biochemistry Department Graduate Studies Symposium |
| 2003-2007 | University of Ottawa Graduate Studies Tuition Award |
| 2002 | University of Ottawa Graduate Entrance Scholarship |
| 1998-2002 | University of Ottawa Entrance Scholarship (Undergraduate) |

INTERNATIONAL CONFERENCES

- 2009 ***In vivo Barriers to Gene Delivery***, Cold Spring Harbor Laboratory, USA. (Selected Oral Presentation)
- 2009 **5th Annual Conference on Oncolytic Viruses as Cancer Therapeutics**, Banff, Alberta.
- 2007 ***In vivo Barriers to Gene Delivery***, Cold Spring Harbor Laboratory, USA. (Poster)
- 2007 **Synthetic Biology 3.0**, Zurich, Switzerland (Abstract selected for poster presentation)
- 2007 **4th Annual Conference on Oncolytic Viruses as Cancer Therapeutics**, Scottsdale, Arizona (Selected Abstract for Oral Presentation)
- 2005 **3rd Annual Conference on Replicating Oncolytic Virus Therapeutics**, Banff, Alberta, Canada (Poster)
- 2003 **2rd Annual Conference on Replicating Oncolytic Virus Therapeutics**, Banff, Alberta, Canada (Poster)
-